# THE PALAEOBIOLOGY OF THE NON-MAMMALIAN CYNODONTS DEDUCED FROM BONE MICROSTRUCTURE AND STABLE ISOTOPES

**Jennifer Botha**



Thesis presented for the degree of
DOCTOR OF PHILOSOPHY
In the Department of Zoology
UNIVERSITY OF CAPE TOWN

Supervised by:
Professor Anusuya Chinsamy-Turan

November 2002

Declaration:

THE PALAEOBIOLOGY OF THE NON-MAMMALIAN CYNODONTS DEDUCED FROM BONE MICROSTRUCTURE AND STABLE ISOTOPES

Candidate:
Jennifer Botha

Supervisor:
Associate Professor Anusuya Chinsamy-Turan
Department of Zoology
University of Cape Town

I hereby

a) grant the University of Cape Town free license to reproduce the above thesis in whole or in part, for the purpose of research;
b) declare that:
    i) the above thesis is my own unaided work, both in concept and execution and that apart from the normal guidance from my supervisor, I have received no assistance except stated below:
    ii) neither the substance nor any part of the above thesis has been submitted in the past, or is being submitted for a degree in the University or any other university

The thesis is presented by me for examination for the degree of PhD.

signature removed
Jennifer Botha
11-11-2002
Date

ABSTRACT-The biology of six non-mammalian cynodont genera, from basal to more derived forms was examined using bone cross-sectional geometry and histology, as well as stable isotope analyses. The bone histology of multiple postcrania revealed distinct variations in growth pattern between the genera studied. The bone histology of the basal *Procynosuchus* indicates that this animal had a slow, cyclical growth strategy and was probably sensitive to environmental fluctuations. In contrast, the initial growth of the more derived *Thrinaxodon* was rapid and only shows a marked decrease in growth rate with the onset of sexual maturity. The bone histology of the derived *Cynognathus* indicates rapid, sustained growth, whereas the bones of the contemporary *Diademodon* reveal a cyclical growth strategy that alternated between rapid growth during the favourable season and slow or arrests of growth during the unfavourable season. This suggests that the growth of *Diademodon* was more susceptible to seasonal variation than was that of *Cynognathus.* The *Trirachodon* elements also exhibit cyclical growth, but growth cycles are not as marked in some elements compared to the *Diademodon* bones. However, the overall growth strategies of both *Diademodon* and *Trirachodon* suggest that their growth rates may have been lower than that of *Cynognathus.* The most derived non-mammalian cynodont in this study, *Tritylodon,* experienced rapid, sustained growth. This study showed that the growth patterns observed in these non-mammalian cynodonts were not affected by phylogeny alone, but also various other factors, such as ontogeny, inter-elemental variation, sexual dimorphism and environmental fluctuations. Therefore, when interpreting the biology of fossil animals from bone histology, these factors should be considered. Furthermore, due to the inter-elemental variation observed in this study, caution is advised when selecting skeletal elements for bone histological assessments.

Cross-sectional geometry results revealed relatively thick bone walls in the semi-aquatic *Procynosuchus,* which support earlier proposals that this reflects an adaptation for an aquatic lifestyle. Relatively thick bone walls were also found in the fossorial genera and it is proposed that this characteristic may also be an adaptation for digging. The relatively thick bone walls found in the *Diademodon* elements, combined with depleted $\delta^{18}O$ values suggest that this animal was semi-aquatic.

Fourier Transform Infra-red (FTIR) spectroscopic analysis showed that minimal diagenesis occurred in the non-mammalian cynodont enamel and that the overall carbonate content is similar to that of the extant *Crocodylus niloticus.* The oxygen isotope results show directional intra-tooth variability, which suggests seasonal

variation and concurs with earlier palaeoenvironmental assessments that indicate a semi-arid climate with seasonal rainfall.

The combined approach of bone cross- sectional geometry, histology and stable isotope analyses has revealed important insights regarding the lifestyle habits, ontogeny, inter-elemental histovariability and growth strategies of the non-mammalian cynodonts.

For Dru and Doug Botha

"To look is something,
To see what you look at is another,
To understand what you see is another,
To learn from what you understand is something else,
But to act on what you learn is what really matters."

- Winston Churchill

# ACKNOWLEDGEMENTS

There are a number of people I would like to thank for their assistance during this study. Thank you to Kerwin van Willigh and Kholeka Mvumvu from the South African Museum, Iziko Museums of Cape Town Histology Laboratory as well as John Lanham from the Stable Light Isotope Facility at the University of Cape Town for their technical assistance. Many thanks to my supervisor Associate Professor Anusuya Chinsamy-Turan for her advice and to Associate Professor Julia Lee-Thorp for her assistance with the stable isotope chapter. The helpful comments received from Tamara Franz-Odendaal and Jean Jordaan are also appreciated. Special thanks to Dr Sanghamitra Ray for her time, advice and encouragement and to Bruce and Gill Grobbelaar for their support. I am especially grateful to Wayne for always keeping the faith and for his incredible support during the write up of my thesis.

This study was made possible by the material loans from Dr Roger Smith and Derek Ohland of the South African Museum, Iziko Museums of Cape Town; Professor Bruce Rubidge and Dr Michael Raath of the Bernard Price Institute for Palaeontological Research, University of Witwatersrand, Johannesburg; Dr Johann Welman of the Bloemfontein National Museum, Bloemfontein; Johann Neveling of the Council for Geoscience, Pretoria; Dr Jenny Clack from the University of Cambridge and Dr Tom Kemp from Oxford University, England. The National Research Foundation, South Africa is acknowledged for supporting this research.

# TABLE OF CONTENTS

# LIST OF FIGURES

CHAPTER PAGE

# LIST OF TABLES

# CHAPTER ONE
# INTRODUCTION

*This study investigates the biology of six genera within the non-mammalian cynodont lineage using bone cross-sectional geometry, histology and stable isotope analyses. Lifestyle habits are deduced using bone cross-sectional geometry assessments. The bone histology of various, multiple postcranial elements is examined in order to determine the growth patterns of these non-mammalian cynodont genera. Serial intra-tooth carbon and oxygen isotopes are analysed to deduce how seasonal variability is reflected in the teeth of these genera. This study is the first to combine bone histology with stable isotope analyses in order to provide insight into the biological changes that occurred during non-mammalian cynodont evolution. This chapter provides an introduction to the study, the rationale and the general outline of the thesis.*



## 1.1 Introduction

The fossil record of the non-mammalian therapsids, commonly known as the mammal-like reptiles, dates from the Late Carboniferous and their evolution is one of the most significant events in tetrapod history as the group documents the morphological stages that lead to the mammals (Kemp, 1982; Rubidge and Sidor, 2001). The non-mammalian therapsids are divided into five major clades (Figure 1.1), namely the Dinocephalia, Gorgonopsia, Anomodontia, Therocephalia and the Cynodontia (Kemp, 1982; Hopson, 1994; Rubidge and Sidor, 2001).

The only non-mammalian therapsid clade to survive the Triassic period was the Cynodontia (*sensu* Rubidge and Sidor, 2001). The members of this group acquired increasingly more derived mammalian features, such as an enlarged dentary, reduced reflected lamina, bony secondary palate, complex postcanine dentition, reduced lumbar ribs and parasagittal gait, with the first true mammals

appearing by the end of the Triassic (Cluver, 1978; Benton, 1990; Pough, et al., 1996).

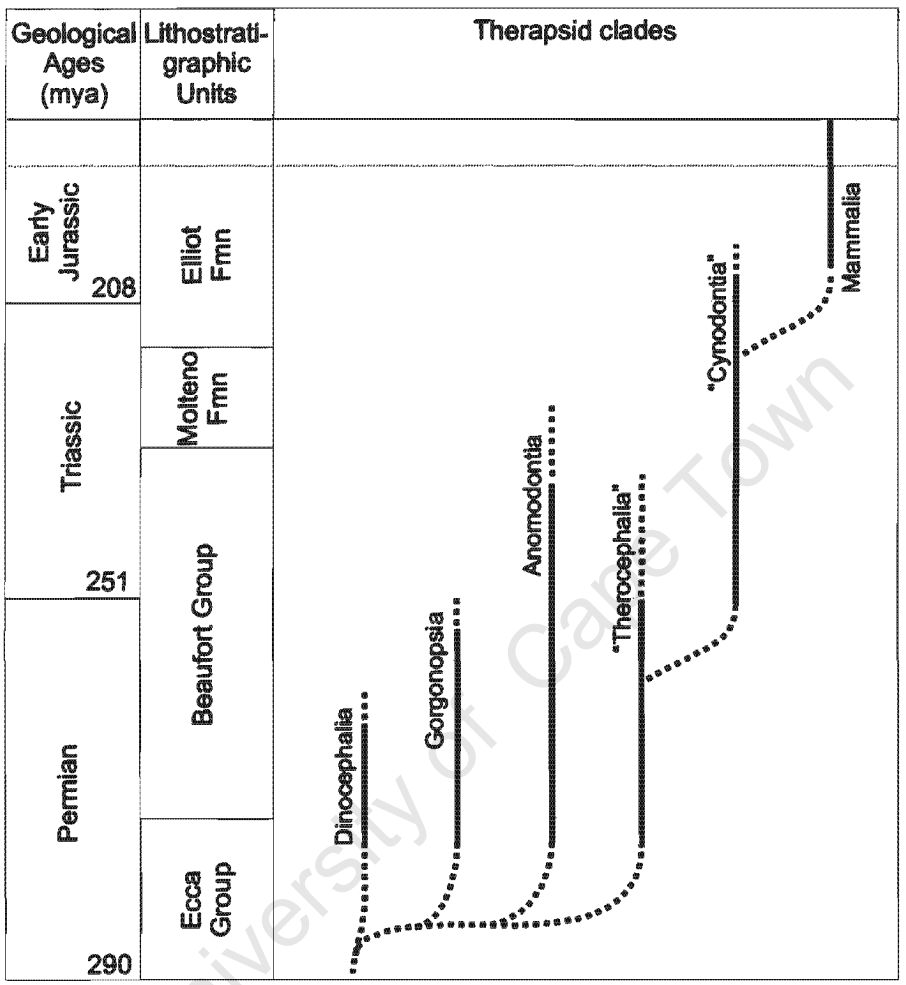


Figure 1.1. Stratigraphic ranges of the various major non-mammalian therapsid clades (modified from Kemp, 1982; Carroll, 1988). "Mya" refers to millions of years ago and "Fmn" refers to formation. Dotted lines indicate uncertain ranges.

The non-mammalian cynodonts are particularly significant as the group is considered to be the best-documented example in the fossil record of an evolutionary sequence connecting two major structural grades: namely the "reptiles"[1] and the mammals (Hopson, 1987). Their extensive fossil record has provided the opportunity for numerous morphological and anatomical studies to

[1] a paraphyletic taxon, consisting of archosaurs, lepidosaurs and chelonians. "Reptiles" in this study refers to extant crocodilians, lepidosaurs and chelonians

be undertaken (e.g. Brink, 1955; Jenkins, 1971; Kemp, 1982; Bennett and Ruben, 1986; Hillenius, 1992; Hopson, 1994).

Although morphological studies have provided extensive information regarding their phylogeny, food acquisition and processing, locomotion and biomechanical adaptations (e.g. Brink, 1955; Grine, 1977; Jenkins, 1971; Kemp, 1982; Hopson, 1971, 1994; Rubidge and Sidor, 2001) little is known about their biology. For example, the manner in which these animals grew and how their growth changed through ontogeny is poorly understood.

### 1.1.1 Rationale and Objectives of Study

Examining the bone histology of an animal provides information regarding its biology and comparing the bone histology of extinct and extant animals has improved the understanding of the ontogeny, individual age, growth, lifestyle adaptations and indirectly the physiology of extinct animals (e.g. Enlow, 1969; Enlow and Brown, 1956, 1957; Ricqlès, et al. 1991; Peabody, 1961; Castanet et al., 1988; Chinsamy, 1991).

Earlier palaeo-histology studies have concentrated mostly on non-avian dinosaur bones (e.g. Ricqlès, 1976; Ricqlès 1980; Reid, 1984a, 1984b, 1987, 1990; Chinsamy, 1990, 1991, 1993a, 1995; Varricchio, 1993; Horner et al., 1999, 2001). In contrast, the Cynodontia have received little attention and studies have included only brief descriptions such as that of Ricqlès (1969) on the bone histology of a *Thrinaxodon* femur, or Ricqlès (1974) who briefly mentioned non-mammalian cynodont bone histology. Another study conducted by Magwene in 1993 included short notes on the femoral bone histology of 14 non-mammalian cynodonts, but the specific diagnosis of the study animals was not known and they were generally labelled as 'gomphodontid', 'tritylodontid' or 'cynodontid'. These studies were based on isolated bones and did not include detailed comparisons of multiple and different skeletal elements.

In this study, multiple postcranial skeletal elements from six non-mammalian cynodont genera were selected. The genera represent early to derived forms, permitting changes in growth patterns to be assessed during different stages of non-mammalian cynodont evolution. Genera studied include *Procynosuchus*, and *Thrinaxodon*, which are early non-mammalian cynodonts and *Cynognathus, Diademodon, Trirachodon* and *Tritylodon*, which represent progressively more derived forms. Figure 1.2 illustrates the phylogenetic relationship among these genera.

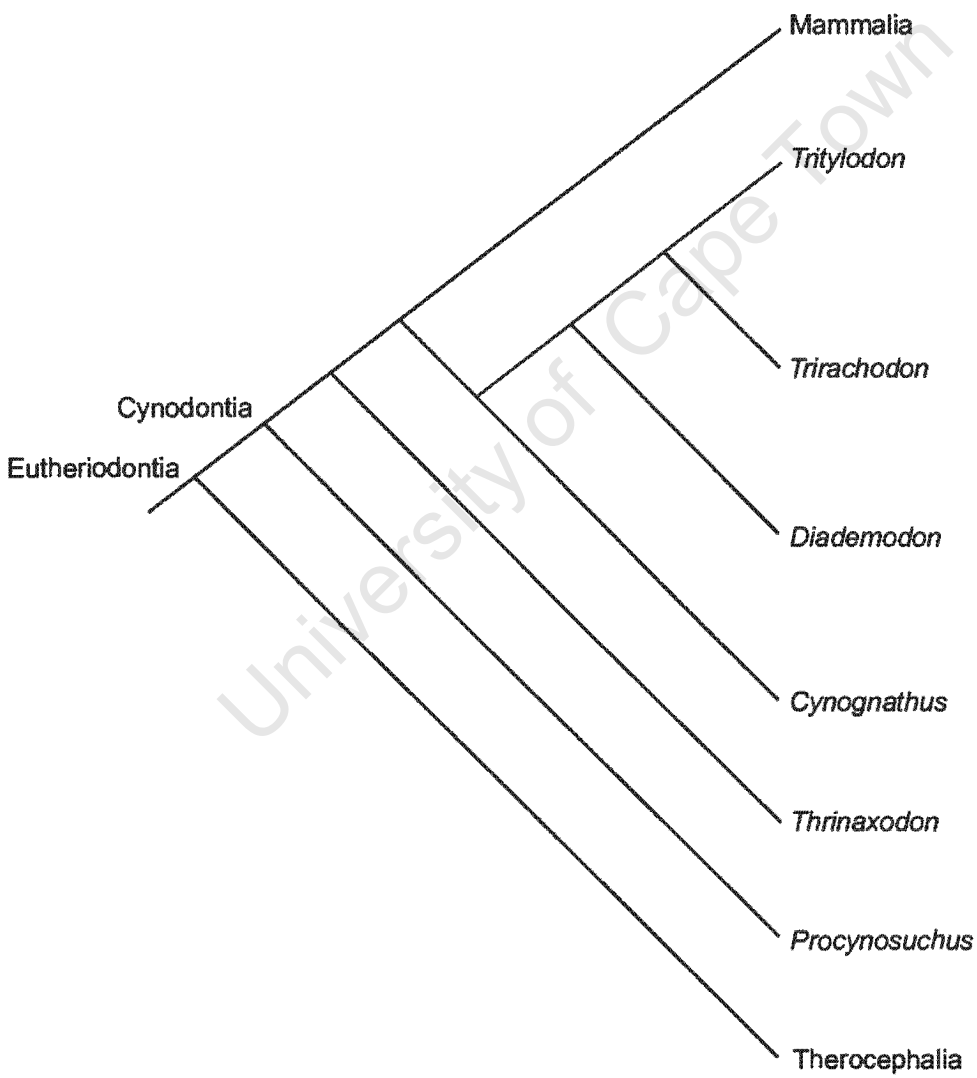




Figure 1.2. Relationships among the non-mammalian cynodonts examined in this study (modified from Rubidge and Sidor, 2001). The Therocephalia form a sister group with the Cynodontia, together called the Eutheriodontia.

*Cynognathus, Diademodon, Trirachodon* and *Tritylodon* are included in the clade Eucynodontia (and more strictly, the clade Cynognathia). Authors such as Brink (1955), Jenkins (1971), Kemp (1982) and Hopson (1994) have found that these genera have increasingly mammal-like cranial and postcranial morphological characteristics. These features include an enlarged dentary, reduced postdentary bones, fusion of the dentaries at the mandibular symphysis, a supplementary contact between the surangular and squamosal lateral to the quadrate-articular jaw joint, acromion process on the scapula and a mammalian phalangeal formula (Rubidge and Sidor, 2001).

The Karoo Supergroup of South Africa is documented as one of the richest fossil records of non-mammalian therapsids and the genera in this study, although not exclusive to the area, form part of this rich fossil assemblage. The remains of these animals were recovered from different Assemblage Zones as shown in Table 1.1. *Procynosuchus* is known from the Late Permian *Cistecephalus* Assemblage Zone (Smith and Keyser, 1995), *Thrinaxodon* from the Early Triassic *Lystrosaurus* Assemblage Zone (Groenewald and Kitching, 1995), *Cynognathus, Diademodon* and *Trirachodon* are known from the Early to Middle Triassic *Cynognathus* Assemblage Zone (Kitching, 1995) and *Tritylodon* from the Early Jurassic *Massospondylus* Range Zone (Kitching and Raath, 1984).

Table 1.1. Biostratigraphy of the Karoo Basin, South Africa. The material used in this study was recovered from the Assemblage Zones indicated in bold (modified from Kitching and Raath, 1984 and Rubidge, 1995). "Mya" and numbers refer to millions of years ago.

| Geological Periods (mya) | Group | Formation | Assemblage Zones |
|---|---|---|---|
| Jurassic | Drakensberg Volcanics | | |
| | | Clarens | |
| 208 | | Elliot | ***Massospondylus*** |
| | | | *Euskelosaurus* |
| | | Molteno | |
| Triassic | Beaufort | Burgersdorp | ***Cynognathus*** |
| | | Katberg | ***Lystrosaurus*** |
| 251 | | Teekloof | *Dicynodon* ***Cistecephalus*** *Tropidostoma* |
| Permian | | Abrahamskraal | *Pristerognathus* *Tapinocephalus* |
| 290 | Ecca | Whitehill | *Mesosaurus* |
| Carboniferous 362 | Dwyka | | |



The aim of this study is to assess evolutionary trends exhibited by the growth patterns of the non-mammalian cynodonts. The examination of different skeletal elements is intended to highlight inter-element histovariability and ensure that the histological comparison between different genera reflects true inter-generic and not inter-element variation. However, since the analysis of bone histology is a destructive process and whole skeletons are generally not available for study, this examination has concentrated mostly on limb bones. These elements do not experience extensive remodelling (particularly the midshaft region) and will permit a reasonable assessment of the ontogenetic

growth of the animal (Francillon-Vieillot et al., 1990b). Depending on availability, other skeletal elements have been incorporated to give an overall view of the bone histology of each genus. The following aspects will therefore be examined:

(i) *the variation in bone cross-sectional geometry between the genera*
(ii) *the histological variation between basal and more derived genera*
(iii) *the histological variation between different skeletal elements*
(iv) *the histological variation within individual skeletal elements*
(v) *the histological variation through ontogeny (subject to availability of material)*

The second part of the study includes an assessment of the seasonal variability experienced by these animals, using stable isotope analyses. The environment plays an important role in affecting the growth of an animal (e.g. Hutton, 1986; Castanet and Baez, 1991; Esteban et al., 1996) and a more complete understanding of non-mammalian cynodont biology can be obtained by examining the seasonal variability of their environment. Stable isotope[2] analysis is a useful technique for interpreting palaeoenvironments and associated environmental fluctuations (Luz et al., 1984; Luz and Kolodny, 1985; Stuart-Williams and Scharcz, 1997; Fricke et al., 1998).

Over the past few decades, studies such as that of Craig (1953), Luz and Kolodny (1985), Kohn (1996) and Fricke et al. (1998) have shown that the isotope signatures in the tissues of living organisms track the isotopic composition of the environment. The nature and amplitude of seasonal variability can be determined by examining the oxygen and carbon isotope signatures in tissues such as bones and teeth (Dansgaard, 1964; Longinelli, 1984; Luz et al., 1984; Lee-Thorp and van der Merwe, 1987; Koch, 1998). More recently, studies such as that of Bocherens et al. (1993), MacFadden (1998), Sharp and Cerling (1998) and Sponheimer and Lee-Thorp (2001) have

[2] chemically identical elements with slightly different atomic masses

found that isotope analysis can also be used to examine palaeoenvironments and various aspects of the biology of extinct animals.

*Thrinaxodon, Cynognathus, Diademodon* and *Trirachodon* teeth were selected for oxygen and carbon isotope analyses in this study. The climate that these animals experienced is thought to have been semi-arid with seasonal rainfall (Tucker and Benton, 1982; Anderson and Anderson, 1983, 1985; Visser, 1991; Smith et al., 1993). If the isotope signature is preserved, the manner in which seasonal variation is reflected in the teeth of these animals can be assessed. Carbon and oxygen isotope analyses will also be performed on extant *Crocodylus niloticus* and will be compared with the fossil isotope results. Fourier Transform Infra-red (FTIR) spectroscopy will be used to check the structural integrity of the non-mammalian cynodont material before proceeding with the stable isotope analyses. FTIR spectra of the extant *Crocodylus niloticus, Varanus, Giraffa camelopardalis* and the extinct *Sivatherium hendeyi* will also be analysed for comparison with the non-mammalian cynodont spectra. Therefore, the aim of this part of the study is to assess:

*(vi) the nature and amplitude of the seasonal variability experienced by the non-mammalian cynodonts, using serial intra-tooth oxygen and carbon isotope analyses*



### 1.1.2 General Outline of Thesis

The following chapter reviews the published literature relating to the palaeobiology of the Cynodontia. It consists of three divisions: a review of earlier theories regarding the thermal physiology of the Cynodontia; an assessment of the use of bone cross-sectional geometry for interpreting lifestyles and a literature review of bone histology and the terminology used.

Chapter three outlines the methods for the palaeobiological aspect of the study. Although identical methods were used to assess the biology of all the genera, the findings are presented separately for each genus. Chapter four provides

the results from the cross-sectional geometry and bone histology analyses of *Procynosuchus*, chapter five includes the results from the same analyses of *Thrinaxodon*, chapter six both *Cynognathus* and *Diademodon* (reasons stated in that chapter), chapter seven, *Trirachodon* and chapter eight, *Tritylodon*.

Chapter nine comprises the palaeoenvironmental part of the study. The stable isotope investigation is considered separately. As such, the literature relating to the palaeoenvironment of the Cynodontia and a brief review of the relevant literature regarding isotope analysis is presented in chapter nine. The method pertaining to the isotope study is also provided in this chapter, together with the results and interpretations, to permit convenient reading.

Chapter ten discusses the results of the biological findings of each genus combined with the stable isotope analyses. Chapter eleven presents a final conclusion and recommendations for the direction of future study.

This study is the first to use a combined approach of bone histology and stable isotope analyses to explore the life history strategies of the non-mammalian cynodonts and to provide essential information relating to the biology of these animals.

# CHAPTER TWO
# PALAEOBIOLOGY LITERATURE REVIEW

*This chapter provides a review of the palaeobiology of the Cynodontia based on earlier studies. Here, the literature relating to non-mammalian cynodont thermal physiology is discussed (2.1). This is followed by a review on the literature relating to the use of limb bone cross-sectional geometry as a technique for examining lifestyle habits (2.2). An update on bone histology terminology is then given, followed by a review of the published literature (2.3).*

## 2.1 Thermal Physiology of the Cynodontia

Much emphasis has been placed on understanding the thermal physiology and metabolic rates of the non-mammalian cynodonts based mainly on anatomical features, such as cranial volume (Hopson, 1980), snout foramina (Brink, 1955, Kemp, 1982), a bony secondary palate (Brink, 1955; Kemp, 1982), posture (Heath, 1968; Carrier, 1987), lumbar rib structure (Brink, 1955; Kemp, 1982) and grooves on the ventral surfaces of the nasal and frontal bones (Kemp, 1982; Hillenius, 1992). In the following section, the hypotheses relating to non-mammalian cynodont physiology that are deduced from morphological characteristics are discussed.

It has been suggested that endothermic animals require large brains due to the complex perceptual abilities and precise sensorimotor control mechanisms associated with high levels of activity (Feduccia, 1973; Hopson, 1977). In order to investigate this suggestion further, Hopson (1980) calculated the cranial volume of the non-mammalian cynodonts *Thrinaxodon* and *Trirachodon* and found it to be approximately 10 to 20% that of extant mammals (encephalization coefficient 0.1-0.2). He suggested that the non-mammalian cynodonts had an intermediate thermal physiology as the cranial volumes fell between that of extant "reptiles" and mammals. However the link between brain size and thermoregulation is still speculative (Bennett and Ruben, 1986; Withers, 1992).

In fact, the values are similar to those of extant monitor and teiid lizards (tegus and whiptails), which are active, intelligent animals, but still ectothermic (Bennett and Ruben, 1986). This suggests that thermal physiology cannot be directly determined from brain size.

The presence of hair is one of the indications of endothermy in extant mammals as it forms an insulating layer thus preventing heat loss and thereby facilitates thermoregulation (Schmidt-Nielson, 1975; Withers, 1992). Unfortunately hair is rarely preserved in the fossil record, as it is proteinaceous. It can therefore rarely be used as evidence of endothermy in palaeobiology studies. However, some authors (e.g. Brink, 1955; Kemp, 1982) interpreted the foramina on the premaxilla and maxilla bones of many non-mammalian cynodonts (as well as some therocephalians and gorgonopsians) as evidence of endothermy. These authors proposed that the foramina supplied blood vessels and nerves to sensory vibrissae. Kemp (1982) further suggested that as vibrissae are modified body hairs, hair had already evolved. In contrast, Bennett and Ruben (1986) argued that rostral foramina do not necessarily indicate the presence of vibrissae. For example, the extant lizard *Tupinambis* also has rostral foramina and they are almost identical to those found in the non-mammalian cynodont *Thrinaxodon* (Estes, 1961). Bennett and Ruben also stated that sensory hairs do not necessarily indicate the presence of a hairy coat and it cannot be assumed that hair first evolved for insulation as the origin and original function of hair is still not well understood.

Another argument for possibly higher metabolic rates in non-mammalian cynodonts involved the presence of muscular fleshy lips, which suggested that food was chewed instead of immediately swallowed. The surfaces of the premaxilla, maxilla and dentary bones of extant crocodilians and lizards contain many tiny foramina often associated with small grooves due to the skin being held tightly against the bone surface. In contrast, the surfaces of these bones in the non-mammalian cynodonts are smooth and contain very few of these tiny foramina. Kemp (1982) proposed that these smooth surfaces indicated the

presence of muscular lips and hence chewing. If this is the case, it would suggest that the non-mammalian cynodonts had a more efficient digestive system compared to extant crocodilians and lizards as chewing may be linked to the increased energy demands of high metabolic rates thus increasing the efficiency of digestion (Pough et al., 1996). However, there have been no studies conclusively linking a smooth snout to the thermal capacity of an animal. As such, this feature should not be used as evidence of endothermy.

In mammals, a secondary bony palate separates the respiratory passage from the buccal cavity, allowing for continuous breathing and increased oxygen consumption, which is necessary in animals with high metabolic rates. Such a secondary bony palate has been found in the more derived non-mammalian cynodonts and has been used as evidence of endothermy (Brink, 1955; McNab, 1978; Kemp, 1982). Yet this feature is present in ectothermic crocodilians and teiid lizards and is absent in endothermic birds (Bennett and Ruben, 1986). Furthermore, many extant ectothermic animals use a fleshy secondary palate to separate the buccal cavity from the respiratory passage. Bennett and Ruben (1986) suggest that a bony palate acts as a surface on which the tongue can manipulate food, facilitating mastication instead of indicating thermoregulatory status. Alternatively, this feature may be associated with mode of life. For example, semi-aquatic crocodilians and turtles have bony secondary palates, completed by soft tissue, as a modification for breathing at the water surface while submerged. Therefore, the original function of the bony secondary palate may not have been thermoregulatory.

The parietal foramen on the dorsal surface of the skull is associated with an epiphyseal complex[1] and it is through which the parietal eye detects the external environment. A parietal foramen (and probably the associated epiphyseal complex) is present in all early tetrapods, including non-mammalian therapsids, but the external connection has disappeared from most living forms

[1] the anterior evagination of the midbrain of early vertebrates, the posterior of which is the pineal (Withers, 1992)

apart from a few extant lizards and the rhynchocephalian *Sphenodon* (Bennett and Ruben, 1986). The whole structure is lost in a few mammals and crocodilians. It is thought that the epiphyseal complex affects thermoregulation or circadian rhythms (photoperiod determination) and that the original function was to control body temperature, when thermoregulation was basically behavioural (Roth and Roth, 1980). Consequently, the loss of the external connection should indicate the beginning of endothermy (at least in those forms that have kept the pineal part of the complex). However, although only extant ectotherms have the complete epiphyseal complex and parietal foramen, the foramen and parietal eye have been independently lost many times during tetrapod evolution and may therefore have nothing to do with the development of endothermy (Bennett and Ruben, 1986).

Heath (1968) suggested that the posture of non-mammalian therapsids was fully erect and this pointed towards endothermy. He argued that a completely erect stance is energetically expensive and therefore a major source of heat production. Yet, Bennett and Ruben (1986) argued that mammalian endothermy depends more on the heat production from the liver, kidney, brain and heart metabolism than on that from skeletal muscle. Furthermore, the non-mammalian cynodont posture was not fully erect, but had a sprawling forelimb and semi-erect hindlimb (Jenkins, 1971; Kemp, 1982; Blob, 2001). Carrier (1987) suggested that although the non-mammalian cynodont posture was not fully erect, the semi-erect stance would have improved the ability for simultaneous breathing and running. The sprawling, lateral undulatory locomotion of extant crocodilians and lizards reduces or prevents simultaneous breathing and running and therefore limits sustained activity (Pough et al., 1996). It was suggested that simultaneous breathing and running would increase sustained activity, which would then facilitate an active lifestyle and hence endothermy. However, there is no direct link between posture and thermoregulation (Bennett and Ruben, 1986; Ruben, 1995). For example, extant ectothermic chelonians, crocodilians (Bakker, 1971) and extant endothermic monotremes (Jenkins, 1971) have a semi-erect stance, which

demonstrates that the posture-thermoregulation correlation is not necessarily distinctive between ecto- and endothermic animals.

A muscular diaphragm is essential for mammalian lung ventilation. Oxygen consumption needs to increase during high levels of activity and a diaphragm facilitates high ventilation rates (Pough et al., 1996). For a diaphragm to be present, the ribs must not restrict the abdomen, so that changes in the thoracic volume can be compensated for by appropriate changes in the abdomen volume. In the more derived non-mammalian cynodonts, the lumbar ribs are greatly reduced and the rib cage becomes very mammal-like suggesting that a diaphragm may have been present (Brink, 1955; Kemp, 1982). Alternatively, as suggested by Bennett and Ruben (1986), these changes may not be linked to diaphragmatic ventilation and endothermy, but instead to increasing agility and activity of the more derived non-mammalian therapsids relative to the early forms. Skeleto-muscular modifications related to the rotation and flexion of the spinal column, such as lumbar rib reduction, may then have developed. Hence, the reduction of the lumbar ribs of non-mammalian cynodonts may or may not be related to the presence of a diaphragm and should not be used as conclusive evidence of endothermy.

In summary, the above anatomical features provide indirect, inconclusive arguments for endothermy in the non-mammalian cynodonts. Bennett and Ruben (1986) proposed that features thought to be associated with endothermy in extinct animals must not be present in any extant ectotherm and must have a distinct and direct link with metabolic rate. Consequently, they suggested that the presence of complex respiratory turbinates provides the best anatomical evidence of endothermy in fossil animals. Complex respiratory turbinates or maxilloturbinate bones are found in the nasal cavities of almost all extant mammals and are involved in the conditioning of inhaled air to the lungs and the absorption of water vapour from the exhaled air (Hillenius, 1992; Ruben, 1995, 1996). Desiccation, associated with high ventilation rates, is prevented by the use of a countercurrent exchange system. Cool inhaled air absorbs heat and

moisture from the turbinal linings. This moist air therefore prevents desiccation of the lungs. The cool air also creates a thermal gradient along the turbinates. Warm exhaled air is then cooled from passing back over the turbinates, which results in condensation and the absorption of water (Hillenius, 1992; Ruben, 1995; Ruben et al., 1997). There are no such complex structures in the nasal cavities of extant "reptiles" (Parsons, 1970), which suggests that these structures evolved to cope with high ventilation rates related to mammalian endothermy (Ruben, 1995). Rudimentary anterolateral ridges for the support of maxilloturbinate bones have been found in non-mammalian therapsids such as *Thrinaxodon* and *Diademodon* (Brink, 1955; Hillenius, 1992), which implies that they may have had high ventilation rates, which is necessary for high metabolic rates.

Bennett and Ruben (1986) also claimed that if a characteristic thought to be associated with endothermy was present in a sister taxon it would suggest ancestral inheritance. Although there are many anatomical and physiological features that separate monotremes from eutherian mammals, the features constituting their thermoregulatory capacities (maintaining high body temperatures, increased capacity for oxygen delivery and utilization) are much the same. Bennett and Ruben (1986) suggested that these common features either arose independently soon after the prototherians (monotremes) and therians (marsupials and placentals) diverged (during the Early Cretaceous) (Crompton and Jenkins, 1973) or they arose within the more derived non-mammalian therapsid lineage. If these features arose after the prototherians and therians diverged, it would indicate improbably high levels of convergence (Bennett and Ruben, 1986; Bennett, 1991). Yet, this kind of evidence is speculative and offers no conclusive proof as to the origin of endothermy.

Apart from anatomical structures, aspects such as predator-prey ratios and biogeographical distribution have also been used as evidence of endothermy in the non-mammalian therapsids. Bakker (1972a, 1980, 1986) has been foremost in maintaining that predator-prey ratios distinguish between extinct

ecto- and endothermic animals. Extant ectothermic vertebrates usually expend approximately 20% of their assimilated energy on secondary productivity (growth and reproduction), whereas extant endotherms expend approximately 1% to 3%, as thermoregulation is energetically expensive (Golley, 1968; Bakker, 1972). Bakker (1972, 1980) suggested that these ratios are reflected in the populations of animal communities that are in a steady state. He argued that ratios within fossil communities can be determined by reconstructing the skeletons of predators and their prey and calculating the biomass of the community. He suggested that a community is endothermic if the predators constitute only 2% to 3% of the animal biomass, whereas a substantially greater ratio of 35% to 60% constitutes an ectothermic community. Bakker (1972) examined non-mammalian therapsids from South Africa and Russia and concluded that their predator-prey ratios were between 10% and 15%, suggesting that they fell somewhere between that of ecto- and endothermic communities. However information from the predator-prey ratios of fossil communities is highly speculative. Firstly it is not known how accurately the fossil record preserves extinct community structures (McNab, 1978; Béland and Russell, 1980; Farlow, 1980; Hotton, 1980) and secondly, the ratios of extant ecto- and endothermic communities can overlap (Bennett and Ruben, 1986). Extinct predator-prey ratios should therefore not be regarded as reliable evidence to argue for or against endothermy.

Bakker (1972) also suggested that non-mammalian therapsids would only have been able to survive during the Late Permian in South Africa if they had been endothermic. He argued that because the climate during the Late Permian was cold, ectotherms could not have survived here. However the ice sheets that dominated Southern Gondwana during the Late Carboniferous disappeared by the Early Permian and the climate became far more equable (Frakes, 1979; Anderson and Anderson, 1983; Parish et al., 1986; Smith et al., 1993). Furthermore, numerous early tetrapods that were almost certainly ectothermic, including the "pelycosaurs"[2] (Rubidge and Sidor, 2001), have been found in

[2] paraphyletic taxon

South Africa during the Late Permian (Smith and Keyser, 1995; Reisz et al., 1998; Modesto et al., 2001).

The non-mammalian cynodonts are regarded as transitional representatives between "reptiles" and the extant mammals and possess morphological characteristics that are found in both groups. It may therefore be expected that they were transitional in their thermoregulatory capacity as well. As the distinction between ecto- and endothermy is not clearly defined, it is difficult to determine the specific point at which these transitional animals ceased being ectothermic and became endothermic (Withers, 1992). The above theories regarding the thermoregulatory capacity of the non-mammalian cynodonts have been inferred from indirect evidence and provide no conclusive proof as to whether they were endo- or ectothermic. Morphological features cannot be used as direct evidence for or against endothermy as those features positively identifying endothermy are usually not preserved in the fossil record (such as blood oxygen carrying capacity, mitochondrial density, lung structure, enzymatic activities, hair, a diaphragm and sweat glands; Ruben, 1995).

Yet, if the indirect features are considered together, in conjunction with the morphological modifications such as an increasingly mammal-like locomotion or those related to obtaining and orally processing food, they may suggest increased ventilation rates and higher rates of metabolism. This may then indicate that some form of endothermy or an intermediate thermal physiology was present among the more derived non-mammalian cynodonts. An assessment of the bone histology of these animals will provide direct information on the pattern and rate of bone deposition and hence growth, which can shed light on aspects of non-mammalian cynodont physiology (see section 2.3 for details).

## 2.2 Bone Cross-Sectional Geometry for the Assessment of Lifestyle Habits

A direct relationship exists between the lifestyle of an animal and the structural design of its bones. For example, fossorial animals (diggers) have thick and relatively short limb bones and a high force moment of their forelimb muscles (Bou et al., 1990; Casinos, et al., 1993). As the lifestyle habits of extinct animals cannot be directly observed, their osteological modifications are important for determining the type of habitat the animal occupied. Numerous studies have used allometry and gross morphology for these examinations (e.g. Kemp, 1980, 1982; Casinos et al., 1993; Bargo et al., 2000). A less frequently used technique that has demonstrated potential for this type of analysis is limb bone cross-sectional geometry. Earlier studies have shown that bone cross-sectional geometry differs according to the type of habitat an animal occupies (terrestrial versus aquatic) (Wall, 1983; Stein, 1989; Bou et al., 1990; Fish and Stein, 1991; Fish, 1993). For instance, the bones of extant sirenians, cetaceans and some aquatic birds as well as the fossil Mesosaurs, Pachypleurosaurs and Champsosaurs (Hua and Buffrénil, 1996; Reid, 1996) have extremely high bone densities, which are achieved through pachyostosis[3] (Buffrénil et al., 1990) osteosclerosis[4] (Damiani, 2000) or pachyosteosclerosis[5] (Francillon-Vieillot et al., 1990b) as aquatic modifications.

In 1983, Wall examined the thickness of the bone walls of 49 mammalian genera and found that most of the aquatic mammals have a significantly higher limb bone density than terrestrial mammals. He proposed that if the compact bone wall exceeds 30% of the average bone diameter, the animal is aquatic or at least semi-aquatic (Wall, 1983). He suggested that the high limb bone density in the aquatic group was to counteract positive buoyancy while in the water.

[3] hyperplasy (excessive development) of the periosteal cortex
[4] reduction or absence of the medullary cavity through inner compaction of bone
[5] combination of pachyostosis and osteosclerosis

Yet, lifestyle habits are not necessarily always clearly discernible. In 1989, Stein compared the limb bone density of a number of semi-aquatic and terrestrial didelphid marsupial and rodent genera and found that although the difference between terrestrial and semi-aquatic genera was significant, the difference between the two groups ceased to be significant when compared with the fully aquatic animals in Wall's (1983) study. Most semi-aquatic taxa swim either on or slightly below the surface of the water and therefore may not have extensive osteological aquatic adaptations. Semi-aquatic taxa must function efficiently both on land and in the water and so their bone density may fall within an optimum range for both types of lifestyle. They often have non-osteological adaptations such as a streamlined body shape, large webbed hind feet, waterproof fur, robust vibrissae, dorso-laterally placed eyes, reduced closable external ears etc. Hence although there appears to be a marked distinction in limb bone density between terrestrial and fully aquatic animals, it may be more difficult to discern the semi-aquatic species on the basis of limb bone density alone (Stein, 1989).

Differences in bone wall thickness can also be ascribed to minimizing energy costs (Alexander, 1985; Currey and Alexander, 1985; Heinrich et al., 1993). In an analysis of tubular bones, Currey and Alexander (1985) suggested that long bones have a minimum mass, thus facilitating locomotion using the least amount of energy. K is the ratio of the internal to external diameter of a bone. If K = 0, then the bone is solid. K increases towards 1 as the walls of the bone become increasingly thinner.

The optimal value of K, which allows bone mass to be minimized, depends on whether the bone is selected for yield or fatigue strength[6], for ultimate strength[7], for impact strength or for stiffness[8] (rigidity). Currey and Alexander (1985) found that if marrow-filled bones are selected for yield strength or fatigue

[6] defined as the progressive loss of strength and stiffness, that occurs prior to failure in materials subjected to repeated loads (Martin and Burr, 1989)
[7] the stress at which the material fails (Withers, 1990)
[8] the ratio of the load and the corresponding deformation (Martin and Burr, 1989)

strength, the K-value should be 0.67, for stiffness, the K-value should be 0.75 and if they are selected for impact loading, they should have a K-value of 0.55. Alternatively the thickness of the bone wall can be expressed as the ratio of the radius to the cortical thickness (i.e. r / t) (Figure 2.1).

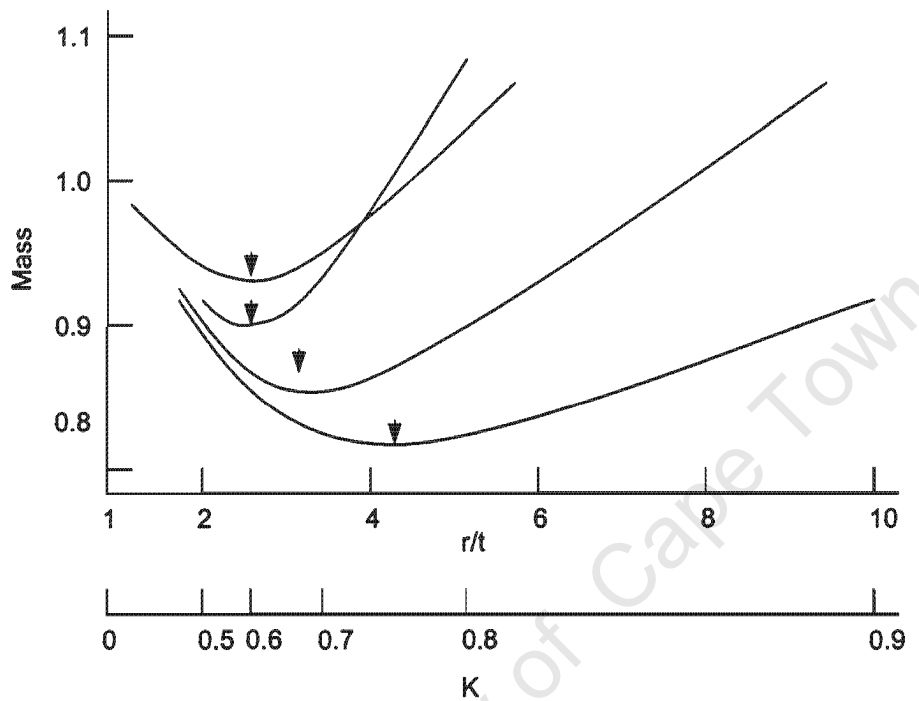


Figure 2.1. Masses of tubular bones, as fractions of the mass of a solid bone of equal length and strength or stiffness, as a function of K and r/t. Arrows indicate optimum value of K (reconstructed from Currey and Alexander, 1985).

In 1993, Magwene studied the cross-sectional geometries of the femoral midshafts of a number of extant crocodilians, lizards and mammals and non-mammalian therapsids. The non-mammalian therapsids included *Edaphosaurus, Biarmosuchus,* indetermined gomphodontids and tritylodontids, as well as *Massetognathus* and *Exaeretodon.* Magwene found that, on average, the non-mammalian therapsids and extant mammals had relatively thinner bone walls than did the crocodilians and lizards and he suggested that they have lighter bones, which are subject to greater bending and torsional stresses. In contrast, crocodilian and lizard limb bones were more robust and stiffer than the non-mammalian therapsid and mammalian limb bones. Magwene proposed that the difference in cortical thickness between the extant

"reptiles" and mammals is due to a skeletal weight saving in the mammals because of their highly active lifestyles. However lifestyle modifications should also be considered in such studies (such as that of Magwene, 1993) as differences in limb bone density may also be due to functional modifications to a habitat and not just phylogeny.

## 2.3 Bone Histology

As the definitions of the terms used to describe bone tissue patterns have varied between different authors in the past, either due to misuse or ambiguity, the following section (2.3.1) provides the terms and definitions used to describe the bone histology observed in this study. Various theories regarding the biology of extinct animals deduced from bone tissue patterns are discussed following the terminology explanation (2.3.2).

### 2.3.1 Terminology

Bone is a rigid form of connective tissue that forms most of the vertebrate skeleton. Bone tissue consists of cells that become embedded in an intercellular matrix, which consists of a mineral component and reinforcing collagen fibres. The main inorganic component is called hydroxyapatite ($Ca_5(PO_4)_3OH$), which is a calcium phosphatic mineral. Inorganic salts such as calcium carbonate, calcium fluoride and magnesium fluoride are also present, but to a lesser extent (Leeson and Leeson, 1981; Cormack, 1987; Francillon-Vieillot, et al., 1990b).

Bone cells are divided into three types, namely osteoblasts, osteocytes and osteoclasts. The cells that are involved in the formation of the bone matrix are called osteoblasts, which become osteocytes when they are entrenched within the bone matrix. The osteocytes lie in spaces called lacunae. These osteocyte lacunae are connected to each other via canaliculi through which the osteocytes extend fine cytoplasmic processes. The canaliculi facilitate the distribution of nutrients and oxygen to the osteocytes. Osteoclasts are found near bone

surfaces and are responsible for the resorption of bone (Leeson and Leeson, 1981; Cormack, 1987).

Skeletal elements differ in structure and are termed long bones, short bones and flat bones. Each bone type differs in shape and structure. Long bones (limb bones) are typically cylindrical and elongated and are divided into the diaphysis, epiphyses and metaphyses. The diaphysis forms the cylindrical shaft and the epiphyses are the regions at the ends of the long bone. The metaphyses are the transitional regions between the epiphyses and the diaphysis (Figure 2.2). Short bones are generally stout, cuboidal or irregular in shape and flat bones show an obvious preferential development within a single plane or single curved surface. Each bone type grows differently and transitions do occur between all three (e.g. ribs) (see Francillon-Vieillot et al., 1990b).



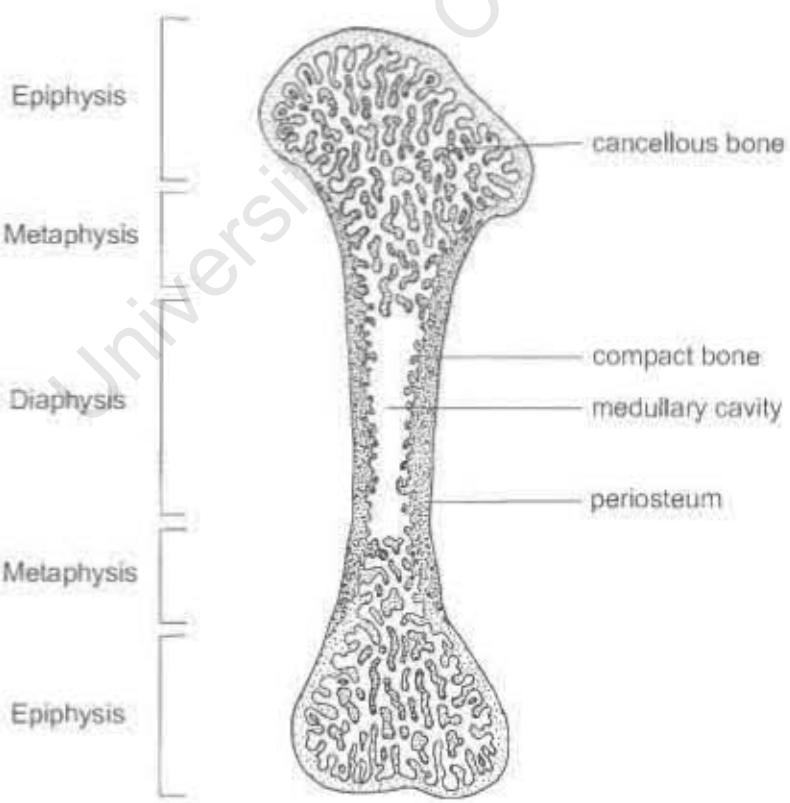


Figure 2.2. Schematic diagram of a typical non-mammalian long bone in longitudinal section, showing the various regions.

A layer of specialised dense connective tissue known as the periosteum, normally covers the surface of most bones (apart from articulating surfaces and regions of tendon and ligament attachment). Lining the bone surfaces of the medullary cavity (the inner, deep region) is another layer of specialised connective tissue known as the endosteum (Francillon-Vieillot et al., 1990b). Bone may be periosteal (resulting from periosteal ossification) or endosteal (resulting from endosteal ossification), depending on whether it is formed on external or internal surfaces, covered by the periosteum or endosteum, respectively (Reid, 1996) (see Figure 2.2).

The bone formed when growing in width is usually periosteal, but may also be mixed i.e. partly periosteal and partly endosteal. Endosteal bone that replaces cartilage during growth (such as growth in length) is known as endochondral bone. Here, cartilage becomes hypertrophic and calcified. It is the first bone type to be formed during early development and later in life is formed at the epiphyses. Cavities form within the bone marrow and trabeculae then form as a result of the resorption of some of the new endochondral bone. Calcified cartilage may occur as little "islands" within the trabeculae and resemble foam-like "bubbles" representing the lacunae that were once occupied by chondrocytes (Reid, 1984a; Francillon-Vieillot et al., 1990b; Reid, 1996).

The endochondral ossification in long bones begins with the development of a cartilaginous model. The midsection of the cartilaginous model becomes calcified and is replaced by bone (see Cormack, 1987 for a detailed discussion). This area is known as the primary centre of ossification. A secondary centre of ossification may also develop in each cartilaginous epiphysis, eventually developing into the bony epiphyses that retain a covering of articular cartilage (Haines, 1969; Leeson and Leeson, 1981; Cormack, 1987). Secondary ossification centres are prominent in the epiphyses of extant mammals, but are absent in non-avian dinosaurs, non-mammalian therapsids and extant crocodilians and turtles (Carter et al., 1998).

Bone can also be distinguished as compact bone or cancellous (spongy) bone according to the overall bone porosity. Compact bone is generally denser than cancellous bone, although the amount of porosity can range from completely compact bone with no spaces to a completely free medullary cavity with few trabeculae. Compact bone typically forms the outer regions of bones and is laid down centrifugally, usually by periosteal deposition (Francillon-Vieillot et al., 1990b; Reid, 1996) (see Figure 2.2). It should be noted however, that although the terms compact and spongy bone are convenient and frequently used, they do not refer to precise, definite histological situations. For example, although the cortex[9] generally consists of compact bone, this is not always the case (e.g. long bones of marine turtles). Furthermore, compact bone can be converted into cancellous bone (e.g. long bones of marine turtles) and vise versa (Francillon-Vieillot et al.; 1990b).

The structural organisation of bone is generally retained even after fossilization. Although the osteocytes, blood vessels (vascular canals) and collagen fibres are destroyed, their position usually remains intact, which facilitates the examination of fossil bone microstructure. During the fossilization process, the hydroxyl component of the hydroxyapatite is displaced and substituted by fluoride to become fluorapatite (Francillon-Vieillot, et al., 1990b; Sponheimer and Lee-Thorp, 1999a). There are also other minerals such as citrate, silicon, sodium, manganese, strontium, zinc, iron, yttrium, arsenic, selenium, barium, lead, thorium and uranium that become incorporated into the inorganic component of bone during fossilization (Parker and Toots, 1970; Francillon-Vieillot, et al., 1990b).

The histological patterns observed in fossil bones are assessed according to the tissue organisations seen in extant taxa. Bone is classified according to several factors, such as the fibrillar organisation (i), the vascular arrangement (ii), the types of bone tissue (iii) and cortical stratification (iv). These classifications involve primary bone, which is deposited where bone did not

[9] region from the medullary cavity to the periphery

previously exist (although it may form on an existing bone surface). The following section describes these classifications and is followed by a brief description of Haversian bone[10] (v) and an explanation of bone remodelling (vi).

**(i) Fibrillar Organisation**

Fibrillar organisation refers to the arrangement of collagen fibres in bone, which are usually grouped into bundles. These arrangements can be distinguished from their orientation (e.g. fibres may be regularly, irregularly, or radially arranged). Although the actual fibrillar structure is not preserved in fossil bone, the alignment of deposited apatite crystals when viewed under polarised light shows the spatial organisation (Reid, 1996). This facilitates the interpretation of the spatial organisation of the original organic matrix. The sections (a), (b) and (c) describe the various bone matrix organisations observed in this study.

**(a) Lamellar Bone Matrix**

Lamellar bone indicates a high level of spatial organisation and consists of successive thin layers called lamellae (Francillon-Vieillot et al., 1990b; Reid, 1996). In each lamella the closely packed collagen fibres are mutually parallel, but the direction changes from one lamella to the next. Each lamella may contain some linear rows of flattened osteocytes with few canaliculi.

**(b) Woven Bone Matrix**

This type of bone matrix consists of coarse and loosely packed collagen fibres of varying size, distributed irregularly throughout the matrix. The osteocyte lacunae are generally globular to round and show a very low spatial organisation (Reid, 1984b; Francillon-Vieillot et al., 1990b; Ricqlès et al. 1991; Reid, 1996). They are also sometimes more abundant and closely packed, compared to other tissues.

[10] secondary bone that may replace primary bone

**(c) Parallel-fibred Bone Matrix**

Parallel-fibred bone tissue consists of closely packed collagen fibres running approximately parallel to each other. Osteocytes are usually flattened and randomly distributed. Under polarised light the tissue appears homogenously light or dark, according to the orientation of the fibres (Francillon-Vieillot et al., 1990b; Reid, 1996). The spatial organisation of this bone tissue is between that of lamellar and woven bone.

**(ii) Vascular Arrangement**

The channels within bone tissue represent the area where lymph, nerves and vascular canals run through the bone tissue. Studies such as that of Enlow (1969), Enlow and Brown (1957) and Currey (1960) have found that the amount and type of channel organisation varies between different extant vertebrate taxa. If fossil bone is well preserved, qualitative and quantitative comparisons of the channels can be made between extinct and extant vertebrates (e.g. Currey, 1962; Enlow and Brown, 1957; Chinsamy, 1991, 1993b; Reid, 1990; Ricqlès, 1976). As these channels include vascular canals, their quantity and organisation will affect the overall efficiency of the bone to distribute nutrients to the bone tissue (Reid, 1996).

Although the channels in bone do reflect vascular canal quantity, Starck and Chinsamy (in press) recently found that the channel shape does not necessarily reflect the exact shape of the vascular canal itself. The examination of extant Japanese quail bones revealed that only about 20% of the channel area contains vascular canals and that more than one vascular canal, sometimes with varying shape, was found within a single channel space. As such, any quantitative analysis should note that the area occupied by these channels reflects the maximum possible area that the vascular canals can occupy.

Vascular canals may become surrounded by centripetally deposited lamellae during periosteal growth to form primary osteons (Francillon-Vieillot et al., 1990b; Reid, 1996).

The vascular canals may form various patterns, which are used in describing bone tissue organisations. The following is a list of structural categories based on the organisation of the channels within the bone tissue and is illustrated in Figure 2.3.

(a) **Simple Longitudinal Canals:** longitudinally oriented channels enclosed within the bone matrix. They are not surrounded by bone lamellae.
(b) **Longitudinal Primary Osteonal Arrangement:** longitudinally oriented primary osteons running parallel to the long axis of the bone arranged irregularly within the bone matrix.
(c) **Longitudinal Primary Osteonal Arrangement Oriented in Radial Rows:** longitudinally oriented primary osteons running parallel to the long axis of the bone arranged in radial rows.
(d) **Longitudinal Primary Osteons in Circular Rows:** longitudinally oriented primary osteons organised in circular rows.
(e) **Laminar Arrangement:** longitudinal primary osteons arranged in successive circumferential layers. Within each vascular layer, circularly oriented primary osteons anastomose between the longitudinally oriented osteons, forming a two dimensional network.
(f) **Plexiform Arrangement:** more densely vascularised compared to laminar bone. The longitudinally oriented canals are connected via radial as well as circular canals, forming a three dimensional network.
(g) **Radiating Arrangement:** radiating primary osteons dominate over longitudinal and circular osteons and represents very fast deposition.
(h) **Reticular Arrangement:** the lamellar primary osteons surrounding the vascular canals are obliquely oriented and irregularly anastomosed forming a very disorganised network of osteons.

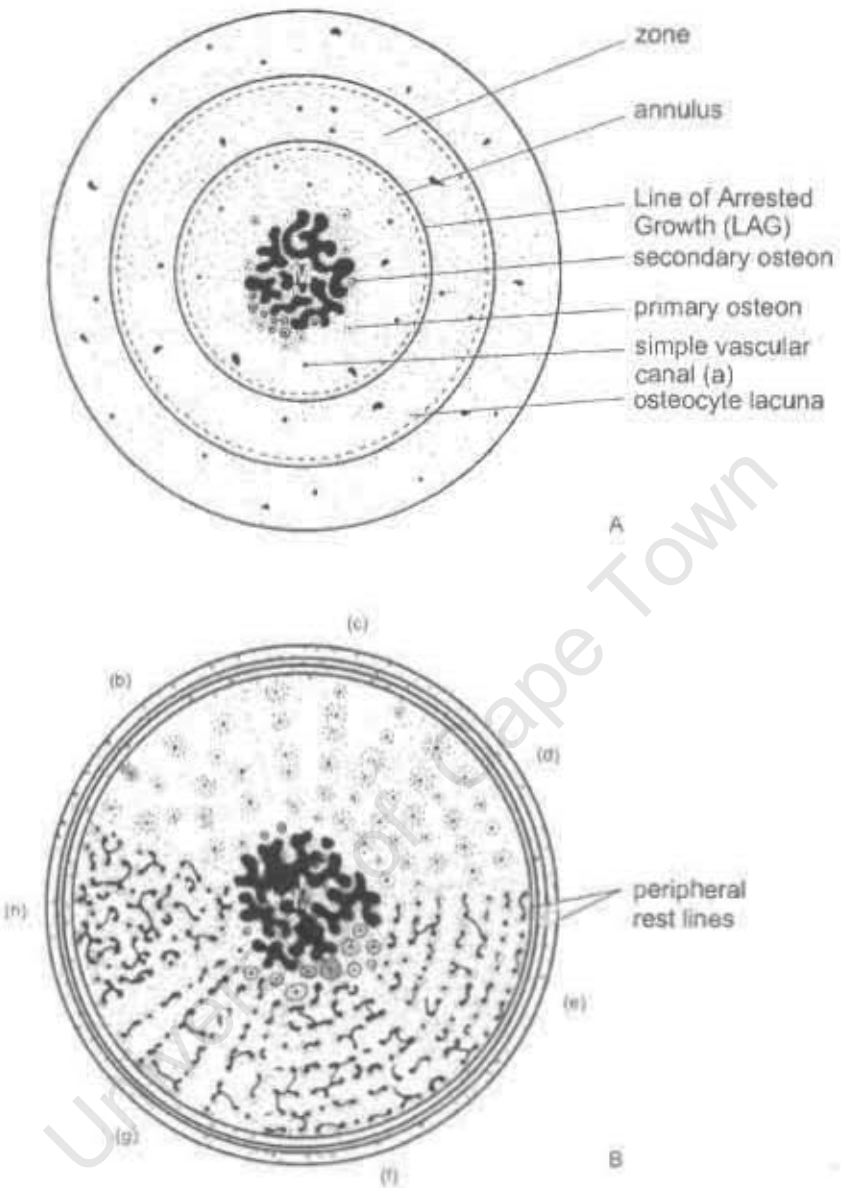




Figure 2.3. A schematic diagram of transverse sections through the midshaft of a limb bone, showing zonal bone (A) and azonal bone (B). (a) to (h) represent the different vascular arrangements that may be found in bone tissue. (a) is more commonly associated with the bone type found in A, however any of the vascular organisations (from (a) to (h)) may occur within either zonal (A) or azonal bone (B). Combinations of the organisations may also occur within an individual bone. (a), simple vascular canal arrangement; (b), longitudinal primary osteonal arrangement; (c), longitudinal primary osteonal arrangement oriented in radial rows; (d), longitudinal primary osteons in circular rows; (e), laminar arrangement; (f), plexiform arrangement; (g), radiating arrangement; (h), reticular arrangement. Accretionary bone is represented as peripheral rest lines at the outer margin of B. M indicates medullary cavity.

### (iii) Types of Bone Tissue

#### (a) Lamellar Bone Tissue

This bone tissue, characterised by a lamellar bone matrix, is usually poorly vascularised (Francillon-Vieillot et al., 1990b; Reid, 1996). It is frequently associated with zonal bone tissue (see section 2.3.1 iv-a), although it may occur azonally as well.

#### (b) Woven-fibred Bone Tissue

This bone tissue consists mostly of a woven bone matrix. It is laid down rapidly as fine cancellous tissue, instead of as compact bone and is generally found in embryos or very fast growing young individuals. When woven bone includes primary osteons, the tissue is known as fibro-lamellar bone (Ricqlès, 1980, et al., 1991; Reid, 1984b, 1996; Francillon-Vieillot et al., 1990b). The term 'fibro-lamellar' includes various typological categories such as laminar, plexiform, reticular and radiating fibro-lamellar bone, according to the vascular canal arrangement (see section 2.3.1 ii).

#### (c) Parallel-fibred Bone Tissue

Parallel-fibred bone is formed from a parallel-fibred matrix and is vascularised by simple primary vascular canals and or primary osteons. It is usually more vascularised than lamellar bone (Francillon-Vieillot et al., 1990b).

It should be noted that all intermediate conditions exist between these various tissue types and are not always clearly defined.

### (iv) Cortical Stratification

Bone tissue may exhibit various structural discontinuities. An abrupt change n the direction of growth, either from inward to outward, or vise versa, is termed a "reversal". The line separating the centrifugally deposited periosteal bone and centripetally deposited endosteal bone is termed a reversal line (Enlow, 1963).

If bone deposition is simply interrupted and then resumed, the interruption is marked by an interruption or resting line.

**(a) Zonal Bone**

When growth is intermittently interrupted by a series of concentric growth rings, the tissue is termed zonal bone (Reid, 1996). The growth rings consist of zones bounded by annuli or rest lines (Lines of Arrested Growth) or both annuli and rest lines. Zones are thick regions of bone corresponding to periods of fast growth, whereas annuli are thin regions of bone corresponding to periods of slow growth. The zones of the simplest zonal tissues consist of avascular bone (Reid, 1996). The zones of more complex tissues contain vascularised parallel-fibred or fibro-lamellar bone with relatively abundant, globular osteocytes and sometimes a dense network of canaliculi. Annuli are narrow, avascular or poorly vascularised regions, consisting of parallel-fibred bone, or more commonly, of lamellar bone. The osteocytes inside the annuli are usually flattened and the canaliculi are generally poorly developed or absent. Lines of Arrested Growth (LAG) may occur alone, or before/after an annulus (as single, double or even multiple lines) and they correspond with temporary, complete cessations in growth (Francillon-Vieillot, et al., 1990b; Reid, 1996) (Figure 2.3A).

When zonal bone is combined with a lamellar bone tissue, the tissue is called lamellar-zonal bone (Enlow, 1963; Reid, 1984b; Francillon-Vieillot et al., 1990b; Ricqlès et al., 1991; Chinsamy and Dodson, 1995). Most extant "reptile" bone consists of lamellar-zonal bone tissue. Studies on extant crocodilians using a tetracycline antibiotic, to stain the skeletal elements of known-age Nile crocodiles (*Crocodylus niloticus*) have revealed that one zone and one annulus are deposited in one year (Hutton, 1986). Tetracyclines are used as vital markers of growing parts of bones and teeth. Once administered (usually by injection), the antibiotic becomes localised in particular regions of bones and teeth

where it appears in thin sections and fluoresces under ultra-violet light (Klevezal, 1996). Hutton (1986) found that a broad zone was deposited during the warm rapid growing season and a narrow annulus was deposited during the cool non-growing season. Although there is no proof that the growth rings in fossil animals are annual (Peabody, 1961), no other type of cycle is known to produce such stratification (Reid, 1990).

**(b) Azonal Bone**

When bone tissue does not contain any cyclically developed growth rings (i.e. interruptions in growth) and corresponding zones, the tissue is termed azonal (Figure 2.3B).

**(c) Accretionary Bone**

Animals that exhibit a determinate growth strategy i.e. stop growing after they reach a maximum size, may still experience a minor thickening of the bones at the periosteal surfaces (Reid, 1996). Small amounts of slowly growing bone are laid down at the sub-periosteal surface, which may continue throughout the animal's life. Such accretionary bone is usually poorly vascularised and represents a slowing down in the growth rate of the animal (Cormack, 1987). If rest lines are present within this slowly forming tissue, they are called peripheral rest lines (Figure 2.3B). In contrast, some animals exhibit an indeterminate growth strategy, whereby they continue to grow throughout their lives and never reach a maximum size. Most extant crocodilians, lizards etc. experience an indeterminate growth strategy whereas most extant birds and mammals experience a determinate growth strategy and usually exhibit peripheral rest lines in their bones (Reid, 1996).

### (v) Haversian Bone

Haversian bone is compact bone constructed from secondary osteons, which replaces primary bone by a process called Haversian reconstruction (Francillon-Vieillot et al., 1990b; Reid, 1996). Secondary osteons result from the remodelling of existing primary osteons. The inner surface of a primary osteon (the primary bone around the vascular canal) is resorbed to form a large resorptive space. Layers of lamellar bone are then centripetally deposited on the surface of this enlarged canal. Secondary osteons are always designated by a cementing line, which marks the furthest extent of bone removal and appears irregular and scalloped as it represents resorbed bone surfaces. At first, the interstitial bone surrounding the secondary osteons is still primary bone, but as more secondary osteons are deposited, the primary bone becomes replaced and undergoes secondary reconstruction. Resorption spaces may begin to encroach on older secondary osteons and when successive generations of closely packed secondary osteons intersect each other, the Haversian bone becomes dense Haversian bone (see Figure 2.4) (Enlow, 1963; Francillon-Vieillot et al., 1990b; Reid, 1996).

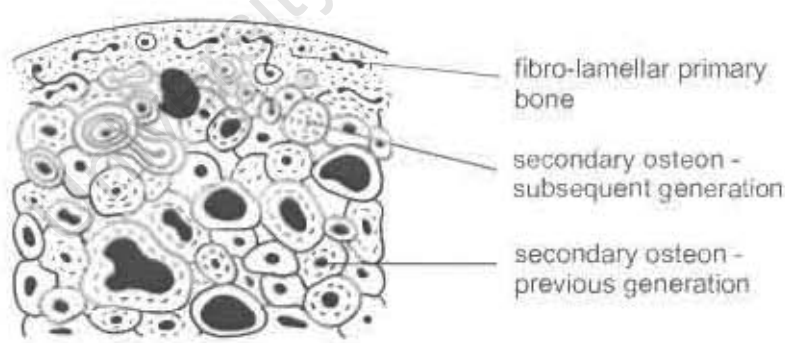


Figure 2.4. Dense Haversian bone replacing primary fibro-lamellar bone tissue. Modified from Francillon-Vieillot et al. (1990b).

Metabolic starvation resulting in damage to the vascular system (Currey, 1960), osteocyte death and biomechanical adaptation to physical strain (Currey, 1962; Enlow, 1963; Crompton, 1989) are among the suggestions for secondary osteon formation, but Amprino's 1967 suggestion that phosphocalcic metabolism is the cause, has received the most support.

**(vi) Bone Remodelling**

During growth, bone continually changes size and shape through the process of bone remodelling. This process occurs both inside (internal remodelling) and at the periphery of the bone. It is usually related to the early development of an animal, but can also be associated with mechanical constraints and physiological demands later in life (Amprino, 1967; Ricqlès et al., 1991). Hence, bone remodelling can affect both primary and secondary bone (Francillon-Vieillot, et al., 1990b). As a bone grows, it increases in both length and diameter. As it lengthens, the diameter of the metaphysis is reduced because the bone tissue in this area must be converted into the lengthening diaphysis, which is of smaller diameter (Figure 2.5). The localised process of reshaping is known as metaphyseal remodelling and takes place by periosteal resorption and consequent endosteal deposition. Bone remodelling is associated with (a) secondary cancellous bone, (b) compacted coarse cancellous bone, (c) compacted fine-cancellous endochondral bone and (d) inner circumferential lamellae.

As the size of the metaphyseal diameter decreases, the cross-sectional shape of each successive level also changes. The cortex shifts, relative to the long axis of the bone in order to align it with the curvature of the shaft during growth. The spatial transfer (usually lateral) and repositioning of bone or parts of bone during growth is known as bone drift. The process is so termed as the cortex appears to 'drift' in one or more directions by the removal of bone from certain areas and the addition of bone on corresponding surfaces. The protuberances in various areas of the bone also undergo bone drift and become relocated along the shaft (Enlow, 1963; Francillon-Vieillot, et al., 1990b).

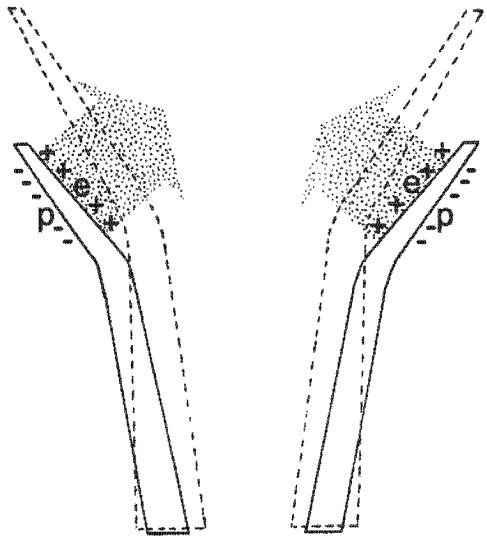


Figure 2.5. Metaphyseal relocation and reduction. Bone is removed from the periosteal surface (p) and deposited on the endosteal surface (e), thereby decreasing the metaphyseal diameter. Modified from Enlow (1963).



**(a) Secondary Cancellous Bone**

Secondary deposits of lamellar bone may replace bone removed during internal remodelling. The bone that is replaced may be endochondral bone, periosteal, Haversian compact bone or older endosteal cancellous bone. Medullary cancellous bone can be recognised as secondary either by the encroachment on the surrounding compact bone or if it spreads gradually outwards, into dense Haversian tissue (Reid, 1984a).

**(b) Compacted Coarse Cancellous Bone**

During inward growth of the cortex, the cancellous bone in the medullary cavity may become compacted by the deposition of bone within the cancellous spaces. It has a characteristically convoluted irregular appearance resulting from the deposition of new bone on the older, irregularly oriented surfaces of the original cancellous trabeculae (Enlow, 1969). Compacted coarse cancellous bone is more developed where bones undergo external resorption during metaphyseal remodelling or lateral drifting. This allows bone to maintain a compact external cortex, if the original compact bone has been completely removed (Reid, 1984a).

**(c) Compacted Fine Cancellous Endochondral Bone**

During metaphyseal reduction, fine cancellous trabeculae, produced by endochondral replacement of cartilage, may be converted into compact bone by the relocation of the cortex into the former medullary area. As the inward advancing cortex invades medullary cancellous bone, the remnants of any endochondral spicules that survived the formation and reformation of coarse cancellous trabeculae become incorporated into the new cortex resulting in cancellous compaction (Enlow, 1963).

**(d) Inner Circumferential Endosteal Lamellae**

Once the metaphysis reaches the dimensions of the diaphysis, metaphyseal reduction ceases. The diaphysis continues to increase in diameter through periosteal deposition. As endosteal growth proceeds into areas of cancellous bone, a compact cortex consisting of irregular lamellar convolutions is produced. However, if endosteal growth proceeds into areas of the metaphysis or diaphysis that have few or no cancellous trabeculae, the new layer of bone consists of even, regularly arranged sheets of endosteal lamellae (Enlow, 1963; Cormack, 1987).



### 2.3.2 Implications of Bone Tissue Patterns

Bone tissue patterns are used to interpret aspects of the biology of extinct animals. The following sections (i), (ii) and (iii) briefly describe the factors affecting bone tissue organisation and section (iv) provides the views on deducing palaeophysiology from bone histology.

**(i) Histological Variation between Skeletal Elements**

Bone is a highly dynamic, complex structure that undergoes continuous renewal or regeneration throughout an individual's life. Histological patterns are a result of biomechanical and physiological requirements, which differ between skeletal elements depending on the individual adaptations of the particular element. Histological variation is therefore expected between the elements of an individual skeleton and has been documented in a number of studies (e.g.

Enlow and Brown, 1957; Amprino, 1967; Ricqlès, 1976; Reid, 1984a; Horner et al., 1999; Starck and Chinsamy, in press).

Comprehensive studies such as that of Horner et al. (1999), Curry (1999) and Sander (2000) have documented the histological variation between skeletal elements that differ in structure, i.e. long bones, short bones and flat bones.

In a study involving the hadrosaurid *Hypacrosaurus stebingeri*, Horner et al. (1999) found that the largest bones, such as the femur and tibia were least affected by Haversian reconstruction compared to the short bones. Furthermore, Curry (1999) found that *Apatosaurus* radius and ulna histology differs from that of the scapulae (flat bone). She found that the radii and ulnae grew continually at sustained rates, whereas the scapulae exhibited a cyclical growth rate. The scapulae also exhibited areas of lower vascularisation, whereas the vascularisation in the radii and ulnae was uniformly distributed. Curry (1999) suggested that these patterns in the scapulae implied slower growth rates compared to the radii and ulnae. Sander (2000) also suggested, in a study on the limb bones of Tendaguru sauropods, that LAGs were scarce in these elements because they were the largest and therefore fastest growing bones. LAGs are usually more prominent in smaller bones due to the low rate of bone deposition. Klevezal (1996) also found similar features in mammalian skeletons. Furthermore, Starck and Chinsamy (in press) have found that the skeletal elements of Japanese quail (*Coturnix japonica*) that underwent experimentally imposed adverse conditions responded differently from those of birds under normal conditions. The elements of the experimental birds deposited significantly less primary periosteal bone than the birds under normal conditions. Their study also showed inter-elemental histovariability, whereby the mid-diaphyseal regions of the humerus and femur increased in cross-sectional thickness faster than the radius, ulna or tarsometatarsus.

**(ii) Skeletochronology**

Researchers have used the method of skeletochronology to assess the age of an individual on the basis of LAG or annulus counts (Castanet and Cheylan, 1979; Castanet et al., 1996) and it has been used on extant crocodilians and lizards for several years (Castanet and Cheylan, 1979; Hutton, 1986; Castanet et al., 1988; Caetano, 1990; Francillon-Vieillot et al., 1990a; Chinsamy, 1993a; Chinsamy et al., 1995; Castanet, 1994; Wake and Castanet, 1995; Castanet et al., 1996; Esteban et al., 1996; Márquez et al., 1997). It has been accepted that each LAG or annulus (growth ring) corresponds to one year, which allows the age of the individual to be calculated.

As earlier growth rings near the medullary cavity may be removed by endosteal resorption in older individuals, back calculations (LeClair, 1990) are used to obtain the total count. It involves using the width of the initial zones of the smallest and presumably youngest individual to obtain an estimation of the number of resorbed growth rings, which is then added to the total count (Smirina, 1974; Chinsamy, 1993a).

As histovariability between different skeletal elements causes growth ring counts to differ within an individual, skeletochronology is usually best conducted on the limb bones of an animal (Castanet and Smirina, 1990). The midshaft regions of limb bones experience the least amount of reconstruction compared to other element types and so exhibit the most accurate number of growth rings (Chinsamy, 1990, 1991; Francillon-Vieillot, et al., 1990b; Horner et al., 1999).

**(iii) Sexual Maturity**

In many extant species, a decrease in the width between successive growth rings may occur when sexual maturity is reached (Castanet and Smirina, 1990; Castanet and Baez, 1991). Such a feature can aid in identifying the onset of sexual maturity in fossil animals. In bone where growth rings are absent, an abrupt transition in tissue pattern may occur. For example, a tissue pattern that is rapidly formed may change to one that is more slowly formed. However, this

change in pattern reflects a decrease in the diametric growth rate, but may not necessarily indicate attainment of maximum size (especially if large amounts of bone are deposited after the transition). It may instead indicate that sexual maturity has been reached (Castanet and Smirina, 1990; Sander, 2000).

**(iv) Deductions Relating to Palaeophysiology from Bone Histology**

Earlier studies such as that of Ricqlès (1974, 1976, 1980) and Bakker (1972b, 1980, 1986) suggested that the thermal physiology of an extinct animal could be deduced from its bone histology. They used the presence of fibro-lamellar bone, which is a rapidly forming tissue, and dense Haversian bone (more usually found in mammals) as evidence of endothermy in non-avian dinosaurs and non-mammalian therapsids. However, authors such as Bouvier (1977), Reid (1984a, 1984b, 1987), Spotila et al. (1991) and Chinsamy and Rubidge (1993) have since contested this argument. Although the presence of fibro-lamellar bone tissue does indicate rapid osteogenesis, it is not in itself proof of endothermy. Enlow (1963) found that the bones of young crocodiles contained uninterrupted fibro-lamellar bone and growth rings only appeared in older individuals. Furthermore, Reid (1984b) found fibro-lamellar bone tissue in adult *Crocodylus porosus* and in wild *Alligator mississipiensis* from North Carolina (1997). In contrast, growth rings have been found in endothermic polar bears (Chinsamy et al., 1998) and hibernating mammals (Klevezal, 1996).

The histological differences observed in extant ecto- and endotherms are not always clearly defined. For example, small birds, bats, shrews and rodents, which have some of the highest metabolic rates, exhibit simple avascular lamellated bone, which resembles the tissue found in lizards and amphibians (Reid, 1984b). Dense Haversian bone is also absent from these animals and can therefore have no direct causal connection with high metabolic rates. Furthermore, as a secondary tissue replacing primary bone, dense Haversian tissue is influenced by various non-thermal factors (e.g. muscular attachments, Reid, 1984a). Dense Haversian bone is also not restricted to endotherms

(Bouvier, 1977) and has been found in turtles, crocodilians and tortoises (Reid, 1997).

Therefore, although lamellar-zonal bone is mainly found in extant "reptiles" and fibro-lamellar bone in mammals and birds, there are exceptions. It is now widely agreed that many non-avian dinosaurs possibly possessed a growth strategy intermediate between that of endotherms and ectotherms (Ricqlès, 1983; Reid, 1984a; Chinsamy, 1990, 1993a). However a number of researchers (e.g. Reid, 1984b, Chinsamy and Rubidge, 1993) caution that deductions regarding palaeophysiology are speculative. In fact there is no direct relationship between bone histology and thermoregulation (Chinsamy, et al., 1994).

Studies have also assessed the growth rates of different types of fibro-lamellar tissue, claiming that different fibro-lamellar organisations (e.g. laminar, plexiform, reticular, radial etc.) correspond to different growth rates (Castanet et al., 2000; Horner et al., 2000). However Starck and Chinsamy (in press) recently found that similar bone tissue types do not necessarily suggest similar bone depositional rates. In a study on the bone deposition rates of Japanese quail (*Coturnix japonica*), they found that the rate of bone formation was significantly influenced by environmental/experimental conditions, skeletal element and age. They also observed that one type of fibro-lamellar tissue covered the full range of bone deposition rates previously associated with different types of bone tissue (Castanet et al., 1996, 2000). Thus caution is advised when attributing specific bone deposition rates to similar tissues in extinct animals.

Although the thermal physiology of an extinct animal cannot be directly determined using the analysis of bone histology, the method can be used to directly assess the growth of the animal, which provides information relating to its biology.

# CHAPTER THREE
# METHODS
## PALAEOBIOLOGICAL TECHNIQUES

### 3.1 Macro-measurements

Where available, the total lengths, midshaft diameter, proximal and distal widths of all study specimens were measured. Measurements of the complete specimens were used to estimate the total lengths of the incomplete elements using allometry.

All specimens and associated skulls were photographed using either a Nikon Coolpix 995 digital camera or a Pentax SP500 camera (using black and white, 100 ASA film). When the Pentax SP500 camera was used, Ilford Ilfotec HC film developer and Ilford Hypam rapid fixer were used to develop the film. Ilford Multigrade paper developer and Ilford photographic paper were used to print photographs.



### 3.2 Cross-Sectional Geometry

#### 3.2.1 Relative Bone Wall Thickness

The relative bone wall thickness of each bone was measured in microns (µm) using an eyepiece micrometer in a Nikon Alphaphot-2 YS2 polarising petrographic microscope (at 20X magnification). Four measurements of the bone wall were taken and the mean calculated as shown in Figure 3.1. This bone wall mean was divided by the mean bone diameter and the final value is expressed as percentage relative bone wall thickness (RBT). Measurements were taken from the midshaft region of the bone, using the mean of two values per element. As the transition between the cortex and medullary cavity is not always sharp due to the presence of bony trabeculae in the medullary cavity, the RBT measurement refers to the minimum thickness of the compact bone.

D = $(d_1 + d_2) / 2$
T = $(t_1 + t_2 + t_3 + t_4) / 4$

D = diameter
T = bone wall thickness

**RBT = (T/D) x100**

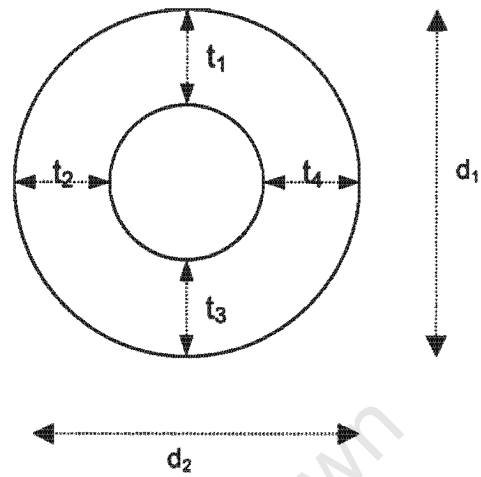


Figure 3.1. Schematic representation of the relative bone wall thickness (RBT) measurements, expressed as a percentage.

### 3.2.2 K-values

K-values were calculated by dividing the medullary cavity value by the diameter value as shown in Figure 3.2. Two values were taken from each section to obtain a mean.

$k_1 = mc_1 / d_1$
$k_2 = mc_2 / d_2$

k = k-value
d = diameter
mc = medullary cavity

**$k = (k_1 + k_2) / 2$**

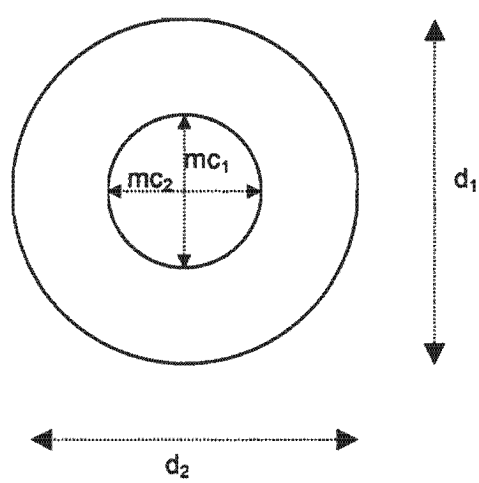


Figure 3.2. Schematic representation of the K-value measurements.

## 3.3 Preparation of Fossil Bone for Histological Examination

The method for the preparation of fossil bone follows that of Chinsamy and Raath (1992) with a few modifications. Elements were serially sectioned where possible in order to view the histological variation along an element.

### 3.3.1 Embedding Specimens for Sectioning

As fossil bones tend to be brittle, they must be embedded in a suitable mounting medium to prevent them from shattering or disintegrating during sectioning and grinding processes. The specimens were embedded in plastic containers using Araldite (AY 103) and hardener (HY 951). Araldite is a mounting resin, which does not damage or interfere with the bone structure. Prior to embedding, the inside of each container was coated with Vaseline (petroleum jelly) to prevent the resin from sticking to the sides of the container after setting. The containers and embedded specimens were then placed in a vacuum dessicator to remove bubbles and left to cure for 24 hours.

### 3.3.2 Sectioning Embedded Bone

The region where the bone was sectioned was carefully documented as bone tissue structure differs between bones and between different regions of the same bone. This documentation permits comparative analysis between different bones. Each specimen was cut into small blocks (consisting of bone embedded in Araldite) using an Imptech C 10 abrasive cutter. The blocks were labelled with a diamond-tipped pen. The bones were cut transversely in the diaphyseal region and longitudinally in the metaphyseal regions and consequently divided into proximal, shaft and distal regions (Figure 3.3).

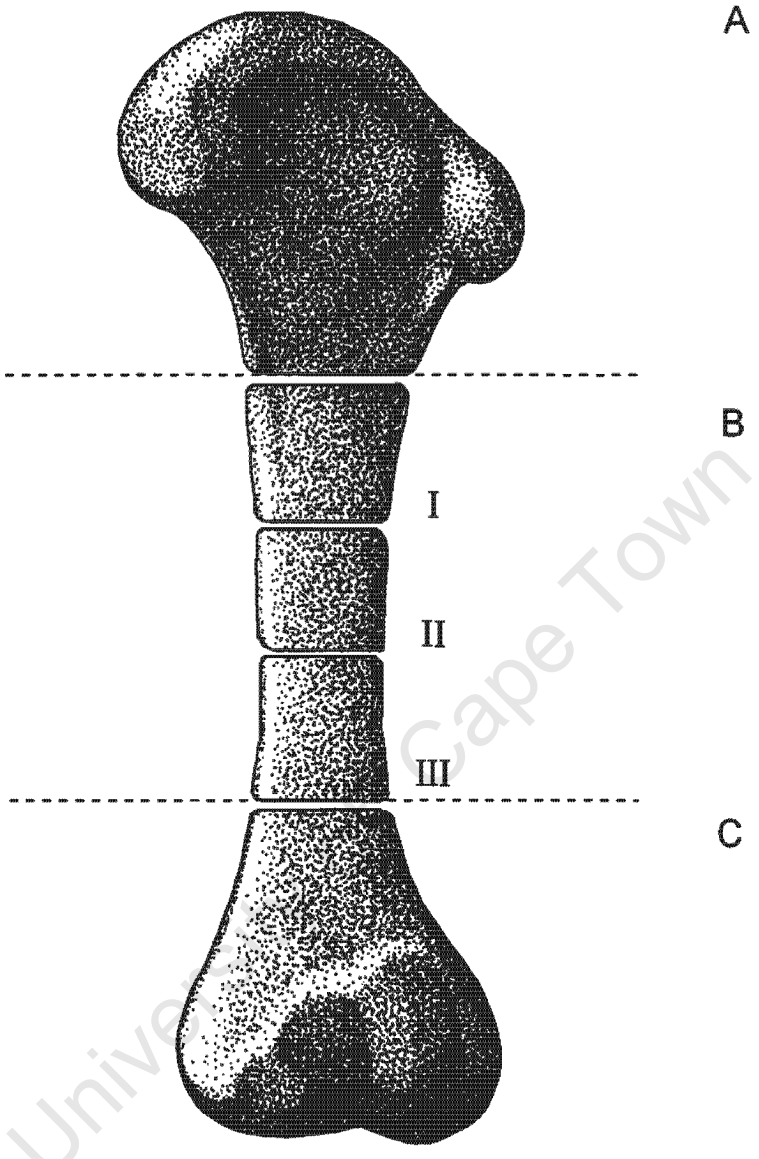




Figure 3.3. Representation of bone divisions. Each bone was divided into a proximal (A), shaft (B) and distal (C) region. The shaft region was further divided into smaller sections (I, II, III) for convenient handling.

### 3.3.3 Grinding One Surface for Affixing to Slide

The cut surface of each block was ground down mechanically on successively finer abrasive grinding discs (320, 600 and 1200 grit), using an Imptech 30 DVT Grinder Polisher, until the surface was completely flat and smooth. The Grinder Polisher consists of two rotating lap-wheels. Waterproof abrasive grinding discs are fixed to one lap-wheel and the other lap-wheel contains a fixed smooth, felt, polishing disc. The discs were used in decreasing grit size (320, 600 and 1200 grit) to remove marks on the cut surface left by the abrasive cutter and the polishing disc was used to give the surface a final polish using Struers OP-U suspension fluid.

### 3.3.4 Mounting and Labelling the Resin Block

The polished surface of each resin block was then mounted onto a petrographic frosted glass slide using the resin adhesive, Epotek. Frosting enhances the resolution and provides better adhesion for the mounting medium. The slide itself was also labelled using a diamond tipped stylus. A Buehler section-cutting Isomet 11-1180 Low Speed Saw was then used to feed the slide with attached block onto a water-cooled, rotating, diamond-encrusted blade, which cut a 200µm thick section from the main block.

### 3.3.5 Finishing/Polishing

The resulting thin sections were ground down and polished using the abrasive and polishing discs and suspension fluid (as described above). The slides were examined under a microscope at intervals to check the thickness and amount of visibility of bone microstructure.

The resulting slides were viewed using a Nikon Alphaphot-2 YS2 polarising petrographic microscope (at 20 to 200X magnification), which allows viewing under polarised light. Photographs were taken using a Nikon FDX-35 camera that was fitted to the microscope.

### 3.4 Quantification of Channel Area

Quantification of the area occupied by channels in the bone of a given section of fossil bone gives an approximate indication of how vascularised that area was when the animal was alive. This quantification does not give the absolute channel area, but instead the maximum possible area occupied by the channels (refer to Starck and Chinsamy's research in section (ii) of 2.3.1). The channel area in each bone was calculated to determine the presence or absence of a trend in the amount of vascularisation between different genera as well as during ontogeny.

Measurements were standardised using transverse thin sections of the mid-diaphysis in the mid-cortical region of each bone. An image capturing computer program, Asymetrix Digital Video Producer 3.0 (1994) was used to capture images at 10X magnification from a Nikon Alphaphot-2 YS2 petrographic microscope.

An Image Analysis computer program, Jandel Scientific Sigma Scan/Image Analysis (Pro 4, 1993) was then used to analyse the images. After randomly selecting a field of view in the mid-cortex, every third field of view from that point was examined. The surface area of each channel in the field of view was calculated by tracing the perimeter of the channel and flooding the encircled area. The sum of the surface area of all channels in that field of view was then calculated (in microns). Two thin sections in the mid-diaphyseal region of each bone were analysed and the mean of the two taken. This measurement was converted into a percentage. As these channels would have included lymph and nerves as well as vascular canals when the individual was alive, it is recognised that the vascular canals may not have occupied the entire channel area. Each vascular percentage obtained is therefore a representative of the maximum amount of vascularisation in the midshaft of each bone.

### 3.5 Statistical Analyses

As bone histology is a destructive process, few specimens were available for this examination. The sample sizes in this study are generally too low to perform detailed statistical analyses. Therefore, most of the quantifications (relative bone wall thickness or channel area) have been presented graphically as box and whisker plots to two standard errors. This type of presentation clearly indicates how similar or different the data points are to each other, when statistical tests cannot be performed. However, when statistical analyses could be conducted, independent 1-tailed t-tests and one-way ANOVA's (Statistica 5.5, 1984) were used to establish significant differences.

# CHAPTER FOUR
# *PROCYNOSUCHUS* BIOLOGY

*Summary*

*This chapter includes the use of cross-sectional geometry and bone histology to examine the biology of the Late Permian, semi-aquatic, non-mammalian cynodont Procynosuchus. A brief account of its morphological characteristics based on earlier studies is given and is followed by a section on the material used in this study. The results obtained from the cross-sectional geometry study indicate a relatively thick bone wall (30.4%) with a low K-value of 0.33. These values support Wall's 1983 proposal of increased limb bone densities in aquatic or semi-aquatic animals in order to counteract buoyancy while in the water. The results obtained from the histological examination suggest that Procynosuchus had a cyclical growth strategy that was possibly seasonally influenced. Histological patterns suggest the possible onset of sexual maturity in some elements. The presence of poorly, vascularised lamellar-zonal bone tissue indicates that the overall growth of Procynosuchus was slow.*



## 4.1 Functional Morphology

*Procynosuchus,* reaching a length of approximately 60cm, was an early non-mammalian cynodont that lived during the Late Permian. This animal had the most "reptilian" jaw musculature of all the non-mammalian cynodonts, as the teeth did not occlude and they were continually replaced. The upper and lower teeth continually moved past each other, causing food to be torn between them. This modification would have been useful for crushing tough insect cuticles and it has been proposed that *Procynosuchus* was probably an insectivore (Kemp, 1979, 1982). However, a few more derived mammal-like features are also present. These features include an incomplete secondary palate and a reduction in the lumbar ribs, thereby separating the vertebral column into thoracic and lumbar regions (Kemp, 1979, 1980, 1982).

The zygopophyses of the lumbar vertebrae are horizontally oriented, which allowed the posterior part of the body and tail to undulate. This specialised modification suggests that *Procynosuchus* was semi-aquatic (Kemp, 1980). The limb bones and feet are also extremely flat, implying that the limbs were

used as paddles. Furthermore, the haemal arches between the tail vertebrae are elongated, possibly increasing the surface area of the tail as a swimming organ (Kemp, 1980, 1982).

## 4.2 Materials and Localities

Three *Procynosuchus* elements, namely radius, clavicle and rib fragments (each from separate individuals) were examined in this study (Table 4.1).

Table 4.1. The *Procynosuchus* specimens used in this study and the localities from where the specimens were recovered. The clavicle and radius were excavated from localities in the *Cistecephalus* Assemblage Zone, Teekloof Formation, Beaufort Group, South Africa (Figure 4.1). The rib was excavated from the Luangwa Valley, Zambia (Figure 4.2). Several sections were taken from each element in order to facilitate a detailed histological analysis. See Appendix 1 for institutional abbreviations.

| District | Specimen number | Skeletal element | Number of sections | Region sectioned |
|---|---|---|---|---|
| Fraserburg | SAM-PK-K8511 | clavicle | 8 | midshaft |
| Nieu-Bethesda | B/P/I/3747 | radius | 7 | proximal/midshaft |
| Luangwa Valley | TSK34 | rib | 4 | midshaft |

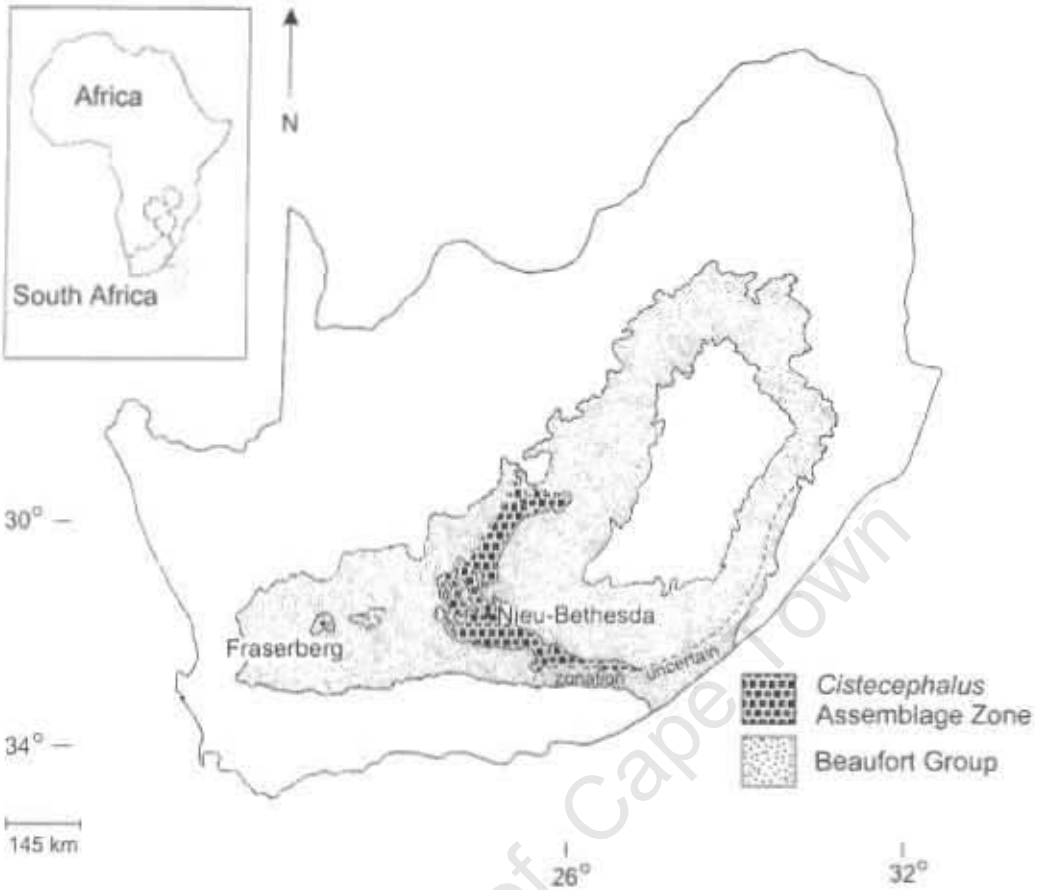


Figure 4.1. *Cistecephalus* Assemblage Zone, Teekloof Formation, Beaufort Group, South Africa. The radius (B/P/I/3747) and clavicle (SAM-PK-K8511) were recovered from localities near the towns Nieu-Bethesda and Fraserburg respectively. Map compiled from the Reader's Digest Illustrated Atlas of Southern Africa (1994) and Smith and Keyser (1995).



The *Cistecephalus* Assemblage Zone (Late Permian, Tatarian Stage; Harland et.al., 1990) is characterised by the presence of the dicynodonts *Diictodon*, *Pristerodon*, *Emydops*, *Cistecephalus*, *Aulacephalodon* and *Oudenodon* and includes the non-mammalian cynodont *Procynosuchus*. Fossils are mostly preserved in interchannel mudrocks and are usually isolated and dispersed (Smith and Keyser, 1995). The presence of highly sinuous channel patterns, ephemeral stream sedimentation and playa-type gypsum precipitation suggests that the climate was semi-arid with seasonal rainfall (Smith et al., 1993).

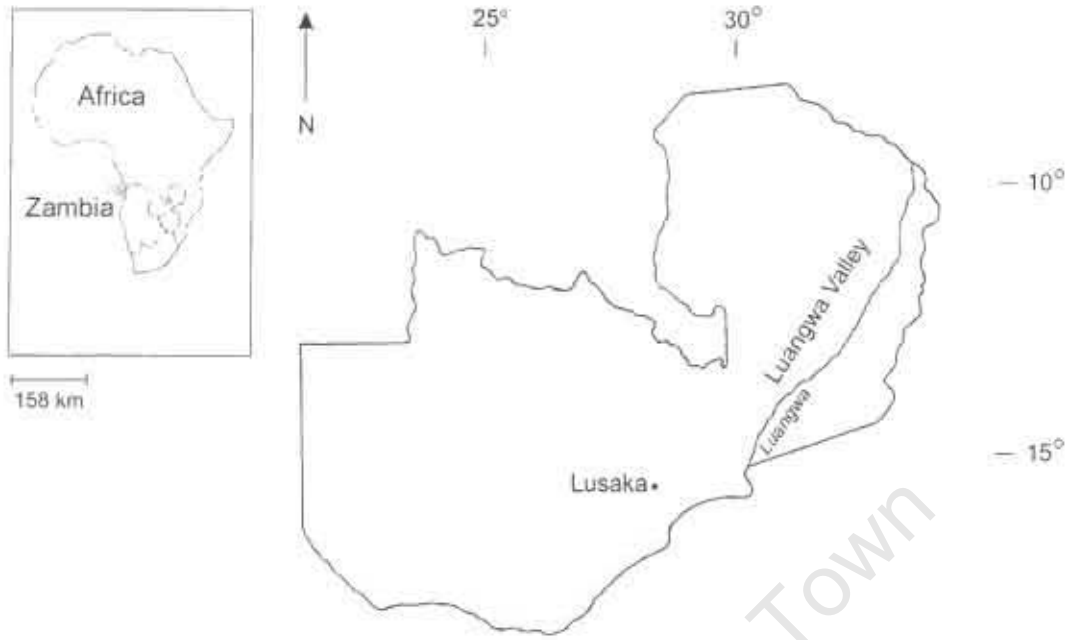


Figure 4.2. Luangwa Valley, Zambia. The *Procynosuchus* rib fragment TSK34 was recovered from the Luangwa Valley (approximately 12° 20'S 32° 00'E). Map modified from the Reader's Digest Illustrated Atlas of Southern Africa (1994).

## 4.3 Results

### 4.3.1 Macro-analysis

Measurements were taken from each specimen, the purpose of which was to calculate the maximum length of each element and hence determine the percentage adult size (% adult in Table 4.2) for each element. Due to the fragmentary nature of the material however, the skeletal proportions and percentage adult size could not be calculated.

Table 4.2. Gross measurements of *Procynosuchus* skeletal elements.

| Specimen number | Skeletal element | Diameter (mm) | Proximal width (mm) | Length (mm) | % Adult |
|---|---|---|---|---|---|
| B/P/I/3747 | radius | 8.24 | 14.27 | - | - |
| SAM-PK-K8511 | clavicle | 3.29 | - | - | - |
| TSK34 | rib | 3.02 | - | - | - |

Relative bone wall thickness (RBT) and K-values were calculated for the radius. In order to standardise comparisons between genera and with material examined in earlier studies, only limb bone RBT and K-values were calculated in this study. As such, clavicle and rib values have not been included. The RBT value of the radius was calculated as 30.4% and the K-value as 0.33 (see Appendix 2 for detailed results).

### 4.3.2 Micro-analysis

A detailed histological analysis was conducted on the clavicle, radius and rib. The overall bone tissue is zonal, consisting of fibro-lamellar or lamellar tissue, interrupted by annuli of lamellar-zonal tissue or LAGs.

In cross-sectional view, 79% of the cortex (medullary cavity to mid-cortex) of the radius (B/P/I/3747) contains fibro-lamellar bone alternating with narrow annuli consisting of lamellar tissue. The tissue in the outer 21% of the cortex then becomes poorly vascularised lamellar-zonal bone (Figure 4.3). The vascular canals in the fibro-lamellar region are mostly longitudinally oriented primary osteons, whereas the lamellar-zonal region contains simple longitudinal and radial vascular canals. Secondary osteons are observed in the peri-medullary region. The osteocyte lacunae are globular in both the fibro-lamellar and lamellar-zonal regions. The canaliculi radiate from the osteoycte lacunae when preserved. Large cancellous spaces and an extensive network of bony trabeculae reveals extensive secondary remodelling in the medullary cavity, which becomes more extensive towards the metaphysis of the bone. Longitudinal sections show a dense network of bony trabeculae with few cancellous spaces in the proximal metaphysis. Sharpey's fibres are observed on the anterior and posteromedial surface of the bone in the proximal metaphyseal region.

The cortex of the clavicle (SAM-PK-K8511) consists entirely of lamellar-zonal bone tissue and the vascular canals are mostly simple longitudinal and radial canals (Figure 4.4). The globular osteocyte lacunae radiate branched

canaliculi, but the canaliculi are rarely preserved. LAGs become more closely spaced towards the sub-periosteal surface compared to the rest of the cortex and often become multiple (many occurring close together). Secondary osteons are observed in the peri-medullary region and large cancellous spaces are more extensive towards the ventral side of the bone, eventually reaching the surface towards the medial end. Sharpey's fibres are observed on the dorsal and anterior surfaces of the bone.

The rib fragment (TSK34) shows lamellar-zonal bone tissue with extensive secondary remodelling around the medullary cavity. The peri-medullary region contains abundant primary and secondary osteons, whereas the outer cortex, near the periphery of the bone, exhibits a marked decrease in vascularisation with few primary osteons and some simple longitudinal vascular canals (Figure 4.5). The osteocyte lacunae and canaliculi are similar to the radius and clavicle.

The percentage channel area was quantified for the radius (B/P/I/3747) and clavicle (SAM-PK-K8511) and the results are shown in Figure 4.6.

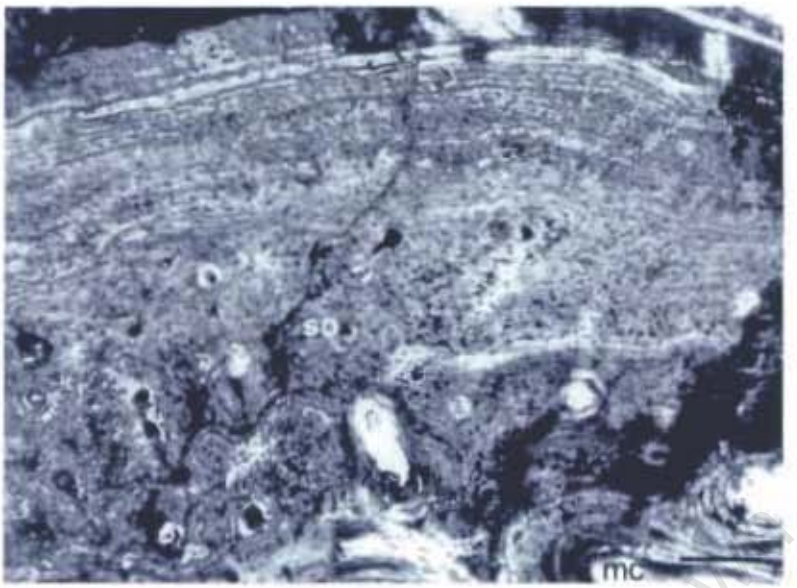


Figure 4.5. Transverse section of the *Procynosuchus* rib TSK34. The tissue is lamellar-zonal. Vascularisation is low, decreasing further towards the sub-periosteal surface. Secondary osteons are observed in the mid-cortex.

Scale bar =125µm

so, secondary osteon; mc, medullary cavity

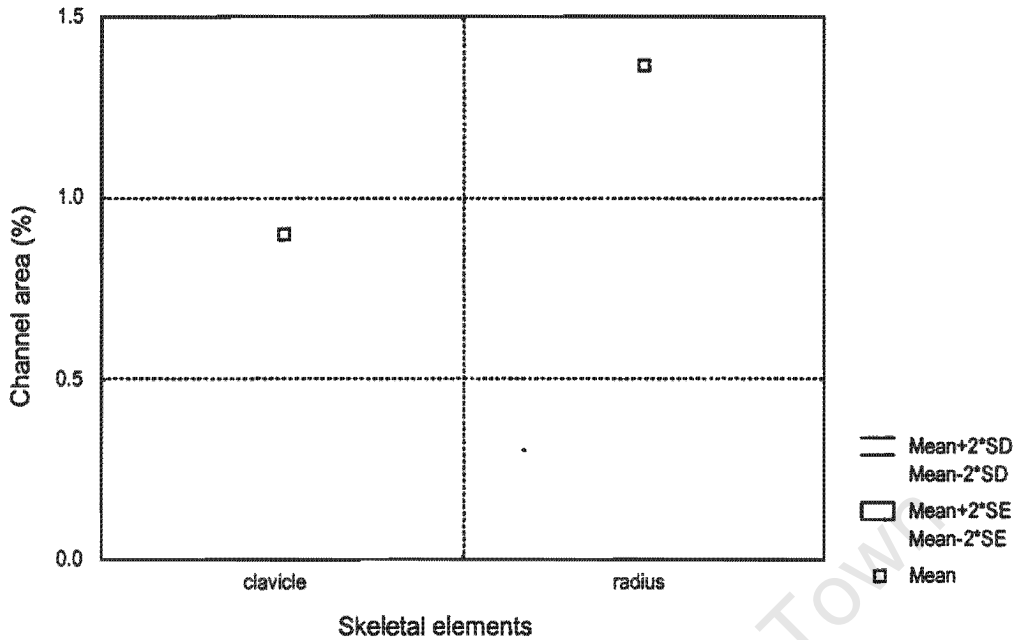


Figure 4.6. Midshaft percentage channel area of the *Procynosuchus* clavicle (SAM-PK-K8511) and radius (B/P/I/3747).

Although the values cannot be tested statistically due to the small sample size, Figure 4.6 clearly shows that the radial midshaft percentage channel area (1.37%) is higher than that of the clavicle (0.9%).

### 4.4 Interpretations

A high limb bone density in aquatic mammals has been cited as a means of controlling their buoyancy while in the water (e.g. Wall, 1983; Stein, 1989; Fish and Stein, 1991). It has been previously suggested, from morphological characteristics (Kemp, 1980, 1982), that *Procynosuchus* was semi-aquatic. The radial RBT value (30.4%), coupled with Wall's suggestion that the bone wall thickness of aquatic or at least semi-aquatic animals should exceed 30%, supports Kemp's suggestion that *Procynosuchus* may have been semi-aquatic. To be absolutely thorough, a number of various limb bones would need to be evaluated to determine if this RBT value was maintained throughout all the limb bones of *Procynosuchus*. Although a lack of available material precludes such an assessment, the radial value in this study supports similar findings of increased limb bone density, not only in semi-aquatic mammals (Wall, 1983;

Fish and Stein, 1991), but in semi-aquatic crocodilians as well (*Crocodylus niloticus,* Chinsamy 1991; *Alligator,* Magwene, 1993; Appendix 3). Furthermore, Stein (1989) found significant differences in limb bone density between two groups of semi-aquatic and terrestrial mammals, but the differences were less distinct when the two groups were compared with a group of fully aquatic mammals. The radius was the only element where the differences remained distinct, which suggests that although the sample size for examining *Procynosuchus* bone cross-sectional geometry is small, the radius is perhaps a good representative of the skeleton, when assessing relative bone wall thickness.

As a semi-aquatic animal, *Procynosuchus* would have needed to function efficiently on land as well as in the water. The radial K-value of 0.33 suggests that the radius is selected for impact loading and ultimate strength. This implies that the radius is strong enough not to break under impact loading (during walking or running), or fracture under the greatest bending moments (e.g. the strain of muscle action on the bone during sitting or standing) expected to act on it (Chinsamy, 1991). Currey and Alexander (1985) also found the femoral K-value of the semi-aquatic *Alligator* to be low (0.22) and the humeral value of the aquatic manatee (*Trichechus manatus*) to be zero, having no medullary cavity at all. The low radial K-value of *Procynosuchus* supports the proposal that aquatic or semi-aquatic animals have relatively thick bone walls, possibly to counteract buoyancy while in the water.

With regard to the bone histology of this animal, only three skeletal elements were available for study. Rates of bone growth are known to vary between skeletal elements. Hence, the small sample size in this study poses difficulty in assessing interelemental histovariability. However, the radius is a good representation of overall bone tissue organisation as limb bones undergo less secondary reconstruction compared to other types of elements. Secondly, the appearance of slowly forming lamellar-zonal bone towards the outer margin of the radius, the general decrease in vascularisation and more closely spaced

growth rings towards the periphery, in both the radius and clavicle, suggests that these elements belong to mature individuals.

The intermittent interruptions in growth indicate that *Procynosuchus* had a cyclical growth strategy, which may have been influenced by the semi-arid climate and seasonal rainfall prevalent at the time. *Procynosuchus* may have grown rapidly during the warm favourable season and more slowly or sometimes not at all (indicated by the presence of LAGs) during the colder wet winter. Alternatively, as *Procynosuchus* was probably a semi-aquatic insectivore (Kemp, 1979, 1980, 1982), its favourable growing season may have been when insects were more abundant.

The shift to an overall slowly forming lamellar-zonal tissue organisation and decrease in the distance between successive LAGs in the radius suggests an overall slowing down in growth and probably indicates the attainment of adulthood. Maximum size had probably not been reached as the large amount of lamellar-zonal tissue suggests that growth continued, but at a slower rate. The transition may instead indicate the onset of sexual maturity (Castanet and Baez, 1991; Reid, 1996; Sander, 2000). *Procynosuchus* probably grew rapidly during the favourable season until it reached sexual maturity and then more slowly as an adult, even during the active growing season. In addition, the shift from annuli to LAGs, shown in the radius, indicates that growth did not just slow down during the unfavourable season, but ceased completely, implying a substantial decrease in growth rate.

The radial percentage channel area (1.37%) is higher than that of the clavicle (0.9%), which is to be expected as the moderately vascularised fibro-lamellar tissue in the radius would have increased the overall percentage channel area. The lower percentage channel area and slowly forming lamellar-zonal cortex of the clavicle suggests that it grew more slowly than the radius. Rapidly forming bone tissue would be expected to contain abundant vascular canals (Reid, 1996) for the efficient transport of oxygen, nutrients and waste products, which

would facilitate rapid bone growth. The low percentage channel area in these elements further suggests that *Procynosuchus* was a relatively slow growing animal.

Secondary osteons are more abundant in the *Procynosuchus* rib compared to the other elements, indicating that the rib underwent more secondary remodelling compared to the radius and clavicle.

Sharpey's fibres were observed on the posteromedial side of the radius. Sharpey's fibres consist of bundles of coarse collagenous fibres and they are found in the outer layers of bone. They anchor the periosteum to the bone and are conspicuously abundant at points of insertion of ligaments and tendons (Leeson and Leeson, 1981). The Sharpey's fibres seen here may indicate the insertion of the biceps on the radial ridge (Jenkins, 1971). The Sharpey's fibres that were observed on the dorsal and anterior sides of the medial end of the clavicle possibly indicate the origin of the cleido-mastoid musculature (Jenkins, 1971).

Juvenile extant crocodilians are known to exhibit rapidly forming fibro-lamellar tissue, but they lose this ability as they grow older and tend to display typical, slowly forming lamellar-zonal bone (Reid, 1997). Chinsamy (1991) found the percentage vascularisation (= percentage channel area in the current study) of adult *Crocodylus niloticus* cortical femoral tissues to be 1.85%, similar to that of *Procynosuchus*. *Procynosuchus* growth probably depended on environmental temperature, similar to that of extant crocodilians and it appears to have lost the ability of forming fibro-lamellar bone when adulthood was reached.

# CHAPTER FIVE
# *THRINAXODON* BIOLOGY

*Summary*

*This chapter includes an examination of the biology of the non-mammalian cynodont Thrinaxodon, using the analysis of bone cross-sectional geometry and histology. A brief description of its morphological characteristics based on earlier studies is provided, followed by a materials section. The relative bone wall thickness values obtained from the cross-sectional geometry study (22%-27%) do not suggest that Thrinaxodon had any modifications for a lifestyle requiring a high limb bone density. The adult radii and ulnae have significantly thicker bone walls than the younger femora and humeri. The K-values (0.46-0.54) indicate that the elements are selected for impact loading and ultimate strength. The limb bones were divided into different age classes according to their percentage adult size, prior to thin sectioning. The analysis of their bone histology showed that the age classes could also be distinguished by the differences in their tissue organisation. Late juvenile elements have rapidly growing fibro-lamellar tissues in the peri-medullary region, but also contain a peripheral region that suggests a slower growth rate compared to the tissues in the inner cortex. Late sub-adults and early adults display more extensive fibro-lamellar tissue and higher overall vascularisation compared to the late juveniles, which suggests that these elements grew faster than the late juveniles. Older elements display parallel-fibred regions at the sub-periosteal surface, which becomes more extensive with age. An annulus in the mid-cortex of the sub-adult femur indicates an episodic slowing down in bone growth. No other element contained growth rings therefore this annulus may represent an individual response to a particularly stressful unfavourable season. Overall growth was rapid until the appearance of slowly forming parallel-fibred bone, which may indicate the onset of sexual maturity.*



## 5.1 Functional Morphology

*Thrinaxodon* was a small, short-limbed carnivore that grew to a body length of approximately 50 cm (Brink, 1954; Carroll, 1988). It represents a more derived stage in non-mammalian cynodont evolution after *Procynosuchus* (Kemp, 1982). *Thrinaxodon* has a larger temporal fenestra and more robust zygomatic arch compared to that of *Procynosuchus,* producing a more derived adductor jaw musculature. The enlarged dentary has expanded and the postdentary bones are correspondingly smaller. The coronoid process is also larger than

*Procynosuchus* and extends right up into the temporal fenestra (Fourie, 1974). Contrary to *Procynosuchus*, a complete bony secondary palate is present (Watson, 1920; Parrington, 1933). However, the basic alternate tooth replacement is still present in *Thrinaxodon* as in *Procynosuchus* (Estes, 1961; Crompton, 1963). *Thrinaxodon* has a double occipital condyle similar to extant mammals, instead of a single condyle as in extant crocodilians, lizards etc. (Hopson, 1963; Grine et al, 1979b; Kemp, 1982; Carroll, 1988). The most notable postcranial development in *Thrinaxodon* is an expansion of the inner part of the rib shaft to form a series of closely interlocking plates. Several functional implications of the intercostal plates in cynodonts have been proposed. These include the management of a powerful musculature (Gregory and Camp, 1918), preventing the rib cage from collapsing during the contraction of a possible diaphragm (Gregory and Camp, 1918; Brink, 1956, 1958), strengthening of the vertebral column (Jenkins, 1971) as well as maintaining the rigidity of the vertebral column by preventing lateral bending (Kemp, 1982).

*Thrinaxodon* had a more erect posture compared to *Procynosuchus*, with the hindlimbs pulled in closer to the body (Jenkins, 1971, Kemp, 1982, Carroll, 1988, Benton, 1990).

Although there have been several morphological studies conducted on *Thrinaxodon* (Jenkins, 1971; Kemp, 1982; Carroll, 1988), none of these studies have interpreted aspects of its biology using bone histology. In 1969, Ricqlès examined the bone histology of a *Thrinaxodon* femur, but the study was limited as it was not a comprehensive multi-element analysis.

### 5.2 Materials and Localities

Ten limb bones (including humeri, radii, ulnae, femora) were obtained for histological analysis (Table 5.1). In some instances several types of elements were obtained from a single individual. Multiple sections from each element were studied for a detailed analysis.

Table 5.1. The *Thrinaxodon* specimens used in this study and the localities from where the specimens were recovered. All localities are situated in the *Lystrosaurus* Assemblage Zone, Katberg Formation, Beaufort Group, South Africa (Figure 5.1). The radius B/P/I/4282a and the ulna B/P/I/4282b were taken from the same individual. The femora SAM-PK-K8004a and SAM-PK-K8004b are the right (a) and left (b) femora of one individual. Appendix 1 provides the institutional abbreviations.

| District | Specimen number | Skeletal element | Number of sections | Region sectioned |
|---|---|---|---|---|
| Bergville | B/P/I/5208 | humerus | 11 | complete |
| | B/P/I/5018 | ulna | 11 | complete |
| Bethulie | B/P/I/4282a | radius | 11 | complete |
| | B/P/I/4282b | ulna | 12 | complete |
| | SAM-PK-K8004a | femur | 6 | proximal/midshaft |
| | SAM-PK-K8004b | femur | 8 | complete |
| Bulwer | B/P/I/2820 | humerus | 13 | complete |
| Harrismith | SAM-PK-K1221 | humerus | 10 | proximal/midshaft |
| Newcastle | B/P/I/1730 | radius | 11 | complete |
| Unkown | SAM-PK-K1395 | femur | 4 | midshaft |

The *Lystrosaurus* Assemblage zone (Early Triassic, Early Scythian Stage; Harland et al., 1990) is characterised by *Lystrosaurus* and *Procolophon* and the absence of *Dicynodon lacerticeps* (Groenewald and Kitching, 1995). The environment was warm and temperate, with seasonal rainfall and floods (using sedimentary facies; Tucker and Benton, 1982).

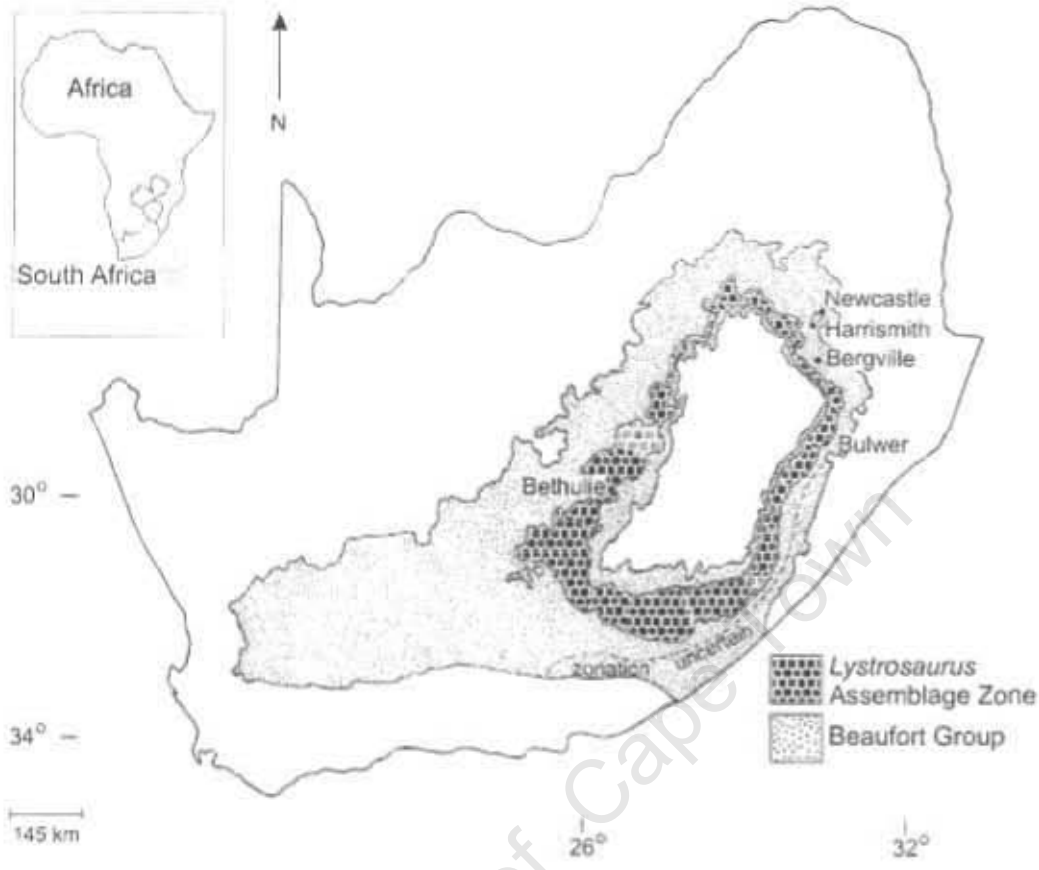


Figure 5.1. *Lystrosaurus* Assemblage Zone, Katberg Formation, Beaufort Group, South Africa. The material was recovered from localities near the towns Bergville, Bethulie, Bulwer, Harrismith and Newcastle. Map compiled from the Reader's Digest Illustrated Atlas of Southern Africa (1994) and Groenewald and Kitching (1995).



## 5.3 Results

### 5.3.1 Macro-analysis

The midshaft diameter, proximal width and lengths of each limb bone were measured. The various measurements were then used to calculate the percentage adult size of each element (Table 5.2), which gives an approximation of individual age.

Table 5.2. Gross measurements of the *Thrinaxodon* limb bones.

| Specimen number | Skeletal element | Diameter (mm) | Proximal width (mm) | Length (mm) | % Adult |
|---|---|---|---|---|---|
| B/P/I/2820 | humerus | 4.77 | 12.94 | 30.37 | 75.85 |
| SAM-PK-K1121 | humerus | - | 13 | 32.57 | 81.34 |
| B/P/I/5208 | humerus | 5.41 | 11.38 | 33.46 | 83.57 |
| B/P/I/4282a | radius | 2.98 | 6.18 | 32.23 | 96.65 |
| B/P/I/1730 | radius | 3.54 | 7.02 | 33.34 | 100 |
| B/P/I/5018 | ulna | 6.09 | 10.67 | 31.87 | 93.12 |
| B/P/I/4282b | ulna | 5.22 | 6.61 | 33.09 | 96.65 |
| SAM-PK-K8004a | femur | 1.84 | - | 18.74 | 41.98 |
| SAM-PK-K8004b | femur | - | 2.28 | 18.74 | 41.98 |
| SAM-PK-K1395 | femur | 3.83 | 11.03 | 34.53 | 77.35 |

The largest bone (radius B/P/I/1730), considered to represent an adult individual, is used as a standard to compare and assess all the other elements and is considered to be 100% of adult size. Measurements were not entered for the specimens SAM-PK-K1121, SAM-PK-K8004a and SAM-PK-K8004b due to their fragmentary nature.

The limb bones have been divided into different age classes according to their percentage adult size shown in Table 5.2. As the femora SAM-PK-K8004a and SAM-PK-K8004b are approximately 42% of the adult size, they are designated as late juveniles. The humerus B/P/I/2820 is approximately 75% of the adult size and is classed as a late sub-adult, as is the SAM-PK-K1395 femur at 77.35% of the adult size. The elements that are 80% to 84% of the adult size are designated early adults, whereas those above the 84% adult size are classed as adult.

Where possible, relative bone wall thickness (RBT) measurements (Figure 5.2) and K-values (Table 5.3) were taken from the midshaft regions of the limb bones. Using an independent t-test (1-tailed), a significant difference in RBT was found between the sub-adult elements (humeri and femora) and the adult elements (radii and ulnae) ($t_s = -2.592$; $df = 18$; $p < 0.05$). Appendix 2 provides detailed results.

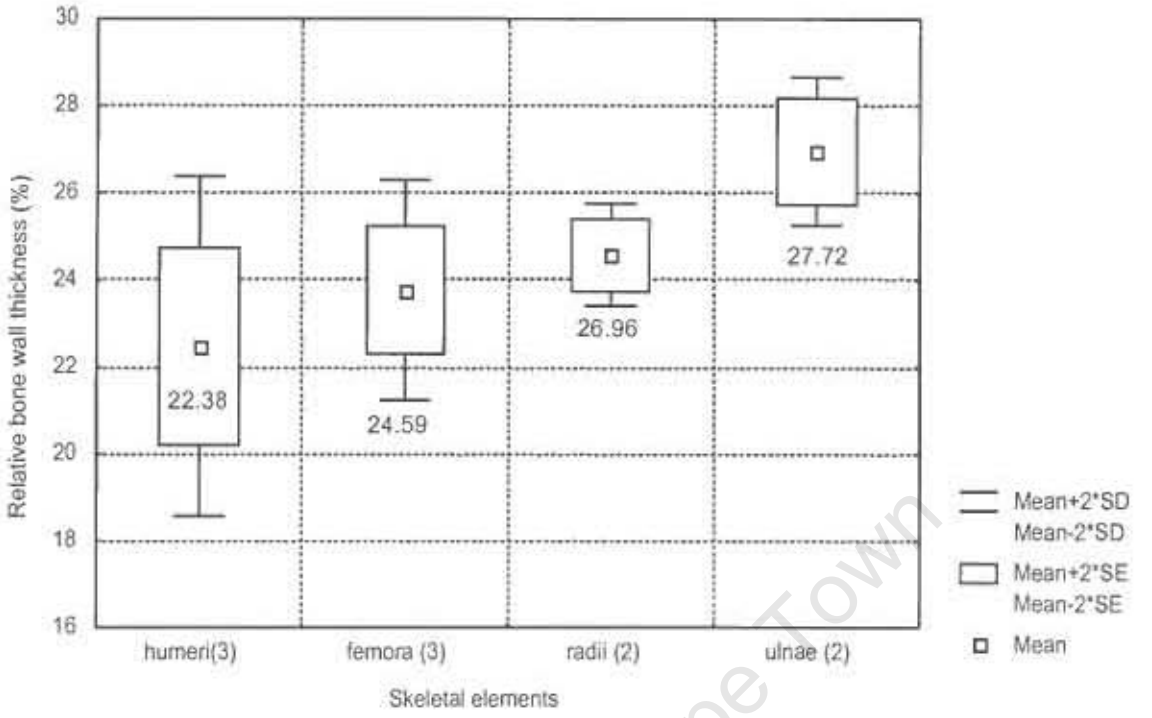


Figure 5.2. Comparison of the relative bone wall thickness values between the *Thrinaxodon* limb bones. Numerical values associated with the boxes represent the average percentage RBT of each element type. The numbers in brackets indicate the number of elements used to obtain the value for each type of element.

Table 5.3. Mean K-values of the *Thrinaxodon* limb bones. The same number of individuals was used to calculate the K-values (as indicated by n).

| Skeletal element | n | Mean K-value | Standard Deviation |
|---|---|---|---|
| humeri | 3 | 0.54 | ±0.03 |
| femora | 3 | 0.52 | ±0.032 |
| radii | 2 | 0.51 | ±0.035 |
| ulnae | 2 | 0.46 | ±0.098 |

No significant difference was found between the K-values (one-way ANOVA, $F = 1.582$; $p > 0.05$).

### 5.3.2 Micro-analysis

A comprehensive histological analysis was conducted on all elements in order to obtain an overall view of the histology of *Thrinaxodon*. The overall bone tissue generally consists of fibro-lamellar bone, which becomes parallel-fibred towards the periphery. The globular osteocyte lacunae are abundant and radiate branched canaliculi. The vascular canals in the fibro-lamellar tissue are mostly longitudinally oriented primary osteons with radial anastomoses. The parallel-fibred region contains fewer vascular canals compared to the fibro-lamellar tissue.

The late juvenile right and left femora (SAM-PK-K8004a and SAM-PK-K8004b respectively) do not contain a distinct parallel-fibred peripheral region, but the osteocyte lacunae become more organised and the tissue becomes less vascular towards the sub-periosteal surface (Figure 5.3). Secondary osteons are absent. The bony trabeculae at the ends of the bones are sparse. However, those that are present lie parallel to the long axis of the bone or form separate islets in the centre of the metaphyses.

The femur SAM-PK-K1395 is approximately 77% of the adult size and is considered a late sub-adult. An annulus of parallel-fibred bone is observed in the mid-cortex, which contains flattened osteocyte lacunae. A narrow, poorly vascularised region at the sub-periosteal surface contains osteocyte lacunae that appear more organised than the rest of the cortex. This may correspond to another annulus or the onset of slowly forming bone tissue (Figure 5.4). A few Sharpey's fibres are observed on the ventral side of the bone.

The three humeri that were examined fall between 75% and 84% of the adult *Thrinaxodon* size. A thin layer of circumferential endosteal lamellar tissue, containing a mixture of globular and flattened osteocyte lacunae, surrounds the medullary cavity in the midshaft region of the early adult humerus SAM-PK-K1121 (Figure 5.5). This layer disappears towards the metaphyses, where large cancellous spaces and bony trabeculae near the medullary cavity become

more extensive. Secondary remodelling is more extensive on the dorsal side of all three elements compared to the ventral side and resorption is generally more extensive in the early adult humerus (B/P/I/5208). The vascular canals radiate out towards the sub-periosteal surface and the resorption cavities extend almost to the surface in the delto-pectoral crest regions. Compacted coarse cancellous bone is present towards the metaphyseal regions. Secondary osteons are absent from all three elements. Thin bony trabeculae form a spacious network at the ends of the bones. A narrow region of parallel-fibred bone is seen at the outer margin of SAM-PK-K1121 (Figure 5.5) and a similar area of organised osteocyte lacunae is observed in B/P/I/5208 (Figure 5.6).

The radius B/P/I/1730 is the largest adult *Thrinaxodon* element in the sample and was used to determine the percentage adult size for all the *Thrinaxodon* elements in the study (Table 5.2). The second radius (B/P/I/4282a) examined is approximately 97% the length of the radius B/P/I/1730. The fibro-lamellar tissue is less vascular and the peripheral parallel-fibred region is thicker and more distinct compared to that of the humeri and femora (Figure 5.7). Longitudinally oriented primary osteons with occasional radial anastomoses as well as radially oriented vascular canals can be seen in the cortex. Multiple layers of very poorly vascularised endosteal lamellar tissue surround the medullary cavities (Figure 5.7), but these layers disappear towards the metaphyses where large cancellous spaces near the medullary cavity become prominent. Compacted coarse cancellous tissue becomes progressively more extensive towards the metaphyses, where the primary compact tissue becomes almost non-existent. The resorption cavities are also more extensive on the anterior side of the bone. Sharpey's fibres are observed on the posteromedial side of the bone. An intricate network of thin bony trabeculae, sometimes forming isolated islets is present towards the epiphyses of both elements.

The tissue of the ulnae B/P/I/5018 (93.12% adult length, Table 5.2) and B/P/I/4282b (96.65% adult length, Table 5.2) is similar to that of the radii (Figure 5.7). A few small secondary osteons are observed scattered throughout the cortex of B/P/I/5018. Multiple layers of endosteal lamellar tissue surround the medullary cavities in the midshaft regions (Figure 5.8). Resorption cavities are more extensive in the metaphyses, especially on the anterior side of the bone. Both elements exhibit a few Sharpey's fibres in the ulna crest regions. A loose intricate network of thin bony trabeculae is present at the ends of the bones.

A schematic diagram showing the histological variation between the different elements at various ages is provided in Figure 5.9. This figure clearly illustrates the ontogenetic variation in vascularity and tissue organisation within the *Thrinaxodon* limb bones.

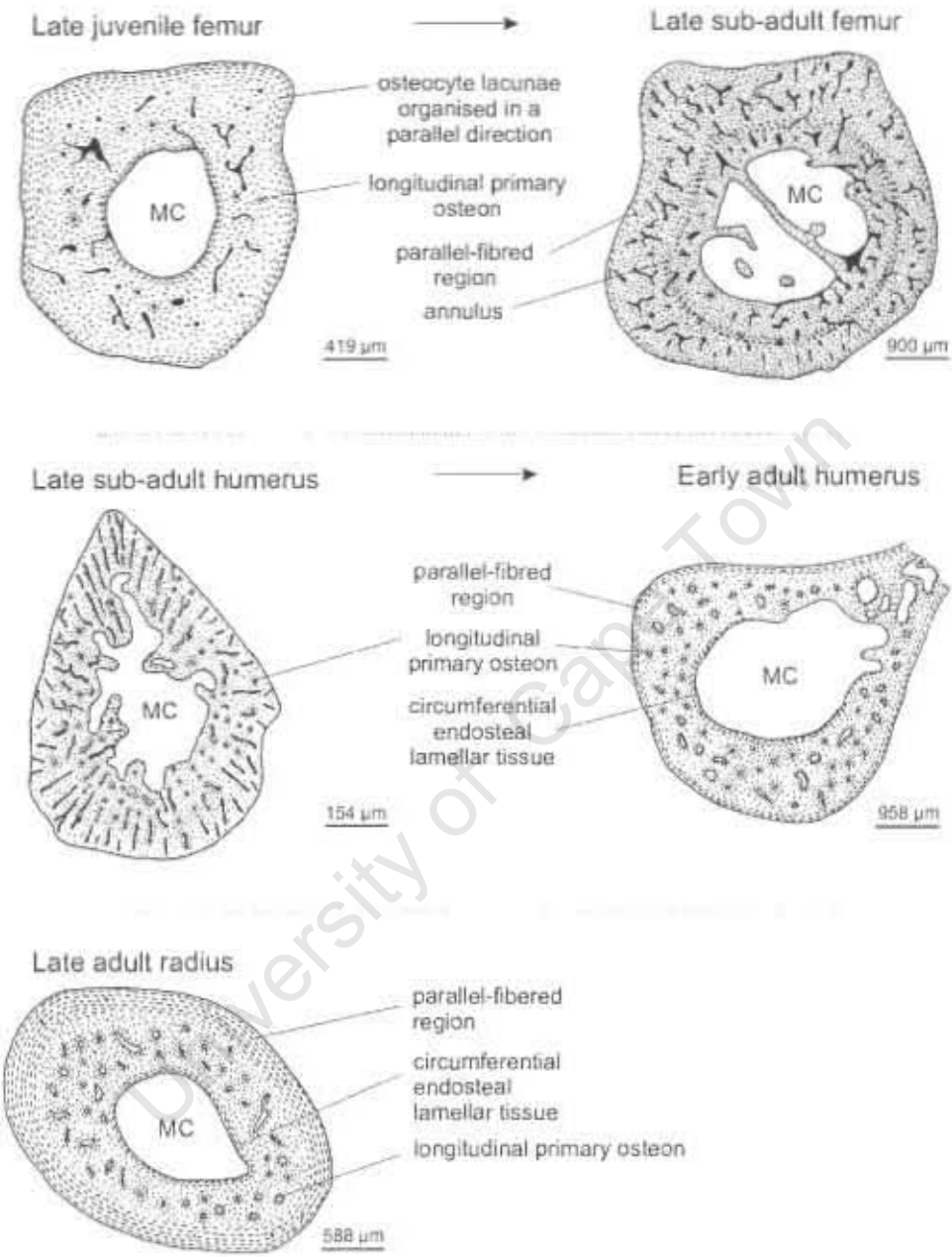


Figure 5.9. Schematic histology of the histological variation between the *Thrinaxodon* elements at various ages. MC indicates medullary cavity.

The midshaft percentage channel area was calculated in order to quantify the extent of vascularisation in the midshaft regions of each limb bone and is shown in Figure 5.10.

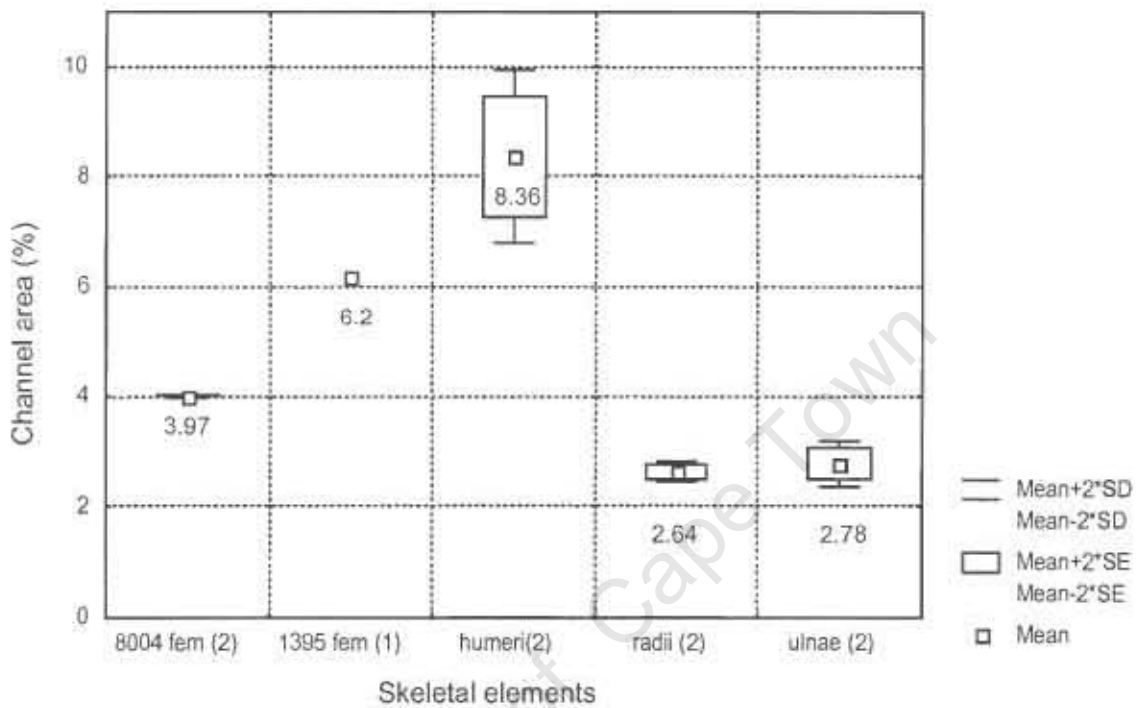


Figure 5.10. The midshaft percentage channel area of the *Thrinaxodon* skeletal elements. The values of the late juvenile femora (SAM-PK-K8004a and b) and the late sub-adult femur that is 77% of the adult size (SAM-PK-K1395) are notably different and are therefore plotted separately. The channel area of the humerus SAM-PK-K1121 was not quantified due to poor preservation. The values associated with the boxes represent the mean percentage channel area and the numbers in brackets indicate the number of elements used to obtain the percentage channel area value for each type of element .

A one-way ANOVA revealed a significant difference in midshaft percentage channel area between the different element types ($F = 22.26903$; $p < 0.05$), except between the radii and ulnae. Independent t-tests (1-tailed) showed that the differences lay between the humeri and femora ($ts = 4.243$; $df = 7$; $p < 0.05$); the humeri and radii ($ts = 5.63$; $df = 4$; $p < 0.05$); the humeri and ulnae ($ts = 7.792$; $df = 6$; $p < 0.05$) and between the femora and ulnae ($ts = 2.776$; $df = 7$; $p < 0.05$), but not between the radii and ulnae. The humeri have a

significantly higher percentage channel area compared to any of the other elements, including the late juvenile femora.

### 5.4 Interpretations

The relative bone wall thickness values range from 22% to 27% (Figure 5.2). The morphology of *Thrinaxodon* does not indicate any modifications for a lifestyle that would require an increase in limb bone density (such as aquatic, arboreal or fossorial) and the relatively low RBT values support this. The adult radii and ulnae have significantly higher RBT values than the younger femora and humeri, which support earlier findings that relative bone wall thickness increases with age (Heinrich and Biknevicus, 1998).

The K-values (0.46-0.54) suggest that these elements are selected for impact loading and ultimate strength (Currey and Alexander, 1985), similar to *Procynosuchus*. The radial (0.51) and ulna (0.46) K-values are slightly lower than the humeral (0.54) and femoral values (0.52) (Table 5.3). Currey and Alexander (1985) found that the distal limb bones in their study have lower K-values than the proximal bones possibly because the distal elements are more vulnerable to impacts and low values might then be selected. However, these lower values may also correspond to age.

The limb bones were divided into different categories according to their percentage adult size, prior to thin sectioning. The analysis of their bone histology showed that the categories could also be distinguished by the differences in their tissue organisation. The fibro-lamellar tissue in the late juvenile femora indicates rapid growth (Francillon-Vieillot, et al., 1990b; Reid, 1996), but the osteocyte lacunae become progressively more organised towards the sub-periosteal surface (Figure 5.3). The increased organisation and lower vascularisation towards the periphery, suggest a slower growth rate, compared to the peri-medullary region as vascular density is known to be positively correlated with growth rate in osseous tissues (Ricqlès, 1983; Erickson and Tumanova, 2000).

The late sub-adult femur (SAM-PK-K1395) and humerus (B/P/I/2820) and the early adult humeri exhibit more extensive fibro-lamellar tissue and higher overall vascularisation than that of the late juvenile femora. This suggests that these elements experienced faster growth than did the late juvenile elements. Immature individuals usually have highly vascular tissues due to the high energy requirement of rapid growth. The types of growth exhibited by the elements in the different age classes (late juvenile – late sub-adult – early adult) may represent a sigmoidal growth pattern. Animals that grow in this manner usually experience a relatively slow increase in body mass early in ontogeny, during a stage called the lag phase. The lag phase is followed by a sustained rapid growth period called the logarithmic or exponential stage during which most of the adult body mass is attained. The final stage is called the stationary phase and is characterised by a plateauing of growth late in ontogeny (late adults) as growth gradually ceases or at least slows down considerably (Erickson and Tumanova, 2000).

Apart from the late sub-adult femur (SAM-PK-K1395), which contains an annulus in the mid-cortex (Figure 5.4), growth rings are absent from all elements. The overall absence of growth rings suggests that growth was continuous throughout the year and did not cease during the unfavourable season. The annulus in the sub-adult femur may represent a local response or a particularly stressful unfavourable season, whereby growth slowed down during that period. The presence of fibro-lamellar tissue after the annulus indicates that the interruption in growth was episodic and that growth resumed once the favourable season returned.

The appearance of increasingly organised osteocyte lacunae at the periphery of the late sub-adult femur and early adult humeri, suggests the start of an overall slowing down in growth. The radii and ulnae exhibit this change in bone growth more clearly as parallel-fibred bone (Figures 5.7, 5.8), which consists of highly organised, poorly vascularised tissue. This general decrease in growth rate may also represent the onset of sexual maturity, similar to *Procynosuchus*

(Castanet and Baez, 1991; Reid, 1996; Sander, 2000). Inner circumferential lamellae, which indicate that the adult size has been reached (Cormack, 1987; Reid, 1996), are also observed surrounding the medullary cavity of the radii and ulnae (Figures 5.7, 5.8). Apart from age, the more extensive slowly forming tissues in the radii and ulnae may also be due to inter-element histovariability. The radii and ulnae may grow more slowly than the humeri and femora, so explaining the extensive appearance of parallel-fibred bone. If this is the case, late adult humeri and femora would exhibit more parallel-fibred bone than late sub-adult or early adult specimens, but this type of bone would not become as extensive as that in the radii and ulnae.

Bone drift observed throughout the delto-pectoral crest regions of the humeri is possibly due to the presence of the deltoid musculature, namely M. pectoralis and M. brachialis (cf. Jenkins, 1971). Bone drift occurs in the delto-pectoral crest regions due to the relocation of the protuberance along the bone shaft during growth. Sharpey's fibres observed in the distal metaphysis of the late sub-adult femur (SAM-PK-K1395) may indicate the origin of the M. femoro-tibialis (cf. Jenkins, 1971) as Sharpey's fibres occur in areas of muscle insertion (Leeson and Leeson, 1981).

Sharpey's fibres also observed on the posteromedial side of the radii may indicate the insertion of the biceps. Resorption cavities were found to be more prominent in the region of the ulna crest, which runs distally down the anteromedial side of the bone. Sharpey's fibres were also present in this region, indicating the possible origin for the insertion of a radio-ulnar interbone ligament (cf. Jenkins, 1971).

# CHAPTER SIX
# *CYNOGNATHUS* AND *DIADEMODON* BIOLOGY

*Summary*

*This chapter includes a study of the biology of the contemporaneous non-mammalian cynodonts Cynognathus and Diademodon, through the examination of their cross-sectional geometry and bone histology. Their fossilized remains are frequently found in the same deposits and in the absence of diagnostic cranial material, their postcranial skeletons are considered indistinguishable from each other. As such, part of the material obtained for the study of these genera could not be positively identified as either genus from their morphological features. Hence the results for both genera are included in this chapter. A brief description of the morphological characteristics of these genera, based on earlier studies is provided, followed by a section on the materials and localities. The results obtained from the histological analysis revealed distinct histological patterns for each genus, which has facilitated the positive identification of their limb bones on the basis of their bone histology, when associated cranial material is absent. A significant difference in relative bone wall thickness (RBT) between the early sub-adult Cynognathus humerus (22.35%) and late sub-adult and adult femora (33.07%) was found. Almost all the Diademodon elements have RBT values exceeding 30%. A fossorial or semi-aquatic lifestyle is suggested. The K-values of both genera suggest that the limb bones are selected for impact loading and ultimate strength. The uninterrupted fibro-lamellar tissue of Cynognathus, containing abundant vascular canals in a plexiform arrangement, suggests a rapid, sustained growth strategy. Cynognathus may have grown independently of environmental conditions. The tissue organisation of Diademodon is zonal suggesting that it had a cyclical growth strategy, which may have been seasonally influenced. The Diademodon material includes an ontogenetic series of the humerus and femur and a partial ontogenetic series of the tibia allowing histological variation through ontogeny to be observed in a number of different elements. The extent of this material allows deductions regarding the changes in growth strategy through ontogeny to be made for this genus.*

*Cynognathus* and *Diademodon* were contemporaneous during the Early to Middle Triassic and their remains are frequently found in the same fossil assemblages. Although they have distinctive cranial and dental morphologies, their postcranial skeletons appear to be indistinguishable from one another (Brink, 1955; Jenkins, 1971), with the exception of slight differences in the neural spines and centra of the vertebral column (Brink, 1955). This poses a

difficulty in distinguishing their postcrania when no associated cranial material is preserved. Diagnostic positively identified postcranial elements (using associated cranial material) were used to examine the bone histology of *Cynognathus* and *Diademodon*. A number of limb bones from a bone bed identified as *Cynognathus/Diademodon* were also examined to determine the possibility of distinguishing between their postcrania on the basis of their bone histology.

## 6.1 Functional Morphology

*Cynognathus* was a large, robust carnivorous non-mammalian cynodont that reached up to 2m in length. The cranium of *Cynognathus* is characterised by a long, narrow snout, enlarged dentary bone, robust orbital bar and zygomatic arch and an unusually large squamosal. The sectorial teeth have wear-facets indicating that the teeth occluded and were probably used in a shearing action to cut up meat (Seeley, 1908; Broom, 1911, 1913; Gregory and Camp, 1918; Kemp, 1982).

*Diademodon* was a large omnivorous (Grine, 1978) non-mammalian cynodont, similar in size to *Cynognathus*. The cranium is characterised by a narrow snout, wide orbital region and antero-dorsally placed eyes (Seeley, 1895a; Watson, 1911; Kemp, 1982). The temporal fenestrae are large and separated from one another by a narrow, high sagittal crest (Kemp, 1982). The postorbital region of the zygomatic arch is also unusually deep (Brink, 1955; Hopson, 1994). *Diademodon* is one of the first non-mammalian therapsids to exhibit a combination of a mammal-like jaw adductor musculature and precise postcanine occlusion (Grine, 1976, 1977, 1979b; Kemp, 1982). The development of tooth occlusion facilitated the modification of different tooth types to encompass a varied diet (Hopson, 1991; Rowe, 1993).

As more derived non-mammalian cynodonts, *Cynognathus* and *Diademodon* had a semi-erect stance instead of the more sprawling gait of the earlier non-mammalian cynodonts. The acetabulum of the hindlimb is deeper and smaller

than in earlier non-mammalian cynodonts, while the articulating head of the femur is a large sphere set off at an angle to the shaft of the bone. The femur could only fit into the acetabulum if the knee joint lay fairly close to the body throughout the stride, which caused the hindlimb to move in a more parasagittal plane. In contrast, the forelimb stance remained sprawling. The glenoid restricted the movements of the humerus, forcing it to remain in a horizontal position. Despite the primitive action of the forelimb however, the more erect hindlimb gait would have increased locomotory power. The hind feet would also have been spaced closer together and would have improved maneuverability needed for activities such as prey capture or evasion of predators (Brink, 1956; Kemp, 1982).

## 6.2 Materials and Localities

The positively identified diagnostic *Cynognathus* material consists of three limb bones, a scapula and a rib and that of *Diademodon* consists of ten limb bones and two ribs. *Cynognathus* elements are relatively difficult to obtain as *Cynognathus* material is rarely found in the field (possibly because it is a carnivore). Eleven limb bones from the bone bed diagnosed as *Cynognathus/Diademodon* were also examined (Table 6.1).

All elements were excavated from the *Cynognathus* Assemblage Zone, Beaufort Group, South Africa (Figure 6.1). The *Cynognathus* Assemblage Zone (Early to Middle Triassic, Late Scythian to Early Anisian Stage; Harland, et al., 1990) is characterised by the non-mammalian cynodonts, *Cynognathus, Diademodon* and *Trirachodon,* the dicynodont, *Kannemeyeria* and the absence of *Lystrosaurus.* The presence of ephemeral stream sandstones indicates a semi-arid climate with seasonal rainfall (Smith et. al., 1993).

Table 6.1. The *Cynognathus* and *Diademodon* specimens used in this study and the various localities from where they were recovered. Those elements that have the same specimen abbreviations were obtained from single individuals. Where possible multiple sections from each element were studied for a detailed analysis. See Appendix 1 for institutional abbreviations.

| District | Genus | Specimen number | Skeletal element | Number of sections | Region sectioned |
|---|---|---|---|---|---|
| Aliwal North | *Cynognathus* | SAM-PK-K6235a | femur | 30 | complete |
| | | NMQR3019a | femur | 4 | midshaft |
| | | NMQR3019b | scapula | 2 | fragment |
| | | SAM-PK-K6235b | ulna | 2 | midshaft |
| | | NMQR3019c | rib | 1 | midshaft |
| | *Diademodon* | SAM-PK-K1332 | rib | 4 | midshaft |
| Burgersdorp | *Diademodon* | B/P/I/3772 | humerus | 18 | complete |
| | *Diademodon/* | NMQR1208a | humerus | 18 | complete |
| | *Cynognathus* | NMQR1208b | humerus | 17 | complete |
| | | NMQR1208c | humerus | 14 | complete |
| | | NMQR1208d | humerus | 12 | proximal |
| | | NMQR1208e | humerus | 10 | proximal |
| | | NMQR1208f | femur | 15 | complete |
| | | NMQR1208g | tibia | 8 | complete |
| | | NMQR1208h | tibia | 10 | complete |
| | | NMQR1208i | tibia | 10 | complete |
| | | NMQR1208j | tibia | 8 | complete |
| Lady Frere | *Diademodon* | UMCZ T492 | humerus | 3 | midshaft |
| | | UCMZ T495 | femur | 3 | midshaft |
| | | UCMZ T503 | femur | 4 | midshaft |
| | | UCMZ T493 | femur | 4 | midshaft |
| | | UCMZ T447 | tibia | 5 | midshaft |
| | | UCMZ T448 | fibula | 4 | midshaft |
| Rouxville | *Diademodon* | NMQR2682 | rib | 8 | midshaft |
| Unknown | *Diademodon* | SAM-PK-K8971a | humerus | 13 | midshaft/ distal |
| | | SAM-PK-K8971b | radius | 16 | midshaft |
| | | SAM-PK-K8971c | ulna | 12 | midshaft |

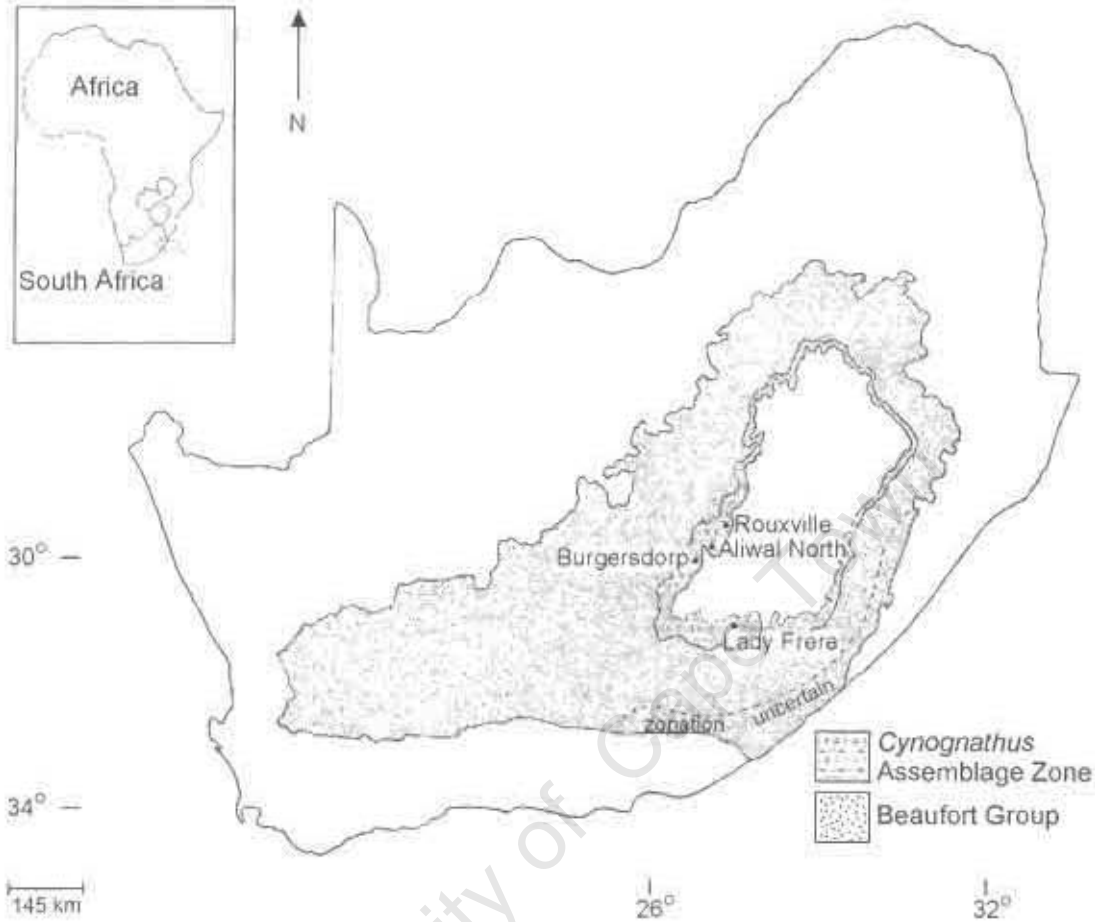


Figure 6.1. *Cynognathus* Assemblage Zone, Burgersdorp Formation, Beaufort Group, South Africa. The material was excavated from localities near the towns Aliwal North, Burgersdorp, Lady Frere and Rouxville. Map compiled from the Reader's Digest Illustrated Atlas of Southern Africa (1994) and Kitching (1995).

## 6.3 Results

### 6.3.1 Macro-analysis

Where possible, the diameter, proximal width and total length of each skeletal element was measured to obtain the percentage adult size of each element. The bone histology of the various diagnostic *Cynognathus* and *Diademodon* skeletal elements was analysed and the defining histological characteristics for each genus was determined. These characteristics were then used to positively identify the postcrania (NMQR1208) from the Burgersdorp bone bed as either *Cynognathus* or *Diademodon* (Table 6.2).

Table 6.2. Gross measurements of the *Cynognathus* and *Diademodon* skeletal elements. The largest *Cynognathus* femur NMQR3019a represents an adult and is considered to be approximately 100% of the adult size. It has been used to obtain the percentage adult size of the smaller femur SAM-PK-K6235a. The *Cynognathus* ulna (SAM-PK-K6235b) diameter was not measured due to distortion, but as it belongs to the same individual as SAM-PK-K6235a, it will be the same percentage adult. Percentage adult values for the *Cynognathus* scapula and rib were not obtained as they are fragmentary. The largest tibia (NMQR1208j) was positively identified as *Diademodon* and was used to estimate the percentage adult size of all the *Diademodon* elements.

| Genus | Specimen number | Skeletal element | Diameter (mm) | Proximal width (mm) | Length (mm) | % Adult |
|---|---|---|---|---|---|---|
| *Cynognathus* | NMQR1208a | humerus | 19.01 | 57.61 | 140.4 | 77.5 |
| | SAM-PK-K6235a | femur | 21.98 | 82.63 | 190.1 | 68.4 |
| | NMQR3019a | femur | 32.24 | - | 278 | 100 |
| | SAM-PK-K6235b | ulna | - | - | - | 68.4 |
| | NMQR3019b | scapula | 31.61 | - | - | - |
| | NMQR3019c | rib | 19.02 | - | - | - |
| *Diademodon* | SAM-PK-K8971a | humerus | 8.48 | - | 57.36 | 31.66 |
| | UMCZ T492 | humerus | 8.55 | 26.36 | 70.41 | 38.87 |
| | B/P/I/3772 | humerus | 7.89 | 26.31 | 75.57 | 41.72 |
| | NMQR1208b | humerus | 12.9 | 42.71 | 107.7 | 59.45 |
| | NMQR1208c | humerus | 17.33 | 54.69 | 127.2 | 70.19 |
| | NMQR1208d | humerus | 22.6 | 75.11 | 172.4 | 95.17 |
| | NMQR1208e | humerus | 22.61 | 71.57 | 173.6 | 95.85 |

| Genus | Specimen number | Skeletal element | Diameter (mm) | Proximal width (mm) | Length (mm) | % Adult |
|---|---|---|---|---|---|---|
| *Diademodon* | SAM-PK-K8971b | radius | 5.09 | - | 56.15 | 31.6 |
| | SAM-PK-K8971c | ulna | 6.22 | - | 51.21 | 31.6 |
| | UCMZ T495 | femur | 12.6 | 29.53 | 93.67 | 48.5 |
| | UCMZ T503 | femur | 11.3 | 40.88 | 103.1 | 53.38 |
| | NMQR1208f | femur | 20.85 | - | 161.7 | 83.7 |
| | UCMZ T493 | femur | 14.5 | - | 118.6 | 61.42 |
| | NMQR1208g | tibia | 10.9 | 22.7 | 90.7 | 58.67 |
| | NMQR1208h | tibia | 13.7 | 28.2 | 98.7 | 63.67 |
| | UCMZ T447 | tibia | 13.4 | 21.75 | 111.9 | 72.36 |
| | NMQR1208i | tibia | 21.6 | 44.3 | 140.6 | 90.89 |
| | NMQR1208j | tibia | 24.2 | 47.4 | 154.7 | 100 |
| | UCMZ T448 | fibula | 6.23 | - | 76.94 | 76.94 |
| | NMQR2682 | rib | 21.55 | - | - | - |
| | SAM-PK-K1332 | rib | 23.46 | - | - | - |

Three ontogenetic ranges, (humeral, femoral and tibial) were obtained from the *Diademodon* elements. The elements were divided into age classes according to their percentage adult size shown in Table 6.2 and are presented graphically in Figures 6.2, 6.3 and 6.4.

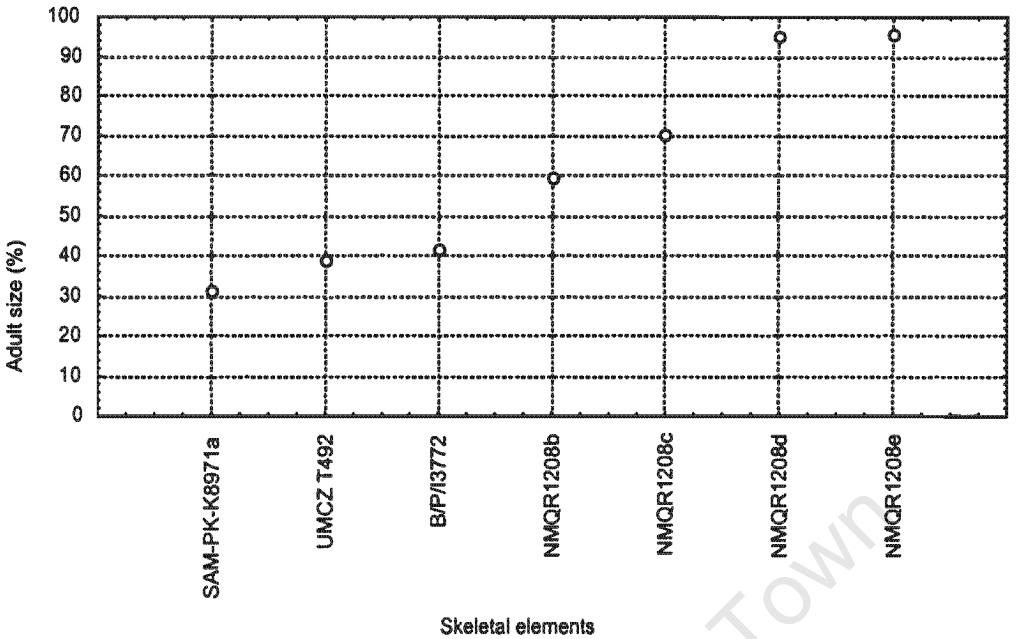


Figure 6.2. Graphic representation of the *Diademodon* humeral ontogenetic series. Those humeri below 50% adult size are classed as early sub-adults, those from 50% to 70% as late sub-adults and those above 80% are categorised as adults.

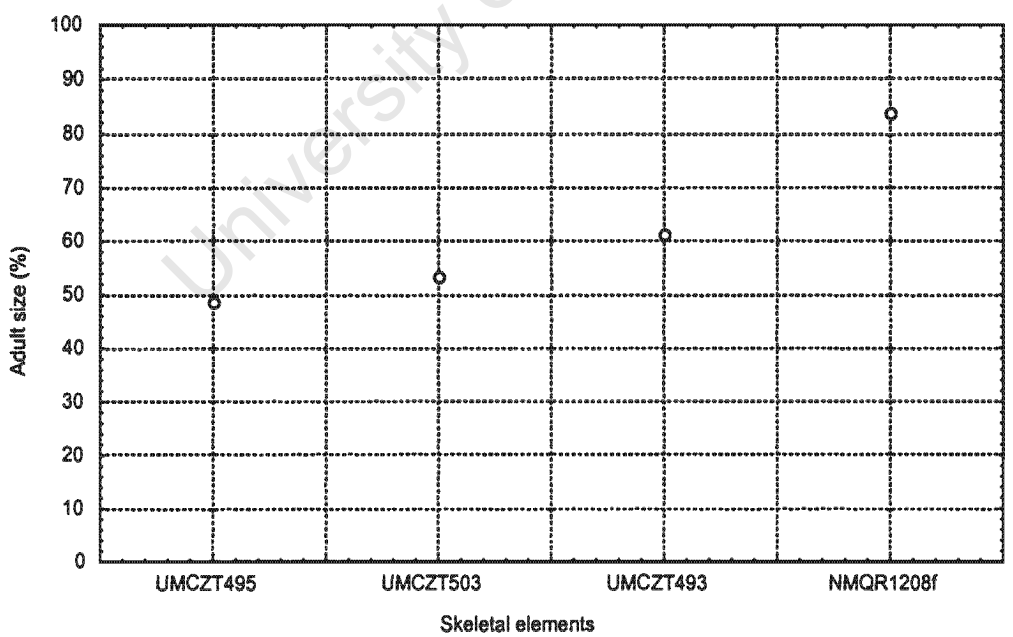


Figure 6.3. Graphic representation of the *Diademodon* femoral ontogenetic series. The femora UMCZ T495 and UMCZ T503 are designated sub-adults, the femur UMCZ T493 is classed as a late sub-adult and the femur NMQR1208f as an adult.

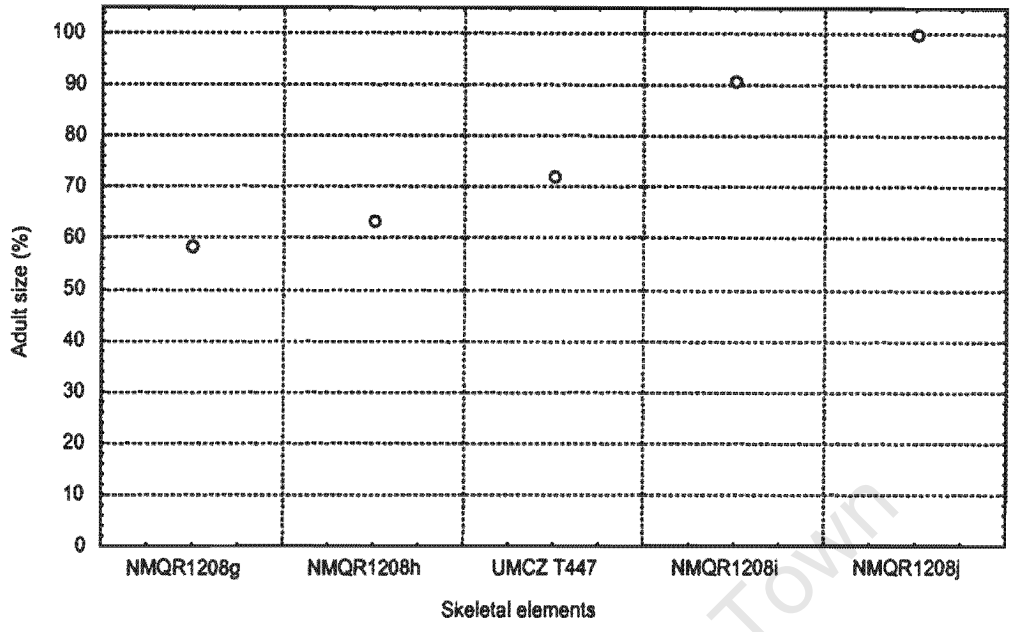


Figure 6.4. Graphic representation of the *Diademodon* tibia ontogenetic series. The tibiae below 80% adult size are classed as sub-adults, whereas those above 80% are considered adults.

### (i) Cross-Sectional Geometry of *Cynognathus*

The humerus NMQR1208a, excavated from the Burgersdorp bone bed, was positively identified as *Cynognathus* on the basis of its bone histology (see section 6.3.2). Relative bone wall thickness (RBT) and K-values were calculated for the *Cynognathus* femora and humerus. RBT measurements were taken from the midshaft regions of each bone and are presented as a percentage (Figure 6.5).

The average *Cynognathus* femoral RBT percentage of 33.07% is significantly higher (independent 1-tailed t-test: $t_s$ = -8.738, df = 4, $p < 0.05$) than the humeral value of 22.35%. The average femoral K-value (0.34) is also significantly lower than the humeral K-value 0.56 (independent 1-tailed t-test: $t_s$ = 8.918, df = 4, $p < 0.05$) (See Appendix 2 for detailed RBT and K-value results).

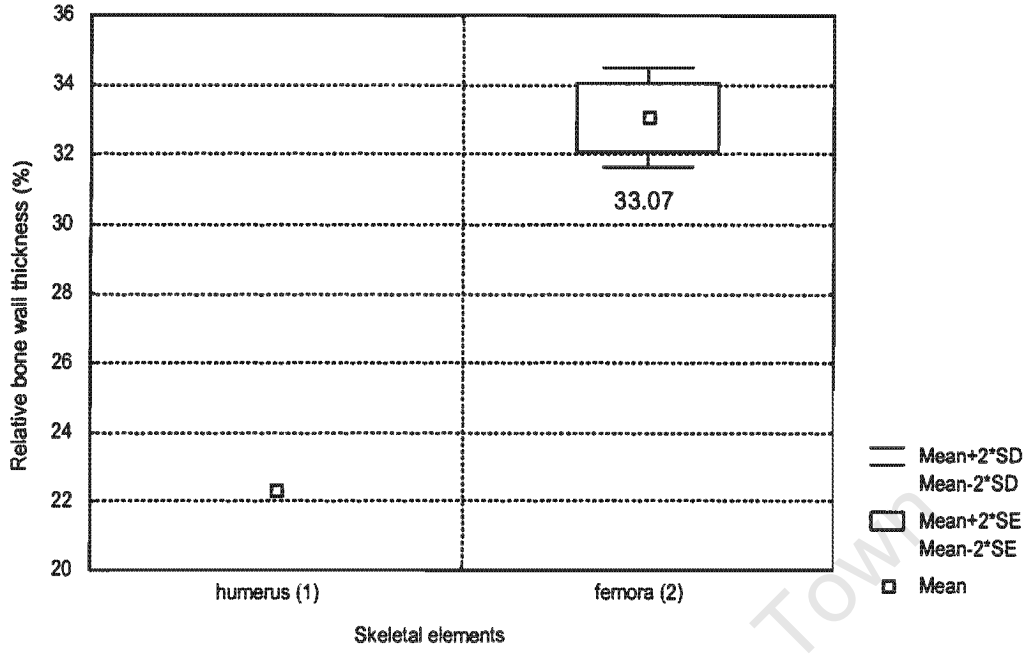


Figure 6.5. *Cynognathus* midshaft relative bone wall thickness percentages. The numerical value associated with the box represents the average femoral percentage RBT. The number of individual elements examined for each type of element is indicated by the numbers in brackets. The ulna is distorted and has been excluded.

### (ii) Cross-Sectional Geometry of *Diademodon*

Relative bone wall thickness and K-values were also calculated for the *Diademodon* limb bones, using the midshaft regions. They have been presented first in tabular form (Table 6.3) for comparing individual values between the different types of elements. K-values are also shown in Table 6.3. Appendix 2 gives the detailed RBT and K-value calculations.

Table 6.3. The *Diademodon* limb bone percentage relative bone wall thickness (RBT) and K-values. All values (apart from SAM-PK-K8971a, UMCZ T495, 503, 493) exceed 30%.

| Specimen number | Skeletal element | %RBT | K-value |
|---|---|---|---|
| SAM-PK-K8971a | humerus | 27.04 | 0.46 |
| UMCZ T492 | humerus | 36.97 | 0.27 |
| B/P/I/3772 | humerus | 36.62 | 0.27 |
| NMQR1208b | humerus | 38.54 | 0.24 |
| NMQR1208c | humerus | 35.44 | 0.3 |
| NMQR1208d | humerus | 42.47 | 0.15 |
| NMQR1208e | humerus | 34.8 | 0.3 |
| SAM-PK-K8971b | radius | 31.97 | 0.37 |
| SAM-PK-K8971c | ulna | 32.68 | 0.37 |
| UMCZ T495 | femur | 21.29 | 0.54 |
| UMCZ T503 | femur | 25.91 | 0.48 |
| UMCZ T493 | femur | 28.65 | 0.43 |
| NMQR1208f | femur | 33.98 | 0.33 |
| NMQR1208g | tibia | 38.48 | 0.23 |
| NMQR1208h | tibia | 33.13 | 0.33 |
| UMCZ T447 | tibia | 34.57 | 0.31 |
| NMQR1208i | tibia | 35.94 | 0.29 |
| NMQR1208j | tibia | 31.12 | 0.39 |
| UMCZ T448 | fibula | 40.4 | 0.2 |



An increase in the humeral and femoral relative bone wall thickness occurs with age (shown in Figures 6.6 and 6.7). Although the mean value of the adult tibiae is slightly lower than that of the sub-adult tibiae, they are extremely similar (Figure 6.8). The sub-adult tibia, NMQR1208g, has a value of 38.48% (Table 6.3), which is higher than any of the other tibiae and has therefore probably scewed the sub-adult tibia mean. The RBT value of the adult NMQR1208j tibia (31.12%) is also lower than the other adult tibia, NMQR1208i and has probably caused a similar shift in the mean adult tibia RBT value.

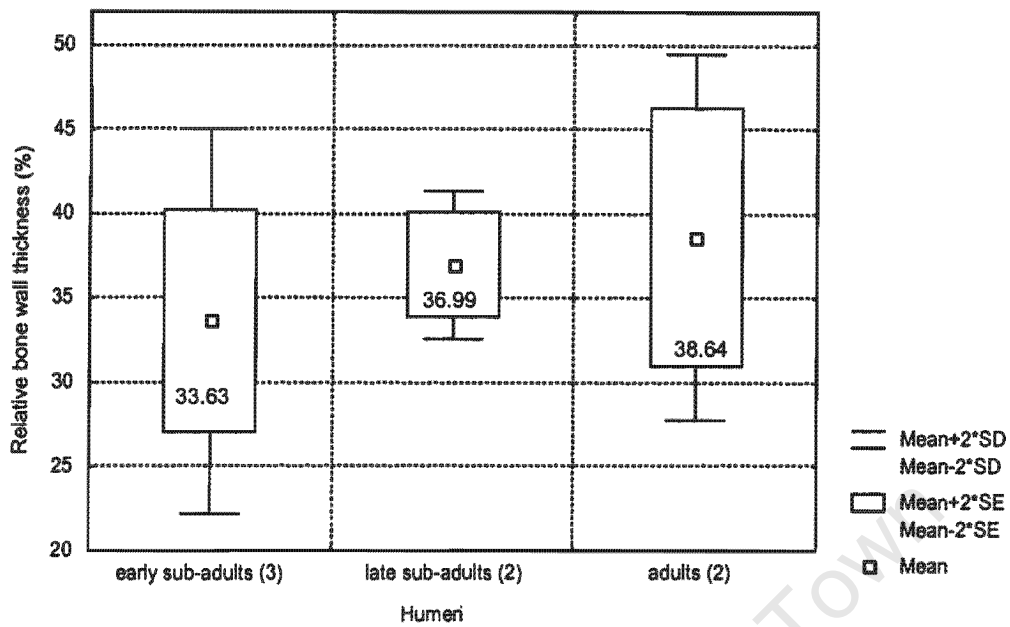


Figure 6.6. *Diademodon* midshaft relative bone wall thickness values of the humeral age classes. The values associated with the boxes represent the means of each age class. The number of individual elements used to calculate the percentage RBT for each type of element is indicated by the numbers in brackets.

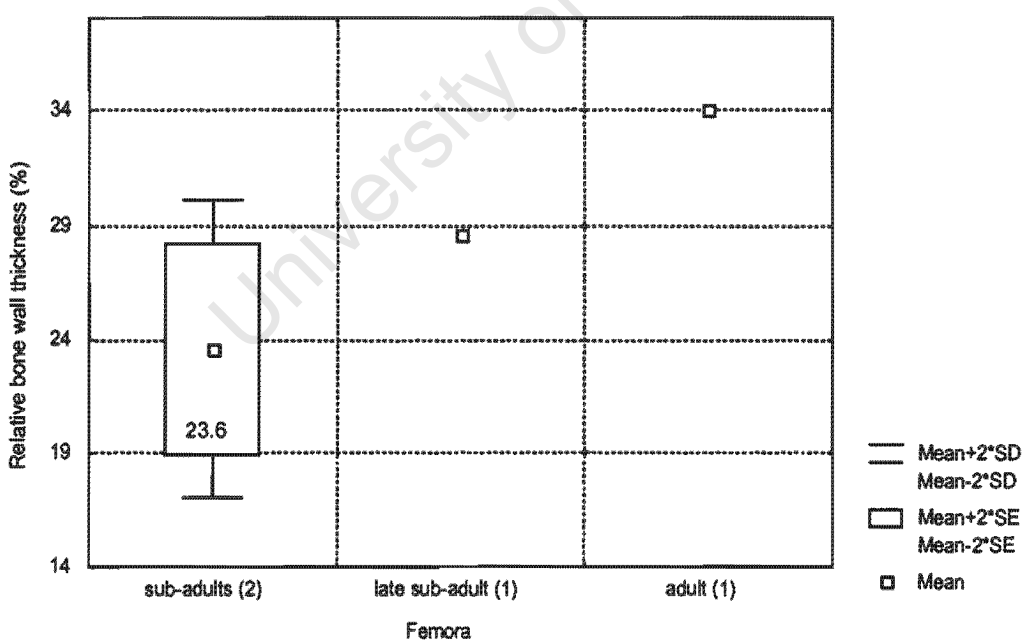


Figure 6.7. *Diademodon* midshaft percentage relative bone wall thickness values of the various femoral age classes. The value associated with the box and numbers in brackets as in Figure 6.6.

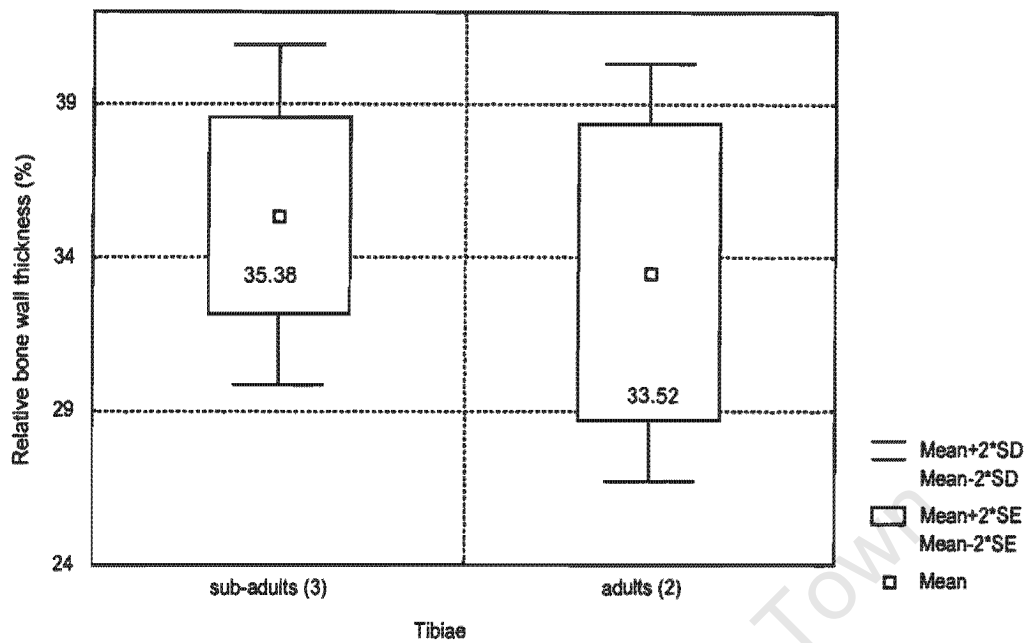


Figure 6.8. *Diademodon* midshaft relative bone wall thickness values of the tibia age classes. The values associated with the boxes and those in brackets as in Figure 6.6.

### 6.3.2 Micro-analysis

The overall bone tissue of the diagnostic *Cynognathus* elements consists of uninterrupted, highly vascularised fibro-lamellar tissue. The vascular canals form a plexiform arrangement, where circumferential vascular canals dominate. Branched canaliculi radiate from globular osteocyte lacunae, but the canaliculi are generally not well preserved. In contrast, the overall bone tissue of the diagnostic *Diademodon* elements is zonal. Zones consist of fibro-lamellar bone tissue with various vascular arrangements ranging from a dominance of longitudinally oriented primary osteons to a reticular network. The osteocyte lacunae are globular and radiate branched canaliculi. The annuli consist of lamellar bone tissue with few, flattened osteocyte lacunae. They are narrow and either avascular or poorly vascularised with occasional vascular anastomoses crossing over them. LAGs are sometimes present before or after the annuli.

The distinct differences in bone histology between the two genera have facilitated the positive generic identification of the postcrania from the

Burgersdorp bone bed (NMQR1208). Out of the 11 postcrania, one humerus (NMQR1208a) was positively identified as *Cynognathus*, whereas the rest of the limb bones were positively identified as *Diademodon*. A histological description of the bones of *Cynognathus* and *Diademodon* follows. The postcrania from the Burgersdorp bone bed have been added to increase the sample size of each genus.

**(i) Bone Histology of *Cynognathus***

The bone tissues of the positively identified femora (SAM-PK-K6235a; NMQR3019a) consist of uninterrupted fibro-lamellar bone tissue (Figure 6.9). The vascular canals are abundant and form a plexiform vascular arrangement. Small secondary osteons are present around the medullary cavities, but these are rare. Circumferential endosteal lamellar tissue is observed surrounding the medullary cavities of both elements. Bone drift is observed in the lesser trochanter and on the medial side of the bone, towards the distal end of SAM-PK-K6235a. There is a change in the orientation of the vascular canals and the cortex is thicker on the dorsal side of the bone, in the lesser trochanter region. Coarse cancellous bone is more prominent on the dorsal side of the bone, from the proximal metaphysis to the midshaft and on the ventral side of the bone, from the midshaft to the distal metaphysis. Secondary remodelling reaches the sub-periosteal surface in the greater trochanter region. The bone tissue is slightly less vascular at the sub-periosteal surface, compared to the rest of the cortex. Sharpey's fibres are observed on the ventral side of the bone, in the region of the lesser trochanter. A few Sharpey's fibres can also be seen on the ventral side of the bone in the distal metaphyseal region of SAM-PK-K6235a.

The bone tissue of the ulna SAM-PK-K6235b is very similar to that of the femur and it belongs to the same individual (SAM-PK-K6235a). It also consists of highly vascularised uninterrupted fibro-lamellar tissue in a plexiform arrangement (Figure 6.10). There are a few small secondary osteons in the peri-medullary region and a slight decrease in vascularisation is observed at the outer margin.

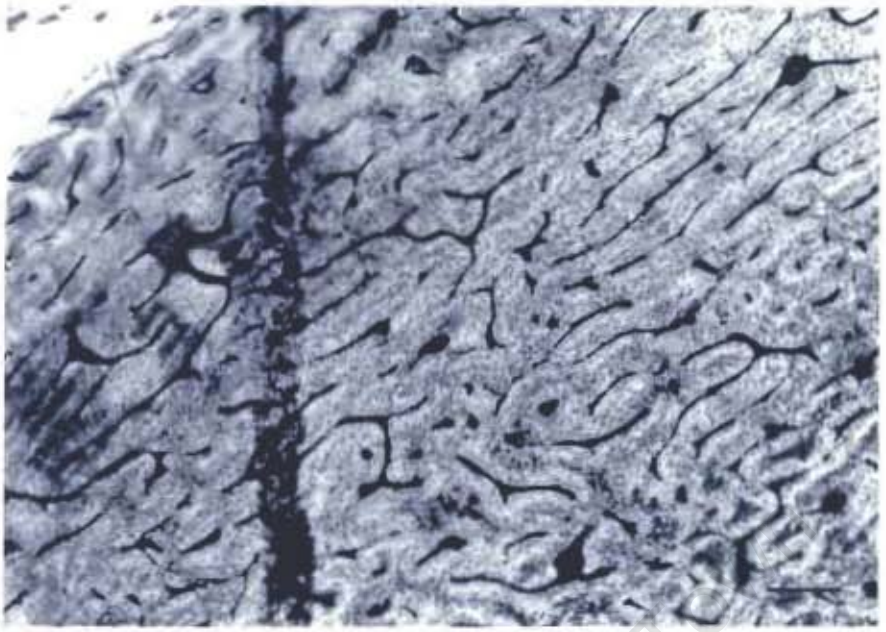

Figure 6.9.

Figure 6.10.

Figure 6.9. Transverse section of the *Cynognathus* femur SAM-PK-K6235a, showing uninterrupted fibro-lamellar bone tissue with abundant vascular canals, arranged in a plexiform arrangement. A slight decrease in vascularisation is observed at the periphery of the bone.

Figure 6.10. Transverse section of the *Cynognathus* ulna SAM-PK-K6235b, showing a similar bone tissue to the femur shown above.

Scale bars = 250µm

The bone tissue of the humerus NMQR1208a consists of similar tissues to the femora and ulna. The vascular canals are uniformly distributed throughout the cortex, right to the periphery of the bone (Figure 6.11). The vascular canal arrangement is a mixture of plexiform and reticular networks. Primary osteons are observed throughout the cortex and secondary osteons are present around the medullary cavity, but these are rare. Bone drift occurs in the delto-pectoral crest region and compacted coarse cancellous bone is more extensive here. The vascular canals radiate out from the medullary cavity in this region. Secondary remodelling is more extensive on the medial and dorsal sides of the bone and it also increases around the ectepicondylar and entepicondylar foramena. Separated spicules of bony trabeculae, sometimes joining to form a network, are present at the ends of the bone.

The tissue of the scapula NMQR3019b consists of fibro-lamellar tissue with a mixture of longitudinally oriented primary and secondary osteons. Numerous Sharpey's fibres are observed and a LAG is seen at the sub-periosteal surface. Abundant globular osteocyte lacunae are present, similar to the humeri and femora. The canaliculi are not preserved. Dense Haversian bone is observed in the peri-medullary region. Figure 6.12 shows large erosion cavities near the sub-periosteal surface.

The bone tissue of the rib NMQR3019c is highly vascularised and contains a mixture of longitudinally oriented primary and secondary osteons, which extend to the periphery of the bone (Figure 6.13). Two annuli can be seen at the sub-periosteal surface in one region of the bone.

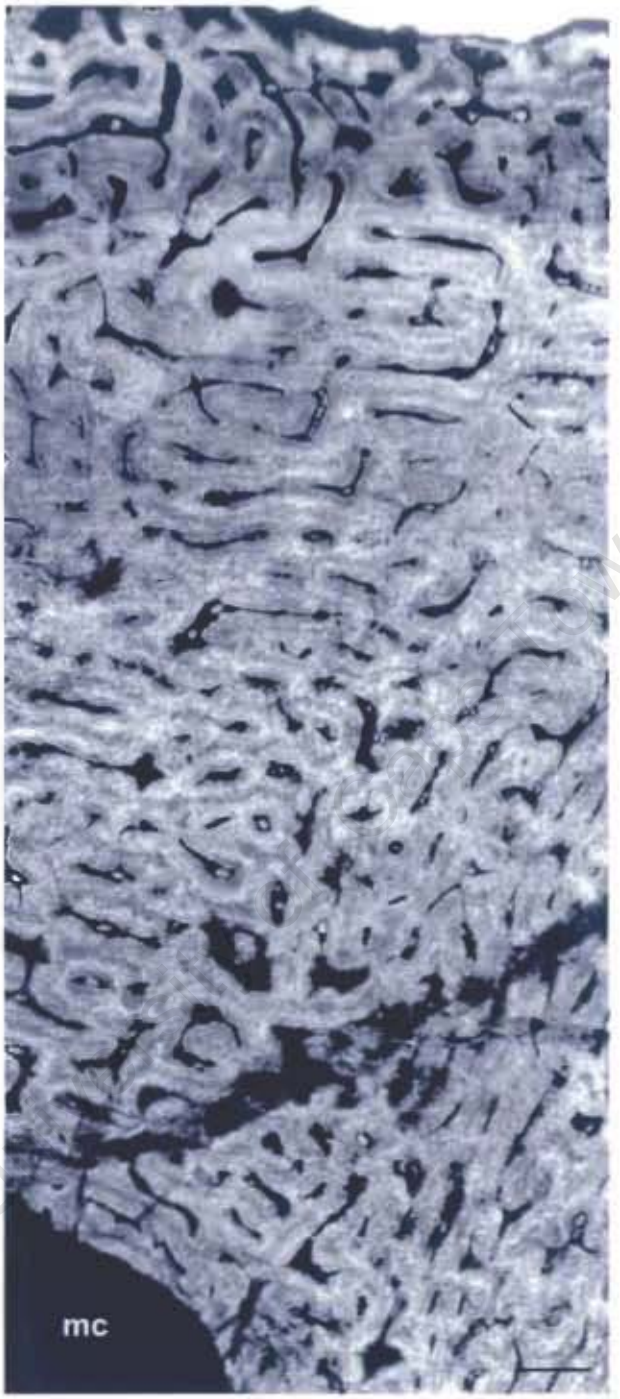


Figure 6.11. Transverse section of the *Cynognathus* humerus NMQR1208a, showing the highly vascularised, uninterrupted fibro-lamellar tissue, similar to the previous femur and ulna.

Scale bar = 250μm

mc, medullary cavity

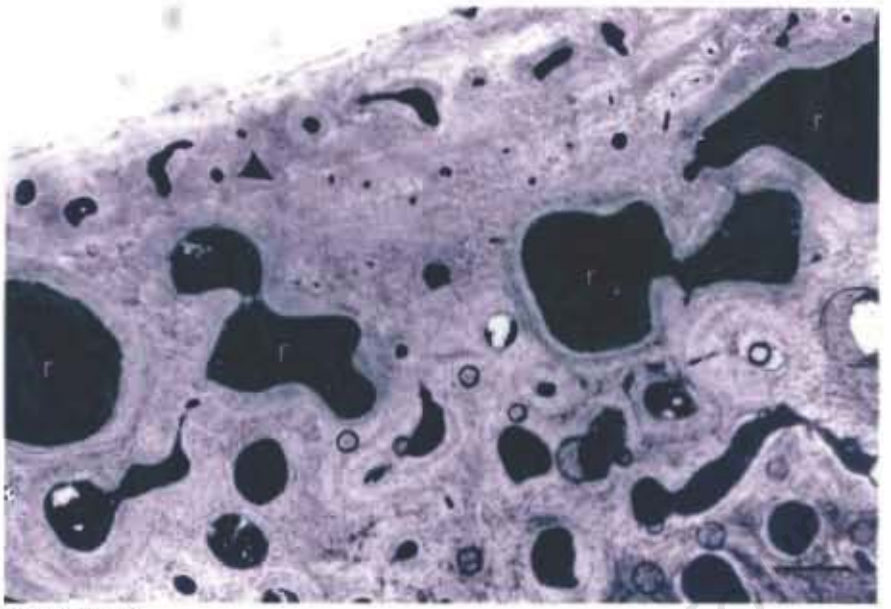


Figure 6.12.

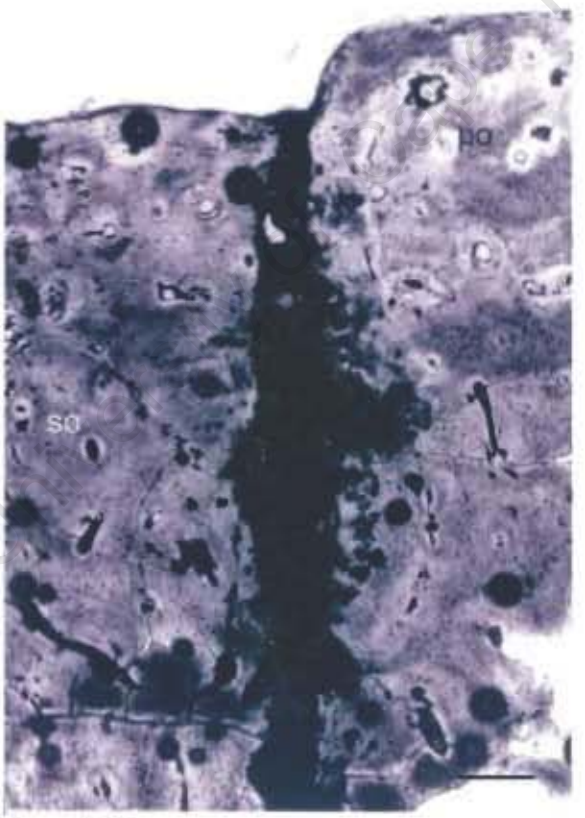


Figure 6.13.

Figure 6.12. Transverse section of the *Cynognathus* scapula NMQR3019b. Large resorption cavities are abundant and reach the sub-periosteal surface in places. A LAG is observed near the periphery of the bone (►).

Figure 6.13. Transverse section of the *Cynognathus* rib NMQR3019c. Primary and secondary osteons are abundant throughout the cortex.

Scale bars = 250µm
po, primary osteon; so, secondary osteon; r, resorption cavity

The midshaft percentage channel area was calculated for the *Cynognathus* humerus (NMQR1208a), femora (SAM-PK-K6235a, NMQR3019a) and ulna (SAM-PK-K6235b) in order to quantify the vascular density of the tissues.

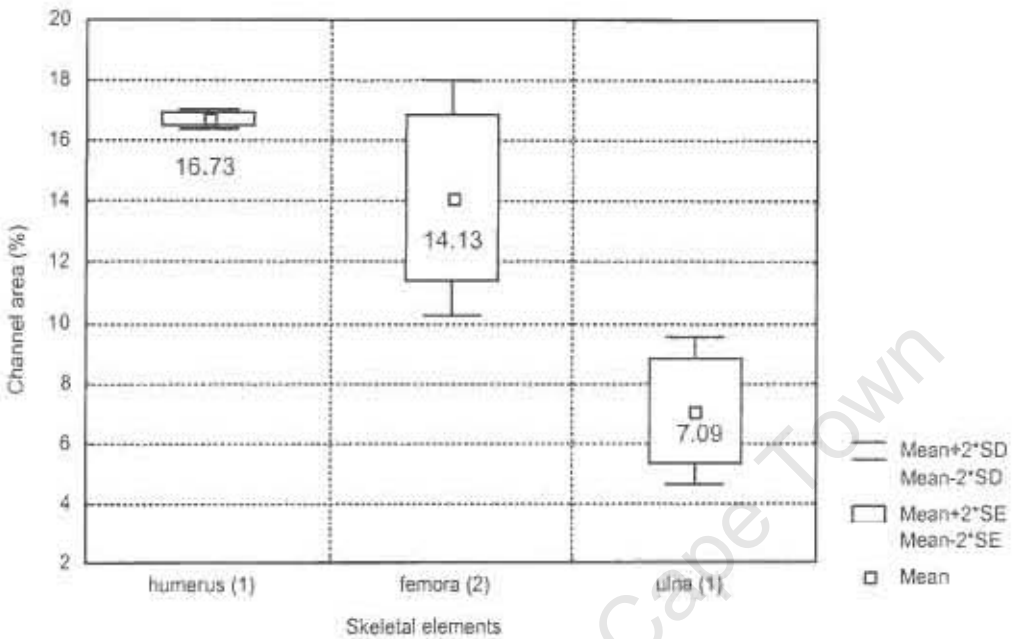


Figure 6.14. The midshaft percentage channel area of the *Cynognathus* humerus, ulna and femora. The values associated with the boxes indicate the mean values. The numbers in brackets indicate the number of individual elements used to calculate the percentage channel area for each type of element.

The percentage channel area of the ulna is significantly lower than that of the humerus and femora (independent 1-tailed t-test: $t_s = -5.56$; $df = 4$; $p < 0.05$).

**(ii) Bone Histology of *Diademodon***

The *Diademodon* humeral material consists of two diagnostic humeri (positively identified through associated cranial material) and four humeri excavated from the Burgersdorp bone bed that were positively identified as *Diademodon* using the diagnostic material.

The vascular canals in the early sub-adult humeri SAM-PK-K8971a (Figure 6.15) and UMCZ T492 (Figure 6.16) form a reticular arrangement in the mid-cortex, becoming plexiform in some places at the sub-periosteal surface. A slight decrease in vascularisation is seen at the sub-periosteal surface of SAM-

PK-K8971a (Figure 6.15). The two annuli observed in this element are narrow and poorly vascularised. Longitudinal sections show a dense network of bony trabeculae in the distal metaphysis and secondary remodelling is more extensive in this region. The two annuli in UMCZ T492 are also narrow and poorly vascularised. Circumferential endosteal lamellar tissue surrounds the medullary cavity in some areas and secondary remodelling has just begun in the medullary cavity region.

Six annuli are observed in the humerus B/P/I/3772 and LAGs are present after some of the annuli (Figure 6.17). Secondary osteons are observed in the medullary cavity region. Although this element is designated as an early sub-adult, it is slightly larger and probably older (41.72% adult size) than the other two early sub-adult elements. There is a slight decrease in vascularisation at the periphery and the vascular canals are smaller in diameter here. Longitudinal sections show a dense network of bony trabeculae in the metaphyses.

In comparing the early sub-adult humeri with the late sub-adult and adult humeri, the latter contain more secondary osteons, annuli and LAGs compared to the early sub-adults. The humeri range in length from 57.36 mm (SAM-PK-K8971a) to 173.64 mm (NMQR1208e). The vascular canals in the late sub-adults are mostly longitudinal with radial anastomoses whereas those of the adult humeri form a laminar arrangement. The overall tissue arrangement of the adult humeri is also more organised than that of the early sub-adults. A varying decrease in vascularisation is observed at the sub-periosteal surface in all elements (Figure 6.18). Multiple layers of endosteal lamellar tissue can be seen around the medullary cavities of the late sub-adult humeri. LAGs are present in all elements, except the adult humerus NMQR1208e, in which only annuli occur. Vascular canals radiate out from the medullary cavity on the ventral distal side of the late sub-adult humerus NMQR1208c. A network of bony trabeculae interspersed with trabecular islets is observed in the metaphyses. Bone drift is observed in the delto-pectoral crest region of all the humeri and secondary remodelling is more extensive in this area. Compacted coarse cancellous bone can also be seen in this region (Figure 6.19).

The tissue organisation of the *Diademodon* radius (SAM-PK-K8971b) and ulna (SAM-PK-K8971c) is very similar and to avoid repetition are described together. The humerus SAM-PK-K8971a, the radius SAM-PK-K8971b and the ulna SAM-PK-K8971c all belong to the same individual. Vascular canals are mostly longitudinally oriented primary osteons with radial anastomoses (Figures 6.20, 6.21). Secondary osteons are seen around the medullary cavities. Two annuli are observed in the radius and one in the ulna. The annuli in both elements are poorly vascularised and occasional radial anastomoses cross over the annuli. Bone drift can be seen in the ridge of the radius. Secondary remodelling becomes very extensive towards the metaphyses, occupying almost the entire cross sectional area in both elements. Compacted coarse cancellous bone is present around the medullary cavities. Longitudinal sections reveal a trabecular network similar to the humerus SAM-PK-K8971a.


Figure 6.20. Transverse section of the early sub-adult *Diademodon* radius SAM-PK-K8971b. Annuli (►) are observed interrupting the fibro-lamellar tissue and longitudinal primary osteons are abundantly distributed throughout the cortex.

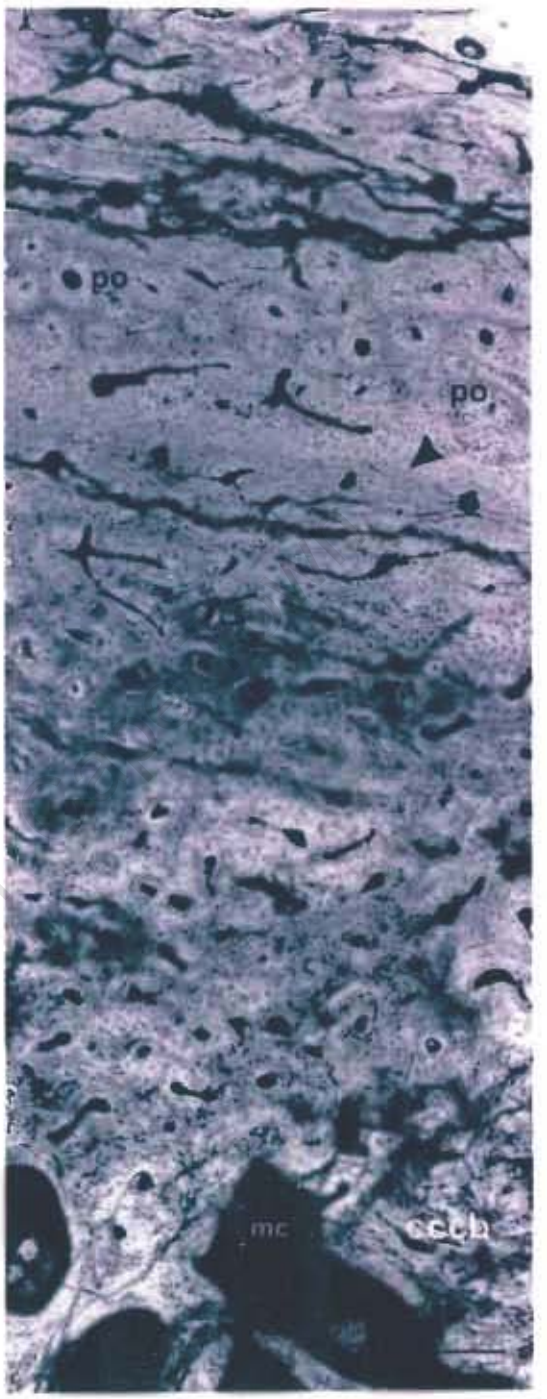


Figure 6.21. Transverse section of the early sub-adult *Diademodon* ulna SAM-PK-K8971c. The tissue exhibits abundant longitudinal primary osteons similar to the radius. An annulus in the mid-cortex is indicated by (►). Compacted coarse cancellous bone is seen in the vicinity of the medullary cavity.

Scale bars = 125µm
mc, medullary cavity; po, primary osteon; cccb, compacted coarse cancellous bone

The tissue of the *Diademodon* femora is similar to that of the humeri. The annuli are poorly vascularised and LAGs are absent from the sub-adult femora (UMCZ T495 and T503). One LAG is observed after the outermost annulus in the late sub-adult femur (UMCZ T493). The sub-adult tissues are highly vascularised and contain reticular to plexiform arrangements and many circumferentially oriented vascular canals (Figure 6.22).

There are fewer vascular canals in the late sub-adult and adult femora and they are mostly longitudinal with radial anastomoses. Circumferential endosteal lamellar tissue is present in a small region around the medullary cavity in the late sub-adult and surrounds the medullary cavity in the centre of the adult femur midshaft. Compacted coarse cancellous bone is also observed in the peri-medullary regions.

Small secondary osteons are present around the medullary cavity of the adult femur. There is also a localised radial orientation of vascular canals on the ventral side in the region of the lesser trochanter. The wide annuli (7 observed) in the inner and mid-cortex become narrower towards the periphery and the LAGs become multiple at the periphery of the medial side of the bone. Although some areas of the bone are diagenetically altered, localised growth at the sub-periosteal surface after the last LAGs can still be observed as shown in Figure 6.23. The osteocyte lacunae are haphazardly arranged and primary osteons are abundant. Secondary remodelling is slightly more extensive on the dorsal side of the distal metaphysis of this element.

The tissues of the *Diademodon* tibiae and fibula are very similar and are described together. The vascular canals of all the elements (tibiae NMQR1208g, h, i, j and UMCZ T447 and the fibula UMCZ T448) are mostly longitudinally oriented primary osteons with radial anastomoses (Figure 6.24). Circumferential endosteal lamellar tissue is observed around the medullary cavities of the sub-adult tibiae (UMCZ T447, NMQR1208g and NMQR1208h) and the fibula UMCZ T448. The osteocyte lacunae are flattened here. LAGs are absent from the two smallest tibiae, but multiple LAGs appear at the sub-periosteal surface of the sub-adult (UMCZ T447) and the adult tibiae (Figures 6.24, 6.25), and a wider region of lamellar tissue compared to the rest of the cortex, is observed at the periphery of the fibula (Figure 6.26). A decrease in vascularisation can be seen at the outer margin of the adult tibia NMQR1208j (Figure 6.25). Secondary osteons are present around the medullary cavities of the sub-adult UMCZ T447, the adult tibiae (more common in the area of bone drift) and the fibula. Secondary remodelling is slightly more extensive towards the anterior side of the fibula.

The tissues of the *Diademodon* ribs NMQR2682 and SAM-PK-K1332 are extensively remodelled and large resorption cavities extend to the sub-periosteal surface as shown in the rib NMQR2682 of Figure 6.27. The osteocyte lacunae are globular and radiate canaliculi similar to that of the long bones. Distinct LAGs, which are sometimes multiple, are observed in the outer cortex.

Figures 6.28 to 6.30 provide schematic transverse sections of the various elements in each age class and highlight the changes in vascularity and tissue organisation through ontogeny.

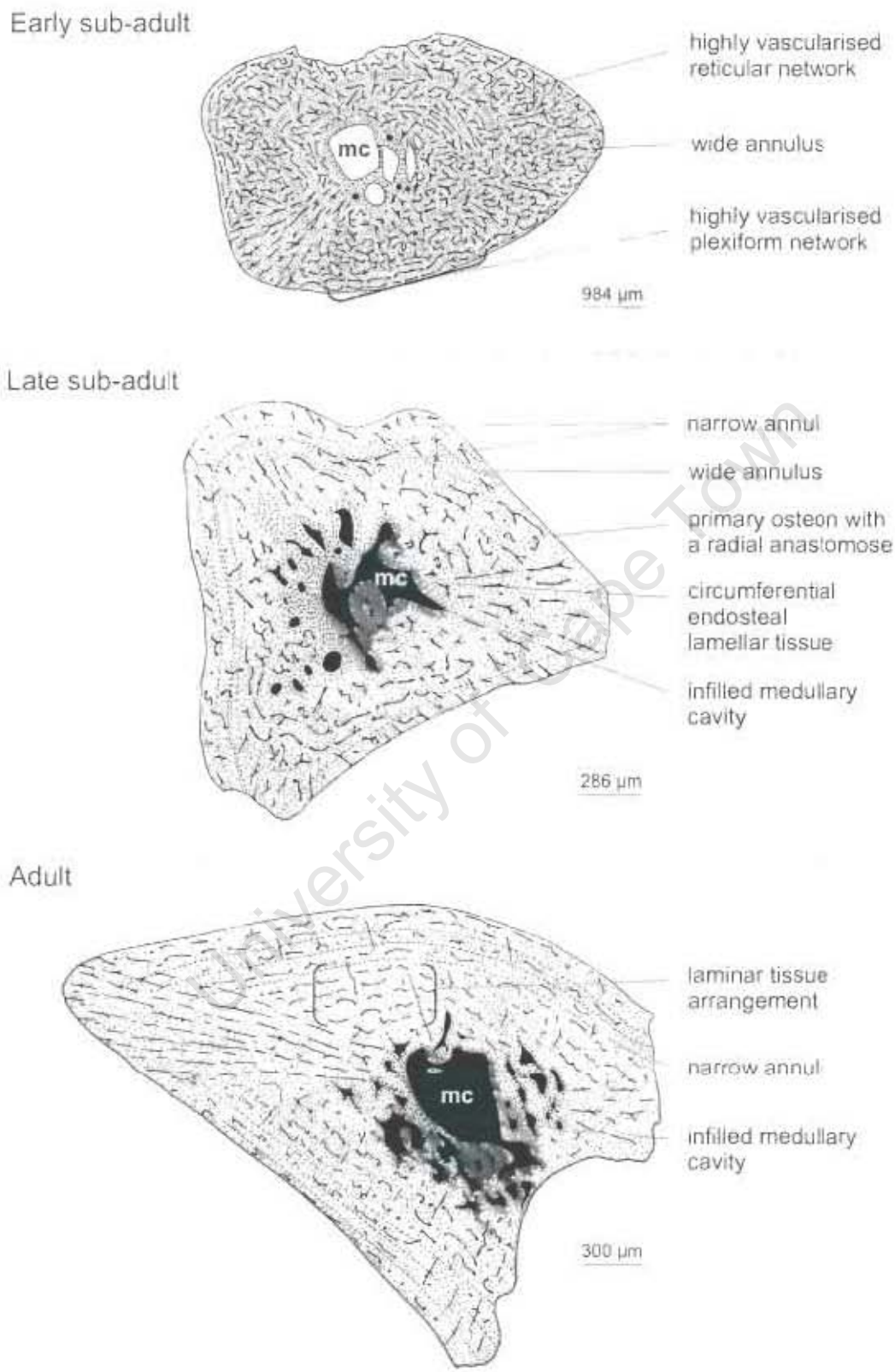


Figure 6.28. Schematic histology of the humeral ontogenetic series of *Diademodon* showing the changes in histological organisation through ontogeny. MC indicates medullary cavity

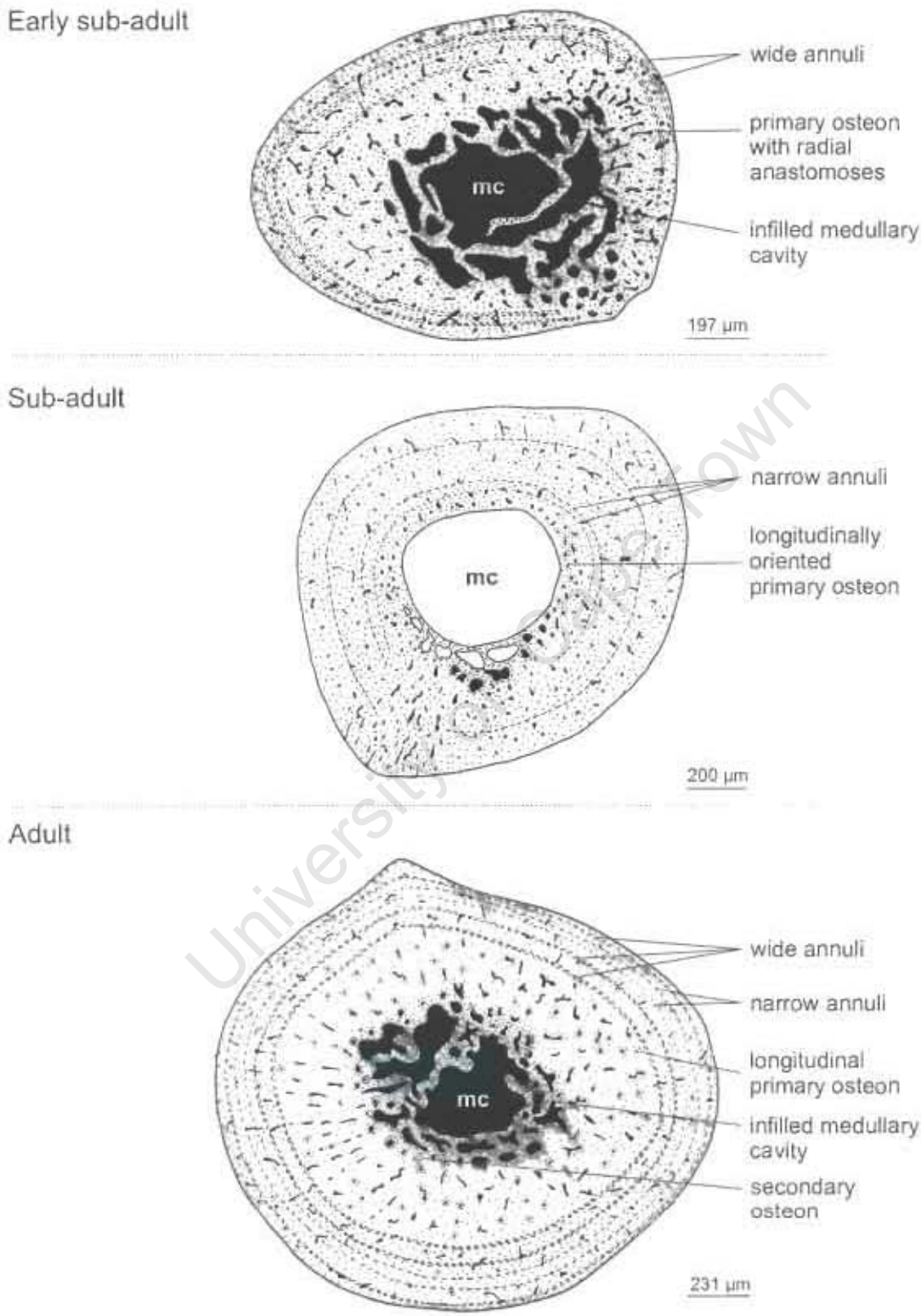


Figure 6.29. Schematic histology of the femoral ontogenetic series of *Diademodon* showing the histological variation through ontogeny. MC indicates medullary cavity.

Sub-adult

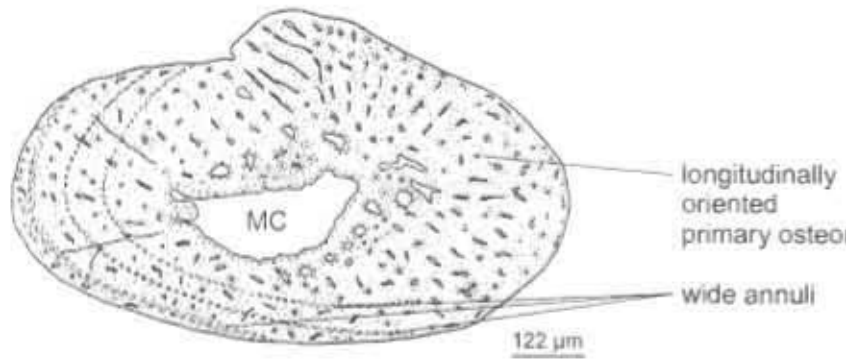


Adult

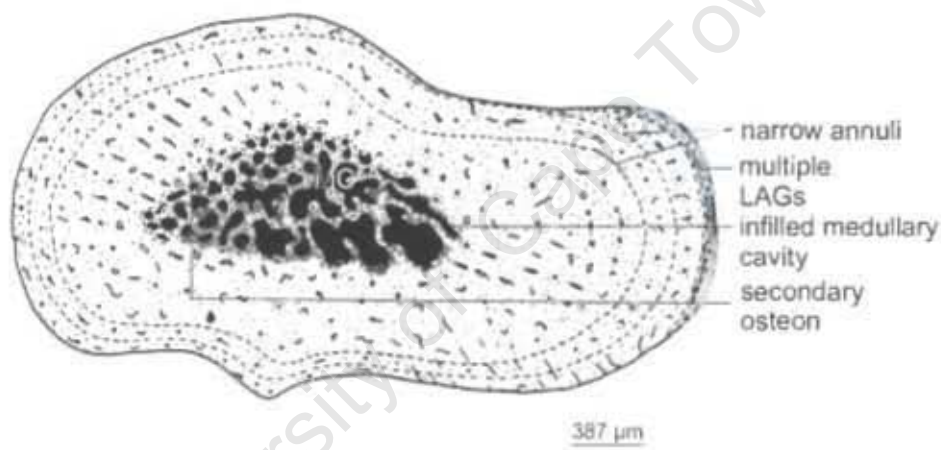




Figure 6.30. Schematic histology of the tibia ontogenetic series of *Diademodon* showing the changes in tissue organisation through ontogeny. MC indicates medullary cavity.

Where possible, the percentage channel area was calculated for each element, using the midshaft region. The values are presented graphically for the humeral, femoral and tibia ontogenetic series. The radius (SAM-PK-K8971b), ulna (SAM-PK-K8971c) and fibula (UMCZ T448) values are 7.28%, 4.56% and 1.52% respectively. Although not statistically significant, a trend of decreasing vascular density with age is shown for each age class (Figures 6.31, 6.32 and 6.33). In addition, if the tibiae are compared with the humeri and femora, the sub-adult and adult tibia values are lower than those of the other sub-adult and adult elements. The sub-adult fibula vascular density is also lower than that of any of the other elements in the sub-adult age class.

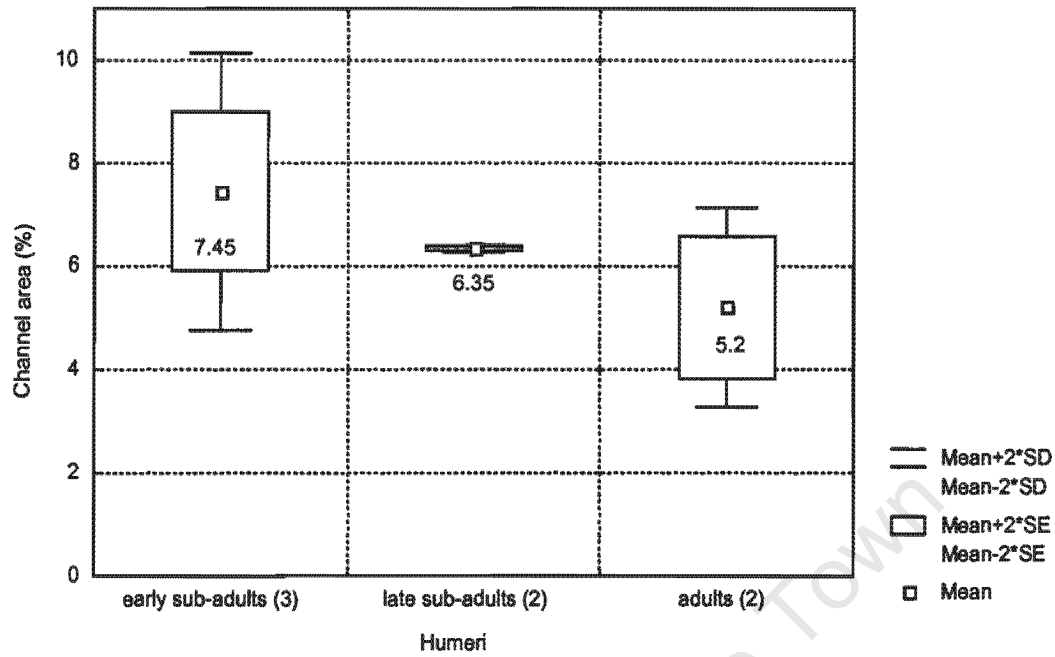


Figure 6.31. *Diademodon* midshaft percentage channel area of the humeral ontogenetic series. The number of elements used to obtain the percentage channel area for each age class is indicated by the numbers in brackets. Values associated with the boxes represent the mean value for each age class.

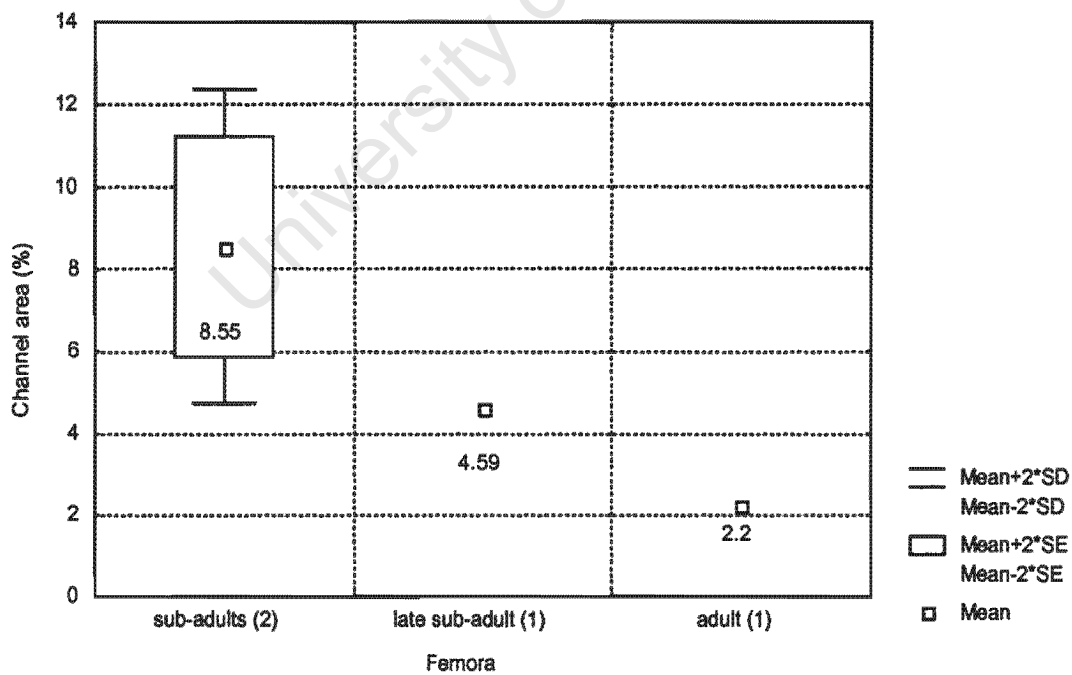


Figure 6.32. *Diademodon* midshaft percentage channel area of the femoral ontogenetic series. The values associated with the box and the numbers in brackets as in Figure 6.31.

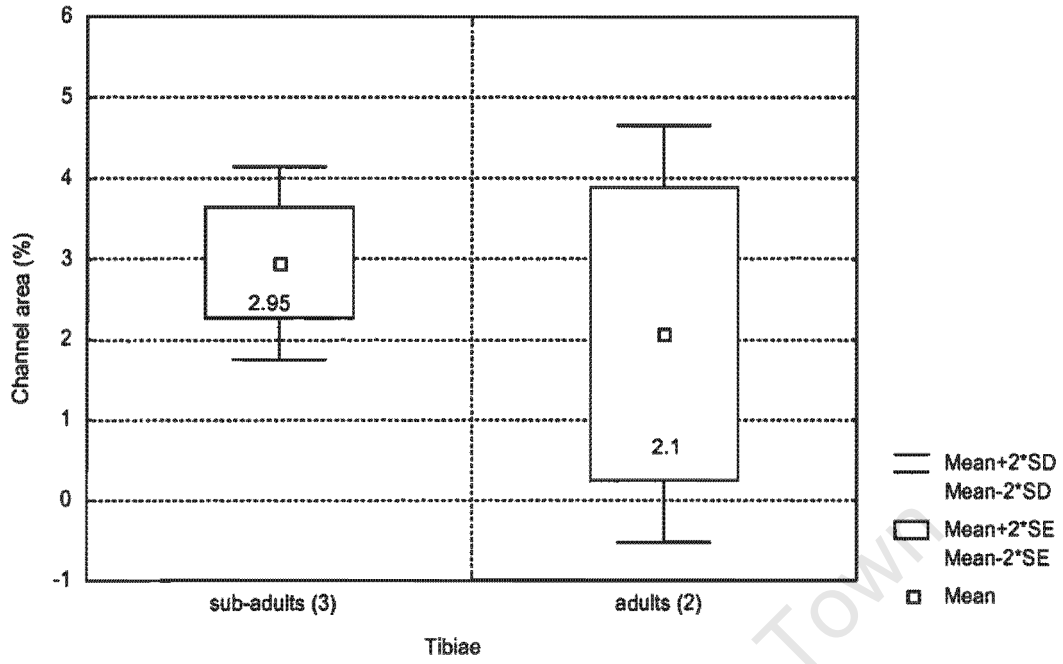


Figure 6.33. *Diademodon* midshaft percentage channel area of the tibia ontogenetic series. The numbers associated with the boxes and values in brackets as in Figure 6.31.

## 6.4 Interpretations

### 6.4.1 *Cynognathus* Biology

The RBT values of the *Cynognathus* humerus (22.35%) and femora (33.07%) were found to be significantly different. This may be due to a difference in element age as the bone histology of the humerus indicates that this element is from a younger individual than the femora. An older humerus may have a higher RBT value, but more material is required in order to deduce this. *Cynognathus* is not known to possess any modifications for a specific lifestyle that would require a high limb bone density. More material is required to make reasonable deductions regarding the lifestyle habits of this animal. However, *Cynognathus* was a large (up to 2m in length) robust carnivore and the high femoral RBT may be due to biomechanical adaptations to a large size.

The K-values (0.34-0.56) suggest that the limb bones are selected for impact loading and ultimate strength, which is expected due to the large size of this animal. The femoral values are lower than that of the humerus possibly because the femora represent older and therefore larger individuals. Animals

necessary for an active animal. The lower percentage channel area of the ulna (7.09%) compared to the humerus and femora suggests that this element grew more slowly than the other limb bones. Peripheral rest lines are absent from all elements. This suggests that either *Cynognathus* had an indeterminate growth strategy, whereby it grew continuously throughout life or that the largest femur (NMQR3019a), although designated as an adult, represents an early adult, which has not yet reached adult size.

### 6.4.2 *Diademodon* Biology

All the *Diademodon* RBT values exceed 30%, with the exception of an early sub-adult humerus (SAM-PK-K8971a), the sub-adult femora (UMCZ T495, UMCZ T503) and the late sub-adult femur (UMCZ T493) (see Table 6.3). However, the RBT values of the radius and ulna, which belong to the same individual as the humerus SAM-PK-K8971a, exceed 30%. The persistence of such high limb bone densities raises the possibility that *Diademodon* may have been fossorial or semi-aquatic. *Diademodon* is not known to have any particular modifications for a fossorial lifestyle, such as a particularly long olecranon process, large relatively flat, wide and straight ungula phalanges or a modified posture, which is important for digging as the forelimbs need to be released from supporting the animal's weight during digging (Bargo et al., 2000). Bou et al. (1990), in a study on 25 species of insectivores and rodents, found that fossorial animals frequently have relatively thick bones, but this characteristic was not consistent (which is the case with *Diademodon*).

There is no morphological evidence to suggest that *Diademodon* was semi-aquatic either. Wall, (1983) showed that the amphibious *Hippopotamus amphibius* has a very high bone density, yet if the fossilized remains of this animal were found the skeletal morphology would not suggest an amphibious lifestyle. The fact that practically all the *Diademodon* limb bone RBT values exceed 30% strongly suggests a semi-aquatic lifestyle. The only limb bones whose values fall below 30% are the much smaller elements that represent younger individuals. This may be expected as relative bone wall thickness

increases with age (Heinrich and Biknevicus, 1998). *Diademodon* was a relatively large animal, similar in size to *Cynognathus,* but such high values even in the sub-adult elements and some of the early sub-adult elements cannot be explained by large size alone. Secondly, the limb bones of *Diademodon* tend to be relatively slender and Bou et al.'s study (1990) showed that the bones of swimming species tended to have relatively more slender bones than fossorial forms, possibly because movement through water imposes smaller loads than does digging in soil.

If *Diademodon* was semi-aquatic, it would not necessarily possess the morphological modifications that a fully aquatic animal would have, as it would have needed to function efficiently both in the water and on land (Stein, 1989). Modifications for swimming would therefore perhaps be less specialised compared to a fully aquatic animal. Therefore, if *Diademodon* was not an active swimmer and behaved in a similar manner to *Hippopotamus amphibius,* it would not have clear specialised morphological swimming modifications.

The K-values are low and decrease with age. They are closest to those values selected for impact loading and ultimate strength, similar to *Cynognathus*, which is expected, as *Diademodon* was a large animal.

The *Diademodon* material includes an ontogenetic series of the humerus and femur and a partial ontogenetic series of the tibia. The extent of this material allows deductions regarding the changes in growth strategy through ontogeny to be made for this genus. Interruptions in growth, in the form of annuli or LAGs or both, are present in all elements throughout the ontogenetic ranges and suggest that *Diademodon* had a cyclical growth strategy that may have been seasonally influenced as the climate was semi-arid with seasonal rainfall (Smith et al., 1993).

The limb bones were divided into age classes according to their percentage adult size, prior to thin sectioning. The analysis of the bone histology of these

limb bones shows that the histological patterns are in accordance with the age class divisions. The general pattern is that the younger elements exhibit a relatively low RBT, high percentage channel area and poorly organised tissue pattern compared to the older elements. RBT generally increases, the vascular density decreases and the tissue organisation also increases with age.

The reticular to plexiform fibro-lamellar tissue, the high percentage channel area and slight secondary reconstruction in the early sub-adult limb bones is in accordance with young, rapidly growing individuals. The high vascular density is possibly due to higher energy demands during early ontogenetic growth. Interruptions in growth are exhibited as annuli. LAGs are absent in this age class, except in the humerus B/P/I/3772, indicating that generally, there was an intermittent slowing down in bone growth in young individuals, but that growth did not cease completely.

The bone tissue of the radius (SAM-PK-K8971b) and ulna (SAM-PK-K8971c) are both similar to that of the humerus (SAM-PK-K8971a), but the vascular density in the ulna (4.56%) is distinctly lower than the radius (7.28%). The vascular canals in the ulna are mostly longitudinally oriented primary osteons, which indicates rapid growth, but the number of vascular canals is less, leading to a low percentage channel area. This suggests that the ulna grew more slowly compared to the radius or humerus of this individual.

The later sub-adults exhibit higher RBT values and a slightly lower percentage channel area, which decreases towards the sub-periosteal surface. The adult elements have even higher RBT values than the sub-adults, an even lower percentage channel area, LAGs associated with the annuli, more secondary reconstruction and in the humeri and femora, a distinctly more organised tissue pattern. The increase in LAG number with age indicates that not only did growth slow down during the unfavourable season, but that it ceased completely. This suggests an overall slowing down in bone growth with age. The progressive increase in secondary reconstruction with an increase in

element size also suggests that it is age related. The overall vascular density of the adult humeri (5.2%) is higher than that of the adult femur (2.2%) and adult tibiae (2.1%), which suggests that the humeri may have grown more rapidly than the femora or tibiae.

Compacted coarse cancellous tissue is observed in the delto-pectoral crest regions of the humeri and is probably due to M. pectoralis and M. brachialis (cf. Jenkins, 1971). Secondary remodelling and bone drift is more extensive proximomedial to the tibia ridge and may be the origin of a pedal dorsiflexor (cf. Jenkins, 1971).

The bone tissue of *Diademodon* is notably less vascularised than that of *Cynognathus*. This is probably due not only to the lower number of vascular canals in the *Diademodon* bone tissue, but also to the presence of avascular or poorly vascularised annuli in the cortex, which would decrease the overall vascularisation of the tissue. The uninterrupted fibro-lamellar bone tissue in *Cynognathus* results in a higher overall vascularisation of the cortex. These vascularisation differences as well as the difference in their overall tissue organisation, may suggest that *Diademodon* was less active than *Cynognathus*.

The fibula, sub-adult tibia (UMCZ T447) and adult tibiae (NMQR1208i and NMQR1208j) exhibit multiple LAGs thoughout the cortex. The multiple LAGs cover a larger cross-sectional area at the periphery of the adult tibiae, compared to the rest of the cortex. These multiple LAGs may represent peripheral rest lines. If this is the case, it would suggest that *Diademodon* had a determinate growth strategy. *Diademodon* would then have reached a maximum size and would not have grown throughout its life. Only small amounts of accretionary bone would then be deposited each season. On the other hand, the largest humerus, NMQR1208e, is 95.85% of the adult size and does not exhibit multiple LAGs at the sub-periosteal surface, which would be expected, as the element is old enough to do so. Alternatively, the tibia may have grown more slowly than the humerus, exhibiting multiple LAGs as a

general pattern and the increased number of multiple LAGs at the periphery may represent a particularly unfavourable season and may just be a continuation of the multiple LAG pattern seen throughout the rest of the cortex.

Growth rings were not used to estimate individual ages due to a discrepancy in the back calculations. Back calculations use the distance between growth rings in the youngest element to calculate the "missing" growth rings in older elements. Older humeri often exhibit fewer growth rings than younger humeri, which is generally attributed to secondary remodelling and the resorption of earlier growth rings. However, in a number of cases in this study, irrespective of ontogenetic age, growth rings are only present in the *Diademodon* elements from the mid-cortex outwards and sometimes only in the outer cortex. In these cases, there is a large amount of unremodelled primary tissue prior to the growth rings. This observation suggests that back calculations would falsely increase the number of "supposed" growth rings in an element and would therefore incorrectly estimate the individual age.

The overall growth strategy of *Diademodon* alternates between rapidly forming fibro-lamellar bone and slowly forming annuli of lamellar bone early in ontogeny. Older elements exhibit slower growth whereby the fibro-lamellar bone is less vascularised and the interruptions in growth are usually in the form of LAGs and not just annuli (apart from the adult humerus NMQR1208e, which only exhibited annuli).

# CHAPTER SEVEN
# *TRIRACHODON* BIOLOGY

*Summary*

*The cross-sectional geometry and bone histology of the postcrania of the Early to Middle Triassic non-mammalian cynodont, Trirachodon, was examined in order to deduce aspects of its biology. A brief description of its morphological characteristics based on earlier studies is given, followed by a materials and localities section. Cross-sectional geometry results were obtained from elements representing different ontogenetic ages. The relative bone wall thickness values of the sub-adults are less than 30%, whereas the value of an older femur exceeds 30%. Although more material is required to make reasonable deductions regarding the lifestyle habits of this animal, this result agrees with Groenewald et al.'s (2001) proposal that Trirachodon was fossorial. The K-values (0.4 - 0.5) suggest that Trirachodon limb bones are selected for impact loading and ultimate strength, which may be linked to modifications for a fossorial lifestyle. The histological analysis shows fibro-lamellar bone tissue, indicating rapid growth, which is interrupted by growth rings, suggesting that Trirachodon had a cyclical growth strategy that may have been seasonally influenced. Annuli are present, but LAGs are absent from younger elements, suggesting that growth slowed down during the unfavourable season, but did not cease completely. LAGs are more prominent in the older tibiae, suggesting either that overall growth slowed down with age or that the tibiae grew more slowly than the other elements, or both. Interruptions in growth are absent from the radius, but a region of parallel-fibred bone is observed towards the sub-periosteal surface. The younger femur and tibia diameters are larger than those of the older femur and tibiae. The lack of a size/histology correlation in this case may be due to a species difference or sexual dimorphism.*



## 7.1 Functional Morphology

*Trirachodon*, a derived herbivorous non-mammalian cynodont, is closely related to *Diademodon*, the main differences being a smaller body size (up to 50cm in length, similar in size to *Thrinaxodon*) and a difference in the structure and number of the postcanines. *Trirachodon* has fewer postcanines, which are shorter anteroposteriorly and broader transversely than *Diademodon* (Seeley, 1895b; Crompton and Ellenberger, 1957; Kemp, 1982). The skull is also narrower in the posterior region, the zygomatic arches are more slender and

almost parallel and the snout is short and not bulbous as in *Diademodon*. (Seeley, 1895b).

Recent evidence suggests that *Trirachodon* was a burrowing animal (Groenewald et al., 2001). A burrow complex was recently excavated from the Early Triassic, Driekoppen Formation of South Africa and has been attributed to *Trirachodon,* based on a number of disarticulated skulls and skeletons of at least 20 individuals recovered from a nearby, but less well-preserved burrow system. The specimens display typical gomphodont teeth and the canines are well developed, but the incisors are small, which indicates that food processing took place at the back of the mouth. This is in contrast to permanently fossorial animals where food processing mainly involves the incisors, at the front of the mouth. This has lead to the suggestion that *Trirachodon* did not live permanently in the burrows, but surfaced regularly, probably to look for food (Groenewald et al., 2001).

*Trirachodon* had a stance and gait similar to that of *Cynognathus* and *Diademodon* (Kemp, 1982).

*Trirachodon* is one of the few therapsid genera where qualitative morphological changes can be examined within a taxon's stratigraphic range. The earliest form (known only from recently collected material) exhibits sectorial teeth along most of its tooth row, whereas the succeeding morphospecies (*Trirachodon kannemeyeri*), has transversely widened gomphodont teeth in the anterior region of its tooth row, but sectorial teeth at the back of the tooth row. The next succeeding species (*Trirachodon berryi*) has a full complement of gomphodont teeth (Rubidge and Sidor, 2001). Differences between these species may also be exhibited in their growth patterns and may not be limited to their dentition alone.

## 7.2 Materials and Localities

The *Trirachodon* material consists of seven limb bones (radius, ulna, femora, tibiae), two scapulae and two ribs (Table 7.1), recovered from various localities in the *Cynognathus* Assemblage Zone, Beaufort Group, South Africa (see Figure 7.1).

Table 7.1. The *Trirachodon* specimens used in this study and the localities from where the specimens were recovered. The SAM-PK-K5881 specimens were recovered from a bone bed, the CGP1/79 specimens belong to a single individual and the NMQR3282 specimens were found in a matrix that included two similar sized lower jaws. See Appendix 1 for institutional abbreviations.

| District | Specimen number | Skeletal element | Number of sections | Region sectioned |
|---|---|---|---|---|
| Aliwal North | SAM-PK-K5881a | femur | 6 | midshaft/proximal |
| | SAM-PK-K5881b | tibia | 5 | midshaft/proximal |
| | SAM-PK-K5881c | tibia | 3 | midshaft/proximal |
| | SAM-PK-K5881d | rib | 2 | midshaft |
| | SAM-PK-K5881e | rib | 2 | midshaft |
| | SAM-PK-K5881f | scapula | 2 | proximal fragments |
| | SAM-PK-K5881g | scapula | 3 | proximal fragments |
| Bergville | CGP1/79a | radius | 4 | midshaft |
| | CGP1/79b | ulna | 4 | midshaft |
| Kestell | NMQR3282a | femur | 7 | midshaft |
| | NMQR3282b | tibia | 5 | midshaft |

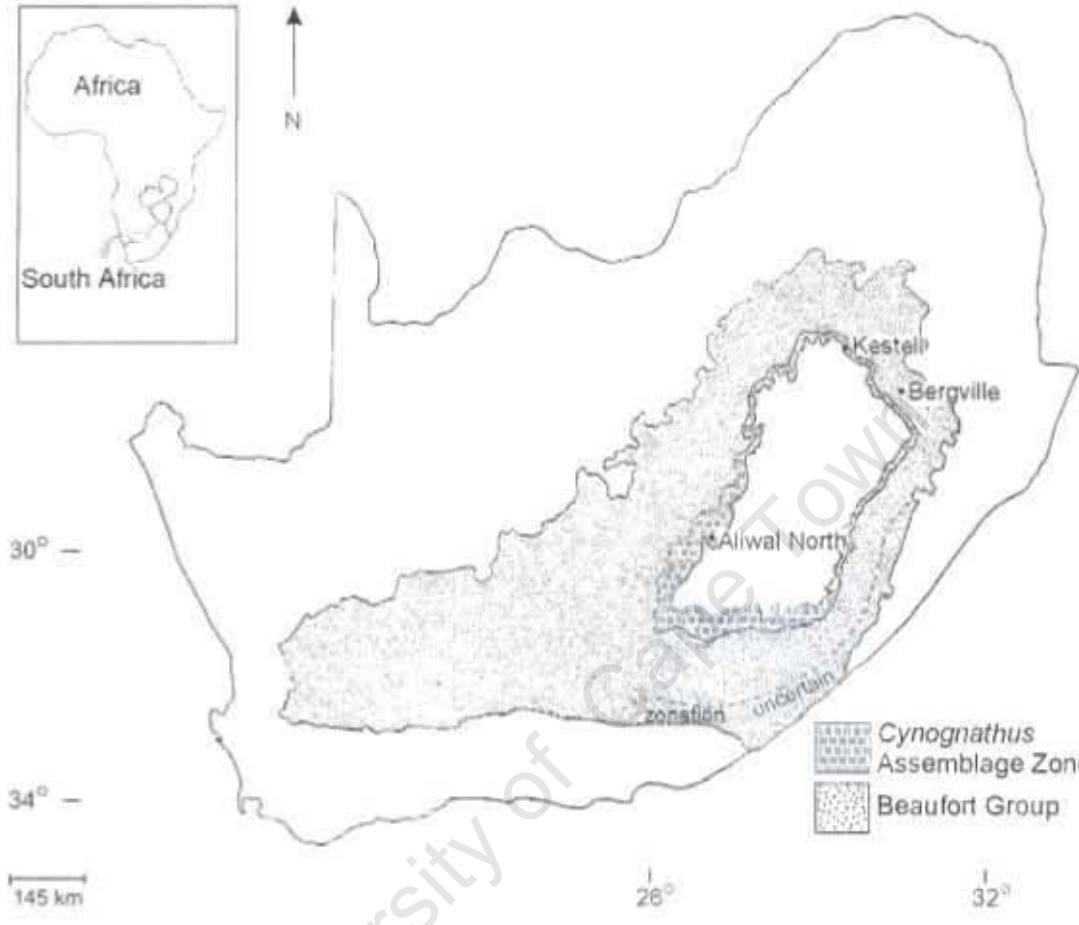




Figure 7.1. *Cynognathus* Assemblage Zone, Burgersdorp Formation, Beaufort Group, South Africa. The material was recovered from localities near the towns Aliwal North, Bergville and Kestell. Map compiled from the Reader's Digest Illustrated Atlas of Southern Africa (1994) and Kitching (1995).

## 7.3 Results

### 7.3.1 Macro-analysis

Where possible, the diameter, proximal width and total length of each skeletal element was measured in order to obtain the percentage adult size (Table 7.2).

Table 7.2. Gross measurements of the various *Trirachodon* skeletal elements.

| Specimen number | Skeletal element | Diameter (mm) | Proximal width (mm) | Length (mm) | % Adult |
|---|---|---|---|---|---|
| CGP1/79a | radius | 3.34 | - | 40.86 | - |
| CGP1/79b | ulna | 5.55 | - | 40.07 | - |
| NMQR3282a | femur | 5.01 | 9.08 | 39.88 | - |
| SAM-PK-K5881a | femur | - | 22 | 89.8 | - |
| NMQR3282b | tibia | 4.76 | 9.15 | 89.8 | 50.15 |
| SAM-PK-K5881b | tibia | - | 13 | 45.14 | 72.22 |
| SAM-PK-K5881c | tibia | - | 18 | 62.5 | 100 |
| SAM-PK-K5881d | rib | 3.24 | - | - | - |
| SAM-PK-K5881e | rib | 2.83 | - | - | - |
| SAM-PK-K5881f | scapula | 3.34 | - | - | - |
| SAM-PK-K5881g | scapula | 7.06 | - | - | - |

Relative bone wall thickness measurements (RBT) (Figure 7.2) and K-values (Table 7.3) were obtained from the limb bones in order to assess the lifestyle habits of *Trirachodon*. Measurements were taken from the midshaft regions of each bone.

Figure 7.2 shows that there is not a marked variation in RBT between the different elements, although the mean value of the femur SAM-PK-K5881a is higher than that of the femur NMQR3282a.

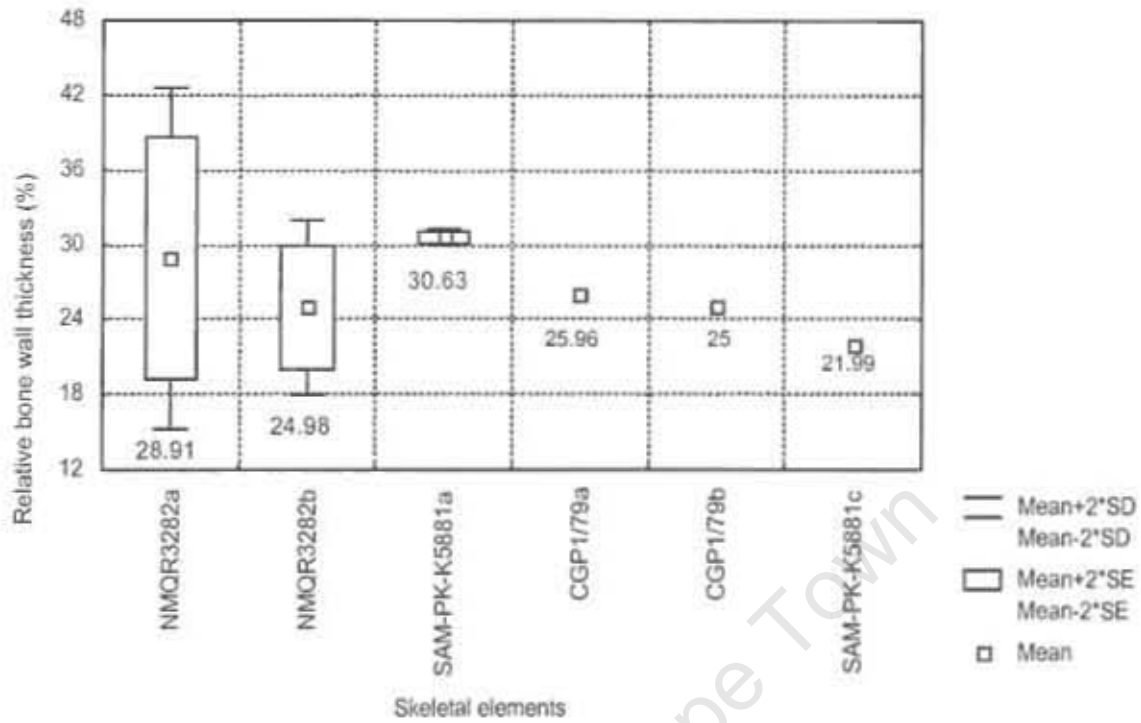


Figure 7.2. Relative bone wall thickness values of the *Trirachodon* limb bones. The values associated with the boxes indicate the mean value of those individuals. NMQR3282a and SAM-PK-K5881a are femora, NMQR3282b and SAM-PK-K5881c are tibiae, CGP1/79a is a radius and CGP1/79b is an ulna.

Table 7.3. *Trirachodon* limb bone K-values. The rest of the limb bones could not be measured due to their fragmentary nature.

| Specimen number | Skeletal element | K-value |
|---|---|---|
| CGP1/79a | radius | 0.47 |
| CGP1/79b | ulna | 0.5 |
| NMQR3282a | femur | 0.43 |
| SAM-PK-K5881a | femur | 0.4 |
| NMQR3282b | tibia | 0.5 |

### 7.3.2 Micro-analysis

A detailed histological analysis of the *Trirachodon* postcrania was undertaken. The tissue organisation of all elements is zonal. In most elements, the zones consist of moderately vascularised fibro-lamellar tissue, which alternate with either poorly vascularised annuli or LAGs.

The femur NMQR3282a exhibits highly vascularised fibro-lamellar tissue and is interrupted by two narrow incomplete annuli (Figure 7.3). The vascular canals are arranged in a reticular network and the osteocyte lacunae are globular and radiate branched canaliculi. The inner annulus forms an almost complete circle, disappearing on the ventro-medial side and the outer annulus disappears on the dorso-lateral and ventro-medial sides of the bone. The annuli are poorly defined, but the osteocyte lacunae are more organised in these regions and can be distinguished from the rest of the cortical tissue. There is no indication of a decrease in vascularisation at the periphery and little secondary remodelling is present.

The bone tissue of the femur SAM-PK-K5881a consists of fibro-lamellar tissue (Figure 7.4), which is slightly less vascularised than the femur NMQR3282a. The osteocyte lacunae are similar to the femur NMQR3282a described above, but they become more organised in a parallel-fibred region of bone, observed at the outer margin. Small secondary osteons are seen around the medullary cavity towards the metaphysis. Bone drift occurs in the lesser trochanter region, where reworked tissue almost reaches the sub-periosteal surface. The dorsal and lateral sides of the bones contain more compact tissue than the ventral and medial regions. The vascular canals form a radial network from the medullary cavity to the surface in the region of the lesser trochanter and a network of bony trabeculae can be seen in the proximal metaphysis in longitudinal section.

The radius (CGP1/79a) and ulna (CGP1/79b) are described together as they were obtained from a single individual. The bone tissue of the radius consists

of moderately vascularised, fibro-lamellar tissue, which becomes less vascularised and more organised towards the periphery to form parallel-fibred bone (Figure 7.5). Vascular canals vary from longitudinal primary osteons with radial anastomoses to radially oriented canals. The ulna exhibits zonal bone tissue, consisting of moderately vascularised fibro-lamellar tissue, intermittently interrupted by poorly vascularised annuli of lamellar tissue (Figure 7.6). The vascular canals are mostly longitudinally oriented primary osteons. A reversal line is observed in the peri-medullary region. The osteocyte lacunae in both bones are similar to the femora and a few small secondary osteons are recognised in the peri-medullary regions. Sharpey's fibres are seen in the ulna crest region.

The tissue of the tibia NMQR3282b (Figure 7.7) is very similar to that of the femur NMQR3282a. The moderately vascularised tissue forms a reticular network and is interrupted by two narrow poorly defined annuli, similar to the femur NMQR3282a.

Longitudinally oriented primary osteons dominate the tissues of the tibiae SAM-PK-K5881b and SAM-PK-K5881c. The tissue is intermittently interrupted by annuli, which are sometimes associated with LAGs (Figure 7.8). The globular osteocyte lacunae contain radiating canaliculi, similar to the elements just described above. Secondary osteons are observed, distributed throughout the cortex, in both elements. Extensive secondary remodelling can be seen, especially on the medial side in SAM-PK-K5881c as thin sections were taken mostly from the proximal metaphyseal region. The more proximal sections of SAM-PK-K5881b show extreme secondary remodelling which reaches a parallel-fibred region at the periphery of the bone.


Figure 7.5.

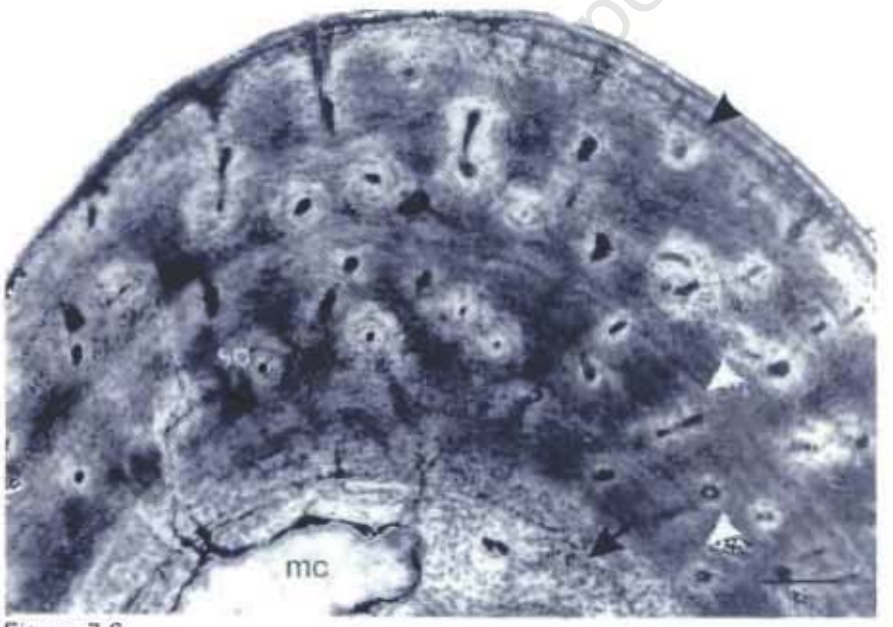


Figure 7.6.

Figure 7.5. Transverse section of the *Trirachodon* radius CGP1/79a. The tissue alters from fibro-lamellar bone in the mid-cortex to parallel-fibred tissue towards the outer margin (➔).

Figure 7.6. Transverse section of the *Trirachodon* ulna CGP1/79b. The fibro-lamellar tissue is intermittently interrupted by annuli (➤) and a reversal line is observed in the peri-medullary region (➔). A few secondary osteons are distributed throughout the cortex.

Scale bars =125μm
mc, medullary cavity; so, secondary osteon

The bone tissue of the scapulae SAM-PK-K5881f and SAM-PK-K5881g consist of fibro-lamellar tissue, interrupted by annuli. The annuli are more prominent in the smaller scapula (SAM-PK-K5881f). One annulus can be seen towards the sub-periosteal surface of SAM-PK-K5881g. Longitudinally oriented primary osteons dominate in SAM-PK-K5881f (Figure 7.9), whereas radial anastomoses are associated with the vascular canals in SAM-PK-K5881g (Figure 7.10). Secondary osteons are observed scattered throughout the cortex in SAM-PK-K5881f, but are more abundant in the peri-medullary region.

The ribs SAM-PK-K5881d and SAM-PK-K5881e consist of moderately vascularised fibro-lamellar bone interrupted occasionally by LAGs (Figure 7.11). In some places, multiple LAGs occur together at intervals. The vascular canals are mostly longitudinally oriented primary osteons and are just as abundant at the surface as they are in the mid-cortex. Secondary osteons are common and may reach the outer cortex in some areas, but are more abundant around the medullary cavity. Numerous trabeculae extend into the medullary cavity area and abundant small resorption cavities are present.

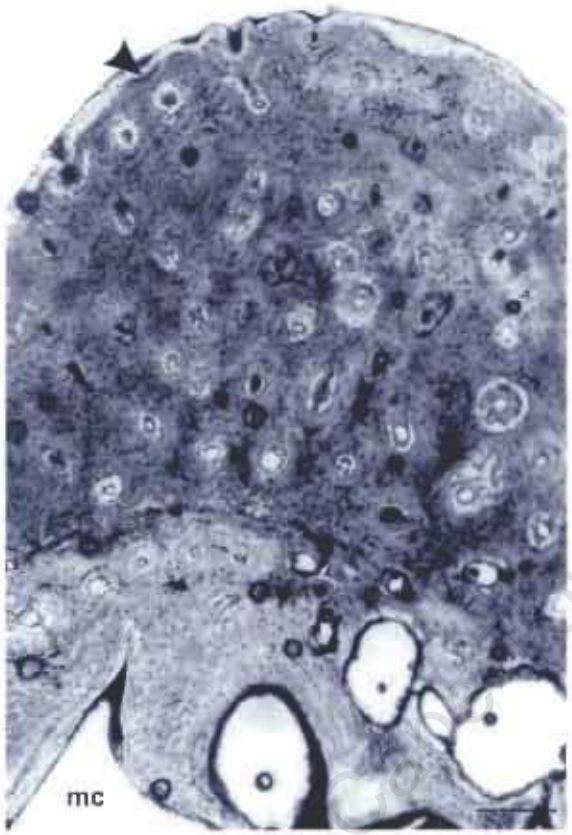


Figure 7.9.

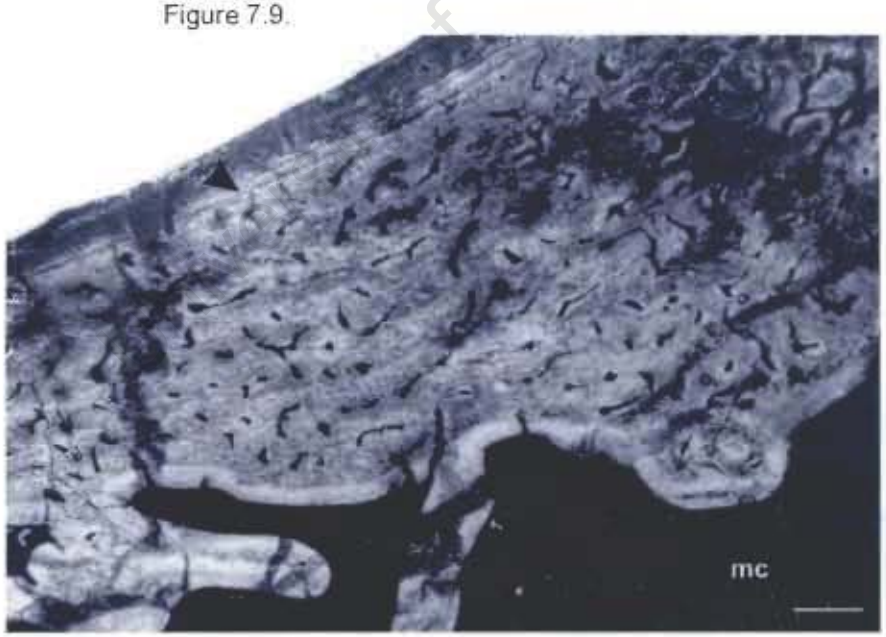


Figure 7.10.

Figure 7.9. Transverse section of the *Trirachodon* scapula SAM-PK-K6881f. Longitudinal primary and secondary osteons are abundant. An annulus is observed at the outer margin (►).

Figure 7.10. Transverse section of the *Trirachodon* scapula SAM-PK-K6881g. The vascular canal organisation differs markedly from the scapula SAM-PK-K5881f, shown above. A LAG at the sub-periosteal surface is indicated by (►). There are few longitudinally oriented primary osteons and numerous radial anastomoses.

Scale bars =125μm

so, secondary osteon; po, primary osteon; mc, medullary cavity


Figure 7.11. Transverse section of the *Trirachodon* rib SAM-PK-K5881d, showing abundant longitudinally oriented primary and secondary osteons throughout the cortex. A LAG is shown near the outer margin (►).

Scale bar =125µm

po, primary osteon; so, secondary osteon; mc, medullary cavity

The channel area was quantified for all the limb bones except the tibia, SAM-PK-K5881b, as no midshaft region was available. Figure 7.12 shows a marked distinction between the percentage channel area of the femur NMQR3282a and tibia NMQR3282b and the rest of the limb bones.

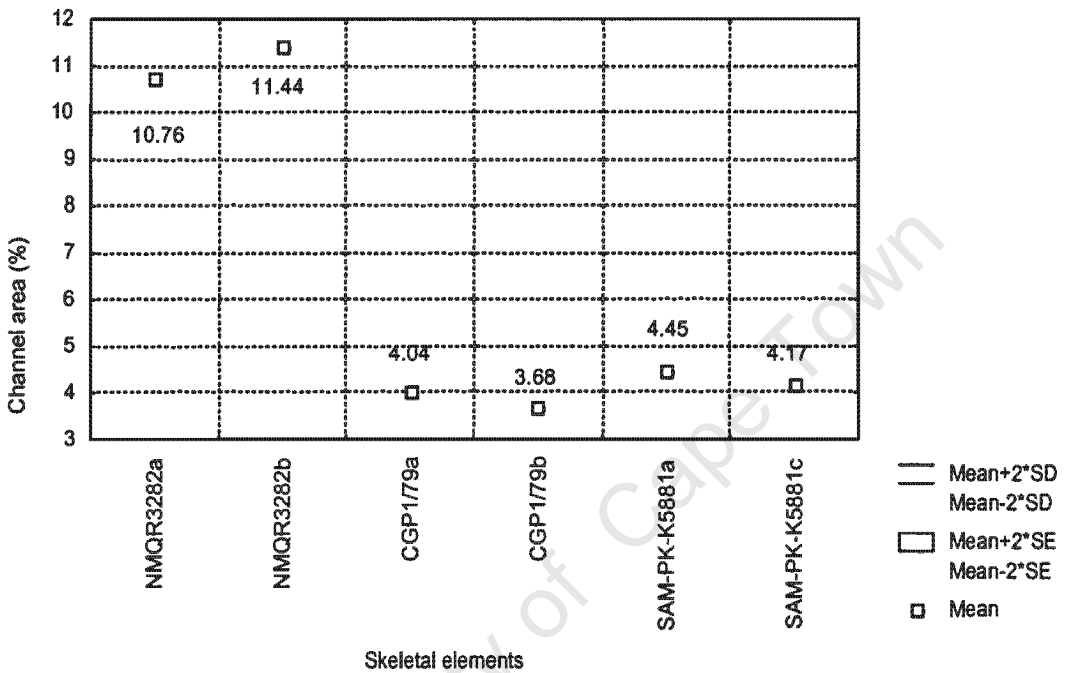


Figure 7.12. *Trirachodon* midshaft percentage channel area. Individual elements have been plotted separately due to distinct differences in their percentage channel area. NMQR3282a and SAM-PK-K5881a are femora, NMQR3282b and SAM-PK-K5881c are tibiae, CGP1/79a is a radius and CGP1/79b is an ulna.



## 7.4 Interpretations

*Trirachodon* specimens are rare, which has posed a difficulty in obtaining gross limb bone measurements for the estimation of percentage adult sizes for the elements in this study. Hence, most of the individual ages were estimated using bone histology analysis.

The femur NMQR3282a and tibia NMQR3282b were found with two similar sized lower jaws, identified as *Trirachodon,* in a block of matrix. The elements may both belong to one individual, but if they are not, they are from similar sized individuals and hence are probably similar in ontogenetic age. The fibro-

lamellar tissue and abundant vascular canals (10.76% channel area in the femur and 11.44% in the tibia) in a reticular network indicates rapid growth. There is also no decrease in vascularisation towards the sub-periosteal surface of either element, suggesting that growth was still rapid at the time of death. Such characteristics suggest that these elements represent a late juvenile or early sub-adult stage/s (depending on whether they represent one or two individuals).

Although it is not known what the percentage adult size of the radius CGP1/79a and ulna CGP1/79b is, the parallel-fibred bone in the outer cortex of the radius indicates a slowing down in bone growth, which suggests that this individual was probably a late sub-adult. The relatively low percentage channel area of both elements (radius 4.04%; ulna 3.68%) also supports this suggestion.

The postcrania recovered from the Aliwal North bone bed (SAM-PK-K5881) represent several individuals of various sizes and probably stages in ontogenetic age, as they have all been diagnosed as a single species, *Trirachodon kannemeyeria*. The tibia SAM-PK-K5881b, at approximately 72% of the adult size, represents a late sub-adult and the tibia SAM-PK-K5881c is designated as an adult. The size of SAM-PK-K5881c, abundance of well-defined annuli and LAGs, secondary remodelling and distribution of secondary osteons throughout the cortex supports these estimations.

Although the femur NMQR3282a is ontogenetically younger than the femur SAM-PK-K5881a, they exhibit similar mean RBT values. These values indicate a relatively thick bone wall and agree with the proposal that *Trirachodon* was fossorial (Groenewald et al., 2001), especially since both femora of varying ontogenetic age exhibit relatively thick bone walls. As a fossorial animal, relatively thick limb bones would be advantageous for digging (Bou et al., 1990; Casinos et al., 1993). Although a humerus is required to establish if both fore and hindlimbs are modified, the femur of the naked mole rat (*Heterocephalus glaber*), which lives in extensive burrow complexes, also has a percentage RBT

of approximately 31%. Furthermore, a number of burrowing or digging lizards such as *Gerrhonotus grantis, Heloderma suspectum* and *Phrynosoma douglassi* and the new world porcupine *Erethizon,* which is known to burrow, also have femoral RBT values above 30% (see Appendix 3).

The K-values (0.4 - 0.5) suggest that *Trirachodon* limb bones are selected for impact loading and ultimate strength (Currey and Alexander, 1985), similar to *Cynognathus* and *Diademodon. Trirachodon* is smaller than either *Cynognathus* or *Diademodon*, but it may have needed robust limbs for added support during digging.

The presence of fibro-lamellar bone tissue indicates that the overall growth of *Trirachodon* was rapid. The presence of growth rings in almost all the elements studied however, suggests that *Trirachodon* experienced a cyclical growth strategy. The annuli and LAGs indicate that growth slowed down during the unfavourable growing season or in older individuals, even ceased. *Trirachodon* is found in the same deposits as *Cynognathus* and *Diademodon* and it therefore probably experienced similar climatic conditions to these animals (Smith et al., 1993). Hence, these intermittent interruptions in growth may be due to a sensitivity to changes in a seasonal environment.

LAGs are more prominent in the older tibiae SAM-PK-K5881b and SAM-PK-K5881c, suggesting that the overall growth was slower than the other elements. Futhermore, the percentage channel area of the tibia SAM-PK-K5881c (4.17%) is distinctly lower than that of the younger tibia, NMQR3282b (11.44%). This indicates that the overall growth slowed down with age.

Although most of the *Trirachodon* material is fragmentary, the diameter of each element could usually be measured. There is a notable difference in diameter and therefore probably overall size, between the sub-adult femur (NMQR3282a) and tibia (NMQR3282b) and the older femur (SAM-PK-K5881a) and tibiae (SAM-PK-K5881b, SAM-PK-K5881c). It would be expected that the

histologically younger elements would have a smaller diameter than the older ones, however this is not the case. The diameter of the histologically younger NMQR3282 elements is wider than that of the histologically older SAM-PK-K5881 elements. The size difference may be due to taxonomic differences. The NMQR3282 material was collected from Kestell and has only been identified to genus level. This material may therefore represent any of the three morphospecies described by Rubidge and Sidor (2001). The SAM-PK-K material, containing the rest of the specimens, was collected from Aliwal North and has been identified as *Trirachodon kannemeyeria*. The two samples may therefore belong to different species, which may have been different sizes.

Another possibility for the differences in size may be sexual dimorphism. It is possible that the rapid growth in the large femur and tibia (NMQR3282a and NMQR3282b) could be due to selection pressure for large size early in ontogeny, which would be advantageous in male competition for females. Sexual dimorphism, whereby males grow more quickly than do the females has been found in the American alligator, (*Alligator mississippiensis*), box turtles, (*Terrapene* spp.), agama lizards, (*Agama* spp.) and copperhead snakes (*Agkistrodon contortrix*) (Sander, 2000). Alternatively, females may have grown more quickly than males in order to be able to reproduce at an earlier age. Females are known to outsize males in some mammals such as hyenas, bats and whales, as large size provides extra protection and warmth. This phenomenon is also found in birds of prey as well as some reptiles, amphibians (Márquez, et al., 1997) and fish (Ralls, 1976).

# CHAPTER EIGHT
# *TRITYLODON* BIOLOGY

*Summary*

*This chapter includes an examination of the biology of the derived Early Jurassic non-mammalian cynodont, Tritylodon, through the study of the cross-sectional geometry and bone histology of its postcrania. The morphological characteristics of this genus are given, based on earlier published literature. The materials and localities are then provided. The cross-sectional geometry analysis indicates a relatively thick bone wall, possibly as a modification for digging. The histological examination reveals a moderately vascularised uninterrupted, fibro-lamellar bone tissue, which suggests that Tritylodon grew rapidly. Growth rings are absent from all elements except one radius, which may be due to a particularly stressful, unfavourable growing season. The view that many different types of elements should be used when conducting histological studies to assess the histo-variability between elements is emphasised.*

## 8.1 Functional Morphology

According to Rubidge and Sidor (2001), the tritylodontids represent the most highly derived members of the Cynognathia. *Tritylodon* was a relatively long (up to 100 cm in length), slender and short-limbed herbivorous non-mammalian cynodont, with an extremely mammal-like postcanine dentition (Owen, 1884; Seeley, 1895c; Grine et al., 1979a; Kemp, 1982; King, 1996). This animal has an extremely large temporal fenestra and narrow crest-like intertemporal region. With the loss of the postorbital bone (Petronievics, 1917), the orbit and temporal fenestra became confluent, similar to that of primitive mammals (Kemp, 1982). The postcanine teeth are multi-rooted, a feature that is found only in mammals. Canines are absent, but have been replaced by incisors and a long diastema separates the incisors from the enlarged cheek teeth (Kühne, 1943; King, 1996). This animal may have been root-eating, the long incisors being well adapted for digging out and breaking off roots and the molars well-suited to grinding (Broom, 1910). In addition, Sues (1985) noted a long and robust olecranon process on the ulna, which further suggests that this animal was fossorial. The postcranial skeleton is also more mammal-like. Compared to other non-mammalian cynodonts, the humerus is more slender and the

processes are less prominent. The costal plates on the ribs have been lost (Kemp, 1982). The posture and gait of the hindlimb are also comparable with those of primitive extant mammals (Carroll, 1988).

## 8.2 Materials and Localities

The *Tritylodon* material consists of seven limb bones and a rib (Table 8.1) recovered from various localities in the *Massospondylus* Range Zone, Elliot Formation, South Africa (see Figure 8.1).

Table 8.1. The *Tritylodon* material used in this study and the localities from where the specimens were recovered. Those specimens with the same specimen abbreviations were obtained from one individual. Appendix 1 gives the institutional abbreviations.

| District | Specimen number | Skeletal element | Number of sections | Region sectioned |
|---|---|---|---|---|
| Bethlehem | B/P/I/5167 | radius | 10 | complete |
| Clarens | B/P/I/5671 | humerus | 8 | distal |
| Fouriesburg | B/P/I/4785a | humerus | 8 | complete |
| | B/P/I/4785b | radius | 2 | midshaft |
| | B/P/I/4785c | rib | 4 | midshaft |
| Ladybrand | B/P/I/5160 | humerus | 3 | midshaft/proximal |
| | B/P/I/5089 | humerus | 4 | distal |



The Elliot Formation is a typical fluvial redbed succession that is of Late Triassic (Norian) to Early Jurassic (Toarcian) age (Smith and Kitching, 1997). It is composed mostly of floodplain mudstones, siltstones and various grades of sandstone. This formation is often known as the "red beds" due to the diagenetic oxidation of iron, derived from ferruginous silicate and clay minerals, which causes a red colouration (Smith et al., 1993). The middle of the Elliot Formation is marked by a distinctive change in the mudrock colour, which has been interpreted as being the onset of ephemeral stream flow conditions due to an increase in aridity. The Upper Elliot contains mudrocks that are more varied in colour and more fissile, with characteristic siliceous septarian nodules. They

contain minor interbedded sheet sandstones that are often well bioturbated with burrows (Smith and Kitching, 1997).

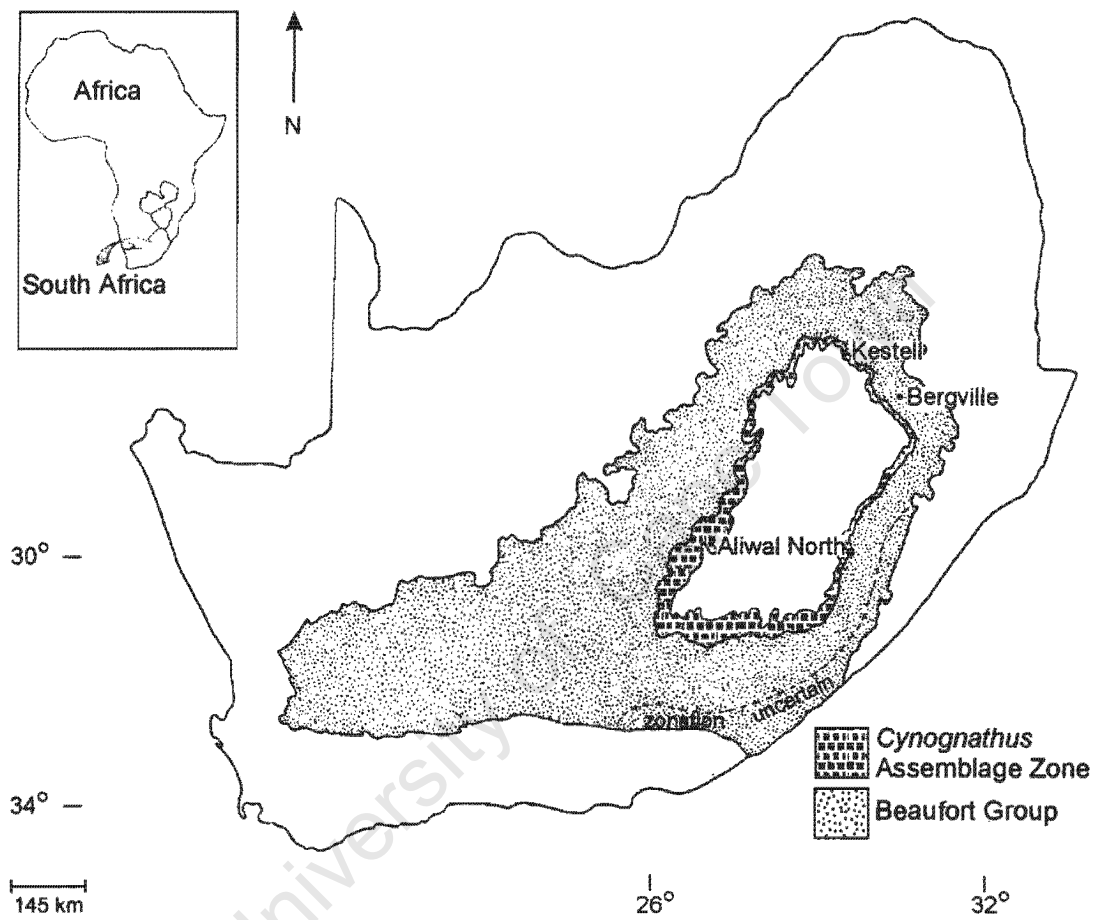


Figure 8.1. Elliot Formation, South Africa. The material was recovered from localities near the towns Bethlehem, Clarens, Fouriesburg and Ladybrand. Compiled from Kitching and Raath (1984), the Reader's Digest Illustrated Atlas of Southern Africa (1994) and Smith pers. comm (2002).

The *Massospondylus* Range Zone lies in the Middle to Upper Elliot Formation (Early Jurassic, Toarcian Stage; Smith and Kitching, 1997). This informal zone was proposed by Kitching and Raath in 1984 and is characterised by the dominance of the prosauropod, *Massospondylus* and the dinosaurs *Syntarsus, Heterodontosaurus, Lesothosaurus* and *Fabrosaurus*. It has not yet been formally designated by the South African Council of Stratigraphy and is therefore not shown in Figure 8.1. A thin horizon in this zone contains an abundance of *Tritylodon* fossils and has been given the name, *Tritylodon* Acme Zone. Fossil fish, crocodilians and a proganochelid turtle, *Australochelys africanus*, as well as *Erythrotherium* and *Megazostrodon*, the first true mammals from South Africa, are also known from this zone (Kitching and Raath, 1984; MacRae, 1999).

## 8.3 Results

### 8.3.1 Macro-analysis

The diameter, proximal width and total length of each skeletal element was obtained for the calculation of the percentage adult size of each element (Table 8.2), so providing individual age estimations for each element. Due to the paucity of *Tritylodon* skeletons, the percentage age of the radius B/P/I/5167 could not be estimated as a fully adult radius was not available for comparison.



Table 8.2. Gross measurements of the *Tritylodon* skeletal elements. The radius B/P/I/4785b and rib B/P/I/4785c belong to the same individual as the humerus B/P/I/4785a.

| Specimen number | Skeletal element | Diameter (mm) | Proximal width (mm) | Length (mm) | % Adult |
|---|---|---|---|---|---|
| B/P/I/5160 | humerus | 7.55 | - | 55.07 | 66.87 |
| B/P/I/4785a | humerus | 7.23 | 22.31 | 52.77 | 64.08 |
| B/P/I/5089 | humerus | 7.64 | - | 55.77 | 67.72 |
| B/P/I/5671 | humerus | 10.03 | - | 82.35 | 100 |
| B/P/I/5167 | radius | 5.99 | 11 | 34.9 | - |
| B/P/I/4785b | radius | - | - | - | 64.08 |
| B/P/I/4785c | rib | 2.72 | - | - | 64.08 |

The relative bone wall thickness (RBT) of the midshaft regions of the humeri B/P/I/5160 and B/P/I/4785a and the radii B/P/I/5167 and B/P/I/4785b was calculated (see Appendix 2 for detailed results). The K-values of these limb bones were also calculated. Figure 8.2 gives the relative bone wall thickness values and indicates a relatively high RBT value. The mean humeral K-value is 0.3 (standard deviation of 0.012) and the mean radial value is 0.32 (standard deviation of 0.057).

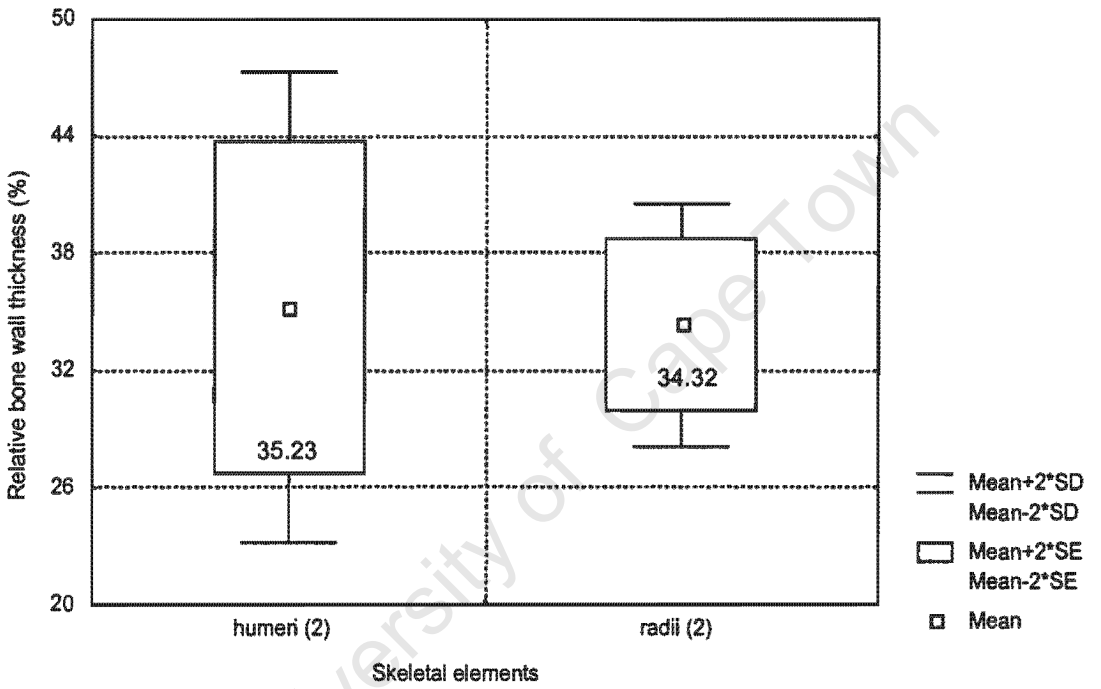




Figure 8.2. *Tritylodon* midshaft relative bone wall thickness values. Numerical values associated with the boxes represent the mean percentage RBT. The numbers in brackets indicate the number of individual elements used to obtain the RBT value of each type of element.

There is no significant difference in relative bone wall thickness between the humeri and radii.

### 8.3.2 Micro-analysis

Histological analyses reveal that the bone tissue of *Tritylodon* consists of a moderate to highly vascularised, fibro-lamellar bone tissue. The osteocyte lacunae are globular and radiate branched canaliculi. Of the seven elements studied, only the radius, B/P/I/5167, exhibited growth rings.

All the humeri in this examination are diagenetically altered, but the overall tissue organisation can still be observed. The vascular arrangement consists mostly of longitudinally oriented primary osteons. Interruptions in the bone tissue are absent (Figure 8.3). Circumferential endosteal lamellar tissue surrounds the medullary cavity in the centre of the midshaft of B/P/I/5160 and bone drift can be seen in B/P/I/4785a. Compacted coarse cancellous bone is observed in the distal metaphysis of B/P/I5671. The bony trabeculae in the smallest humerus B/P/I/4785a lie mainly parallel to each other at the end of the bone. The rest of the humeri contain a network of thin bony trabeculae with many small cancellous spaces in the metaphyses. Compacted coarse cancellous bone is observed in the delto-pectoral crest regions.

The tissue of the radius B/P/I/5167 consists of moderately vascularised, fibro-lamellar bone, interrupted near the sub-periosteal surface by two annuli (Figure 8.4). A LAG is observed after the outermost annulus. The vascular canals consist of a mixture of longitudinal simple canals and primary osteons. Circumferential endosteal lamellar tissue surrounds the medullary cavity. There is no decrease in vascularisation towards the periphery. Secondary remodelling is extensive in the metaphyseal region. The radius, B/P/I/4785b, belongs to the same individual as the humerus B/P/I/4785a. The radius was attached to the humerus and was therefore sectioned slightly obliquely due to its position relative to the humerus. The fibro-lamellar tissue of the radius B/P/I/4785b is uninterrupted (Figure 8.5), but a slight change in tissue organisation is observed at the periphery. There are less osteocyte lacunae here and they form a more organised arrangement and lie in the same general orientation. They may represent an area of parallel-fibred bone, but this cannot be confirmed due to the poor preservation at the periphery.

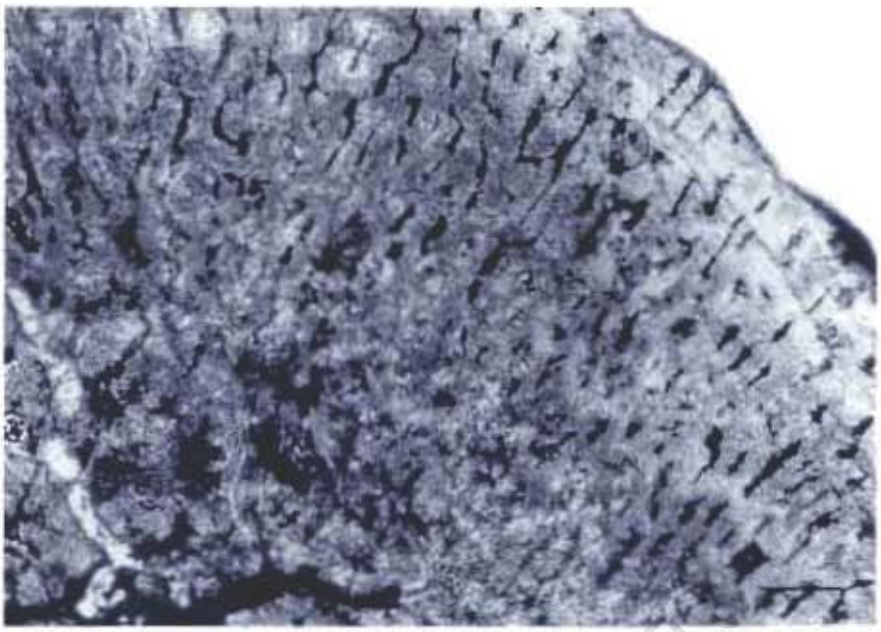

Figure 8.3.

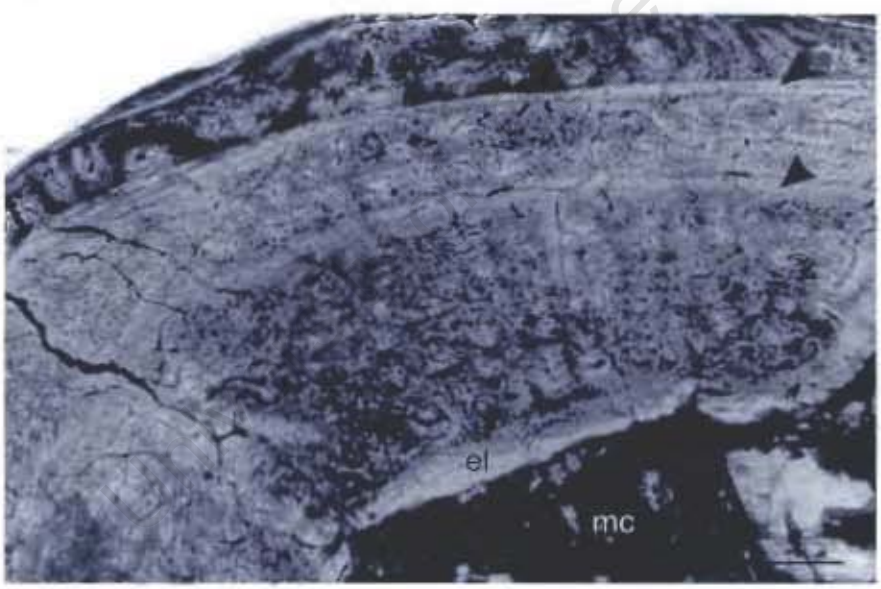


Figure 8.4.

Figure 8.3. Transverse section of the *Tritylodon* humerus B/P/I/4785a. Although not very well preserved, an uninterrupted fibro-lamellar tissue can be discerned.

Figure 8.4. Transverse section of the *Tritylodon* radius B/P/I/5167. The fibro-lamellar tissue is interrupted by two annuli (►) and a LAG is observed after the outermost annulus. Circumferential endosteal lamellar tissue surrounds the medullary cavity in some areas.

Scale bars =250μm

el, endosteal lamellar tissue; mc, medullary cavity

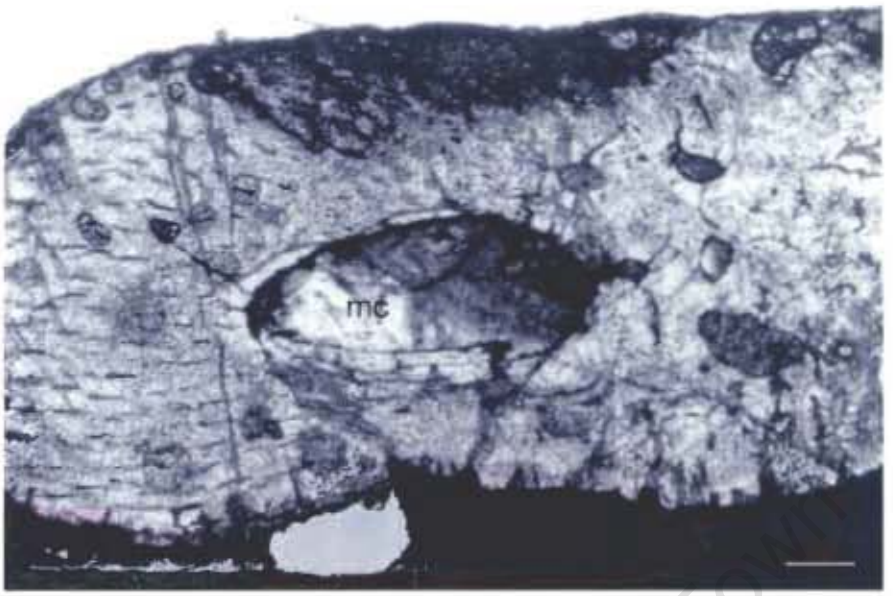


Figure 8.5. Transverse section of the *Tritylodon* radius B/P/I/4785b. This bone was attached to the humerus B/P/I/4785a and was sectioned slightly obliquely. However, the uninterrupted fibro-lamellar bone is still observed.

Scale bar =250μm

mc, medullary cavity

The tissue of the rib B/P/I/4785c is similar to that of the limb bones. The tissue is moderately vascularised and growth rings appear to be absent. Abundant osteocyte lacunae radiate branched canaliculi and a mixture of longitudinally oriented primary and secondary osteons are distributed throughout the cortex.

The percentage channel area of the two radii and the humerus B/P/I/4785a was calculated. Figure 8.6 shows that the tissues are moderately vascularised and no significant difference was found between the two types of elements.

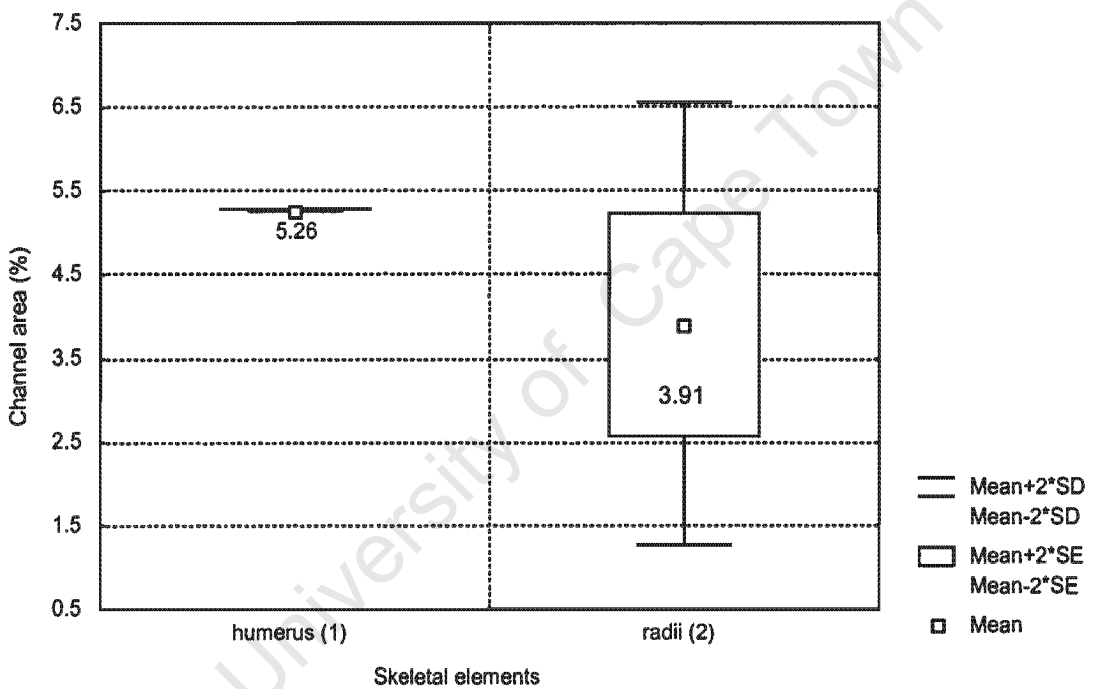




Figure 8.6. *Tritylodon* midshaft percentage channel area of the radii B/P/I/4785b and B/P/I/5167 and the humerus B/P/I/4785a. The number of individual elements that were used to calculate the percentage channel area for each type of element is indicated by the values in brackets. The number associated with the box indicates the mean radial channel area value.

## 8.4 Interpretations

The RBT values of the *Tritylodon* humeri and radii (35.23% and 34.32% average respectively) indicate a relatively thick bone wall. *Tritylodon* was a herbivore with a rodent-like dentition and the tusk-like second incisors are well adapted for eating roots (Broom, 1910). Furthermore, the relatively thick bone walls of the humeri and radii are in accordance with the proposal that *Tritylodon*

was fossorial (Sues, 1985) and these values suggest that, at least the forelimb, may have been modified for digging.

The analysis of the bone histology revealed a moderately vascularised fibro-lamellar bone tissue, indicating rapid growth. Longitudinally oriented primary osteons are abundant in most of the elements, again suggesting rapid growth. Growth rings are absent from all elements except the radius B/P/I/5167 (Figure 8.4). The elements in this study consist of humeri, radii and a rib. The second radius, B/P/I/4785b did not exhibit any growth rings. This suggests that the growth rings observed in the radius B/P/I/5167 are not indicative of a cyclical growth strategy, but a response of this particular individual. Smaller elements usually grow more slowly than limb bones (Sander, 2000) and the rib, which is a small element, does not exhibit any interruptions in growth. The rib represents an individual that is approximately 65% of the adult size and is probably old enough to be used in assessing growth. Furthermore, a study conducted by Chinsamy et al. (2002.) examined a *Tritylodon* femur and also found growth rings to be absent. The growth rings found in this radius may indicate a particularly stressful growing season for this individual. It is also possible that this individual experienced some form of injury or disease that may have caused bone deposition to temporarily cease. As the rest of the *Tritylodon* elements studied exhibit azonal bone, it is likely that this genus grew in a sustained manner.

The observed rest lines in the radius and lack thereof in the rest of the elements in this examination highlights the fact that bone histological analyses should include as many different types of elements as possible, as many individuals need to be examined before reasonable deductions regarding a genus can be made.

# CHAPTER NINE
# CHEMICAL ANALYSES OF ENAMEL

*Summary*

*Intra-tooth oxygen and carbon isotope analyses of non-mammalian cynodont enamel carbonate were conducted in order to assess the nature and amplitude of the seasonal variability reflected in their teeth. Extant Crocodylus niloticus teeth were analysed for comparison. Prior to the isotope analyses, Fourier Transform Infra-red spectroscopy (FTIR) was used to assess the integrity of the biological apatites. FTIR absorbance spectra were obtained from extant Giraffa camelopardalis, Varanus and Crocodylus niloticus enamel and dentine as well as the Pliocene Sivatherium hendeyi enamel for comparative purposes. The FTIR absorbance spectra showed that the non-mammalian cynodont enamel resembles biological apatite. Carbonate levels are similar to the extant Crocodylus niloticus and Varanus enamel, but a slight difference in the proportion of the $v_4$ phosphate peaks, between the extant and fossil enamel spectra was observed. The non-mammalian cynodont $\delta^{13}C$ values fall within the expected $C_3$ plant range, as the terrestrial Triassic flora was fundamentally $C_3$. The oxygen isotope results show patterned $\delta^{18}O$ intra-tooth variation, which likely indicates seasonal changes, as earlier studies have found that the climate was semi-arid with seasonal rainfall. The average $\delta^{18}O$ values of the Diademodon individuals are significantly more depleted than those of the rest of the non-mammalian cynodont genera studied. This may suggest that this animal was nocturnal and/or semi-aquatic.*



## 9.1 Introduction

### 9.1.1 Stable isotopes

The relative mass differences of environmental isotopes (hydrogen, carbon, nitrogen, oxygen and sulphur) can lead to measurable isotopic partitioning or fractionation between substances during physical and chemical processes. Substances are "labelled" with distinct isotopic ratios (Koch, 1998), which living organisms incorporate into their tissues and therefore reflect the isotopic ratios of the environment. Hence, organisms can be used to interpret climatic and ecological information within ecosystems (Bocherens, et al., 1996).

Typically, isotopic ratios are expressed as the ratio of the two most abundant isotopes of a given element (such as oxygen, carbon or nitrogen) and are

standardised against a known reference gas. The natural abundance of stable light isotopes is small and by convention is expressed as parts per thousand (‰), using the δ (delta) notation, where

$$\delta = [(R_{sample} / R_{standard}) - 1] \times 1000$$

and R is the ratio between the heavy and light isotopes, in this study either $^{13}C/^{12}C$ or $^{18}O/^{16}O$ (Craig, 1953).

Oxygen isotopic ratios obtained from skeletal tissues such as bones and teeth provide information relating to environmental fluctuations (e.g. Luz et al., 1984; Luz and Kolodny, 1985; Stuart-Williams and Scharcz, 1997; Fricke et al., 1998). The temperature of biomineral formation and the $\delta^{18}O$ value of body water principally determine the oxygen isotope signatures of skeletal tissues. As mammals maintain relatively constant body temperatures, their skeletal tissue $\delta^{18}O$ values are controlled more by body water composition than temperature. The composition of body water is controlled by the mass balance and fractionation of oxygen as it enters and exits the body. Oxygen enters the body as inspired oxygen (atmospheric oxygen), drinking water and food water (ingested water). Oxygen is lost as liquid water in urine, sweat and faeces and as water vapour and $CO_2$ in respiratory gases (Bryant and Froelich, 1995). Atmospheric $\delta^{18}O$ values are well-mixed and kept relatively constant, so the $\delta^{18}O$ value of ingested water is the major factor affecting the oxygen isotopic ratios in bones and teeth (Luz and Kolodny, 1985; Kohn, 1996; Kohn et al., 1996).

The main source of ingested water is meteoric water (surface, fluvial, lacustrine etc.), the isotopic composition of which is sensitive to climatic factors such as mean annual temperature and amount of precipitation (Dansgaard, 1964). As the isotopic composition of skeletal tissues is mainly controlled by the $\delta^{18}O$ value of body water, these tissues can be used to obtain information relating to

environmental temperature and precipitation (Luz and Kolodny 1985; Bocherens et al., 1996; Stuart-Williams and Schwarcz, 1997).

Oxygen is present in both phosphate ($PO_4^{3-}$) and carbonate ($CO_3^{2-}$) ions in enamel apatite and a high correlation exists between $\delta^{18}O$ phosphate and $\delta^{18}O$ carbonate (Bryant, et al., 1996b). Studies have concentrated on phosphate to obtain oxygen, as the P-O chemical bond is stronger than the C-O bond in carbonate. This makes the phosphate oxygen less susceptible to isotopic exchange than carbonate oxygen (Shemesh et al., 1983; Longinelli, 1984; Luz and Kolodny, 1989; Iacumin et al., 1996; Sponheimer and Lee-Thorp, 1999a). However, recent studies have shown that biogenic oxygen signals can be reliably obtained from enamel carbonate back to at least Miocene age (Bocherens, et al., 1996; Cerling et al., 1997; MacFadden, 1998; Sponheimer and Lee-Thorp, 1999a, 1999b). The analysis of the $\delta^{18}O$ of carbonate is easier, less expensive and is determined simultaneously with $\delta^{13}C$, yielding information from both oxygen and carbon in one analysis (Bryant, et al., 1996b). For these reasons and because phosphate analysis is not available at the University of Cape Town, carbonate was used to obtain the $\delta^{18}O$ and $\delta^{13}C$ values examined in this study.

Carbon isotopic ratios provide information relating to the ecology of animals (e.g. DeNiro and Epstein, 1978; van der Merwe and Medina, 1989, 1991; Ostrom and Fry, 1993). Carbon isotopic ratios in plants are influenced by temperature, light intensity, water stress and salinity, but are primarily determined by the type of photosynthetic pathway the plants use. Plants discriminate against the heavier $^{13}C$ isotope in favour of the lighter $^{12}C$ isotope during photosynthesis, which leads to distinct isotopic ratios in plant tissues (Berry, 1988). Plants using the $C_3$ or Calvin Cycle photosynthetic pathway (including most trees, shrubs, herbs and temperate grasses) (Cerling et al., 1991) exhibit $\delta^{13}C$ values between -30‰ and -23‰. Plants using the $C_4$ or Hatch-Slack photosynthetic pathway (including all warm weather grasses) possess $\delta^{13}C$ values between -15‰ and -12‰. Plants using CAM or the

Crassulacean Acid Metabolism photosynthetic pathway (mostly succulents) possess $\delta^{13}C$ values that nearly cover the entire $C_3$ and $C_4$ $\delta^{13}C$ range (Cerling, et al., 1991). Herbivores incorporate ingested plant $\delta^{13}C$ isotope signatures intc their tissues and due to physiological processes, have $\delta^{13}C$ values that are slightly more positive than the plants themselves (Ostrom and Fry, 1993; Bocherens et al., 1994; Barrick, 1998; MacFadden, 1998). Therefore, extant herbivores feeding exclusively on $C_3$ plants have $\delta^{13}C$ values for mineral carbonate of approximately -17‰ to -10‰, whereas those feeding on $C_4$ plants have $\delta^{13}C$ values of about –4‰ to +2‰ (Lee-Thorp et al., 1989). Herbivores during the Triassic probably incorporated $\delta^{13}C$ isotope signatures of $C_3$ plants only, as the terrestrial flora was fundamentally $C_3$ until the Late Miocene (at least 12 million years ago). $C_4$ plants then evolved during the Late Miocene and spread worldwide to become the dominant flora of today (Cerling et al., 1991; Ehleringer et al., 1997).

The material used in this study consists of tooth enamel from several non-mammalian cynodont genera. As tooth enamel is laid down incrementally from the top of the crown to the base of the crown (Figure 9.1), short-term seasonal changes that occur during enamel growth are recorded in individual teeth (Fricke and O'Neil, 1996; Fricke et al., 1998). Fricke and O'Neil (1996) found a 5.6‰ intra-tooth oxygen isotopic variability in 500 year old Bison teeth. They proposed that intra-tooth variability provided valuable information on the extent of $\delta^{18}O$ environmental seasonality. A time series, of changes in ingested water $\delta^{18}O$ values, along the direction of tooth growth, which in turn reflects variability in the local climate, can therefore be obtained (Fricke et al., 1998).

The length of season reflected in the tooth enamel depends on how long the enamel takes to form. The rate of tooth replacement in young *Alligator mississippiensis* is between eight and sixteen months (Edmund, 1969) and the replacement rate decreases with age. Although non-mammalian cynodonts also experienced multiple tooth replacement, it is thought that *Thrinaxodon* (Osborn and Crompton, 1973) and the more derived genera such as

*Cynognathus, Diademodon* and *Trirachodon*, had a slower rate of tooth replacement compared with the early non-mammalian cynodonts (Hopson, 1971). Little research has been done on rates of reptilian enamel formation, but Line (2000) found that enamel in an extant crocodilian took approximately 2.5 months to form. In contrast, human enamel takes several years to form. If the tooth replacement rates of the more derived non-mammalian cynodonts were between that of extant "reptiles" and mammals, it is likely that their rates of enamel formation were also between the two groups. Therefore, the amount of season reflected in their teeth is likely to be several months.

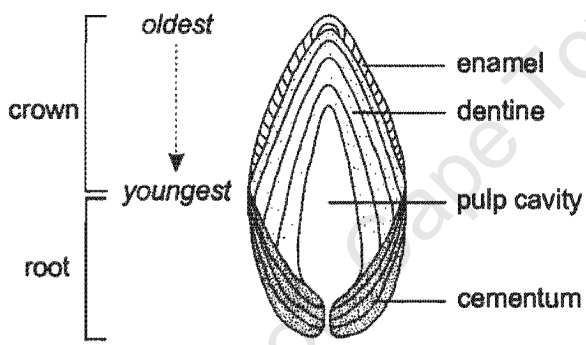


Figure 9.1. A schematic longitudinal section of a typical mammalian canine tooth. Enamel covers the crown of the tooth and is supported by the underlying dentine. Modified from Carlson (1990) and Fricke and O'Neil (1996).



Studies have shown that if the integrity of the isotopic signatures in biological apatite of fossil animals remains intact, useful information for the interpretation of palaeoenvironments can be obtained (e.g. Bryant et al., 1996c; Reinhard et al., 1996; Koch, 1998; Sharp and Cerling, 1998). However, measuring isotopic ratios from fossil tissues is complicated by the possible alteration of the apatite structure during the fossilization process (Sharp et al., 2000). Tooth enamel is more resistant to physical and chemical alteration as it has a lower organic content, is compact with little pore space and contains larger apatite crystals compared to dentine or bone (LeGeros, 1991). For this reason, tooth enamel and not bone or dentine, has been used for the stable isotope analyses in this study.

### 9.1.2 Fourier Transform Infra-red Spectroscopy

Since the non-mammalian cynodont enamel dates from the Early to Middle Triassic, some diagenetic alteration is expected. However, if the structural integrity of the biological apatite remains intact, diagenetic alteration is likely to be low and the results obtained from the stable isotope analyses can be accepted with greater confidence. Measures such as nuclear magnetic resonance, scanning and transmission electron microscopy (LeGeros, 1991) can be used to assess the integrity of extant material, but fewer options are available for the examination of fossil material. Studies (e.g. Michel et al., 1995; Sponheimer and Lee-Thorp, 1999a) have shown that Fourier Transform Infra-red spectroscopy (FTIR) is a useful technique for assessing the integrity of fossil biological apatite. Enamel contains carbonate substituted in two existing anionic sites, which play an important role in the mineral phase of enamel. Most of the carbonate is located at the trivalent phosphate ($PO_4^{3-}$) sites, generally designated as type B carbonate, whereas a lesser amount is located in the monovalent hydroxyl anionic ($OH^-$) sites and is generally designated as type A carbonate (Rey et al., 1991). The location and proportions of type A and B carbonate alter to some extent due to recrystallisation resulting in another form of apatite (e.g. fluorapatite; LeGeros and Tung, 1983). FTIR spectroscopy allows the crystallographic structure of the fossil enamel to be assessed for alterations in the type A and B carbonate ions.

In FTIR spectroscopy, the frequencies (wavenumber) ($cm^{-1}$) at which the compound absorbs infra-red radiation are measured. This produces an absorption spectrum, indicating both frequency and intensity of the various functional groups. The functional groups (e.g. $HPO_4^{2-}$, $PO_4^{3-}$, $CO_3^{2}$) absorb infra-red at specific frequencies, which allows the chemical composition of the compound to be identified. The absorption spectra of biological apatites differ from that of other carbonate minerals such as calcite and to some extent, from each other, allowing diagenetic minerals in fossil material to be detected (LeGeros, 1991; Sponheimer and Lee-Thorp, 1999a). This technique has been used in this study, prior to isotope analysis, to assess the structural integrity of

the fossil enamel apatite. If the fossil material still resembles biological apatite, it is likely that diagenesis is minimal and the results of the isotope analyses will represent the biological apatite.

Indices calculated from the spectra can be used to quantitatively determine the changes in crystallographic structure. Indices, shown in Figure 9.2, reflecting the amount of type B carbonate to phosphate (BPI), the amount of type A carbonate to phosphate (API), the relative amount of B- to A-site carbonate (BAI) and the "crystallinity" (PCI) of each sample were calculated using absorption bands in the $\nu_3$ carbonate (1415 $cm^{-1}$, 1540 $cm^{-1}$) and $\nu_4$ phosphate domains (565 $cm^{-1}$, 590 $cm^{-1}$, 605 $cm^{-1}$) (Sponheimer and Lee-Thorp, 1999a). These absorption bands are appropriate to use, as they do not overlap, so facilitating a clear examination of the A- and B-sites (Rink and Schwarcz, 1995; Sponheimer and Lee-Thorp, 1999a). The index ratios calculated from the absorption bands are shown in Table 9.1.



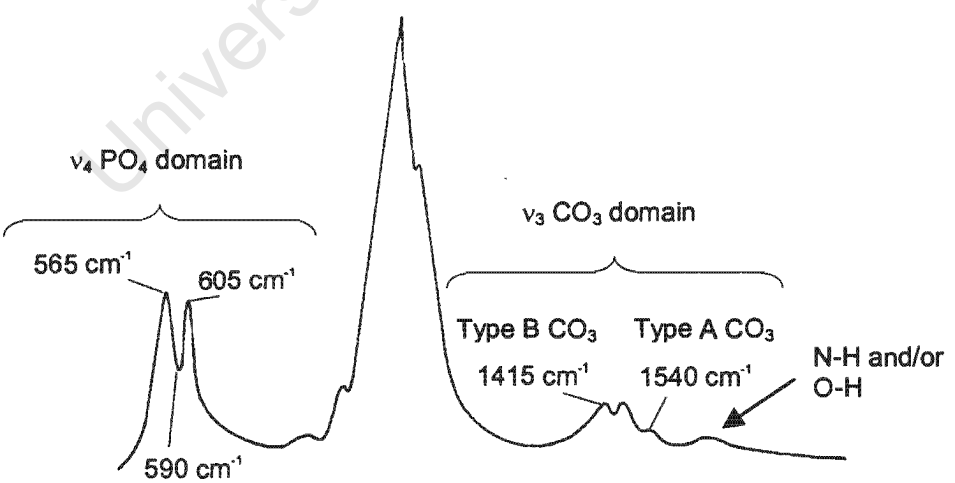


Figure 9.2. Typical FTIR absorbance spectrum of a biological apatite showing the phosphate (565 $cm^{-1}$, 605 $cm^{-1}$ and 590 $cm^{-1}$) and carbonate peaks (1415 $cm^{-1}$ and 1540 $cm^{-1}$). The arrow indicates an N-H and/or O-H peak at 1640 $cm^{-1}$.

Table 9.1. Indices calculated from intensities at the various absorbance bands (following that of Sponheimer and Lee-Thorp, 1999a).

| Indices | Abbreviation | Ratios |
|---|---|---|
| Amount of type B $CO_3$ to $PO_4$ | BPI | 1415 $cm^{-1}$ / 605 $cm^{-1}$ |
| Amount of type A $CO_3$ to $PO_4$ | API | 1540 $cm^{-1}$ / 605 $cm^{-1}$ |
| Relative amount of B- to A $CO_3$ | BAI | 1415 $cm^{-1}$ / 1540 $cm^{-1}$ |
| "crystallinity" | PCI | (565 $cm^{-1}$ + 605 $cm^{-1}$) / 590 $cm^{-1}$ |

BPI has been used to quantitatively determine the overall carbonate content in biological and synthetic apatites as it closely tracks the overall carbonate content (LeGeros, 1991). Figure 9.3 represents the relationship between BPI and the percentage carbonate weight determined by LeGeros (1991) from synthetic apatites and has been used in this study to estimate the overall carbonate content in the study material.



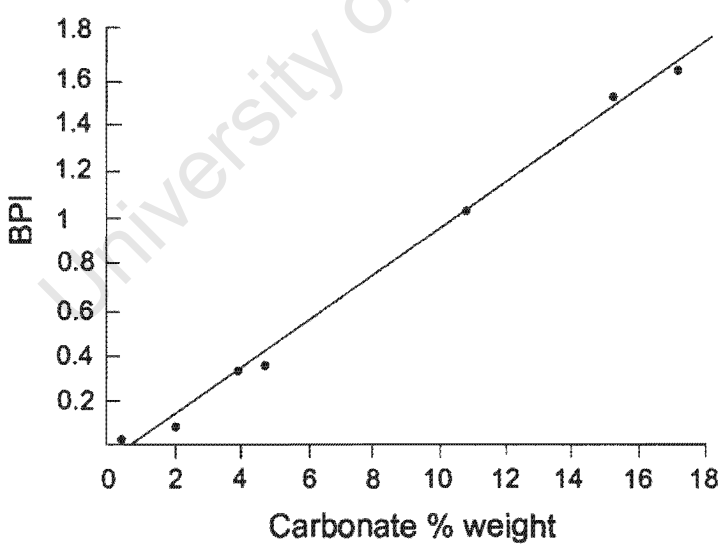


Figure 9.3. Determination of the percentage carbonate by weight using the BPI index for synthetic carbonate apatites. Modified from LeGeros (1991) after Sponheimer and Lee-Thorp (1999a).

## 9.2 Materials and Methods

### 9.2.1 Materials

The material used in the Fourier Transform Infra-red spectroscopic analysis, for examining the enamel apatite structure, prior to isotope analysis, includes nine extant *Crocodylus niloticus* (Nile crocodile) teeth, one extant *Varanus* (monitor lizard) tooth, one extant *Giraffa camelopardalis* (giraffe) molar and one fossil *Sivatherium hendeyi* (short-necked giraffe) molar. The non-mammalian cynodont material includes two *Cynognathus,* two *Diademodon* and one *Trirachodon* canine (Tables 9.2 and 9.3).

The material used for isotope analysis consists of three extant *Crocodylus niloticus* teeth and one *Thrinaxodon,* two *Cynognathus,* eight *Diademodon* and two *Trirachodon* canines (Tables 9.2 and 9.3). Canine teeth take longer to develop than other tooth types and therefore provide a longer record of the isotopic signature. Furthermore, restricting analyses to one tooth type excludes inter-tooth variability that may occur during tooth growth (Reinhard et al., 1996).

All the specimens were obtained from South Africa. See Appendix 1 for institutional abbreviations.



### 9.2.2 Methods

**(i) Fourier Transform Infra-red Spectroscopy**

As the non-mammalian cynodont, extant *Crocodylus niloticus* and *Varanus* samples were very small, they were not treated with the standard sodium hypochlorite and acetic acid pre-treatment. These substances remove the organic and mineral contaminants in order to remove the highly soluble (high carbonate content) mineral component. However, one extant *Giraffa camelopardalis* enamel sample and one dentine sample were given the standard pre-treatment prior to FTIR analysis to compare pre-treated and unpre-treated samples. 1.8 mg of enamel was obtained from each tooth using a low-speed rotary drill with a 1.5 mm diamond-tipped bit.

Table 9.2. Localities of the various specimens examined in the FTIR spectroscopic and stable isotope analyses for comparison with the non-mammalian cynodont material.

| Genus | Specimen number | Locality | FTIR | Isotopes |
|---|---|---|---|---|
| *Crocodylus niloticus* | CROC1 | Le Bonheur Crocodile Farm, Stellenbosch | | ✓ |
| | CROC2 | | | ✓ |
| | CROC3 | | | ✓ |
| | CROC6 | | ✓ | |
| | CROC7 | | ✓ | |
| | CROC8 | | ✓ | |
| | CROC9 | | ✓ | |
| | CROC10 | | ✓ | |
| | CROC11 | | ✓ | |
| | CROC12 | | ✓ | |
| | CROC13 | | ✓ | |
| | CROC14 | | ✓ | |
| *Varanus* | 1 | University of Cape Town | ✓ | |
| *Giraffa camelopardalis* | 1a | Kruger National Park | ✓ | |
| | pre-treated 1b | Skukuza | ✓ | |
| *Sivatherium hendeyi* | SAM-PQL43928 | Langebaanweg ~ 5 million years old | ✓ | |

Table 9.3. Localities of the non-mammalian cynodont material used for FTIR spectroscopic and stable isotope analyses in this study. FTIR analysis was not conducted on *Thrinaxodon* due to a lack of available material.

| Genus | Specimen number | Assemblage Zone | Locality | FTIR | Isotopes |
|---|---|---|---|---|---|
| *Thrinaxodon* | B/P/I/5020 | *Lystrosaurus* | unknown | | ✓ |
| *Cynognathus* | SAM-PK-K3029 | *Cynognathus* | Burgersdorp | ✓ | ✓ |
| | B/P/I/1675d | | | ✓ | ✓ |
| *Diademodon* | UMCZ T504a, | *Cynognathus* | Lady Frere | ✓ | ✓ |
| | 504b, | | | ✓ | |
| | 443, 470, 471, 472, | | | | ✓ |
| | 473, 474, 487 | | | | ✓ |
| *Trirachodon* | SAM-PK-K5881(1) | *Cynognathus* | Aliwal North | ✓ | |
| | SAM-PK-K5881(2) | | | | ✓ |
| | SAM-PK-K5881(3) | | | | ✓ |

*Giraffa camelopardalis* samples were treated with 3.5% sodium hypochlorite (diluted 50:50 with distilled water) for 30 minutes. The samples were then centrifuged in an Eppendorf centrifuge 5410 for 3.5 minutes, the sodium hypochlorite removed by an aspirator and the samples rinsed with distilled water. The soluble components ($CaCO_3$) were removed using 0.1 M acetic acid for 15 minutes. The samples were again centrifuged and the acetic acid aspirated off. Each sample was given a final rinse with distilled water and freeze-dried overnight.

*Crocodylus niloticus* and *Varanus* samples were not pre-treated as initial pre-treatment experiments resulted in the loss of too much enamel. The non-mammalian cynodont teeth were not pre-treated either as only very small amounts of enamel could be drilled off the teeth and this amount would have been lost during pre-treatment. The purpose of pre-treatment is to remove diagenetic carbonate from samples found in carbonate-rich matrices. As the *Crocodylus niloticus* and *Varanus* teeth are extant, they were not found in such material. Similarly, the non-mammalian cynodont teeth were not excavated from carbonate rich sediments and therefore pre-treatment was not necessary.



Each sample was ground together with 300 mg of potassium bromide in an agate mortar and compressed into transparent discs under a pressure of 10 tons. The transparent FTIR discs were placed in a Perkin Elmer FT-IR Spectrometer Paragon 1000 and the resulting FTIR absorbance spectra were recorded. Sixteen scans of each sample were taken, using a range of 4000 – 500λ, at a resolution of 8 $cm^{-1}$. The spectra were downloaded to the Perkin Elmer Grams Analyst 1000 computer program (version 3.01A, Level II, 1991) where they were standardised by adjusting the baseline and then analysed.

In addition to the enamel spectra, extant *Crocodylus niloticus* and *Varanus* dentine spectra were also obtained. As their enamel is extremely thin, both enamel and dentine spectra were obtained in order to distinguish between the two to ensure that dentine had not been incorporated into the enamel sample.

These dentine spectra were also compared with the *Giraffa camelopardalis* dentine spectrum.

**(ii) Stable Isotope Analyses**

Enamel was serially drilled in bands along the teeth, from the top of the crown to the base of the crown, parallel to the occlusal surface (Figure 9.4), using a low-speed rotary drill with a 1.5 mm diamond-tipped bit. Each sample per band weighed approximately 0.7 mg.

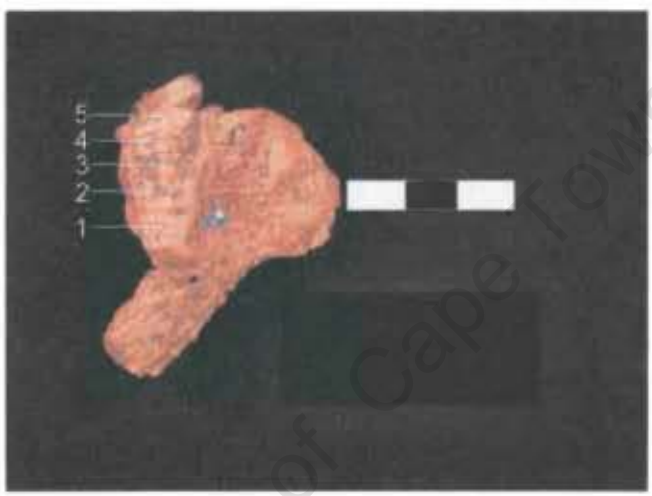


Figure 9.4. Serially sampled *Diademodon* canine tooth. The numbers, 1-5 (from top of crown to bottom of crown), represent bands drilled along the tooth.

Isotopic ratios were measured using a Finnigan Mat 252 mass spectrometer. $CO_2$ was obtained by acid hydrolysis using 100% pure phosphoric acid ($H_3PO_4$) at 70°C and collected by cryogenic distillation. Standards (NBS 18, NBS 20, Carrara Z and Lincoln Limestone) were used to obtain a 4-point regression curve, which was used to calibrate the sample data. Ratios are reported relative to the PDB standard (marine carbonate: belemnite from the Pee Dee Formation) (Bocherens et al., 1993; Fogel and Cifuentes, 1993).

## 9.3 Results

### 9.3.1 Fourier Transform Infra-red Spectroscopy

The Fourier Transform Infra-red spectroscopic results are presented first as this analysis was conducted prior to the stable isotope analyses.

### (i) Fourier Transform Infra-red Spectra of Extant Taxa

#### (a) Effects of Pre-treatment on the Extant *Giraffa camelopardalis* Enamel and Dentine

FTIR absorbance spectra of the unpre-treated and pre-treated enamel and dentine *Giraffa camelopardalis* are shown in Figures 9.5 and 9.6 respectively. As shown in the spectra, pre-treatment had very little observable effect on the *Giraffa camelopardalis* enamel other than sharpening the peaks and reducing the carbonate very slightly (Figure 9.5A, 9.5B). In contrast, pre-treatment has notably affected the dentine as shown in Figure 9.6A and 9.6B (arrow), by the increased 1654 $cm^{-1}$ peak (assigned to N-H and/or O-H) of the unpre-treated spectrum.

#### (b) *Crocodylus niloticus* and *Varanus* Spectra

The enamel spectra for *Crocodylus niloticus* (Figures 9.7A, 9.8A) and *Varanus* are easily distinguishable from their respective dentine spectra (Figures 9.7B, 9.8B). The peaks of the enamel $\nu_3$ carbonate are higher than those of the dentine $\nu_3$ carbonate. In addition, the dentine ~1657 $cm^{-1}$ absorbance peaks (indicated by arrows) are markedly higher relative to the $\nu_3$ domain than the respective enamel peaks. In comparing the *Varanus* spectra with the *Crocodylus niloticus* spectra, the *Varanus* ~1657 $cm^{-1}$ enamel peak is clearly higher than that of *Crocodylus niloticus*.

#### (c) Extant Mammalian, *Crocodylus niloticus* and *Varanus* Enamel Spectra

A higher ~1657 $cm^{-1}$ absorbance peak is observed in the enamel *Crocodylus niloticus* (arrow in Figure 9.7A, absorbance 0.30552) and *Varanus* (arrow in Figure 9.8A, absorbance 0.32054) compared to the enamel *Giraffa camelopardalis* spectra (Figures 9.5A, 9.5B, average absorbance 0.19754). As a general trend however, the overall *Crocodylus* and *Varanus* absorbance is lower (i.e. less mineral) than the *Giraffa camelopardalis* enamel spectra.

**(ii) Fourier Transform Infra-red Spectra of Extinct Taxa**

**(a) *Sivatherium hendeyi* and *Giraffa camelopardalis* Enamel Spectra**

The *Sivatherium hendeyi* spectrum highlights some of the affects of fossilization on mammalian enamel apatite. The overall profile of this spectrum is similar to that of the *Giraffa camelopardalis*, but the overall absorbance is substantially lower (Figure 9.9). In addition, the difference in peak height, between the 565 $cm^{-1}$ phosphate peak and 605 $cm^{-1}$ phosphate peak in the $\nu_4$ phosphate domain of *Sivatherium hendeyi*, is not as great as that of *Giraffa camelopardalis* (Figure 9.9, arrow).

**(b) Non-mammalian Cynodont Enamel Spectra**

The *Cynognathus* (Figure 9.10) and *Diademodon* (Figure 9.11) enamel spectra are similar in appearance to the extant *Giraffa camelopardalis* and *Crocodylus niloticus* spectra, whereas the *Trirachodon* spectrum shows differences. The *Trirachodon* spectrum contains several extra peaks that the other two fossil spectra do not have (indicated by arrowheads in Figure 9.12). For example, the *Trirachodon* ~1654.6 $cm^{-1}$ peak (arrowhead a, absorbance 0.30388), has a higher absorbance than those of *Cynognathus* (0.21465) or *Diademodon* (0.2366). The ~1280 $cm^{-1}$ (arrowhead b) and ~745.48 $cm^{-1}$ (arrowhead c) peaks in *Trirachodon* are also absent from the *Cynognathus* and *Diademodon* spectra.

**(c) Non-mammalian Cynodont and Extant Enamel Spectra**

A notable feature of the *Cynognathus* and *Diademodon* spectra is that the 565 $cm^{-1}$ phosphate peak, in the $\nu_4$ phosphate domain, has a higher absorbance than the 605$cm^{-1}$ phosphate peak, whereas the converse applies to the extant *Giraffa camelopardalis* (Figures 9.5A, 9.5B, arrows), *Crocodylus niloticus* (Figure 9.7A, open arrow) and *Varanus* (Figure 9.8A, open arrow) enamel spectra. Furthermore, the non-mammalian cynodont carbonate absorbance peaks are relatively higher than the extant *Giraffa camelopardalis* enamel spectra and are similar to that of *Crocodylus niloticus* and *Varanus*.

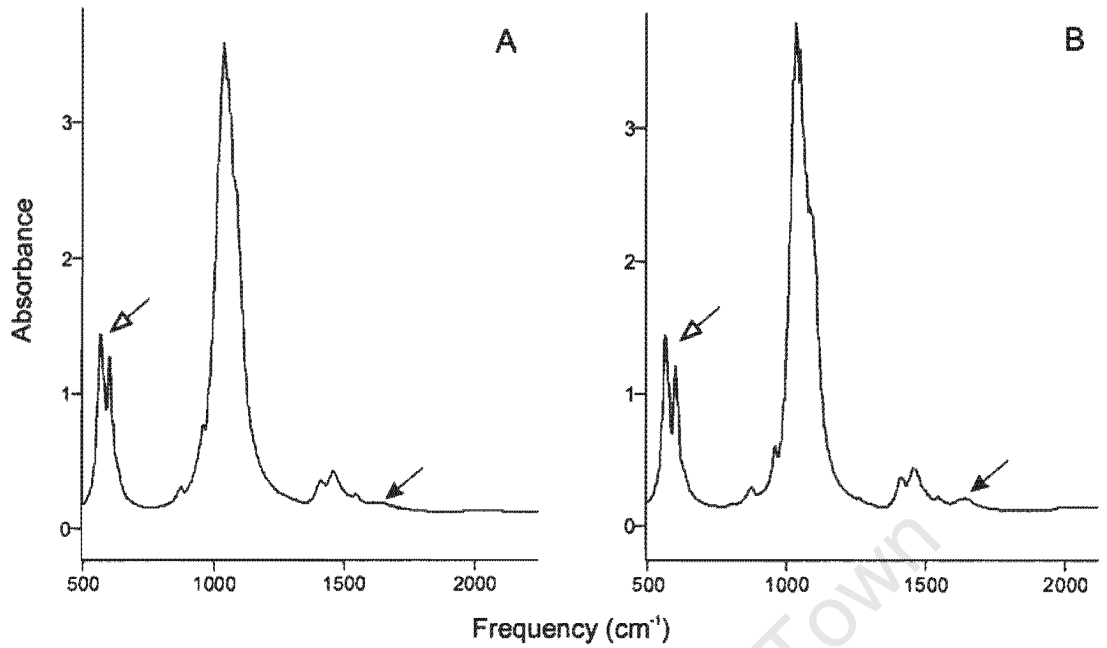


Figure 9.5. Unpre-treated (A) and pre-treated (B) extant *Giraffa camelopardalis* enamel FTIR spectra. Open arrows indicate $\nu_4$ $PO_4$ domain, closed arrows indicates the 1654cm$^{-1}$ peak.



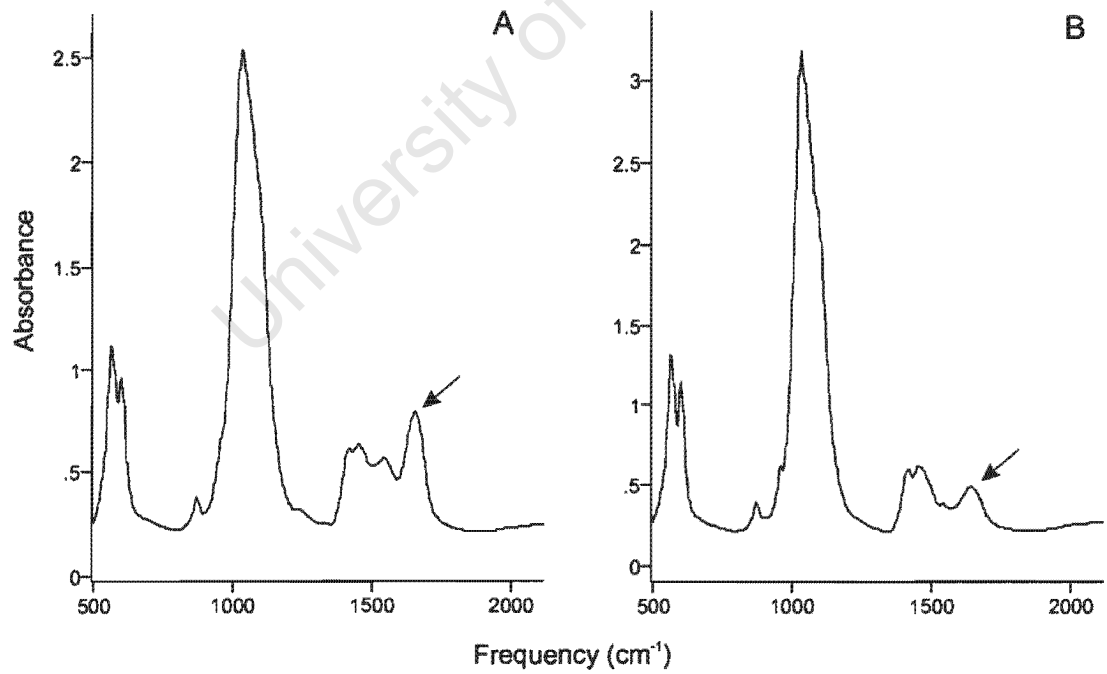


Figure 9.6. Unpre-treated (A) and pre-treated (B) extant *Giraffa camelopardalis* dentine FTIR spectra. Arrows indicate the 1657cm$^{-1}$ peak.

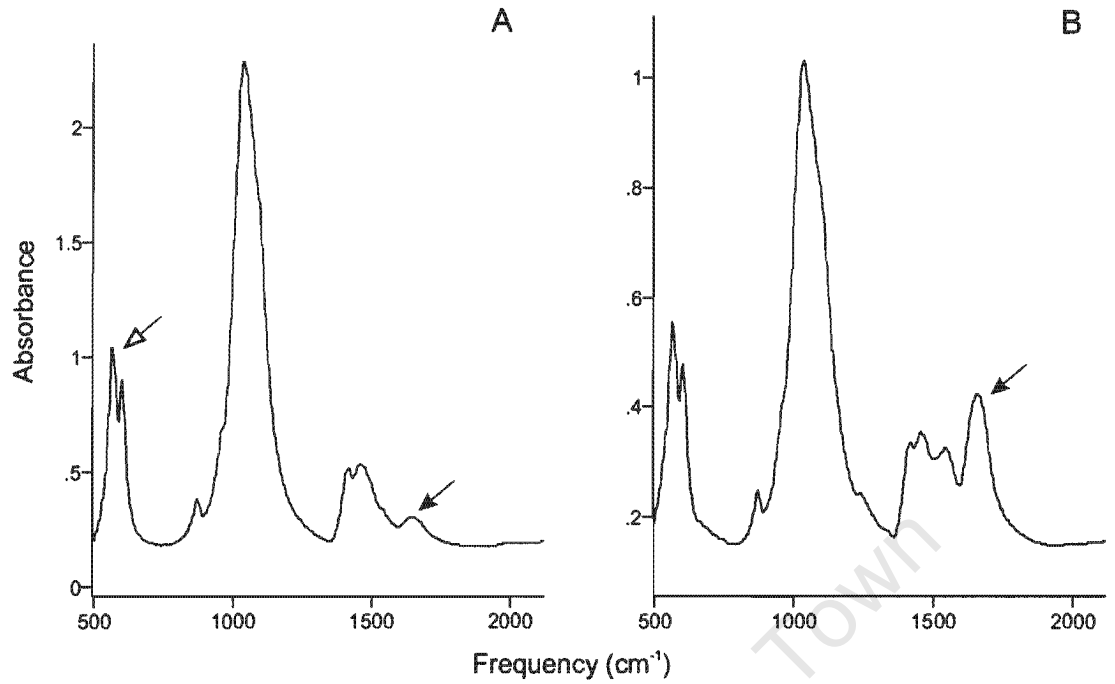


Figure 9.7. Extant *Crocodylus niloticus* enamel (A) and dentine (B) FTIR spectra. Open arrow indicates $\nu_4$ $PO_4$ domain and closed arrows indicate the 1657cm$^{-1}$ peak.

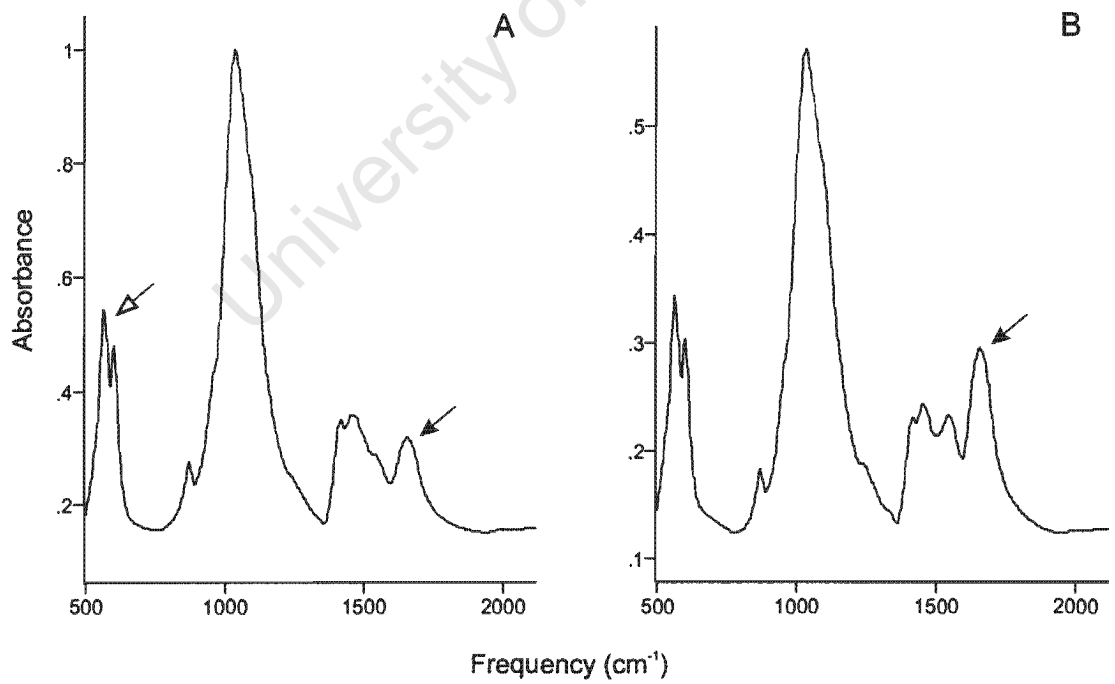


Figure 9.8. Extant *Varanus* enamel (A) and dentine (B) FTIR spectra. Open arrow indicates $\nu_4$ $PO_4$ domain. Closed arrows indicate the 1657cm$^{-1}$ peak.

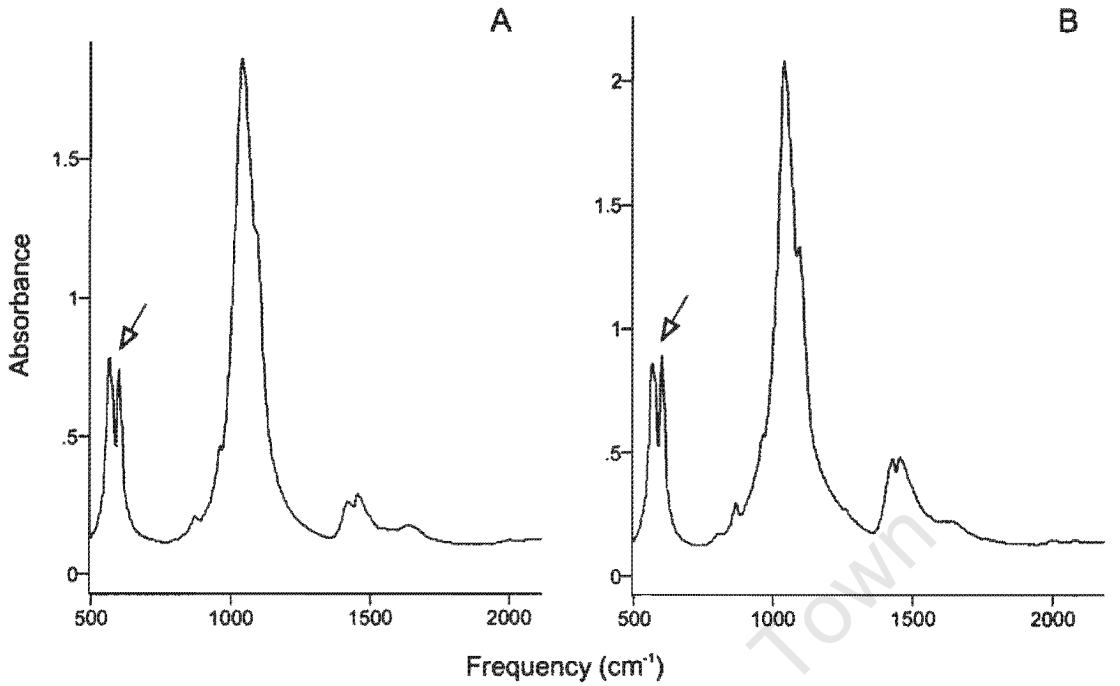


Figure 9.9. *Sivatherium hendeyi* enamel FTIR spectrum. Open arrow indicates $\nu_4$ $PO_4$ domain.

Figure 9.10. *Cynognathus* enamel FTIR spectrum. Open arrow indicates $\nu_4$ $PO_4$ domain.

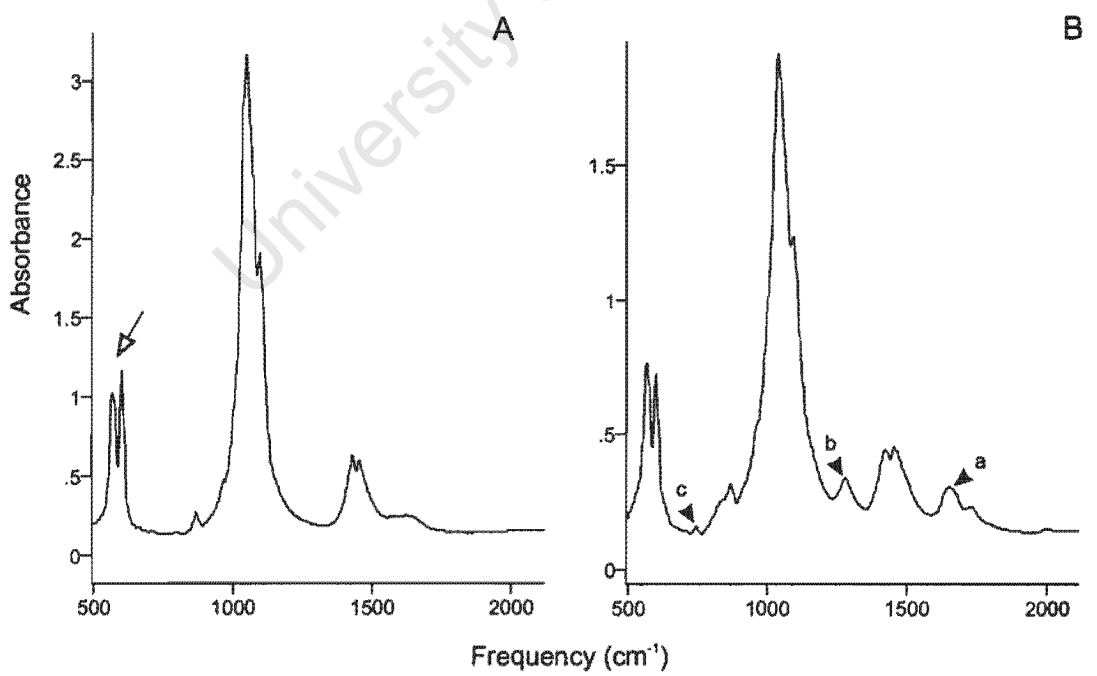


Figure 9.11. *Diademodon* enamel FTIR spectrum. Open arrow indicates $\nu_4$ $PO_4$ domain.

Figure 9.12. *Trirachodon* enamel FTIR spectrum. Arrowheads indicate (a) 1654.6cm$^{-1}$, (b)1280cm$^{-1}$ and (c) 745.48cm$^{-1}$ peaks.

The indices calculated from the intensities at the absorbance bands given in Table 9.1, are presented in Table 9.4. The peaks used for calculating the fossil indices are in similar positions to those of the extant spectra, apart from the peak indicating type B carbonate in the $\nu_3$ carbonate domain, which has shifted slightly to the right. Detailed calculations are given in Appendix 4.

Table 9.4. Indices of extant and fossil enamel obtained from the FTIR absorbance spectra. The overall carbonate content ($CO_3\%_{wt}$) has been estimated using the graphic relationship between BPI and carbonate percentage weight modified from LeGeros (1991), shown in Figure 9.3.

| Taxon | Specimen number | BPI | API | BAI | PCI | $CO_3\%_{wt}$ |
|---|---|---|---|---|---|---|
| *Giraffa camelopardalis* | 1a | 0.316 | 0.167 | 1.545 | 3.183 | 3.75 |
| | pretreated 1b | 0.312 | 0.186 | 1.666 | 3.855 | 3.75 |
| *Crocodylus niloticus* | 6 | 0.57 | 0.369 | 1.547 | 2.71 | 6.25 |
| | 7 | 0.577 | 0.316 | 1.826 | 2.764 | 6.25 |
| | 8 | 0.603 | 0.367 | 1.644 | 2.648 | 6.5 |
| | 9 | 0.606 | 0.38 | 1.596 | 2.632 | 6.5 |
| | 10 | 0.649 | 0.4 | 1.621 | 2.623 | 7 |
| | 11 | 0.506 | 0.311 | 1.629 | 2.79 | 5.75 |
| | 12 | 0.545 | 0.337 | 1.619 | 2.773 | 6 |
| | 13 | 0.555 | 0.355 | 1.564 | 2.704 | 6 |
| | 14 | 0.493 | 0.321 | 1.538 | 2.853 | 5.65 |
| *Varanus* | 1 | 0.717 | 0.591 | 1.213 | 2.51 | 7.25 |
| *Sivatherium hendeyi* | SAM-PQL43928 | 0.354 | 0.227 | 1.561 | 3.279 | 4.15 |
| *Cynognathus* | SAM-PK-K3029 | 0.669 | 0.375 | 1.785 | 3.072 | 7 |
| | B/P/I/1675d | 0.526 | 0.395 | 1.333 | 3.294 | 5.75 |
| *Diademodon* | UMCZ T504a | 0.533 | 0.207 | 2.575 | 3.892 | 5.75 |
| | UMCZ T475 | 0.567 | 0.226 | 2.509 | 3.652 | 6 |
| | UMCZ T504b | 0.574 | 0.256 | 2.246 | 3.732 | 6.15 |
| *Trirachodon* | SAM-PK-K5881 | 0.611 | 0.329 | 1.855 | 3.275 | 6.5 |

The overall carbonate content of the fossil *Sivatherium hendeyi* and extant *Giraffa camelopardalis* (pre-treated and unpre-treated) enamel spectra are similar. However, these values are significantly lower than the extant *Crocodylus niloticus* and *Varanus* carbonate content (independent 1-tailed t-test: $t_s = -7.769$; $df = 11$; $p < 0.05$). In addition, the non-mammalian cynodont

carbonate content is most similar to the extant *Crocodylus niloticus* and *Varanus* values.

In order to observe the generic differences in overall carbonate content more clearly, the results are presented graphically in Figure 9.13.

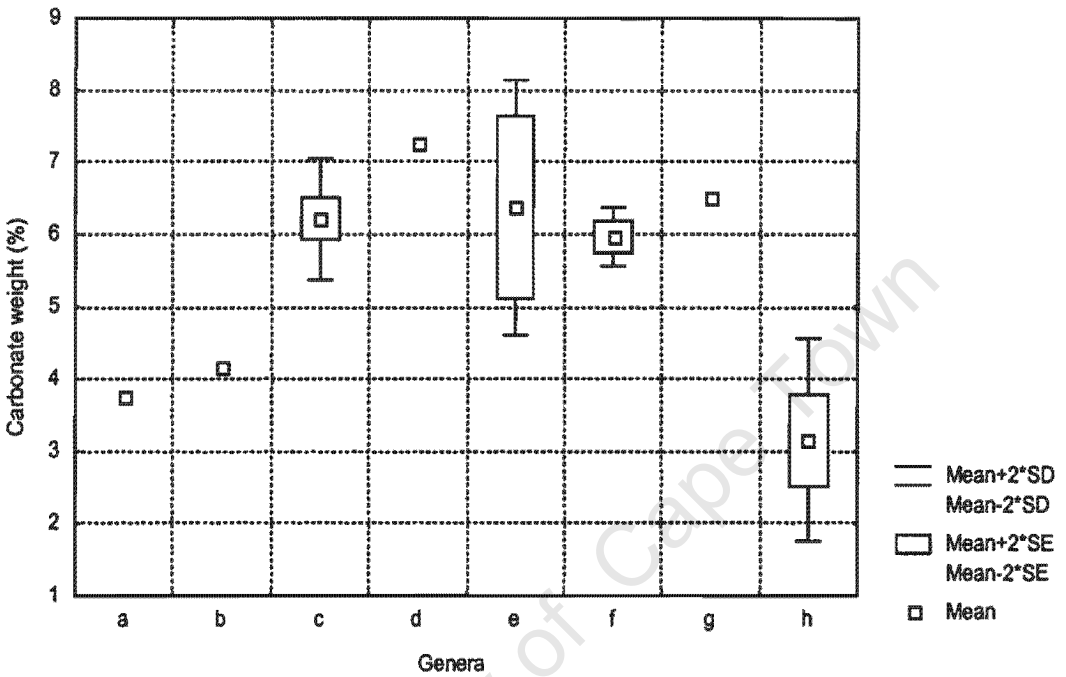


| symbol | name | n |
|---|---|---|
| a | *Giraffa camelopardalis* | 1 |
| b | *Sivatherium hendeyi* | 1 |
| c | *Crocodylus niloticus* | 9 |
| d | *Varanus* | 1 |
| e | *Cynognathus* | 2 |
| f | *Diademodon* | 3 |
| g | *Trirachodon* | 1 |
| h | *extant mammal* * | 5 |

* Sponheimer and Lee-Thorp (1999a)

Figure 9.13. Percentage carbonate weight of each of the genera. The legend gives the full names of the genera presented in the graph and n indicates the number of individual teeth used to obtain the value of each genus. The last letter (h) refers to extant mammalian material taken from Sponheimer and Lee-Thorp (1999a) and has been included to expand the mammalian sample size for comparison with the material in this study. This extant mammalian material includes three bovids, *Raphicerus melanotis, Syncerus caffer, Damaliscus dorcas* and the cercopithecid *Papio cynocephalus* (Sponheimer and Lee-Thorp, 1999a).

The extant and fossil mammalian carbonate content (including values from Sponheimer and Lee-Thorp (1999a), shown in Appendix 5) is significantly lower than the *Crocodylus niloticus, Varanus* and non-mammalian cynodont values (independent 1-tailed t-test: $t_s = -8.10402$, $df = 17$, $p < 0.05$).

### 9.3.2 Stable Isotope Analyses

The $\delta^{13}C$ and $\delta^{18}O$ results are presented graphically in Figures 9.14 to 9.19. Each point, in the graphs, represents a sample taken from one band of each tooth. Each group of points, connected by a line, indicates all the points taken in bands, in one tooth, from the top of the crown (left) through towards the base of the crown (right). Detailed $\delta^{13}C$ and $\delta^{18}O$ values are given in Appendix 6.

#### (i) Extant Isotope Signatures

The *Crocodylus niloticus* $\delta^{18}O$ values range from –2‰ to –5.3‰, whereas the $\delta^{13}C$ values range from –3.9‰ to –8.8‰. Both ratios show high intra-tooth variability (Figure 9.14). Out of the three teeth that were analysed, CROC 1 shows the most intra-tooth variability. However, all the teeth show a variability of more than 1‰ for both $\delta^{18}O$ and $\delta^{13}C$.

#### (ii) Non-mammalian Cynodont Isotope Signatures

The *Thrinaxodon* tooth (B/P/I/5020), shows a high intra-tooth variability, where the $\delta^{18}O$ values range from –10.8‰ to –12.5‰ and the $\delta^{13}C$ values range from -12‰ to -13.3‰ (Figure 9.15). These values vary more than 1‰ in both the $\delta^{18}O$ and $\delta^{13}C$ ratios.

Two *Cynognathus* teeth were analysed (SAM-PK-K3029; B/P/I/1675d). The $\delta^{18}O$ values vary from -10.7‰ to -13.7‰, whereas the $\delta^{13}C$ values range from –10.5‰ to –12‰ (Figure 9.16). Although the values in specimen B/P/I/1675d do not vary considerably, only two samples could be obtained from this tooth. Therefore, it is possible that if more samples had been obtained, the intra-tooth variation would be higher than what is shown in Figure 9.16. However, the

SAM-PK-K3029 tooth shows slightly more variability, although it is less than 1‰. It is important to note that the variability is directional.

Eight *Diademodon* teeth were analysed in this study, which provided a large sample size for the examination of intra-tooth variation. Although the same eight teeth were used to obtain the serial $\delta^{18}O$ and $\delta^{13}C$ values, the results are presented separately due to the large number of teeth. Figure 9.17 shows the $\delta^{18}O$ values of the respective *Diademodon* teeth, which range from -10.3‰ to -16.5‰. The average $\delta^{18}O$ values vary by up to 6‰ (UMCZ T487) and no less than 1.5‰ (average 3.8‰). The *Diademodon* $\delta^{13}C$ values are presented in Figure 9.18 and they vary from -12.2‰ to -15‰. The $\delta^{13}C$ values vary by approximately 1.3‰, not as much as the $\delta^{18}O$ values. However, all eight *Diademodon* teeth show directional intra-tooth variability in their $\delta^{18}O$ and $\delta^{13}C$ ratios.

The *Trirachodon* FTIR spectrum (Figure 9.12) shows that the enamel apatite structure is altered, but the isotope ratios in the teeth still show some intra-tooth variability (Figure 9.19). The $\delta^{18}O$ values range from -7.7‰ to -13‰ and the $\delta^{13}C$ values range from –9.7‰ to –13.4‰. Most predictions suggest that diagenesis results in increased homogeneity. Therefore, either the *Trirachodon* $\delta^{18}O$ and $\delta^{13}C$ values show less variability than they would have if the enamel had not been diagenetically altered, or diagenesis is not so great as to have completely destroyed the isotope signature, so allowing some intra-tooth variation to be discerned. However, more samples are needed to discern whether the variation is directional or not.

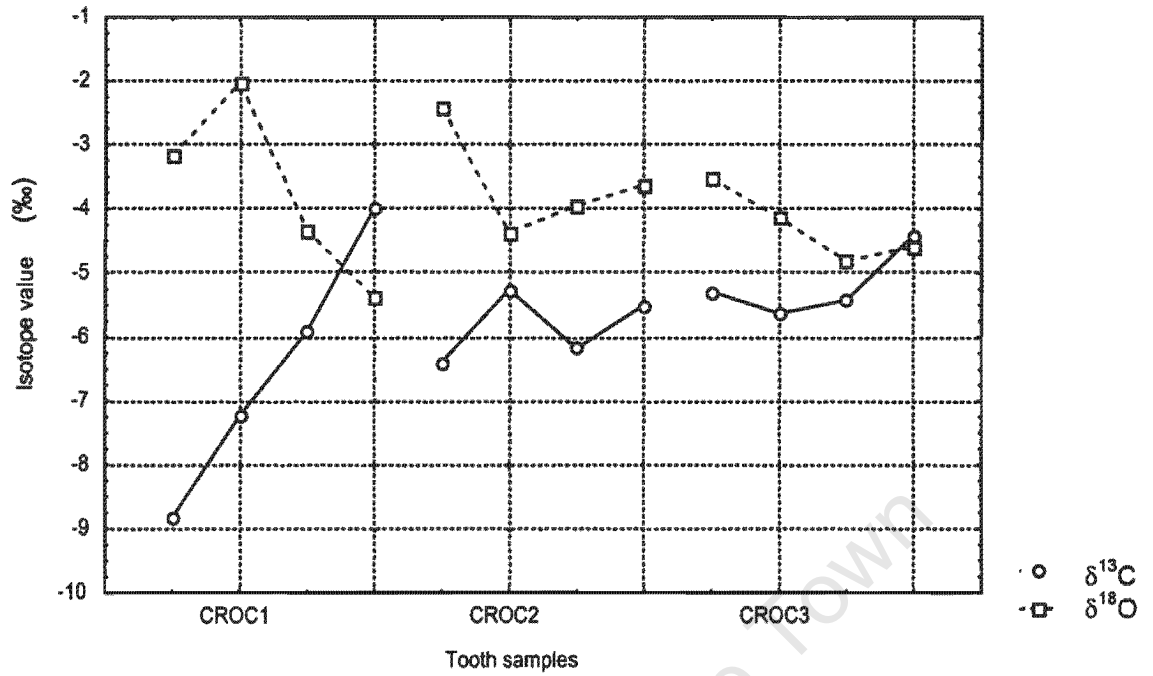


Figure 9.14. $\delta^{13}C$ and $\delta^{18}O$ ratios of the enamel carbonate of extant *Crocodylus niloticus*. Three teeth (CROC1, CROC 2, CROC 3) from three different individuals were analysed.

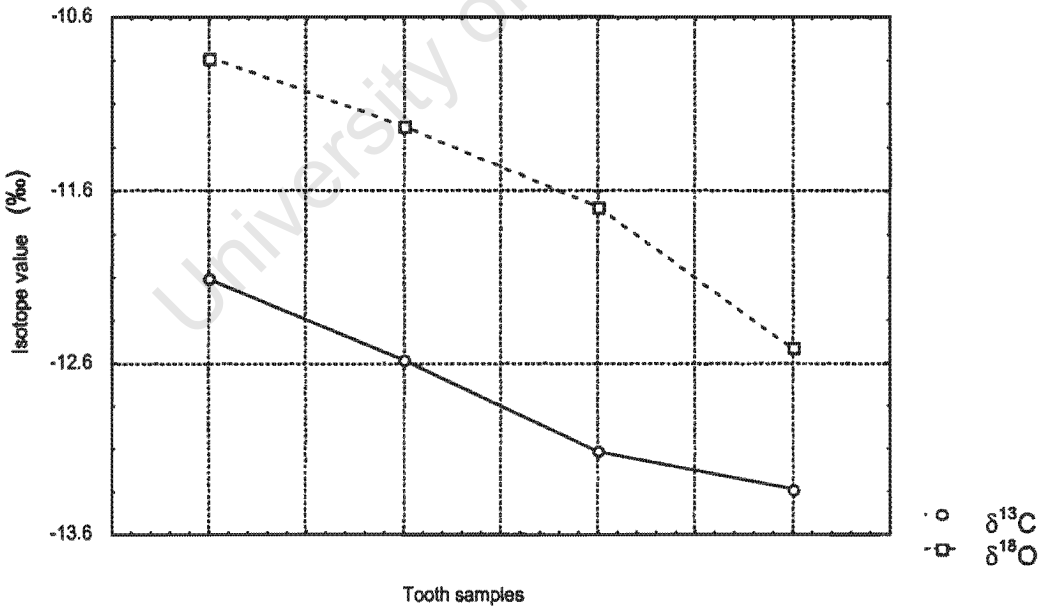


Figure 9.15. $\delta^{13}C$ and $\delta^{18}O$ ratios of the enamel carbonate of the non-mammalian cynodont *Thrinaxodon* specimen (B/P/I/5020). One tooth was analysed.

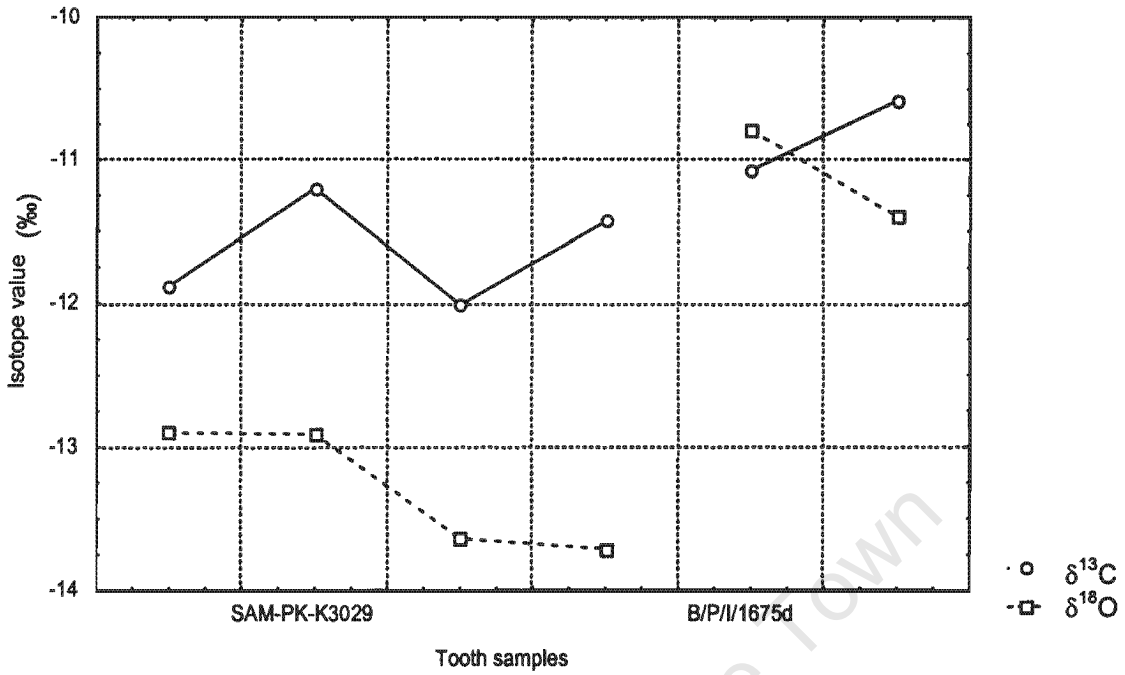


Figure 9.16. $\delta^{13}C$ and $\delta^{18}O$ ratios of the enamel carbonate of the non-mammalian cynodont *Cynognathus*. One tooth from each individual (SAM-PK-K3029 and B/P/I/1675d) was used.

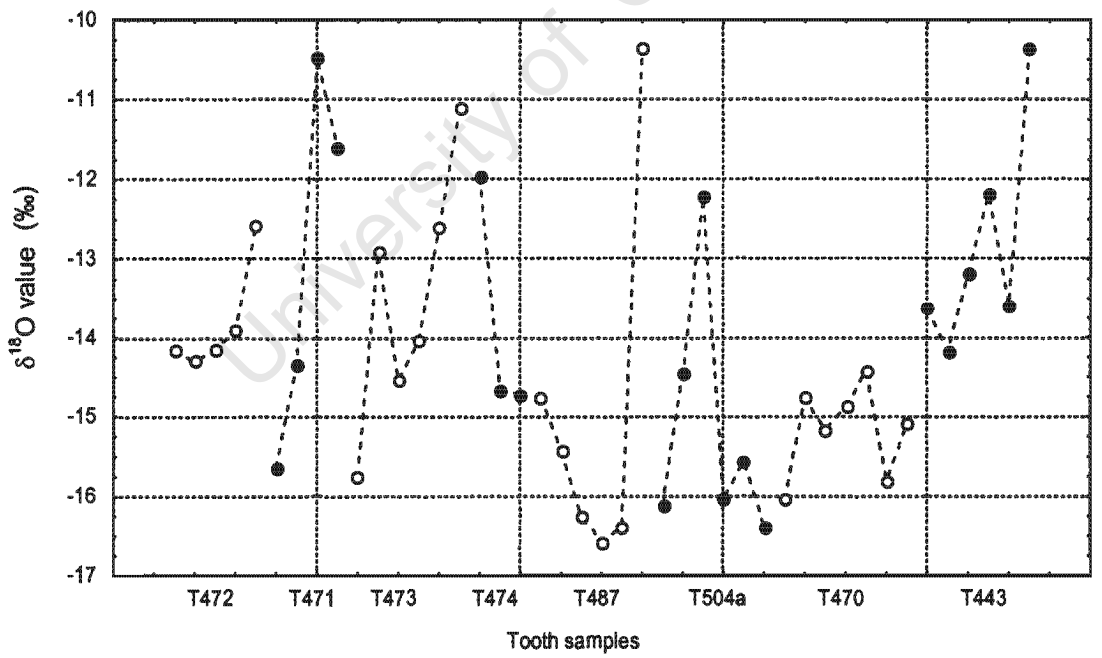


Figure 9.17. $\delta^{18}O$ ratios of the enamel carbonate of the non-mammalian cynodont *Diademodon*. Each group of points represents samples taken along each of eight teeth from several individuals. Open and closed circles are used to distinguish between successive teeth (Each tooth is a UMCZ T specimen, see Appendix 1 for institutional abbreviations).

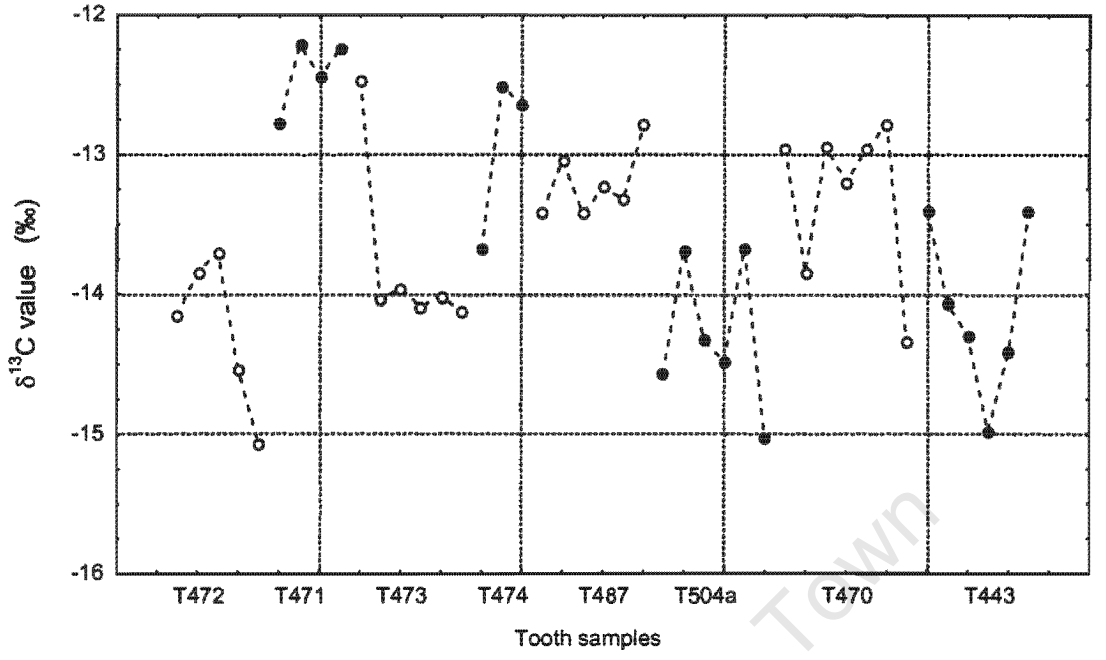


Figure 9.18. $\delta^{13}C$ ratios of the enamel carbonate of the non-mammalian cynodont, *Diademodon.* Open and closed circles as in Figure 9.17.

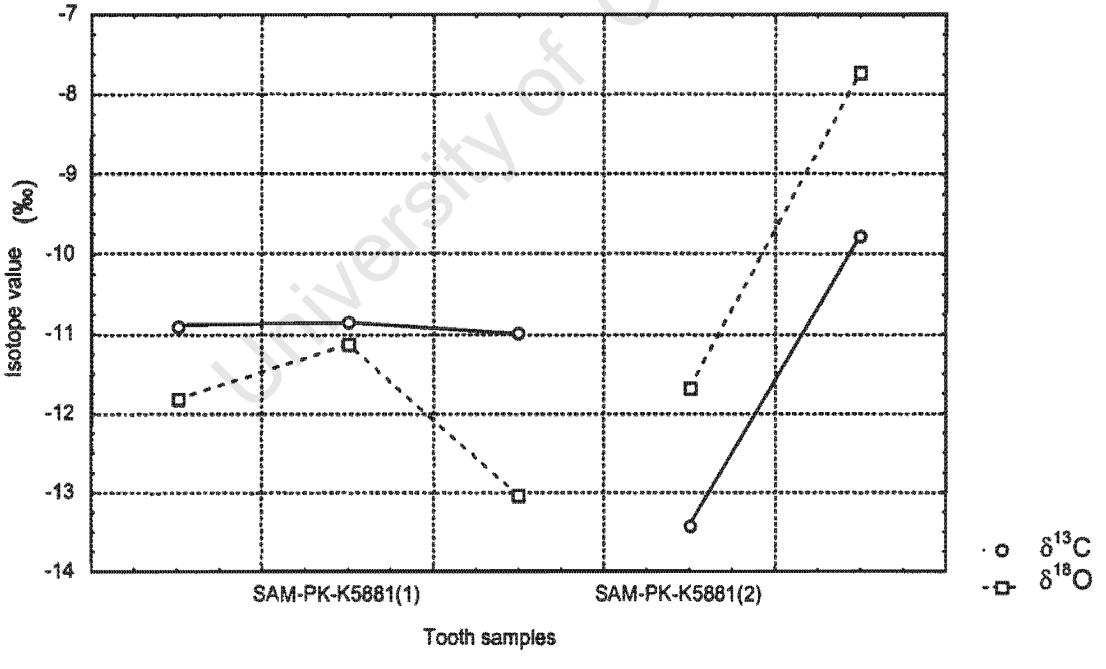


Figure 9.19. $\delta^{13}C$ and $\delta^{18}O$ ratios of the enamel carbonate of the non-mammalian cynodont *Trirachodon.* Two teeth from two different individuals (SAM-PK-K5881(1); SAM-PK-K5991(2)) were sampled.

The mean $\delta^{13}C$ and $\delta^{18}O$ values of each non-mammalian cynodont tooth were plotted against each other (Figure 9.20) to establish any distinctions between them (see Appendix 4 for detailed values).

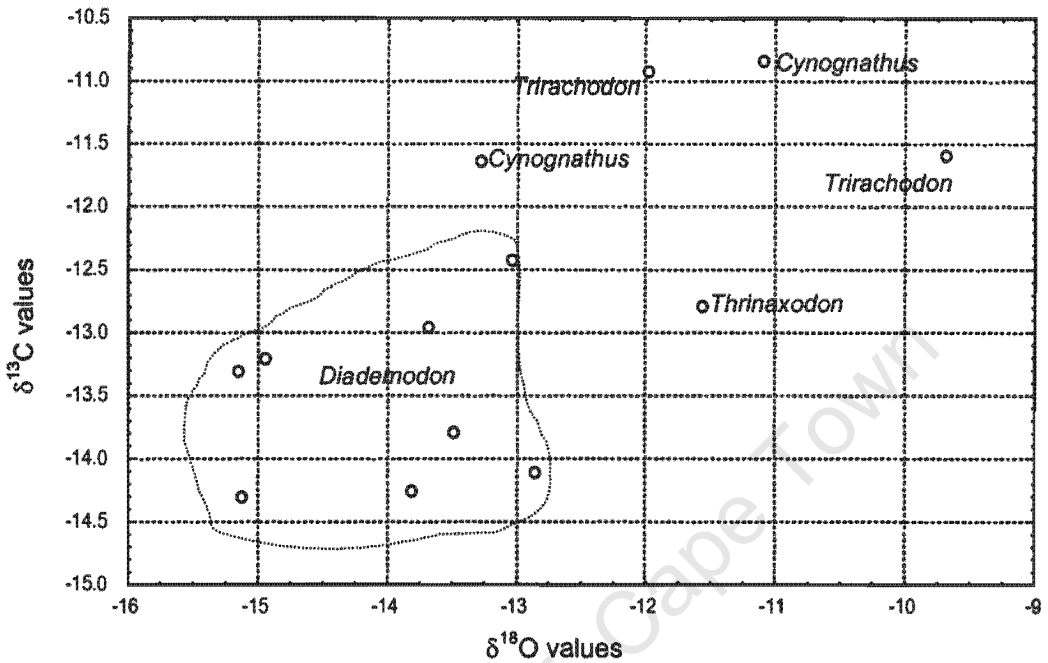


Figure 9.20. $\delta^{13}C$ versus $\delta^{18}O$ ratios of the non-mammalian cynodonts *Thrinaxodon, Cynognathus, Diademodon* and *Trirachodon.*

The *Diademodon* $\delta^{18}O$ and $\delta^{13}C$ values cluster together and are significantly more depleted than the *Thrinaxodon, Cynognathus* and *Trirachodon* ratios (independent 1-tailed t-test: $\delta^{18}O$: $t_s = -4.641$; $df = 56$; $p < 0.05$ and $\delta^{13}C$: $t_s = -7.474$; $df = 56$; $p < 0.05$).

## 9.4 Interpretations

### 9.4.1 Enamel Apatite Structure

The profiles of most of the non-mammalian cynodont spectra resemble biological apatite in spite of the great age of the enamel. The apatite structure is therefore not drastically altered, although it is recognised that some ionic shifts and probably recrystallisation will have occurred.

## (i) Fourier Transform Infra-red Analysis of Extant Taxa

### (a) Effect of Pre-treatment

Pre-treating the extant *Giraffa camelopardalis* enamel had very little affect on the absorbance spectrum (Figure 5A, 5B). In contrast, pre-treatment notably affected the dentine (Figure 6A, 5B). This is to be expected, as dentine contains more organic components than does enamel (LeGeros, 1991) and pre-treatment is a technique for removing organic contaminants.

### (b) Comparison of Extant FTIR Spectra

The higher *Giraffa camelopardalis* 1654 $cm^{-1}$ dentine peak, ~1657 $cm^{1}$ dentine *Crocodylus niloticus* and *Varanus* peaks, compared to the enamel spectra, are further indications that dentine has a higher organic content than does enamel, as shown in earlier studies (e.g. LeGeros, 1991). If this difference is noted in extant taxa, results obtained from fossil dentine may be very different from fossil enamel. Dentine may therefore be more susceptible to diagenesis during fossilization, which suggests that caution should be taken in making deductions from dentine.

Although care was taken in drilling merely the outer surface of the *Varanus* teeth to obtain enamel, the FTIR spectra (Figure 9.8A, 9.8B) show that a small amount of dentine was likely incorporated (shown by the high ~1657 $cm^{-1}$ peak). The *Crocodylus niloticus* and *Varanus* enamel and dentine are the same colour and do not exhibit any observable visual differences, but it proved possible to assess how much enamel was incorporated into a sample by looking at an FTIR spectrum. In this way, enamel thickness can be assessed, providing a way of knowing how deeply a tooth can be drilled. Using this method, it can be seen in this study, that dentine may have been incorporated into the *Varanus* sample, which may have increased the overall carbonate content as the $CO_3$ percentage is higher than any of the other samples in the study.

**(ii) Fourier Transform Infra-red Analysis of Extinct Taxa**

The lower absorbances of the non-mammalian cynodont spectra are probably due to changes that occurred during fossilization. The enamel spectrum of the fossil mammal, *Sivatherium hendeyi,* also exhibits a lower overall absorbance compared to the extant *Giraffa camelopardalis* enamel spectrum (Figures 9.5A, 9.5B and 9.9), which indicates less overall apatite. The difference in proportion between the phosphate peaks of the $\nu_4$ phosphate of the *Cynognathus* and *Diademodon* spectra (Figures 9.10 and 9.11) and the extant *Giraffa camelopardalis, Crocodylus niloticus* and *Varanus* peaks suggests that some diagenetic alteration has occurred. However, the overall profile of the fossil spectra, apart from that of *Trirachodon*, resembles biological apatite, suggesting that diagenesis is minimal. Diagenetic alteration of the *Trirachodon* material appears to be more extensive as shown by the numerous extra peaks in the spectrum (Figure 9.12).

These observed differences between the extant and fossil spectra are due to a re-arrangement of the various ions in the fossil material. According to Krueger (1991), the general mechanisms that can alter the chemical composition of carbonate in fossil apatite are: exogenous carbonate incorporation at B-sites, endogenous carbonate loss at A-sites and endogenous carbonate reorganisation. All the non-mammalian cynodont BPI results are similar to those of *Crocodylus niloticus,* whereas the API values (apart from *Cynognathus*) are less than the *Crocodylus niloticus* values. However, some of the *Diademodon* API values (UMCZ T504a, 475) are similar to the *Sivatherium hendeyi* API value, which suggests that fossilization has affected the non-mammalian cynodont material in the same way. The non-mammalian cynodont type A carbonate peak is extremely low. The type A carbonate has probably not been incorporated into the type B carbonate sites, as the fossil type B carbonate peak does not exceed that of *Crocodylus niloticus.* Hence, exogenous incorporation of carbonate into the type B-sites, is also unlikely. It is possible that the type A carbonate has merely been lost from the type A-site $\nu_3$ carbonate domain due to the fossilization process.

The ratio between the 565 $cm^{-1}$ and 605 $cm^{-1}$ phosphate peaks in the $\nu_4$ phosphate domain differs between extant (Figures 9.5, 9.7, 9.8) and non-mammalian cynodont (Figures 9.10, 9.11) enamel spectra (apart from *Trirachodon*). This indicates that the phosphate in the fossil material has been altered to some extent, over the past 220 million years. The *Sivatherium hendeyi* 565 $cm^{-1}$ and 605 $cm^{-1}$ phosphate peaks are similar to those of the extant spectra and as the *Sivatherium hendeyi* material is only approximately 5 million years old, the observed alteration of the non-mammalian cynodont teeth is probably due to their extreme age. Phosphate is widely used in palaeontological isotope studies as it is thought to be less susceptible to diagenetic alteration compared to carbonate, but as shown from the FTIR results in this study, this may not always be the case. Phosphate may also undergo diagenetic alteration as shown in the $\nu_4$ phosphate of the non-mammalian cynodont FTIR spectra.

The absorbance spectra give an overall profile of the apatite structure, but the indices allow observed variations to be quantified. Extant mammalian enamel indices and overall carbonate content were taken from a study conducted by Sponheimer and Lee-Thorp (1999a) and added to the data obtained in this study (shown in Figure 9.21).

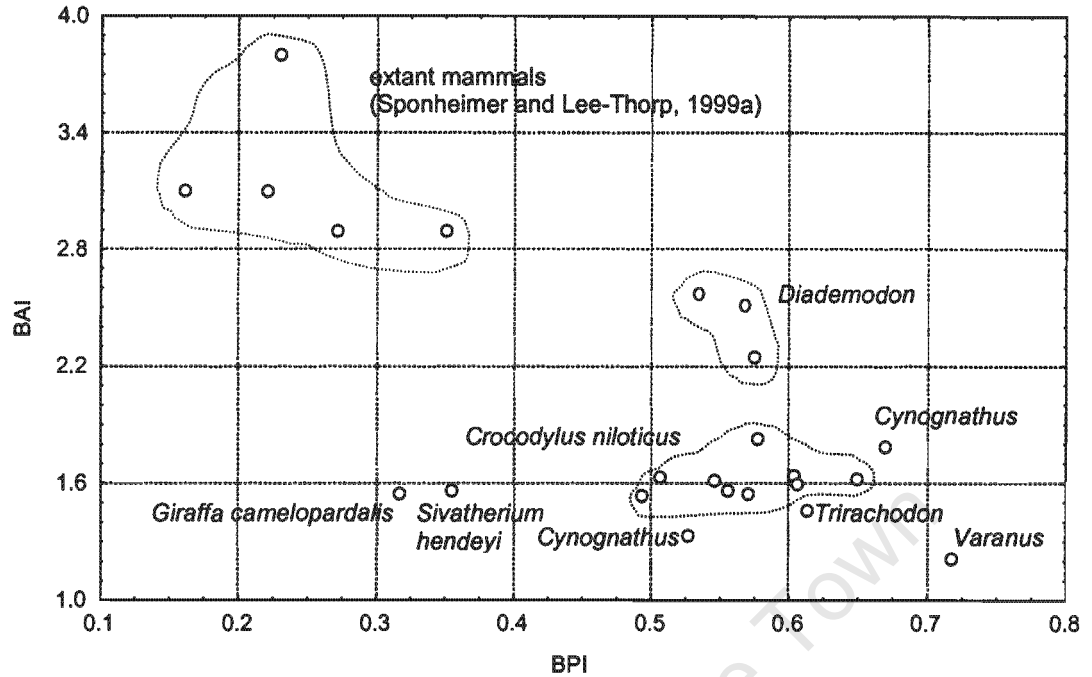


Figure 9.21. BPI versus BAI of the non-mammalian cynodonts, the extant *Crocodylus niloticus, Varanus, Giraffa camelopardalis,* the fossil *Sivatherium hendeyi* and the extant mammalian material from Sponheimer and Lee-Thorp (1999a).

When comparing the two data sets, the BAI indices from their study on extant mammals differ from the BAI *Giraffa camelopardalis* enamel indices in this study. The *Giraffa camelopardalis* was found to have a significantly higher API (independent 1-tailed t-test: $t_s = 2.9021$; df = 4; $p < 0.05$) than those calculated by Sponheimer and Lee-Thorp (1999a), which is probably why this BAI is lower than their values. The reason for this difference in not clear. However, all mammalian BPI indices (extant and extinct), whether from this study or that of Sponheimer and Lee-Thorp differ from the *Crocodylus niloticus, Varanus* and non-mammalian cynodont BPI indices. The mean BPI of *Crocodylus niloticus* and *Varanus* is 0.58 and the mean non-mammalian cynodont BPI is 0.57. In contrast, the extant mammalian BPI, including those indices from Sponheimer and Lee-Thorp, is 0.26. The non-mammalian cynodont BPI is significantly closer to the *Crocodylus niloticus* and *Varanus* mean value than the mammalian value.

As BPI was used to estimate overall carbonate content, a similar result was obtained, where the non-mammalian cynodont carbonate percentage weight (average 6.13%) significantly differs from that of *Giraffa camelopardalis* and *Sivatherium hendeyi* (average 3.75%) and is most similar to the *Crocodylus niloticus* and *Varanus* value (average 6.32%). When these mammalian values are added to the carbonate content values from Sponheimer and Lee-Thorp's study, they still differ significantly from the non-mammalian cynodont results (independent 1-tailed t-test: $t_s = -11.8974$; $df = 22$; $p < 0.05$). These findings suggest that the amount and structural properties of the non-mammlian cynodont carbonate is similar to that of *Crocodylus niloticus* and *Varanus*.

The similarity of the non-mammalian cynodont BPI and carbonate content to the extant *Crocodylus niloticus* and *Varanus* BPI and carbonate content may be due to fossilization, which may cause an increase in type B carbonate, which in turn may increase the BPI (Michel et al., 1995). However, the non-mammalian cynodont spectra profiles indicate biological apatite and the clear distinction between extant mammalian and non-mammalian cynodont values suggests that diagenesis is low. This suggests that the similarity is biological and not due to diagenesis.



### 9.4.2 Stable Isotope Analyses

The *Crocodylus niloticus* oxygen and carbon isotope results exhibit directional intra-tooth variability (Figure 9.14). The variability may be partly due to the ectothermic physiology of the animal as variations in body temperature will affect enamel formation and hence the $\delta^{18}O$ values. However, the large range is probably also due to seasonal variability. These teeth were collected from Stellenbosch in South Africa, which experiences a seasonal climate. In mid- to high latitudes, a positive correlation exists between $\delta^{18}O$ and temperature. The area from where the *Crocodylus niloticus* teeth were obtained experiences warm, dry summers and cool, wet winters. Increased evaporation during the warm summer can lead to isotopic fractionation, causing $\delta^{18}O$ of ingested water to increase during this period. Therefore the more enriched $\delta^{18}O$ values in the

*Crocodylus niloticus* teeth may represent warmer periods, whereas the more negative values, colder periods.

The average non-mammalian cynodont $\delta^{13}C$ value is -13.1‰, (standard deviation = 1.203) which reflects a $\delta^{13}C$ plant range of -25.5‰ to -27.5‰. These values are very similar to today's $C_3$ plant values (Smith and Epstein, 1972). The $\delta^{13}C$ $CO_2$ value of the Triassic is believed to have been approximately -7.4‰ (Ekart et al., 1999, using palaeosol carbonates), which is similar to today's value of -8‰. All Triassic plants used the $C_3$ photosynthetic pathway. Therefore, the fossil $\delta^{13}C$ plant range should be similar to the range of modern values (-30‰ to -23‰) and the results show that this is the case. As these values fall within the expected ranges, they aid in verifying the validity of the oxygen isotope results.

In addition, the *Diademodon* $\delta^{13}C$ values are significantly lower than the rest of the non-mammalian cynodont values (Figure 9.20). Although, there are limitations as to how precisely the carbon isotope values can be interpreted, it is possible that these low $\delta^{13}C$ values are because *Diademodon* was omnivorous. *Trirachodon* as a herbivore, may have eaten different plant matter to *Diademodon*, whereas *Thrinaxodon* and *Cynognathus* were carnivores and may have eaten herbivores that ate plants with different $\delta^{13}C$ values to what *Diademodon* ate. However, more research is needed to verify this suggestion.

With the exception of *Cynognathus,* (whose $\delta^{18}O$ values varied by only 0.81‰), the $\delta^{18}O$ values in the *Thrinaxodon, Trirachodon* and each of the *Diademodon* teeth varied by more than 1‰. It is significant that the intra-tooth variation is directional throughout all the teeth as it may indicate seasonality. The small *Thrinaxodon, Cynognathus* and *Trirachodon* sample size poses a difficulty in assessing seasonal variability in these teeth. However, a 1‰ intra-tooth variability in the *Thrinaxodon* and *Trirachodon* teeth is large enough (Kohn et al., 1999) to suggest that they reflect seasonal variation.

A study conducted on the $\delta^{18}O$ of extant Canadian beaver enamel phosphate found the $\delta^{18}O$ values to vary by approximately 3‰ and the maximum variation to be 3.6‰ (Stuart-Williams and Schwarcz, 1997). Studies have also found a 3.5‰ variation in the $\delta^{18}O$ of fossil bison (approximately 500 years old) and extant sheep enamel phosphate (Fricke and O'Neil, 1996), while a similar variation has been found in the $\delta^{18}O$ of Holocene horse enamel phosphate (Sharp and Cerling, 1998). The variation in $\delta^{18}O$ values of the *Diademodon* enamel is approximately 3.8‰ with a maximum of 6‰ (Figure 9.17). There is no conclusive evidence to indicate whether *Diademodon* was ectothermic or endothermic and it is more difficult to examine seasonality using ectothermic animals. Although studies have claimed that oxygen isotope signatures in the bone phosphate of non-avian dinosaurs can indicate the type of thermal physiology they experienced (Barrick, 1994; Barrick and Showers, 1995; Barrick et al., 1996), there are several problems with this proposal. For example, it has been suggested that intra-bone isotopic variability of an endothermic individual should be very low, i.e. less than 1‰ (Barrick and Showers, 1995). However, it is difficult to ensure that low isotopic variability is due to physiology alone and not diagenetic alteration, as diagenesis tends to decrease isotopic variability. Secondly, studies using this approach have not considered the effect of environmental fluctuations or lack thereof when examining variations in bone phosphate $\delta^{18}O$ (e.g. Barrick and Showers, 1995).

Even if *Diademodon* had a typical ectothermic physiology, similar to extant crocodilians and lizards, the intra-tooth $\delta^{18}O$ variability of up to 6‰, is too high for it to account for variations in body temperature alone (Barrick, pers. comm., 2001). It is more likely that the intra-tooth $\delta^{18}O$ variability in *Diademodon* reflects the extremes of a seasonal climate. Earlier studies have suggested that the environment of the time was semi-arid with a seasonal climate (Tucker and Benton, 1982; Anderson and Anderson, 1983, 1985; Smith et al., 1993), in which warm, dry summers were followed by cool, wet winters (Smith pers. comm. 2001). Therefore, the high $\delta^{18}O$ values in the *Diademodon* teeth may

reflect a spring or summer season, whereas the lower $\delta^{18}O$ values may reflect an autumn or winter season (Fricke and O'Neil, 1996).

The absolute overall $\delta^{18}O$ signature in these animals is more difficult to interpret due to diagenesis. Considering the non-mammalian cynodont FTIR spectra (showing the presence of biological apatite) and the carbon isotope results (showing coherent, expected results), diagenesis is probably minimal. Hence, although specific $\delta^{18}O$ values may not be considered, reasonable interpretations regarding the trends and differences between the genera may be made.

The significantly depleted *Diademodon* $\delta^{18}O$ values compared to the $\delta^{18}O$ values of *Thrinaxodon, Cynognathus* or *Trirachodon* (Figure 9.20) may suggest inherent biological differences. Bocherens, et al. (1996) found that the $\delta^{18}O$ values in *Hippopotamus amphibius* were depleted by approximately 6‰, compared to the rest of the terrestrial herbivores in the study. Bocherens et al., (1996) suggested that the $\delta^{18}O$ values were depleted because of nocturnal terrestrial foraging or diurnal feeding on aquatic vegetation. Evapotranspiration is reduced when plants are not actively photosynthesising, which is usually at night and this may deplete the $\delta^{18}O$ values of animals feeding at this time. Similarly, aquatic plant water is not as enriched in $^{18}O$ as the water in terrestrial plants and may result in lower $\delta^{18}O$ values in those animals feeding on aquatic plants. Bocherens et al. (1996) proposed that because hippopotamuses spend so much time in water, the loss of water from their bodies via transcutaneous evaporation is substantially reduced. Water lost in this way experiences a strong isotope factionation and submergence in water would reduce the loss of $^{18}O$-depleted water. This would produce low $\delta^{18}O$ values in hippopotamus body water compared to terrestrial mammals with large evaporative water loss fluxes.

The semi-aquatic *Crocodylus niloticus* also exhibits relatively low $\delta^{18}O$ values Figure 9.14). Therefore, it is possible that the depleted *Diademodon* $\delta^{18}O$ values support either nocturnal or semi-aquatic habits.

Although diagenesis cannot be excluded, the significantly higher *Thrinaxodon, Cynognathus* and *Trirachodon* $\delta^{13}C$ and $\delta^{18}O$ values compared with those of *Diademodon* suggest that this difference may be due to biological differences and not fossilization. In addition, although the material was collected from different localities in South Africa, all the material was collected from a similar latitude and longitude (30° 40' to 31° 45'S and 26° 20' to 27° 15'E). This then excludes the effect of large-scale differences in rainfall on the material. Any large differences in $\delta^{18}O$ values between the genera is more likely to be due to their biology and not rainfall location differences.

As the non-mammalian cynodont enamel used in this study is of Triassic age, great care was taken in checking the validity of the isotope signatures. The combined results of the FTIR spectroscopy, the coherent, expected $\delta^{13}C$ results and the lack of homogeneity in both the $\delta^{18}O$ and $\delta^{13}C$ values, suggests that reasonable interpretations can be deduced from the trends seen in these isotope results. Although these findings are preliminary and more material needs to be examined, they demonstrate the potential for isotope analysis to be used in studying the palaeobiology and palaeoenvironment of the non-mammalian cynodonts.

# CHAPTER TEN
# DISCUSSION

*Summary*

*The results of the bone cross-sectional geometry, bone histology and stable isotope analyses of the non-mammalian cynodont genera studied are discussed. The bone cross-sectional geometry and stable isotope analyses reveal important implications of the lifestyle habits of these animals (section 10.1). Procynosuchus cross-sectional geometry results suggest that the relatively thick bone walls are an adaptation for an aquatic lifestyle and help prevent positive buoyancy while in the water. As high relative bone wall thickness (RBT) values were also found in the fossorial Trirachodon and Tritylodon, it is proposed that relatively thick bone walls are also an adaptation for a fossorial lifestyle. The high relative bone wall thickness values of the Diademodon limb bones combined with the depleted enamel carbonate $\delta^{18}O$ values suggest that this animal was semi-aquatic. The analysis of the bone histology of these animals revealed distinct growth patterns for each genus. The possible reasons for the observed variability, such as phylogenetic constraints, ontogenetic variation, environmental fluctuations, inter-elemental variability and sexual dimorphism, are discussed in section 10.2. Fourier Transform Infra-red spectroscopic analysis (section 10.3) indicates a significant similarity in BPI and carbonate content between the extant Crocodylus niloticus and non-mammalian cynodont enamel, which suggests a similarity in structural properties. The value of carbon and oxygen isotope analyses to provide information regarding seasonal variability is also discussed (section 10.3). This study has revealed important information relating to the lifestyle habits, ontogeny and growth strategies of non-mammalian cynodonts.*



The objective of this study was to assess whether observable changes in non-mammalian cynodont growth patterns occurred during their evolution. The morphology of these animals exhibit increasingly mammalian characteristics during their evolutionary history (Kemp, 1982; Hopson, 1994; Rubidge and Sidor, 2001), but it is not known if their bone histology also shows such increasingly mammalian features. As multiple elements from different parts of the skeleton were examined, a comprehensive assessment of non-mammalian cynodont bone histology and therefore growth pattern was conducted. The oxygen and carbon isotope analyses performed on the teeth of these animals provided further information relating to their lifestyle habits and their interactions

with the environment. This combined examination, of bone histology and stable isotope analyses, has provided insight into the lifestyle adaptations, ontogeny and growth of these animals.

## 10.1 Lifestyle Implications

The bone cross-sectional geometry assessment has provided fresh insight into the lifestyles of the non-mammalian cynodont genera studied. The high relative bone wall thickness (RBT) value (radius 30.4%) of the semi-aquatic *Procynosuchus* is similar to those values of several semi-aquatic crocodilians, lizards and mammals as shown in Appendix 3. Although no strict specific percentage can designate a lower limit below which an animal is no longer aquatic, the 30% threshold that Wall (1983) proposed as the approximate lower bone wall thickness limit for aquatic or semi-aquatic animals, appears to be adequate (Appendix 3). Hence, as a general trend, the cross-sectional geometry results in this study support the earlier proposals of Wall (1983), Currey and Alexander, 1985; Stein (1989) and Fish and Stein (1991) that limb bone densities in aquatic or semi-aquatic animals are high for counteracting buoyancy in the water. However, relatively thick bone walls were also found in *Trirachodon* (radius, ulna and sub-adult femur, 28%) and *Tritylodon* (humerus and radius 34.77%). As discussed in previous chapters, these two animals are likely to have been fossorial. Earlier studies have found fossorial animals to have particularly thick limb bones (Bou et al., 1990; Casinos et al., 1993), but the relative bone wall thickness of these animals was not examined. Therefore the findings in this study suggest that fossorial animals also have relatively thick bone walls, possibly as an adaptation to digging.

High RBT values found in practically all of the *Diademodon* elements studied may indicate either a fossorial or semi-aquatic lifestyle for this animal (see Chapter 6.4.2). However, the *Diademodon* oxygen isotope signatures are significantly depleted (Figure 9.20), compared to the rest of the non-mammalian cynodont genera studied and may suggest nocturnal or semi-aquatic habits (as discussed in Chapter 9.4.2). When these isotope values are considered in

conjunction with the high RBT values, they strongly suggest a semi-aquatic lifestyle for *Diademodon*. However, the lack of visible skeletal swimming adaptations, suggest that it was probably not an active swimmer. *Diademodon* may have fed in shallow water or behaved in a similar manner to the extant *Hippopotamus amphibious*.

The K-value analysis also showed that although there was some variation between the genera, all the values approach the value of 0.55, which suggests a selection for impact loading and ultimate strength. Animals that are more strongly selected for weight tend to have lower K-values (and high RBT values) than those animals selected for low mass (e.g. the thin bone walls of birds for flight). Thick-walled bones are stronger under localised impact than thin-walled bones and are stronger in bending if the animal is able to tolerate some bone deformation (Currey and Alexander, 1985). However, it should be noted that the *Thrinaxodon* K-values are generally higher than the rest of the genera studied, which agrees with the suggestion that the limb bones of this animal were modified for a fully terrestrial lifestyle. Although *Thrinaxodon* is similar in size to *Procynosuchus, Trirachodon* and *Tritylodon,* which all show modifications in their bone cross-sectional geometry to suggest an aquatic or fossorial life, the *Thrinaxodon* K-values indicate no such adaptations. The differences in K-values between these genera and *Thrinaxodon* therefore probably reflect lifestyle differences and not body size variation.

When comparing the K-values of the elements of similar ontogenetic age in this study, they indicate that the distal elements have lower K-values than the proximal bones. This finding is supported by a study conducted by Currey and Alexander (1985). They found that the extant mammalian distal limb bones in their study also tended to have lower K-values than the proximal bones. Low values may be favourably selected, as distal bones are more susceptible to impacts (Currey and Alexander, 1985).

## 10.2 Factors Affecting Non-mammalian Cynodont Growth Patterns

The results obtained from the bone histology aspects of this research show that the six non-mammalian cynodont genera exhibit distinct differences in growth pattern. Factors such as (i) phylogenetic constraints, (ii) ontogenetic variation, (iii) environmental fluctuations, (iv) inter-elemental histovariability and (v) sexual dimorphism may significantly affect growth and these possibilities are discussed below.

### (i) Phylogenetic Constraints

The non-mammalian cynodonts in this study span a temporal range of some 40 million years. The Late Permian *Procynosuchus* is the most basal non-mammalian cynodont studied. The predominance of poorly vascularised lamellar-zonal bone tissue in the *Procynosuchus* skeleton suggests that the overall growth of this animal was slow and cyclical (Chapter 4.3.2). Independent research has deduced that the climate was seasonal (Smith, et al., 1993) and the bone histology results obtained in this study suggest that *Procynosuchus* growth may have been sensitive to seasonal fluctuations. These findings do not agree with McNab's (1978) proposal that an intermediate metabolic rate, between that of ecto- and endotherms, was established prior to the evolution of the Procynosuchidae. McNab considered the decrease in mass within the Procynosuchidae and the presence of an incomplete secondary bony palate, which may have been completed in life by soft tissue, as evidence that an intermediate metabolic rate had been established prior to the evolution of the procynosuchid group. However, as discussed in Chapter 2.1, a secondary palate may not necessarily indicate endothermy and it is evident from this study that *Procynosuchus* grew in a similar manner to that of extant crocodilians, having a slow overall growth rate, even during the favourable growing season.

The Early Triassic *Thrinaxodon* represents a later stage in the non-mammalian cynodont lineage (see Figure 1.2). The presence of moderately vascularised fibro-lamellar bone tissue suggests that this animal grew relatively quickly, although the parallel-fibred peripheral tissue in older individuals suggests that

the overall growth slowed down with age. The overall growth strategy was not cyclical as in *Procynosuchus* and as the climate was still seasonal (Tucker and Benton, 1982), *Thrinaxodon* may have been less sensitive to seasonal variation. The overall absence of growth rings and presence of fibro-lamellar and parallel-fibred bone suggest that *Thrinaxodon* grew more rapidly than *Procynosuchus*.

The more derived non-mammalian cynodonts investigated in this study are *Cynognathus, Diademodon, Trirachodon* and *Tritylodon* (see Figure 1.2). The first three are all Early to Middle Triassic in age, whereas *Tritylodon* is of Early Jurassic age. The bone histology of *Cynognathus* indicates a rapid and sustained growth strategy even though the environment was seasonal (Tucker and Benton, 1982; Anderson and Anderson, 1983, 1985; Smith et al., 1993), which suggests that *Cynognathus* growth was unaffected by seasonal variation. The bones of *Cynognathus* are also significantly more vascularised than the rest of the genera studied (average of 12.65% compared to 0.27% for *Procynosuchus*; 4.79% for *Thrinaxodon*; 4.56% for *Diademodon*; 6.42% for *Trirachodon* and 4.59% for *Tritylodon*). An animal's growth is relative to the rate at which nutrients and energy are transported to growing tissues (Reid, 1996). Although the link between vascularity and size is not known, it is possible that, the high vascular canal density in *Cynognathus* was necessary for the animal to reach adult size fairly quickly. As the growth strategy of *Cynognathus* was rapid and sustained, it is possible that it differed physiologically from *Procynosuchus* and *Thrinaxodon*.

Given that *Cynognathus* and *Diademodon* were contemporaneous and that their remains are frequently found in the same deposits, it is reasonable to assume that they experienced the same environmental conditions. However, in contrast to *Cynognathus*, *Diademodon* had a moderately vascularised, cyclical growth strategy and may have been more sensitive to seasonal variation than *Cynognathus*. It is possible that *Diademodon's* food supply was seasonally influenced, whereas *Cynognathus,* as a carnivore, would have depended on the

same type of food throughout the year. The growth rate of *Diademodon* may have decreased during the unfavourable season because of food shortage or the presence of less nutritive food (Reid, pers. comm., 2000), but it is also possible that these differences in their growth strategies reflect inherent physiological differences.

The postcranial morphological similarity between *Cynognathus* and *Diademodon* (Brink, 1955; Jenkins, 1971) has posed problems in the past in identifying skeletal remains in the absence of cranial material. The distinct histological patterns observed in this study facilitate a positive identification of the postcranial elements of these genera when cranial material is absent.

The derived herbivorous, non-mammalian cynodont *Trirachodon* exhibits similar growth patterns to that of *Diademodon*, with some differences. Although most of the elements studied exhibit growth rings, indicating that *Trirachodon* had a cyclical growth strategy, a sub-adult femur and a late sub-adult radius exhibit some differences to the rest of the elements studied. Although the cortex of the sub-adult femur is not interrupted by annuli or LAGs, a change in tissue type occurs at the sub-periosteal surface. The tissue changes from fibro-lamellar to parallel-fibred in this region and this may indicate either an overall slowing down in growth or an annulus (Figure 7.4). Similarly, the radius consists of fibro-lamellar bone, which becomes parallel-fibred towards the periphery, but again annuli and rest lines are absent from the inner cortex (Figure 7.5). The differences in tissue organisation between these two bones and the rest of the elements may be due to inter-elemental variation (discussed in more detail in section 10.2 v). It is also possible, however, that earlier growth rings in these bones were resorbed, as the medullary margin is resorptive and large resorption cavities are evident in the medullary cavity regions (Figures 7.4 and 7.5). The overall growth strategy of *Trirachodon* is likely to have been zonal as even the ontogenetically younger elements exhibit zonal growth (Figures 7.3 and 7.7).

The bone histology of *Tritylodon* suggests that it had a rapid, sustained growth strategy even though the climate was semi-arid to arid and seasonal. However, two growth rings were observed in one radius (Figure 8.4) and this suggests that the individual may have responded to extreme fluctuations in environmental temperature and/or precipitation in a way that caused growth to slow down or cease during that period. Furthermore, it is not known if this individual suffered from disease, injury or a biomechanical abnormality that may have initiated enough stress for growth to temporarily cease. As the rest of the six *Tritylodon* elements studied exhibit azonal bone, it is suggested that the overall growth of this animal was less sensitive to seasonal variations as compared to *Diademodon* or *Trirachodon.*

In a study conducted by Chinsamy et al. (2002), on the bone histology of several Mesozoic mammals, it was found that early mammalian taxa had more flexible growth strategies and perhaps not as strong a selection for fast growth rates as do extant mammals. The tissue pattern of the early eutherian mammals in their study indicates a slow, cyclical growth strategy, suggesting that these animals had not yet attained the rapid, sustained growth rates of extant eutherians. The multituberculates in their study exhibited initial fast rates of growth in the form of woven bone, which subsequently became slower forming parallel-fibred bone with rest lines, similar to extant mammals. Extant eutherians generally only form LAGs in their limb bones during hibernation (some rodents, Klevezal, 1996) and in extreme climatic conditions such as polar bears in the arctic (Chinsamy et al., 1998). The *Cynognathus* and *Tritylodon* bones in this study indicate rapid, sustained growth strategies. These growth patterns differ from those of the early eutherians and multituberculates in Chinsamy et al.'s study (2002), as the bone tissue is azonal and peripheral rest lines are absent. If the mammal-like morphological features of these animals are considered with their rapid sustained growth strategies, it is possible that *Cynognathus* and *Tritylodon* had relatively high growth rates, which differed from early eutherians.

Although the *Procynosuchus* elements exhibit mostly lamellar-zonal bone, some fibro-lamellar bone is present in the inner cortex of the radius. The dominant bone tissue of all the other genera studied is fibro-lamellar bone. The bone tissue organisation of the non-mammalian cynodonts more derived than *Procynosuchus*, with an abundance of fibro-lamellar tissue, differs from extant crocodilians and lizard bone histology, which generally exhibit mostly lamellar-zonal bone. Although fibro-lamellar bone has been found within extant crocodilians and lizards (Reid, 1984b, 1997), it is never the dominant tissue type as it is in *Cynognathus* or *Tritylodon*. This observation indicates that these non-mammalian cynodont genera deposited bone at more rapid rates than most extant crocodilians and lizards. However, whether these non-mammalian cynodonts were fully endothermic, cannot be directly interpreted from bone histology.

Earlier studies have found anterolateral ridges in the nasal cavities of *Thrinaxodon* and *Diademodon*, which may suggest that respiratory turbinates were present (Brink. 1955; Hillenius, 1992). As complex respiratory turbinates are found in the nasal cavities of almost all extant mammals, it has therefore been proposed that these non-mammalian cynodonts had high ventilation rates, which may have been associated with endothermy (see Chapter 2.1). Respiratory turbinates prevent desiccation associated with high ventilation rates, but the original function of the maxilloturbinate bones is not known nor whether they were performing this function in *Thrinaxodon* and *Diademodon*.



**(ii) Ontogenetic Variation**

*Procynosuchus* and *Thrinaxodon* are characterised by a marked change in tissue organisation during ontogeny, where the tissue altered from fibro-lamellar to lamellar-zonal tissue in *Procynosuchus* and fibro-lamellar to parallel-fibred bone in *Thrinaxodon*. This abrupt change in the rate at which bone is deposited may indicate that sexual maturity had been reached (Klevezal, 1996). Such a characteristic, signifying a specific life history event, has also been observed in the extant walrus *Odobenus rosmarus* (Klevezal, 1996), the African elephant

*Loxodonta africana* (Jarman, 1983) and in the longbones of Tendaguru sauropods (Sander, 2000). Ontogeny may significantly influence tissue patterns. For example, interruptions in growth are sometimes absent in rapidly growing juveniles, but they occur in older, slower growing individuals (e.g. Enlow, 1969). LAGs also become more prominent and the tissue more organised with age (see *Diademodon,* Chapter 6.3.2 ii). Vascularisation also changes during ontogeny, where tissues become less vascularised with age (e.g. Chinsamy et al., 1995; Curry, 1999; Sander, 2000). This was observed in elements of all the genera in this study and was particularly noticeable in *Diademodon* where an ontogenetic series of the humerus and femur and partial ontogenetic series of the tibia were available for examination (Figures 6.31, 6.32 and 6.33).

**(iii) Environmental Fluctuations**

It is currently thought that the formation of LAGs is an expression of a genetic biological rhythm, which is also dependent on external factors such as seasonality (Castanet and Baez, 1991). The environment therefore plays an important role in determining the extent of cyclical growth. For example, LAG distinctness and intensity appears to be linked with environmental fluctuations. LAGs are generally more distinct in highly seasonal environments and may be reduced in more equable climates (Castanet and Baez, 1991; Esteban et al., 1999). There is also evidence of environmental conditions affecting rates of growth, as it is well known that farmed crocodilians, bred under constant, optimal conditions, grow more rapidly than wild populations (Ross, 1989). The prominence of LAGs in the elements in this study varied, possibly due to ontogeny in the younger elements (e.g. reduced annuli in the *Trirachodon* femur NMQR3282a, Figure 7.3), but some interruptions in growth may be more distinct because of climatic conditions. For example, LAGs may be more prominent or more closely spaced in animals living under drought conditions (Buffrenil and Buffetaut, 1981). It is possible that the annulus in the late sub-adult *Thrinaxodon* femur (Figure 5.4) and rest lines in the *Tritylodon* radius (Figure 8.4) are due to individual responses to particularly harsh local

environmental conditions. As no rest lines were found in the rest of the nine *Thrinaxodon* and six *Tritylodon* elements studied, it is reasonable to suggest that the observed interruptions in growth probably do not represent cyclical growth strategies for these genera.

**(iv) Sexual Dimorphism**

Sexual dimorphism may also cause variations in bone. For example, several *Trirachodon* elements in this study exhibit growth patterns that do not correlate with size (see Chapter 7.4). The diameters of some of the histologically young elements (NMQR3282 femur and tibia) were found to be larger than the diameters of some of the histologically older elements (SAM-PK-K5881 femur and tibiae). A possibility of species differences was discussed in Chapter 7.4, but the possibility of sexual dimorphism was also suggested. If one gender grows more rapidly than the other, body size differences (and hence bone cross-sectional diameters) may occur due to different growth rates. Sexual dimorphism may also cause variations in the bone tissue itself (e.g. osteoporosis, medullary bone in female birds). However, Chinsamy and Barrett (1997) caution against distinguishing the gender of an extinct animal using bone histology, as there is no conclusive quantifiable method of identifying the particular gender. More studies on extant animals are required before reasonable deductions regarding the link between gender and bone histology can be made.

**(v) Inter-elemental Histovariability**

Although the overall tissue pattern between different limb bones is similar, variations were observed between the different types of limb bones. Differences such as vascular density, type and number of growth rings and extent of secondary remodelling were observed, particularly between the proximal and distal limb bones.

The proximal elements of the fore- and hindlimb (humerus and femur) were found to be histologically more similar to each other than they are to the distal

elements (radius, ulna, tibia and fibula). The proximal limb bones generally exhibit a higher percentage channel area (area occupied by the channels in a given section of bone) than the distal elements, suggesting that the proximal elements grew more rapidly than the distal elements. Ontogenetic influences had to be considered, as differences in vascularisation can be attributed to different ontogenetic stages (see section 10.2 ii). For example, differences in percentage channel area between the *Thrinaxodon* sub-adult humeri and femur (7.65% average) and the radii and ulnae (2.71% average) may be at least partly due to ontogenetic differences as the radii and ulnae are from ontogenetically older individuals than the humeri and femur.

The percentage channel area values of the different age classes of *Diademodon* show that the humeri (6.35% sub-adult; 5.2% adult) and femora (4.59% sub-adult; 2.2% adult) are generally more highly vascularised than the distal elements (2.59% sub-adult tibiae and fibula; 2.07% adult tibiae), with the exception of the adult femur. This characteristic is evident even between the elements of a single individual. For example, the humerus SAM-PK-K8971a (7.41%) exhibits greater vascularity than the ulna (4.56%) of the same individual. The *Trirachodon* material consists of ontogenetically varying skeletal elements and therefore only a *Trirachodon* femur, radius, ulna and tibia are available for comparison. Although the difference is not particularly marked the femur (4.45%) still exhibits greater vascularity than the radius (4.04%), ulna (3.68%) and tibia (4.17%) (Figure 7.12). A sub-adult *Tritylodon* humerus and radius examined from a single individual also shows a higher percentage channel area in the humerus (5.26%) compared to the radii (3.15%).

Another histological difference found between the proximal and distal elements was the frequency and prominence of growth lines. LAGs are more frequent and more prominent in the distal elements compared to the proximal elements of *Diademodon* and *Trirachodon*. In the ontogenetically similar *Diademodon* bones, annuli are present in the humeri and femora, but LAGs are absent, whereas both annuli and LAGs, which are sometimes multiple, are present in

When the individual ages of older individuals are determined, back calculations are often used to estimate the number of earlier growth rings that would have been resorbed. These growth rings are then added to the observed number to obtain a total count (Smirina, 1974; Chinsamy, 1993a). However, in some of the *Diademodon* individuals in this study, growth rings are expressed only towards the sub-periosteal surface. The inner tissue is unremodelled and consists of primary tissue. There is therefore a large amount of bone tissue between the medullary cavity and the first growth ring and then distinctly narrower areas of tissue between the successive growth rings. Hence, supposed 'earlier' growth rings would not have been resorbed as the large area consists of primary tissue and adding on supposedly resorbed growth rings was not necessary. Yet, the older elements frequently have fewer growth rings than the younger elements. Most of the humeri were serially sectioned, or if not, at least the midshaft was available for examination. Although intra-elemental variation would have affected the LAG number (e.g. metaphyseal remodelling, compacted coarse cancellous tissue in the delto-pectoral crest region), at least the neutral region of the midshaft, if not most of each bone, could be assessed. Therefore the sectioning should not have influenced the observed growth ring discrepancy. There are other possible reasons for this phenomenon. For example, the *Diademodon* elements generally belong to different individuals from various localities. The various elements may therefore represent different species, which may respond to environmental fluctuations slightly differently. If all the elements represent one species however, the different localities from where the material was recovered, may have experienced slightly different local environmental fluctuations, at least enough to affect LAG number.

This observation in the *Diademodon* elements further cautions the use of back calculating as the width between successive growth rings in the youngest individual is used to count the number of resorbed growth rings in older individuals. Although the width between successive growth rings in older individuals is expected to be quite different from that of younger individuals, the absence of growth rings in the inner primary tissue that has not been resorbed,

is not a general observation. It is expected that discrepancies in LAG counts can occur, due to inter- and intra-elemental histovariability (possibly due to variable local growth conditions) and such discrepancies have been found in earlier studies such as that of Horner et al. (1999). The accuracy of this method depends on several factors, such as the region of bone, type of element, adequate sample size and locality (i.e. similar environment, time span etc.). All these factors should be considered during skeletochronological assessments.

The findings in this study also suggest that the abundance of LAGs and lower vascularisation in the distal elements indicate a slower growth rate compared to the proximal elements. Histological variation between different skeletal elements has also been documented in non-avian dinosaurs (Curry, 1999; Horner et al. 1999, 2000) and extant Japanese quail (Starck and Chinsamy, in press). The findings in this study support Starck and Chinsamy's suggestion that limb bones are better used to interpret overall growth patterns of animals. It is also proposed that due to the histological variation observed between the proximal and distal elements, where possible, elements of both type should be used for growth pattern assessments.

It is recognised that due to the paucity of fossil material, different elements from a single individual are rarely examined for histological analysis. However, caution is advised when selecting between proximal and distal limb bones for histological analyses. A proximal element may indicate an animal's capacity for growth, i.e. the maximum growth rate, but if the bone tissue is azonal, it may falsely imply that overall growth was sustained (as the distal elements may exhibit zonal bone). In contrast, as distal elements appear to have slightly slower growth rates, interruptions in growth are more likely to appear in these elements than in the proximal limb bones. This may then give a more accurate indication as to whether the animal experienced cyclical or sustained growth, but may not reveal the maximum rate at which the animal was able to grow (as proximal limb bones may be azonal). These findings emphasise the importance of examining multiple skeletal elements.

Local variations in bone tissue organisation were also observed in the regions of bony protuberances (ulna crests, femoral trochanters, humeral delto-pectoral crests etc.). A change in the orientation of vascular canals or an increased amount of resorption cavities was sometimes observed in these areas. Compacted coarse cancellous bone was also observed in the metaphyseal regions of bones and particularly in the delto-pectoral crest regions of many humeri.

As a result, the findings of inter- and intra-elemental histovariability in this study are in agreement with earlier proposals (Curry, 1999; Horner et al., 1999; Starck and Chinsamy, in press) that limb bones, particularly the neutral regions of the midshafts, are more reliable than other elements or regions for growth ring assessments.



### 10.3 Chemical Analyses of Enamel Apatite

Most palaeo-isotope studies using fossil tooth enamel have analysed Cenozoic material (e.g. Bocherens et al., 1996; Bryant et al., 1996a; Cerling et al., 1997). Few studies apart from those of Thackeray et al., (1990) and MacLeod et al., (2000) have analysed the isotope signatures from non-mammalian therapsid biological apatite of Permian and Triassic age. However, in both these studies dicynodont tusks that consist entirely of dentine (King, 1981; Hotton, 1986) were used. In the study conducted by MacLeod et al. (2000), no structural testing was performed on the teeth prior to isotope analysis. Although the study conducted by Thackeray et al. (1990) used Fourier Transform Infra-red (FTIR) spectroscopy to assess the integrity of the non-mammalian therapsid dentine and confirmed that the material was still biological apatite, it should be noted that earlier studies (LeGeros, 1991) have found dentine to be more susceptible to diagenetic alteration than enamel (also supported in this study, see Chapter 9.4.1).

The results obtained from the FTIR spectroscopic analysis in this study have demonstrated the potential for examining the structural changes that occur in

non-mammalian therapsid enamel during fossilization. This study is the first to conduct FTIR spectroscopic analysis on such old fossil enamel material (approximately 240 million years old, Early Triassic; Harland, et al., 1990).

The similarity in BPI (amount of type B $CO_3$ to $PO_4$) and carbonate content between the extant *Crocodylus niloticus* and non-mammalian cynodont enamel may indicate a similarity in structural properties (Table 9.4). The non-mammalian cynodont BPI and carbonate content significantly differs from that of the extant *Giraffa camelopardalis* and *Sivatherium hendeyi*. Since non-mammalian cynodont dentition was becoming increasingly mammal-like (e.g. Grine, 1977; Kemp, 1982; Hopson, 1991), it was expected that the non-mammalian cynodont enamel be more similar to the extant mammalian enamel. However, the similarity in BPI and carbonate content with *Crocodylus niloticus* suggests that non-mammalian cynodont apatite structure may still have been similar to that of crocodilians and lizards. Further research into extant crocodilian, lizard and non-mammalian synapsid apatite structure is still required.

The oxygen and carbon isotope signatures of the *Thrinaxodon, Cynognathus, Diademodon* and *Trirachodon* teeth show strong, directional intra-tooth variability. The $\delta^{13}C$ values indicate $C_3$ plants, which is to be expected as earlier studies have found that Triassic terrestrial plants used the $C_3$ photosynthetic pathway. The large *Diademodon* sample size has facilitated the observation of distinct cycles in the *Diademodon* teeth, which probably indicate seasonal fluctuations. This phenomenon is also reflected in the bone histology of this animal (in the form of growth rings, see Chapter 6.4.2). In contrast, although isotopic variability is observed in the *Cynognathus* teeth, seasonal variability is not evident in the bone histology of this animal. The bone histology of *Cynognathus* indicates a sustained growth strategy, whereas the growth of *Diademodon* was cyclical. This suggests that although these contemporary genera experienced similar environmental fluctuations, they responded differently in terms of growth rate.

FTIR spectroscopic and stable isotope analyses were also conducted on extant *Crocodylus niloticus* teeth. Earlier isotope studies have concentrated mainly on extant mammals and therefore most FTIR studies have also examined mammals. This is mainly because mammals have constant body temperatures and variations in the oxygen isotope signature of their tissues will mostly be due to variations of ingested water and oxygen fluxes and not environmental temperature (Longinelli, 1984; Luz, Kolodny and Horowitz, 1984; Bryant and Froelich, 1995; Kohn, 1996). Although crocodilians and lizards do not maintain constant body temperatures and will therefore have large intra-bone and inter-bone isotopic variability (Barrick and Showers, 1995), they can still provide information regarding seasonal variability. The isotopic variability exhibited in their teeth may be enhanced or reduced due to the effect of body temperature, but this has yet to be quantified. Furthermore, the pattern of seasonal variation can still be observed. FTIR spectroscopy provides additional information regarding their tooth structure and although absolute values may not yet be used to determine environmental temperature, isotope analysis still provides important insight into how their teeth record patterns of seasonal fluctuations. There is much scope for research in this area as studies on extant animals are essential for comparing and correctly interpreting information obtained from fossil animals.



This study demonstrates the potential of FTIR spectroscopy for assessing the integrity of non-mammalian therapsid tooth enamel for future palaeo-isotope studies. Palaeo-isotope studies are capable of providing important additional information relating to the biology and ecology of non-mammalian therapsids. The FTIR spectroscopic analysis alone can also provide structural information regarding the biological apatite of very old fossil material, which can lead to a better understanding of the biology of Mesozoic tetrapods.

In summary, this study is the first detailed histological comparison of multiple and different non-mammalian cynodont skeletal elements. It is also the first to combine bone histology with carbon and oxygen isotope analyses to deduce

aspects regarding the biology of these animals. The bone histological study has shown that the overall growth rate of the non-mammalian cynodonts increased as they became more derived (Figure 10.1). The overall increase in bone deposition rate may have been facilitated by endothermy, but this is speculative, as bone histology is not directly linked to physiology (Reid, 1984b; Chinsamy and Rubidge, 1993) and may therefore not reflect the ecto- or endothermic status of the animal.

It is important to note that phylogeny is not the only factor to affect the observed tissue patterns in bone. Factors such as ontogeny, environmental fluctuations, variation between different skeletal elements, sexual dimorphism, disease, biomechanical constraints etc. play important roles in affecting growth rates and bone histology. These factors should be considered when interpreting the growth patterns observed in the bones of fossil animals. This study also emphasises the use of multiple skeletal elements in gaining insight into the overall growth patterns of extinct animals.

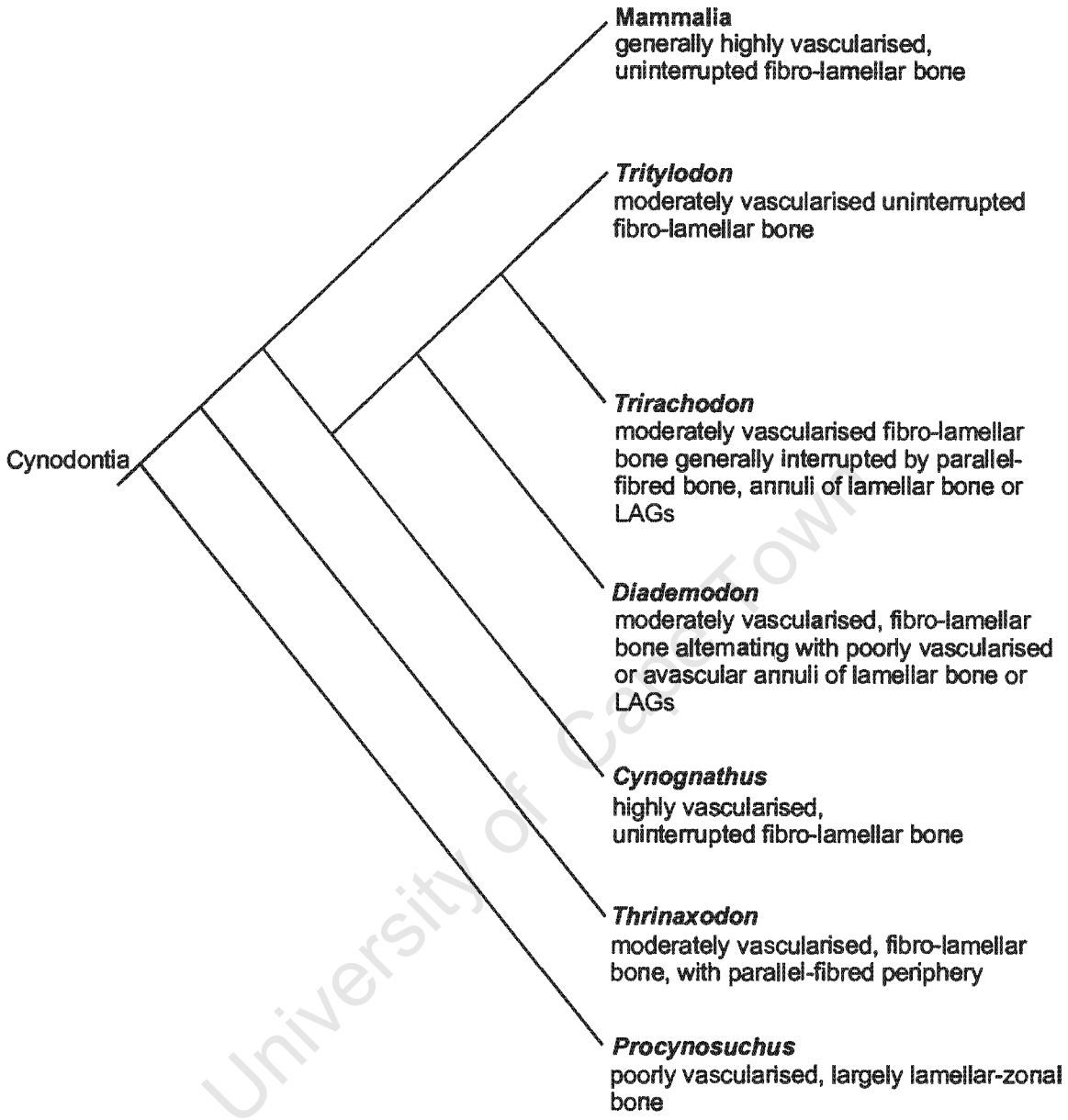




Figure 10.1 Relationships among the six non-mammalian cynodont genera studied, with brief descriptions of the tissue patterns exhibited by the bones of each genus. Tissue organisation varies from largely lamellar-zonal in *Procynosuchus* to uninterrupted fibro-lamellar bone in *Tritylodon*. Vascularisation increases from basal to the more derived genera.

# CHAPTER ELEVEN
# CONCLUSIONS

11.1 The variations in the bone cross-sectional geometry values in this study suggest that habitat and lifestyle are selective factors in producing bone modifications. The semi-aquatic *Procynosuchus* relative bone wall thickness (RBT) value is high, similar to other semi-aquatic animals examined in earlier studies. The relatively thick bone walls of the fossorial *Trirachodon* and *Tritylodon* suggest that this characteristic is also an adaptation for a fossorial lifestyle. The bone cross-sectional geometry results of *Diademodon* and the oxygen isotope analyses suggest that this animal was semi-aquatic. These results show the potential for oxygen isotope analyses to further provide information relating to the lifestyle habits of fossil animals.

11.2 The multi-element bone histology study revealed distinct variations in growth pattern between the non-mammalian cynodont genera. The most basal non-mammalian cynodont in this study (*Procynosuchus*) grew in a slow, cyclical manner whereas the most derived genus (*Tritylodon*) had a rapid, sustained growth strategy and was perhaps less dependent on environmental fluctuations than was *Procynosuchus*. This may indicate an overall increase in growth rate during non-mammalian cynodont evolution. However, the growth strategies of the non-mammalian cynodont genera more derived than *Procynosuchus* and less derived than *Tritylodon* vary considerably. For example, the *Thrinaxodon* elements exhibit rapidly forming fibro-lamellar bone, which becomes slowly forming parallel-fibred bone towards the bone periphery. *Diademodon* and *Trirachodon* both grew in a cyclical manner, although there are some differences between the two genera. The growth cycles in *Trirachodon* do not appear to be as distinct in some elements compared to *Diademodon,* where every element shows distinct, clear growth cycles. The overall growth of these two genera was

not sustained and their growth may have been less rapid than that of *Cynognathus,* which exhibits a rapid, sustained growth strategy.

11.3 The variations in growth pattern observed in these genera may not be due to phylogenetic constraints alone. Factors such as ontogeny, type of element, gender variation or response to the environment also play important roles in affecting patterns of growth. For example the single annulus observed in one *Thrinaxodon* femur or the rest lines in the single *Tritylodon* radius may be due to individual responses to any number of factors (e.g. disease, injury, excessive environmental variations etc.). These results indicate that several factors can affect the histology of bone, which should all be considered when interpreting the growth strategies of fossil animals. Bone histology provides information regarding the life history of a specific element of a particular individual, interpretations of which can be extended to genus level as long as individual variation is considered.

11.4 Histovariability was observed between proximal and distal limb bones where distal limb bones tend to grow more slowly than proximal limb bones. Caution is advised when selecting limb bones for growth pattern interpretations. Proximal limb bones may reflect growth rate capacity, but may also falsely imply high overall growth rates, whereas distal limb bones are more likely to reveal zonal growth, if present, but may not reveal the maximum possible growth rate of the animal. As distal limb bones appear to grow more slowly, it is proposed that they are better for skeletochronology assessments. LAG counts should however be conducted on various limb bones within an individual and, where possible, back calculations should be avoided, as variations in zone width may jeopardize results.

11.5 The assessment of the bone histology of *Cynognathus* and *Diademodon* has facilitated distinguishing between the extremely similar postcrania

when cranial material is absent, showing that bone histology is a useful tool for identification purposes.

11.6 The Fourier Transform Infra-red spectroscopic analysis used to assess the integrity of the non-mammalian cynodont enamel prior to the isotope analyses has shown that FTIR is a useful tool for examining the biological apatite of non-mammalian therapsids and that the BPI and carbonate content of the non-mammalian cynodont enamel is extremely similar to the extant *Crocodylus niloticus* enamel. This indicates that the tooth enamel of these two taxa is structurally similar.

11.7 The $\delta^{13}C$ values fall within the range for $C_3$ plants and these expected results, as well as the directional intra-tooth variability suggest that diagenetic alteration is minimal, as diagenesis tends to reduce isotopic variability. The consistently, cyclical intra-tooth $\delta^{18}O$ values of the *Diademodon* enamel suggest strong seasonal fluctuations, which is in accordance with the cyclical growth strategy exhibited by this animal as well as earlier palaeo-environmental studies.

11.8 This study is the first to use multiple elements to examine the bone histology of non-mammalian cynodonts and has facilitated a detailed, comparative analysis of the biology of these animals. In addition, the combined techniques of bone histology and stable isotope analyses have provided a unique approach to examining aspects of non-mammalian cynodont growth. This study has shown that observable changes in non-mammalian cynodont growth occurred during their evolution. These changes may be linked to phylogeny, although other factors (mentioned above) should also be considered. This study highlights the necessity for multi-element bone histology studies to accurately interpret the growth patterns of fossil animals. It also demonstrates the potential for stable isotope analyses to provide further information regarding lifestyle habits and the interactions of non-mammalian cynodonts with their environment.

# REFERENCES


Alexander, R. 1985. The maximum forces exerted by animals. Journal of Experimental Biology 115:231-238.

Amprino, R. 1967. Bone histophysiology. Guy's Hospital Report 116(2):51-69.

Anderson, J. M. and H. M. Anderson. 1983. Vascular plants from the Devonian to Lower Cretaceous in southern Africa. Bothalia 14:337-344.

---------- and H. M. Anderson. 1985. Palaeoflora of Southern Africa. *Prodromus* of South African megafloras. Devonian to Lower Cretaceous. A. A. Balkema, Rotterdam, 423pp.

Bakker, R. T. 1971. Dinosaur physiology and the origin of mammals. Evolution 25(4):636-658.

---------- 1972a. Dinosaur renaissance. Scientific American 232 (4):58-75.

---------- 1972b. Anatomical and ecological evidence of endothermy in dinosaurs. Nature 238:81-85.

---------- 1980. Dinosaur heresy - dinosaur renaissance. Why we need endothermic archosaurs for a comprehensive theory of bioenergetic evolution; pp. 351-462 *in* R. D. K. Thomas and E. C. Olson, (eds.), A cold look at the warm blooded dinosaurs, Westview Press, Boulder.

---------- 1986. The dinosaur heresies: New theories unlocking the mystery of the dinosaurs and their extinction. William Morrow, New York, 481pp.

Bargo, M. S., S. F. Vizcaíno, F. M. Archuby, and R. E. Blanco. 2000. Limb bone proportions, strength and digging in some Lujanian (Late Pleistocene-Early Holocene) mylodontid ground sloths (Mammalia, Xenarthra). Journal of Vertebrate Paleontology 20(3):601-610.

Barrick, R. E. 1994. Thermal physiology of the dinosauria: evidence from oxygen isotopes in bone phosphate *in* G. D. Rosenberg and D. L. Wolberg (eds.), The Paleontological Society, Indiana University, Indianapolis, 500pp.

---------- and W. J. Showers. 1995. Oxygen isotope variability in juvenile dinosaurs (*Hypacrosaurus*): evidence for thermoregulation. Paleobiology 21(4):552-560.

----------, W. J. Showers, and A. G. Fischer. 1996. Comparison of thermoregulation of four ornithischian dinosaurs and a varanid lizard from the Cretaceous Two Medicine Formation: evidence from oxygen isotopes. Palaios 11:295-305.

-------- 1998. Isotope paleobiology of the vertebrates: ecology, physiology, and diagenesis; pp. 101-137 *in* Isotope paleobiology and paleoecology, The Paleontological Society, Fayetteville.

Béland, P. and D. A. Russell. 1980. Dinosaur metabolism and predator/prey ratios in the fossil record; pp. 85-102 *in* D. K. Thomas and E. C. Olson (eds.), A cold look at the warm-blooded dinosaurs, Westview Press, Boulder.

Bennett, A. F. 1991. The evolution of activity capacity. Journal of Experimental Biology 160:1-23.

-------- and J. A. Ruben. 1986. The metabolic and thermoregulatory status of therapsids; pp. 207-218 *in* N. Hotton III, P. D. MacLean, J. J. Roth, and E. C. Roth (eds.), The ecology and biology of mammal-like reptiles, Smithsonian Institution Press, Washington.

Benton, M. J. 1990. Vertebrate Palaeontology. Chapman and Hall, London, 377pp.

Berry, J. A. 1988. Studies of mechanisms affecting the fractionation of carbon isotopes in photosynthesis; pp. 82-94 *in* P. W. Rundel, J. R. Ehleringer, and K. A. Nagy (eds.), Stable isotopes in ecological research, Springer, Berlin.

Blob, R. W. 2001. Evolution of hindlimb posture in nonmammalian therapsids: biomechanical tests of paleontological hypotheses. Paleobiology 27:14-38.

Bocherens, H., D. B. Brinkman, Y. Dauphin, and A. Mariotti. 1994. Microstructural and geochemical investigations on Late Cretaceous archosaur teeth from Alberta, Canada. Canadian Journal of Earth Science 31:783-792.

--------- M. Friis, A. Mariotti, and K. R. Pedersen. 1993. Carbon isotopic abundances in Mesozoic and Cenozoic fossil plants: Palaeoecological implications. Lethaia 26:347-356.

----------, P. L. Koch, A. Mariotti, D. Geraads, and J.-J. Jaeger. 1996. Isotopic biogeochemistry ($^{13}C$, $^{18}O$) of mammalian enamel from African Pleistocene Hominid sites. Palaios 11:306-318.

Bou, J., M. J. Castiella, J. Ocana, and A. Casinos. 1990. Multivariate analysis and locomotor morphology in insectivores and rodents. Zoologischer Anzeiger 225:287-294.

Bouvier, M. 1977. Dinosaur haversian bone and endothermy. Evolution 31:449-450.

Brink, A. S. 1954. *Thrinaxodon* and some other *Lystrosaurus* Zone cynodonts in the collection of the National Museum, Bloemfontein. Researches of the National Museum, Bloemfontein 1:115-126.

---------- 1955. A study on the skeleton of *Diademodon*. Palaeontologia Africana 3:3-39.

---------- 1956. Speculations on some advanced mammalian characteristics in the higher mammal-like reptiles. Palaeontologia Africana 4:77-96.

---------- 1958. Note on a new skeleton of *Thrinaxodon liorhinus*. Palaeontologia Africana 6:15-22.

Broom, R. 1910. On *Tritylodon* and on the relationships of the multituberculata. Proceedings of the Zoological Society of London:760-768.

---------- 1911. On the structure of the skull in cynodont reptiles. Proceedings of the Zoological Society of London 11:900-905.

---------- 1913. On the shoulder girdle of *Cynognathus*. Annals of the South African Museum 7:20-21.

Bryant, J. D. and P. N. Froelich. 1995. A model of oxygen isotope fractionation in body water of large mammals. Geochimica et Cosmochimica Acta 59:4523-4537.

----------, P. N. Froelich, W. J. Showers, and B. J. Genna. 1996a. Biologic and climatic signals in the oxygen isotopic composition of Eocene-Oligocene equid enamel phosphate. Palaeogeography, Palaeoclimatology, Palaeoecology 126:75-89.

----------, P. N. Froelich, W. J. Showers, and B. J. Genna. 1996b. A tale of two quarries biologic and taphonomic signatures in the oxygen isotope composition of tooth enamel phosphate from modern and Miocene equids. Palaios 11:397-408.

----------, P. L. Koch, P. N. Froelich, W. J. Showers, and B. J. Genna. 1996c. Oxygen isotope partitioning between phosphate and carbonate in mammalian apatite. Geochimica et Cosmochimica Acta 60(24):5145-5148.

Buffrénil, V. and E. Buffetaut. 1981. Skeletal growth lines in an Eocene crocodilian skull from Wyoming as an indicator of ontogenic age and paleoclimatic conditions. Journal of Vertebrate Paleontology 1:57-66.

----------, A. de. Ricqlès, C. E. Ray, and D. P. Domning. 1990. Bone histology of the ribs of the archaeocetes (Mammalia: Cetacea). Journal of Vertebrate Paleontology 10:455-466.

Caetano, M. H. 1990. Use and results of skeletochronology in some urodeles (*Triturus marmoratus*, Latreille 1800 and *Triturus boscai*, Lataste 1879). Annales des Sciences Naturelles, Zoologie 11:197-199.

Carlson, S. J. 1990. Vertebrate dental structures; pp. 531-556 *in* J. G. Carter, (ed.), Skeletal biomineralization: patterns, processes and evolutionary trends, Van Nostrand Reinhold, New York.

Carrier, D. R. 1987. The evolution of locomotor stamina in tetrapods: circumventing a mechanical constraint. Paleobiology 13: 326-341.

Carroll, R. L. 1988. Vertebrate paleontology and evolution. W. H. Freeman, New York, 698 pp.

Carter, D. R., B. Mikic, and K. Padian. 1998. Epigenetic mechanical factors in the evolution of long bone epiphyses. Zoological Journal of the Linnean Society 123:163-178.

Casinos, A., C. Quintana, and C. Viladiu. 1993. Allometry and adaptation in the long bones of a digging group of rodents (Ctenomyinae). Zoological Journal of the Linnean Society 107:107-115.

Castanet, J. 1994. Age estimation and longevity in reptiles. Gerontology 40:174-192.

---------- and M. Baez. 1991. Adaptation and evolution in *Gallotia* lizards from the Canary Islands: age, growth, maturity and longevity. Amphibia-Reptilia 12:81-102.

---------- and M. Cheylan. 1979. Les marques de croissance des os et des écailles comme indicateur de l'âge chez *Testudo hermanni* et *Testudo graeca* (*Reptilia, Chelonia, Testudinidae*). Canadian Journal of Zoology 57:1649-1655.

----------, H. Francillon-Vieillot, and R. C. Bruce. 1996. Age estimation in desmognathine salamanders assessed by skeletochronology. Herpetologica 52(2):160-171.

----------, D. G. Newman, and H. Saint Girons. 1988. Skeletochronological data on the growth, age and population structure of the tuatara, *Sphenodon punctatus*, on Stephens and Lady Alice Islands, New Zealand. Herpetologica 44:25-37.

----------, K. C. Rogers, J. Cubo, and J. J. Boisard. 2000. Periosteal bone growth rates in extant ratites (ostrich and emu). Implications for assessing growth in dinosaurs. Comptes Rendus de l Academie des Sciences Serie III-Sciences de la vie - Life Sciences 323(6):543-550.

---------- and E. Smirina. 1990. Introduction to the skeletochronological method in amphibians and reptiles. Annales des Sciences Naturelles, Zoologie 11:191-196.

Cerling, T. E., J. M. Harris, S. H. Ambrose, M. G. Leakey, and N. Solounias. 1997. Dietary and environmental reconstruction with stable isotope analyses of herbivore tooth enamel from the Miocene locality of Fort Ternan, Kenya. Journal of Human Evolution 33:635-650.

----------, J. Quade, S. H. Ambrose, and N. E. Sikes. 1991. Current events. Fossil soils, grasses, and carbon isotopes from Fort Ternan, Kenya: grassland or woodland? Journal of Human Evolution 21:295-306.

Chinsamy, A. 1990. Physiological implications of the bone histology of *Syntarsus rhodesiensis* (Saurischia: Theropoda). Palaeontologia Africana 27:77-82.

---------- 1991. The osteohistology of femoral growth within a clade: a comparison of the crocodile *Crocodylus,* the dinosaurs *Massospondylus* and *Syntarsus,* and the birds *Struthio* and *Sagittarius.* Ph.D. dissertation, University of Witwatersrand, Johannesburg, 200pp.

---------- 1993a. Bone histology and growth trajectory of the prosauropod dinosaur *Massospondylus carinatus* Owen. Modern Geology 18:319-329.

---------- 1993b. Image analysis and the physiological implications of the vascularisation of femora in archosaurs. Modern Geology 19:101-108.

---------- 1995. Ontogenetic changes in the bone histology of the Late Jurassic ornithopod *Dryosaurus lettowvorbecki.* Journal of Vertebrate Paleontology 15 (1):96-104.

---------- T. Rich, and P. Vickers-Rich. 1998. Polar dinosaur bone histology. Journal of Vertebrate Paleontology 18(2):385-390.

---------- and P. M. Barrett. 1997. Sex and old bones? Journal of Vertebrate Paleontology 17:450.

---------- and P. Dodson. 1995. Inside a dinosaur bone. American Scientist 83:174-180.

---------- and M. A. Raath. 1992. Preparation of fossil bone for histological examination Palaeontologia Africana 29:39-44.

---------- and B. S. Rubidge. 1993. Dicynodont (Therapsida) bone histology: phylogenetic and physiological implications. Palaeontologia Africana 30:97-102.

----------, L. M. Chiappe, and P. Dodson. 1994. Growth rings in Mesozoic birds. Nature, pp. 196-197.

----------, S. A. Hanrahan, R. M. Neto and M. Seely. 1995. Skeletochronological assessment of age in *Angolosaurus skoogi,* a cordylid lizard living in an aseasonal environment. Journal of Herpetology 29:457-460.

----------, J. H. Hurum, Z. Kielan-Jaworowska, and S. Evans. 2002. Growth strategies of Mesozoic mammals. Mesozoic Terrestrial Ecosystems Conference Abstracts, Cape Town.

Cluver, M. A. 1978. Fossil reptiles of the South African Karoo. South African Museum, Cape Town, 54pp.

Cormack, D. H. 1987. Ham's histology. J. B. Lippincott Company, London, 866pp.

Craig, H. 1953. The geochemistry of the stable carbon isotopes. Geochimica et Cosmochimica Acta 3:53-92.

Crompton, A. W. 1989. Bone remodeling in medium-sized mammals and birds in response to slight changes in normal strain levels. 49th Annual Meeting of the Society of Vertebrate Paleontology, University of Texas, Austin, Texas, pp. 18A.

Crompton, A. W. 1963. Tooth replacement in *Thrinaxodon liorhinus* Seeley. Annals of the South African Museum XLVI part XX:479-521.

---------- and F. Ellenberger. 1957. On a new cynodont from Molteno Beds and origin of tritylodontids. Annals of the South African Museum 44:1-14.

---------- and F. A. Jenkins. 1973. Mammals from reptiles: a review of mammalian origins. Annual Review of Earth and Planetary Sciences 1:131-155.

Currey, J. D. 1960. Differences in the blood-supply of bone of different histological types. Quarterly Journal of Microscopical Science 101(3):351-370.

---------- 1962. The histology of the bone of a prosauropod dinosaur. Palaeontology 5(2):238-246.

---------- and M. R. Alexander. 1985. The thickness of the walls of tubular bones. Journal of Zoology, London 206:453-468.

Curry, K. A. 1999. Ontogenetic histology of *Apatosaurus* (Dinosauria: Sauropoda): new insights on growth rates and longevity. Journal of Vertebrate Paleontology 19(4):654-665.

Damiani, R. J. 2000. Bone histology of some Australian Triassic temnospondyl amphibians: preliminary data. Modern Geology 24:109-124.

Dansgaard, W. 1964. Stable isotopes in precipitation. Tellus 16:436-468.

DeNiro, M. J. and S. Epstein. 1978. Influence of diet on the distribution of carbon isotopes in animals. Geochimica et Cosmochimica Acta. 42:495-506.

Edmund, A. G. 1969. Dentition; pp.117-200 *in* C. Gans, (ed.), Biology of the Reptilia. Morphology A., Academic Press, London.

Ehleringer, J. R., T. E. Cerling, and B. R. Helliker. 1997. $C_4$ photosynthesis, atmospheric $CO_2$, and climate. Oecologia 112:285-299.

Ekart, D. D., T. E. Cerling, I. P. Montanez, and N. J. Tabor. 1999. A 400 million year carbon isotope record of pedogenic carbonate: implications for paleoatmospheric carbon dioxide. American Journal of Science 299:805-827.

Enlow, D. H. 1963. Principles of Bone Remodeling. An account of post-natal growth and remodeling processes in long bones and the mandible. C.C.Thomas, Springfield, 131pp.

---------- 1969. The bone of reptiles; pp. 45-80 *in* C. Gans, (ed.), Biology of the Reptilia. Morphology A, Academic Press, London.

---------- and S. O. Brown. 1956. A comparative histological study of fossil and recent bone tissues. Part I. The Texas Journal of Science 8:405-443.

---------- and S. O. Brown. 1957. A comparative histological study of fossil and recent bone tissues. Part II. The Texas Journal of Science 9:136-214.

Erickson, G. M. and T. A. Tumanova. 2000. Growth curve of *Psittacosaurus mongoliensis* Osborn (Ceratopsia: Psittacosauridae) infrared from long bone histology. Zoological Journal of the Linnean Society 130:551-566.

Esteban, M., M. García-Paris, and J. Castanet. 1996. Use of bone histology in estimating the age of frogs (*Rana perezi*) from a warm temperate climate area. Canadian Journal of Zoology 74:1914-1921.

Estes, R. 1961. Cranial anatomy of the cynodont reptile *Thrinaxodon liorhinus*. Bulletin of the Museum of Comparative Zoology 125:165-180.

Farlow, J. O. 1980. Predator/prey biomass ratios, community food webs, and dinosaur physiology; pp. 55-83 *in* R. D. K. Thomas and E. C. Olson, (eds.), A cold look at the warm-blooded dinosaurs., Westview Press, Boulder.

Feduccia, A. 1973. Dinosaurs as reptiles. Evolution 27:166-169.

Fish, F. E. 1993. Comparison of swimming kinematics between terrestrial anc semiaquatic opossums. Journal of Mammalogy 74(2):275-284.

---------- and B. R. Stein. 1991. Functional correlates of differences in bone density among terrestrial and aquatic genera in the family Mustelidae (Mammalia). Zoomorphology 110:339-345.

Fogel, M. L. and L. A. Cifuentes. 1993. Isotope fractionation during primary production; pp. 861 *in* M. H. Engel and S. A. Macko, (eds.), Organic Geochemistry. Principles and Applications, Plenum Press, New York.

Fourie, S. 1974. The cranial morphology of *Thrinaxodon liorhinus* Seeley. Annals of the South African Museum 65(10):337-400.

Frakes, L. A. 1979. Climates throughout geologic time. Elsevier Scientific, New York, 310pp.

Francillon-Vieillot, H., J. W. Arntzen, and J. Géraudie. 1990a. Age, growth and longevity of sympatric *Triturus cristatus, T. marmoratus* and their hybrids

(Amphibia, Urodela): A skeletochronological comparison. Journal of Herpetology 24(1):13-22.

----------, V. de Buffrénil, J. Castanet, J. Geraudie, F. J. Meunier, J. Y. Sire, L. Zylberberg and A. de Ricqlès. 1990b. Microstructure and mineralization of vertebrate skeletal tissues; pp. 471-548 *in* J. G. Carter, (ed.), Skeletal biomineralization: patterns, processes and evolutionary trends., Van Nestrand Reinhold, New York.

Fricke, H. C. and J. R. O'Neil. 1996. Inter- and intra-tooth variation in the oxygen isotope composition of mammalian tooth enamel phosphate: implications for palaeoclimatical and palaeobiological research. Palaeogeography, Palaeoclimatology, Palaeoecology 126:91-99.

----------, W. C. Clyde and J. R. O'Neil. 1998. Intra-tooth variations in $\delta^{18}O$ ($PO_4$) of mammalian tooth enamel as a record of seasonal variations in continental climate variables. Geochimica et Cosmochimica Acta 62:1839-1850.

Golley, F. B. 1968. Secondary productivity in terrestrial communities. American Zoologist 8:53-59.

Gregory, W. K. and C. L. Camp. 1918. Reconstruction of the skeleton of *Cynognathus*. Bulletin American Museum of Natural History 38:538-544.

Grine, F. E. 1976. Postcanine (gomphodont) tooth wear in the mammal-like reptile *Diademodon*: a scanning electron microscope (SEM) study. Electron Microscopy Society of Southern Africa 6:51-52.

---------- 1977. Postcanine tooth function and jaw movement in the gomphodont cynodont *Diademodon* (Reptilia; Therapsida). Palaeontologia Africana 20:123-135.

---------- 1978. Postcanine dental structure in the mammal-like reptile *Diademodon* (Therapsida: Cynodontia). Electron Microscopy Society of Southern Africa 8:123-124.

----------, C. E. Gow, and J. W. Kitching. 1979a. Enamel structure in the cynodonts *Pachygenelus* and *Tritylodon*. Electron Microscopy Society of Southern Africa 9:99-100.

----------, B. D. Hahn and C. E. Gow. 1978. Aspects of relative growth and variability in *Diademodon* (Reptilia: Therapsida). South African Journal of Science 74:50-58.

----------, E. S. Vrba, and A. R. I. Cruickshank. 1979b. Enamel prisms and diphyodonty: linked apomorphies of Mammalia. South African Journal of Science 75:114-120.

Groenewald, G. H. and J. W. Kitching. 1995. Biostratigraphy of the *Lystrosaurus* Assemblage Zone; pp. 35-39 *in* B. S. Rubidge, (ed.), Biostratigaphy of the Beaufort Group (Karoo Supergroup), Council for Geoscience, Pretoria.

---------, J. Welman and J. A. MacEachern. 2001. Vertebrate burrow complexes from the Early Triassic *Cynognathus* Zone (Driekoppen Formation, Beaufort Group) of the Karoo Basin, South Africa. Palaios 16:148-160.

Haines, R. H. 1969. Epiphyses and sesamoids; pp. 81-116 *in* C. Gans, (ed.), Biology of the Reptilia. Morphology A., Academic Press, London.

Ham, A. W. 1965. Histology. J. B. Lippincott Company, Philadelphia, 371pp.

Harland, W. B., R. L. Armstrong, A. V. Cox, L. E. Graig, A. G. Smith, and D. G. Smith. 1990. A geologic time scale. Cambridge University Press, Cambridge, 263pp.

Heath, J. E. 1968. The origins of the thermoregulation; pp. 259-278 *in* E. T. Drake, (ed.), Evolution and the environment, Yale University Press, New Haven, Connecticut.

Heinrich, R. E. and A. R. Biknevicius. 1998. Skeletal allometry and interlimb scaling patterns in mustelid carnivorans. Journal of Morphology 235:121-134.

---------, C. B. Ruff, and D. B. Weishampel. 1993. Femoral ontogeny and locomotor biomechanics of *Dryosaurus lettowvorbecki* (Dinosauria, Iguanodontia). Zoological Journal of the Linnean Society 108:179-196.

Hillenius, W. H. 1992. The evolution of nasal turbinates and mammalian endothermy. Paleobiology 18(1):17-29.

Hopson, J. A. 1963. Tooth replacement in cynodont, dicynodont and therocephalian reptiles. , Yale University, 43pp.

Hopson, J. A. 1971. Postcanine replacement in the gomphodont cynodont *Diademodon*. Zoological Journal of the Linnean Society 50:1-21.

--------- 1977. Relative brain size and behaviour in archosaurian reptiles. Annual Review of Ecology and Sytematics 8:429-448.

--------- 1980. Relative brain size in dinosaurs; pp. 287-310 *in* R. D. K. Thomas and E. C. Olson, (eds.), A cold look at the warm-blooded dinosaurs, Westview Press, Boulder.

--------- 1987. The mammal-like reptiles. A study of transitional fossils. The American Biology Teacher 49:16-26.

--------- 1991. Convergence in mammals, tritheledonts, and tritylodonts. Journal of Vertebrate Paleontology 11(3,Suppl.):36A.

---------- 1994. Synapsid evolution and the radiation of non-eutherian mammals; pp. 190-219 *in* D. R. P. Prothero and R. M. Schoch (ed.), Major features of vertebrate evolution, Paleontological Society, Knoxville.

Horner, J. R, K. Padian, and A. de Ricqlès. 2001. Comparative osteohistology of some embryonic and perinatal archosaurs: developmental and behavioral implications for dinosaurs. Paleobiology 27(1):39-58.

----------, A. de Ricqlès, and K. Padian. 1999. Variation in dinosaur skeletochronology indicators: implications for age assessment and physiology. Paleobiology 25:295-304.

----------, A. de Ricqlès, and K. Padian. 2000. Long bone histology of the hadrosaurid dinosaur *Maiasaura peeblesorum*: growth dynamics and physiology of an ontogenetic series of skeletal elements. Journal of Vertebrate Paleontology 20:115-129.

Hotton, N. III. 1980. An alternative to dinosaur endothermy; pp. 311-350 *in* R. D. K. Thomas and E. C. Olson, (eds.), A cold look at the warm-blooded dinosaurs, Westview Press, Boulder.

---------- 1986. Dicynodonts and their role as primary consumers; pp. 71-82 *in* N. H. Hotton III, P. D. MacLean, J. J. Roth, and E. C. Roth, (eds.), The ecology and biology of mammal-like reptiles, Smithsonian Institution Press, Washington.

Hua, S. and V. de. Buffrénil. 1996. Bone histology as a clue in the interpretation of functional adaptations in the Thalattosuchia (Reptilia, Crocodylia). Journal of Vertebrate Paleontology 16:703-717.

Hutton, J. M. 1986. Age determination of living Nile crocodiles from the cortical stratification of bone. Copeia 2:332-341.

Iacumin, P., H. Bocherens, A. Mariotti, and A. Longinelli. 1996. Oxygen isotope analyses of co-existing carbonate and phosphate in biogenic apatite: a way to monitor diagenetic alteration of bone phosphate? Earth and Planetary Science Letters 142:1-6.

Jarman, P. 1983. Mating system and sexual dimorphism in large, terrestrial, mammalian herbivores. Biological Reviews 58:485-520.

Jenkins, F. A. 1971. The postcranial skeleton of African cynodonts. Problems in the early evolution of the mammalian postcranial skeleton. Peabody Museum of Natural History, New Haven, 216pp.

Kemp, T. S. 1979. The primitive cynodont *Procynosuchus:* functional anatomy of the skull and relationships. Philosophical Transactions of the Royal Society of London 285:73-122.

---------- 1980. The primitive cynodont *Procynosuchus*: structure, function and evolution of the postcranial skeleton. Philosophical Transactions of the Royal Society of London 288:217-258.

---------- 1982. Mammal-like reptiles and the origin of mammals. Academic Press, London, 363pp.

King, G. M. 1981. The functional anatomy of a Permian dicynodont. Royal Society of London Philosophical Transactions 291:243-322.

----------. 1996. Reptiles and herbivory. Chapman and Hall, London, 157pp.

Kitching, J. W. 1995. Biostratigraphy of the *Cynognathus* Assemblage Zone; pp. 40-45 *in* B. S. Rubidge, (ed.), Biostratigraphy of the Beaufort Group (Karoo Supergroup), Council for Geoscience, Pretoria.

---------- and M. A. Raath. 1984. Fossils from the Elliot and Clarens Formations (Karoo Sequence) of the northeastern Cape, Orange Free State and Lesotho, and a suggested biozonation based on tetrapods. Palaeontologia Africana 25:111-125.

Klevezal, G. A. 1996. Recording structures of mammals. Determination of age and reconstruction of life history. A. A. Balkema, Rotterdam, 274pp.

Koch, P. L. 1998. Isotopic reconstruction of past continental environments. Annual Review of Earth Planetary Science 26:573-613.

Kohn, M. J. 1996. Predicting animal $\delta^{18}O$: accounting for diet and physiological adaptation. Geochimica et Cosmochimica Acta 60:4811-4829.

----------, M. J. Schoeninger, and W. W. Barker. 1999. Altered states: effects of diagenesis on fossil tooth chemistry. Geochimica et Cosmochimica Acta 63:2737-2747.

----------, M. J. Schoeninger and J. W. Valley. 1996. Herbivore tooth oxygen isotope compositions: effects of diet and physiology. Geochimica et Cosmochimica Acta 60(20):3889-3896.

Krueger, H. W. 1991. Exchange of carbon with biological apatite. Journal of Archaeological Science 18:355-361.

Kühne, W. G. 1943. The dentary of *Tritylodon* and the systematic position of the Tritylodontidae. Annals and Magazine of Natural History. 10:589-601.

LeClair, R. 1990. Relationships between relative mass of the skeleton, endosteal resorption, habitat and precision of age determination in ranid amphibians. Annales des Sciences Naturelles, Zoologie 11:205-208.

Leeson, T. S. and C. R. Leeson. 1981. Histology. W. B. Saunders, London, 600pp.

Lee-Thorp, J. A. and N. J. van der Merwe. 1987. Carbon isotope analysis of fossil bone apatite. South African Journal of Science 83:712-715.

----------, J. C. Sealy, and N. J. van der Merwe. 1989. Stable carbon isotope ratio differences between bone collagen and bone apatite, and their relationship to diet. Journal of Archaeological Science 16:585-599.

LeGeros, R. Z. 1991. Calcium phosphates in oral biology and medicine. Karger, New York, 201pp.

---------- and M. S. Tung. 1983. Chemical stability of carbonate- and fluoride-containing apatites. Caries Research 17:419-429.

Line, S. R. D. 2000. Incremental markings of enamel in ectothermal vertebrates. Archives in Oral Biology 45:363-368.

Longinelli, A. 1984. Oxygen isotopes in mammal bone phosphate: A new tool for paleohydrological and paleoclimatological research? Geochimica et Cosmochimica Acta 48:385-390.

Luz, B. and Y. Kolodny. 1985. Oxygen isotope variations in phosphate of biogenic apatites, IV. Mammal teeth and bones. Earth and Planetary Science Letters 75:29-36.

---------- and Y. Kolodny. 1989. Oxygen isotope variation in bone phosphate. Applied Geochemistry 4:317-323.

----------, Y. Kolodny, and M. Horowitz. 1984. Fractionation of oxygen isotopes between mammalian bone-phosphate and environmental drinking water. Geochimica et Cosmochimica Acta 48:1689-1693.

MacFadden, B. J. 1998. Tale of two rhinos: isotopic ecology, paleodiet, and niche differentiation of *Aphelops* and *Teleoceras* from the Florida Neogene. Paleobiology 24:274-286.

----------, T. E. Cerling, J. M. Harris, and J. Prado. 1999. Ancient latitudinal gradients of $C_3/C_4$ grasses interpreted from stable isotopes of New World Pleistocene horse (*Equus*) teeth. Global Ecology and Biogeography 8:137-149.

MacLeod, K. G., R. M. H. Smith, P. L. Koch, and P. D. Ward. 2000. Timing of mammal-like reptile extinctions across the Permian-Triassic boundary in South Africa. Geology 28:227-230.

MacRae, C. 1999. Life etched in stone. Fossils of South Africa. The Geological Society of South Africa, Johannesburg, 305pp.

Magwene, P. M. 1993. What's bred in the bone: histology and cross-sectional geometry of mammal-like reptile long bones-evidence of changing physiological and biomechanical demands. MSc dissertation, Harvard University, Cambridge, 54pp.

Márquez, R., M. Esteban, and J. Castanet. 1997. Sexual size dimorphism and age in the midwife toads *Alytes obstetricans* and *A. cisternasii*. Journal of Herpetology 31(1):52-59.

Martin, R. B. and D. B. Burr. 1989. Structure, function, and adaptation of compact bone. Raven Press, New York, 275pp.

Merwe, N. J. van der and E. Medina. 1989. Photosynthesis and $^{13}C/^{18}O$ ratios in Amazonian rain forests. Geochimica et Cosmochimica 53:1091-1094.

---------- and E. Medina. 1991. The canopy effect, carbon isotope ratios and foodwebs in Amazonia. Journal of Archaeological Science 18:249-259.

McNab, B. K. 1978. The evolution of endothermy in the phylogeny of mammals. American Naturalist 112:1-21.

Michel, V., P. Ildefonse, and G. Morin. 1995. Chemical and structural changes in *Cervus elaphus* tooth enamels during fossilization (Lazaret cave): a combined IR and XRD Rietveld analysis. Applied Geochemistry 10:145-159.

Modesto, S., C. A. Sidor, B. S. Rubidge, and J. Welman. 2001. A second varanopseid skull from the Upper Permian of South Africa: implications for Late Permian 'pelycosaur' evolution. Lethaia 34:249-259.

Osborn, J. W. and A. W. Crompton. 1973. The evolution of mammalian from reptilian dentitions. Breviora 399:1-18.

Ostrom, P. H. and B. Fry. 1993. Sources and cycling of organic matter within modern and prehistoric food webs; 861pp *in* M. H. Engel and S. A. Macko, (eds.), Organic geochemistry. Principles and applications, Plenum Press, New York.

Owen, R. 1884. On the skull and dentition of *Tritylodon longaevus*. Quarterly Journal of the Geological Society :151.

Parker, R. B. and H. Toots. 1970. Minor elements in fossil bone. Geological Society of America Bulletin 81:925-932.

Parrington, F. R. 1933. On the cynodont reptile *Thrinaxodon liorhinus*. Annals and Magazines of Natural History. XI:16-24.

Parsons, T. S. 1970. The nose and Jacobson's organ; pp. 99-192 *in* C. Gans, (ed.), Biology of the Reptilia. Morphology B, Academic Press, London.

Peabody, F. E. 1961. Annual growth zones in living and fossil vertebrates. Journal of Morphology 108:11-62.

Petronievics, B. 1917. On the skull of *Tritylodon longaevus,* Owen. Annals and Magazines of Natural History 20:283-289.

Pough, F. H., J. B. Heiser, and W. N. McFarland. 1996. Vertebrate Life. Prentice-Hall, New Jersey, 798pp.

Ralls, K. 1976. Mammals in which females are larger than males. Quarterly Review of Biology 51:245-276.

Reader's Digest. 1994. Reader's Digest illustrated atlas of southern Africa. Reader's Digest, Cape Town, 231pp.

Reid, R. E. H. 1984a. The histology of dinosaurian bone, and its possible bearing of dinosaurian physiology. Symposium of the Zoological Society of London 52:629-663.

---------- 1984b. Primary bone and dinosaurian physiology. Geological Magazine 121:589-598.

---------- 1987. Bone and dinosaurian "endothermy". Modern Geology 11:133-154.

---------- 1990. Zonal "growth rings" in dinosaurs. Modern Geology 15:19-48.

---------- 1996. Bone histology of the Cleveland-Lloyd dinosaurs and of dinosaurs in general, Part I: Introduction: Introduction to bone tissues. Geology Studies 41:25-71.

---------- 1997. How dinosaurs grew; pp. 403-413 *in* J. O. Farlow and M. K. Brett-Surman, (eds.), The complete dinosaur, Indiana University Press, Indianapolis.

Reinhard, E., T. de Torres, and J. O'Neil. 1996. $^{18}O/^{16}O$ ratios of cave bear tooth enamel: a record of climate variability during the Pleistocene. Palaeogeography, Palaeoclimatology, Palaeoecology 126:45-59.

Reisz, R. E., D. W. Dilkes, and D. S. Berman. 1998. Anatomy and relationships of *Elliotsmithia longiceps* Broom, a small synapsid (Eupelycosauria: Varanopseidae) from the Late Permian of South Africa. Journal of Vertebrate Paleontology 18:602-611.

Rey, C., B., C. R. Renugopalakrishnan, M. Shinizu, B. Collins, and M. J. Glimcher. 1991. A resolution-enhanced Fourier Transform Infrared spectroscopic study of the environment of the $CO_3^{2-}$ ion in the mineral phase of enamel during its formation and maturation. Calcified Tissue International 49:259-268.

Ricqlès, A de. 1969. Recherches paléohistologiques sur les os longs des tétrapodes II.-quelques observations sur la structure des os longs des thériodontes. Annales de Paléontologie 55:3-52

---------- 1974. Evolution of endothermy: histological evidence. Evolutionary Theory 1:51-80.

---------- 1976. On bone histology of fossil and living reptiles, with comments on its functional and evolutionary significance; pp. 123-150 *in* A. d'A. Bellairs and C. B. Cox, (eds.), Morphology and biology of reptiles. Academic Press, London.

---------- 1980. (ed.), Tissue structures of dinosaur bone. Functional significance and possible relation to dinosaur physiology; pp. 103-139 *in* D. K. Thomas and E. C. Olson (eds.), A cold look at the warm-blooded dinosaurs, Westview Press, Boulder.

---------- 1983. Cyclical growth in the long limb bones of a sauropod dinosaur. Acta Palaeontologica Polonica 28:225-232.

----------, F. J. Meunier, J. Castanet and H. Francillon-Vieillot. 1991. Comparative microstructure of bone; pp. 1-77 *in* B. K. Hall, (ed.), Bone matrix and bone specific products., CRC Press, Boca Raton.

Rink, W. J. and H. P. Schwarz. 1995. Tests for diagenesis in tooth enamel: ESR dating signals and carbonate contents. Journal of Archaeological Science 22:251-255.

Ross, C. A. 1989. (ed.), Crocodiles and alligators. Merehurst Press, London, 240pp.

Roth, J. J. and E. C. Roth. 1980. The parietal-pineal complex among paleovertebrates: evidence for temperature regulation; pp. 189-231 *in* R. D. K. Thomas and E. C. Olson, (eds.), A cold look at the warm-blooded dinosaurs, Westview Press, Boulder.

Rowe, T. 1993. Early mammal phylogenetic systematics; pp. 129-145 *in* F. S. Szalay, M. J. Novacek, and M. C. McKenna, (eds.), Mammal phylogeny: Mesozoic differentiation, multituberculates, monotremes, early therians, and marsupials, Springer-Verlag, New York.

Ruben, J. 1995. The evolution of endothermy in mammals and birds: from physiology to fossils. Annual Review of Physiology 57:69-95.

---------- 1996. Evolution of endothermy in mammals, birds and their ancestors; pp. 347-376 *in* I. A. Johnston and A. F. Bennett, (eds.), Animals and temperature. Phenotypic and evolutionary adaptation, Cambridge University Press, Cambridge.

---------, A. Leitch, W. Hillenius, N. Geist and T. Jones. 1997. New insights into the metabolic physiology of dinosaurs; pp. 505-518 *in* J. O. Farlow and M. K. Brett-Surman, (eds.), The complete dinosaur, Indiana University Press, Indiana.

Rubidge, B. S. 1995. (ed.), Biostratigraphy of the Beaufort Group (Karoo Supergroup). Council for Geoscience, Pretoria, 46pp.

---------- and C. A. Sidor. 2001. Evolutionary patterns among Permo-Triassic therapsids. Annual Review of Ecology and Systematics 32:449-480.

Sander, M. A. 2000. Longbone histology of the Tendaguru sauropods: implications for growth and biology. Paleobiology 26(3):466-488.

Schmidt-Nielsen, K. 1975. Animal physiology. Adaptation and environment. Cambridge University Press, Cambridge, 699pp.

Seeley, H. G. 1895a. Researches on the structure, organization and classification of the fossil Reptilia. On *Diademdon*. Philosophical Transactions of the Royal Society of London B 185:1029-1041.

---------- 1895b. On the structure, organization and classification of the fossil Reptilia III. On *Trirachodon*. Philosophical Transactions of the Royal Society of London B 186:48-57.

---------- 1895c. On the structure, organization, and classification of the fossil Reptilia. On *Tritylodon longaevus* (Owen). Philosophical Transactions of the Royal Society of London. 185:1025-1028.

---------- 1908. On the dentition of the palate in the South African fossil reptile genus *Cynognathus*. Geological Magazine 5:486-491.

Sharp, Z. D., V. Atudorei and H. Furrer. 2000. The effect of diagenesis on oxygen isotope ratios of biogenic phosphates. American Journal of Science 300:222-237.

---------- and T. E. Cerling. 1998. Fossil isotope records of seasonal climate and ecology: Straight from the horse's mouth. Geology 26:219-222.

Shemesh, A., Y. Kolodny and B. Luz. 1983. Oxygen isotope variations in phosphate of biogenic apatite, II. Phosphorite rocks. Earth and Planetary Science Letters 64:405-416.

Smirina, E. M. 1974. Prospects of age determination by bone layers in Reptilia. Zoologichesky Zhurnal 53:111-117.

Smith, B. N. and S. Epstein. 1972. Two categories of $^{13}C/^{12}C$ ratios for higher plants. Plant Physiology 47:380-384.

Smith, R. and A. W. Keyser. 1995. Biostratigraphy of the *Cistecephalus* Assemblage Zone; pp. 23-28 *in* B. S. Rubidge, (ed.), Biostratigraphy of the Beaufort Group (Karoo Supergroup), Council for Geoscience, Pretoria.

----------. and J. Kitching. 1997. Sedimentology and vertebrate taphonomy of the *Tritylodon* Acme Zone: a reworked palaeosol in the Lower Jurassic Elliot Formation, Karoo Supergroup, South Africa. Palaeogeography, Palaeoclimatology, Palaeoecology 131:29-50.

----------, P. G. Eriksson and W. J. Botha. 1993. A review of the stratigraphy and sedimentary environments of the Karoo-aged basins of southern Africa. Journal of African Earth Sciences 16, No. 1/2:143-169.

Sponheimer, M. and J. A. Lee-Thorp. 1999a. Alteration of enamel carbonate environments during fossilization. Journal of Archaeological Science 26:143-150.

---------- and J. A. Lee-Thorp. 1999b. Oxygen isotopes in enamel carbonate and their ecological significance. Journal of Archaeological Science 26:723-728.

---------- and J. A. Lee-Thorp. 2001. The oxygen isotope composition of mammalian enamel carbonate from Morea Estate, South Africa. Oecologia 126:153-157.

Spotila, J. R., M. P. O'Connor, P. Dodson, and F. V. Paladino. 1991. Hot and cold running dinosaurs: body size, metabolism and migration. Modern Geology 16:203-227.

Starck, J. M. and A. Chinsamy. in press. Bone microstructure and developmental plasticity in birds and other dinosaurs. Journal of Morphology.

Stein, B. R. 1989. Bone density and adaptation in semi-aquatic mammals. Journal of Mammalogy 70(3):467-476.

Stuart-Williams, H. L. Q. and H. P. Schwarcz. 1997. Oxygen isotopic determination of climatic variation using phosphate from beaver bone, tooth enamel, and dentine. Geochimica et Cosmochimica Acta 61:2539-2550.

Sues, H. D. 1985. The relationships of the Tritylodontidae (Synapsida). Zoological Journal of the Linnean Society 85:205-217.

Thackeray, J. F., N. J. van der Merwe, J. A. Lee-Thorp, A. Sillen, J. L. Lanham, R. Smith, A. Keyser, and P. M. S. Monteiro. 1990. Changes in carbon isotope ratios in the late Permian recorded in therapsid tooth apatite. Nature 347:751-753.

Tucker, M. E. and M. J. Benton. 1982. Triassic environments, climates and reptile evolution. Palaeogeography, Palaeoclimatology, Palaeoecology 40:361-379.

Varricchio, D. J. 1993. Bone microstructure of the Upper Cretaceous theropod dinosaur Troodon formosus. Journal of Vertebrate Paleontology 13:99-104.

Visser, J. N. J. 1991. Geography and climatology of the Late Carboniferous to Jurassic Karoo Basin in South-Western Gondwana. Annals of the South African Museum 99:415-431.

Wake, D. B. and J. Castanet. 1995. A skeletochronological study of growth and age in relation to adult size in *Batrachoseps attenuatus*. Journal of Herpetology 29(1):60-65.

Wall, W. P. 1983. The correlation between limb-bone density and aquatic habits in recent mammals. Journal of Vertebrate Paleontology 57:197-207.

Wang, Y., T. E. Cerling, and B. J. MacFadden. 1994. Fossil horses and carbon isotopes: new evidence for Cenozoic dietary, habitat, and ecosystem changes in North America. Palaeogeography, Palaeoclimatology, Palaeoecology 107:269-279.

Watson, D. M. S. 1911. The skull of *Diademodon* with notes on those of some other cynodonts. The Annals and Magazine of Natural History 8:295-330.

---------- 1920. On the Cynodontia. Annals and Magazines of Natural History VI:513-517.

Withers, P. C. 1992. Comparative Animal Physiology. Saunders College, Fort Worth, 949pp.

# APPENDIX 1:

## Institutional abbreviations

Appendix 1: Institutional abbreviations

| Abbreviation | Institution | City | Country |
|---|---|---|---|
| B/P/I | Bernard Price Institute for Palaeontological Research University of Witwatersrand | Johannesburg | South Africa |
| NMQR | Bloemfontein National Museum | Bloemfontein | South Africa |
| SAM-PK-K SAM-PQL | South African Museum | Cape Town | South Africa |
| CGP | Council for Geoscience | Pretoria | South Africa |
| UMCZ T | University of Cambridge | Cambridge | England |
| TSK | University of Oxford | Oxford | England |

# APPENDIX 2:

Relative bone wall thickness (RBT) values and K-value data

Appendix 2: Relative bone wall thickness (RBT) values and K-value data

| Genus | Element | Specimen number | Slide | t1 | t2 | t3 | t4 | mc1 | mc2 | d1 | d2 | T/D.100 % | k-value |
|---|---|---|---|---|---|---|---|---|---|---|---|---|---|
| *Procynosuchus* | radius | B/P/I/3747 | P2-B2 | 2585 | 2365 | 1870 | 1540 | 40 | 61 | 6655 | 7260 | 30.4 | 0.33 |
| | | | | | | | | | | | | | |
| *Thrinaxodon* | humerus | B/P/I/2820 | Tx2-BI 1 | 2035 | 1100 | 825 | 1045 | 48 | 80 | 5500 | 6545 | 20.76 | 0.57 |
| | humerus | SAM-PK-K1121 | Tx1-BI 1 | 2255 | 1100 | 770 | 990 | 43 | 53 | 5390 | 5005 | 24.6 | 0.51 |
| | humerus | B/P/I/5208 | Tx3-BI 1 | 825 | 1650 | 1705 | 1320 | 62 | 44 | 5940 | 5390 | 24.27 | 0.49 |
| | | | Tx3-BI 2 | 715 | 1430 | 1375 | 1375 | 94 | 41 | 7260 | 5060 | 19.87 | 0.58 |
| | radius | B/P/I/4282a | Tx5-BII 1 | 1210 | 935 | 990 | 770 | 39 | 27 | 4345 | 3190 | 25.91 | 0.48 |
| | | | Tx5-BII 2 | 880 | 880 | 770 | 825 | 44 | 31 | 4070 | 3410 | 22.43 | 0.55 |
| | radius | B/P/I/1730 | Tx4-BII 5 | 935 | 825 | 825 | 660 | 30 | 29 | 3410 | 3080 | 25 | 0.5 |
| | | | Tx4-BX | 935 | 715 | 1100 | 660 | 35 | 27 | 3960 | 2860 | 25 | 0.51 |
| | ulna | B/P/I/5018 | Tx9-BI 3 | 1100 | 825 | 1210 | 715 | 18 | 25 | 3300 | 2915 | 30.97 | 0.39 |
| | | | Tx9-BI 4 | 1100 | 495 | 825 | 660 | 40 | 20 | 4125 | 2255 | 27.56 | 0.51 |
| | ulna | B/P/I/4282b | Tx8-BII 1 | 1100 | 660 | 990 | 770 | 36 | 22 | 4070 | 2640 | 26 | 0.48 |
| | | | Tx8-BII 2 | 1155 | 660 | 1320 | 715 | 21 | 40 | 3630 | 3575 | 26.36 | 0.47 |
| | femur | SAM-PK-K8004b | Tx10-BI 1 | 440 | 550 | 550 | 660 | 19 | 25 | 2035 | 2585 | 23.81 | 0.51 |
| | | | Tx10-BI 2 | 550 | 495 | 495 | 495 | 15 | 24 | 1870 | 2310 | 24.34 | 0.51 |
| | femur | SAM-PK-K8004a | Tx11-BII 2 | 440 | 440 | 495 | 550 | 21 | 21 | 2090 | 2145 | 22.73 | 0.54 |
| | | | Tx11-BII 3 | 495 | 550 | 660 | 550 | 20 | 15 | 2255 | 1925 | 26.97 | 0.46 |
| | femur | SAM-PK-K1395 | Tx1395-B1 | 825 | 725 | 1485 | 825 | 104 | 73 | 4910 | 3375 | 23.3 | 0.54 |
| | | | Tx1395-B2 | 900 | 775 | 750 | 750 | 93 | 76 | 3975 | 3425 | 21.45 | 0.57 |
| | | | | | | | | | | | | | |
| *Cynognathus* | humerus | NMQR1208a | CY4-BII 1 | 3300 | 3850 | 6930 | 4455 | 230 | 170 | 22 880 | 17 655 | 22.86 | 0.54 |
| | | | CY4-BII 2 | 3300 | 4518 | 6435 | 4070 | 210 | 220 | 21 285 | 20 688 | 21.83 | 0.56 |
| | femur | SAM-PK-K6235a | C2-BI 2 | 7700 | 6600 | 5720 | 9020 | 145 | 158 | 21 395 | 24 310 | 31.77 | 0.36 |
| | | | C2-BI 1 | 8360 | 7755 | 8140 | 8855 | 114 | 135 | 22 770 | 24 035 | 35.37 | 0.29 |
| | femur | NMQR3019a | C4-BI 1 | 11110 | 9900 | 8470 | 12265 | 185 | 233 | 29755 | 34980 | 32.46 | 0.34 |
| | | | C4-BI 2 | 8955 | 12375 | 11990 | 9625 | 180 | 234 | 30845 | 34870 | 32.68 | 0.35 |

| Genus | Element | Specimen number | Slide | t1 | t2 | t3 | t4 | mc1 | mc2 | d1 | d2 | T/D.100 | k-value |
|---|---|---|---|---|---|---|---|---|---|---|---|---|---|
| *Diademodon* | humerus | SAM-PK-K8971a | D5-B 5 | 2145 | 2200 | 2090 | 3300 | 70 | 76 | 8085 | 9680 | 27.4 | 0.46 |
| | | | D5-B 4 | 2970 | 1870 | 2420 | 1925 | 52 | 94 | 8250 | 8965 | 26.68 | 0.46 |
| | humerus | UMCZ T492 | T492-B 2 | 3190 | 5610 | 3355 | 3630 | 62 | 63 | 9955 | 12 705 | 34.83 | 0.31 |
| | | | T492-B 3 | 2860 | 4785 | 3190 | 6545 | 57 | 26 | 9185 | 12 760 | 39.6 | 0.23 |
| | humerus | B/P/I/3772 | D1-B 6 | 3025 | 3245 | 4125 | 4785 | 29 | 26 | 8745 | 9460 | 41.69 | 0.17 |
| | | | D1-B 4 | 3080 | 3465 | 3300 | 2475 | 68 | 63 | 10 120 | 9405 | 31.55 | 0.37 |
| | humerus | NMQR1208b | CY6-B 6 | 7700 | 8360 | 4125 | 3850 | 62 | 102 | 15 235 | 17 820 | 36.36 | 0.27 |
| | | | CY6-B 5 | 8250 | 4015 | 5280 | 4620 | 30 | 62 | 15 180 | 12 045 | 40.71 | 0.2 |
| | humerus | NMQR1208c | CY5-BI 3 | 4950 | 7700 | 5060 | 6600 | 114 | 93 | 16 280 | 19 415 | 34.1 | 0.33 |
| | | | CY5-BI 4 | 6600 | 5500 | 4675 | 7700 | 85 | 75 | 15 950 | 17 325 | 36.78 | 0.26 |
| | humerus | NMQR1208d | CY1-B 1 | 9900 | 9900 | 11000 | 10175 | 67 | 65 | 24585 | 23650 | 42.47 | 0.15 |
| | humerus | NMQR1208e | CY2-B 1 | 11 220 | 11 550 | 6050 | 7865 | 125 | 92 | 24 145 | 24 475 | 37.73 | 0.24 |
| | | | CY2-B 2 | 7150 | 8250 | 9845 | 7810 | 154 | 188 | 25 465 | 26 400 | 31.87 | 0.36 |
| | radius | SAM-PK-K8971b | D3-BII 3 | 1760 | 2310 | 1100 | 1650 | 41 | 37 | 5115 | 5995 | 30.69 | 0.39 |
| | | | D3-BII 4 | 1375 | 1705 | 2200 | 1925 | 33 | 33 | 5390 | 5445 | 33.25 | 0.34 |
| | ulna | SAM-PK-K8971c | D4b-BII 3 | 990 | 2475 | 1100 | 2640 | 31 | 35 | 3795 | 7040 | 33.25 | 0.36 |
| | | | D4b-BII 4 | 1100 | 2585 | 1045 | 2970 | 35 | 43 | 4070 | 7920 | 32.11 | 0.38 |
| | femur | UMCZ T495 | T495-B2 | 1925 | 1705 | 1870 | 1980 | 113 | 130 | 10 010 | 10 835 | 17.94 | 0.64 |
| | | | T495-B 3 | 1705 | 1815 | 2035 | 1870 | 117 | 22 | 10 175 | 4895 | 24.64 | 0.43 |
| | femur | UMCZ T503 | T503-B 3 | 2585 | 3080 | 2750 | 3575 | 96 | 128 | 10 615 | 13 695 | 24.66 | 0.51 |
| | | | T503-BI | 5170 | 3300 | 3575 | 3245 | 94 | 135 | 13 915 | 13 970 | 27.16 | 0.45 |
| | femur | UMCZ T493 | T493-B5 | 2915 | 4125 | 5060 | 4510 | 105 | 120 | 13750 | 15235 | 28.65 | 0.43 |
| | femur | NMQR1208f | CY8-BI 5 | 7810 | 5775 | 9790 | 6490 | 127 | 93 | 24 585 | 17 380 | 35.58 | 0.29 |
| | | | CY8-BI 4 | 9350 | 5500 | 6380 | 6050 | 120 | 150 | 22 330 | 19 800 | 32.38 | 0.36 |
| | tibia | NMQR1208g | CY12-BI 1 | 3410 | 4400 | 2090 | 3465 | 25 | 50 | 6875 | 10 615 | 38.21 | 0.23 |
| | | | CY12-BI 2 | 3630 | 4125 | 2200 | 4620 | 25 | 52 | 7205 | 11 605 | 38.74 | 0.22 |
| | tibia | NMQR1208h | CY11-BI 1 | 4675 | 4785 | 1925 | 5720 | 44 | 75 | 9020 | 14 630 | 36.16 | 0.28 |
| | | | Cy11-BI 2 | 1650 | 3685 | 5115 | 4840 | 56 | 128 | 9845 | 15 565 | 30.09 | 0.38 |
| | tibia | UMCZ T447 | T447-B2 | 2310 | 5500 | 4235 | 4840 | 51 | 74 | 9350 | 14 410 | 35.53 | 0.29 |
| | | | T447-B 1 | 2200 | 4785 | 3850 | 5280 | 61 | 82 | 9405 | 14 575 | 33.6 | 0.33 |
| | tibia | NMQR1208i | CY10-BII 1 | 4840 | 3575 | 4840 | 3630 | 60 | 75 | 12 980 | 11 330 | 34.73 | 0.31 |
| | | | CY10-BII 2 | 4510 | 9900 | 5390 | 6600 | 60 | 106 | 13 200 | 22 330 | 37.15 | 0.26 |

| Genus | Element | Specimen number | Slide | t1 | t2 | t3 | t4 | mc1 | mc2 | d1 | d2 | T/D.100 | k-value |
|---|---|---|---|---|---|---|---|---|---|---|---|---|---|
| *Diademodon* | tibia | NMQR1208j | CY9-BII 1 | 3575 | 8580 | 4950 | 9900 | 93 | 140 | 13 640 | 26 180 | 33.91 | 0.34 |
| | | | CY9-BII 2 | 3465 | 8415 | 4730 | 6380 | 98 | 222 | 13 585 | 27 005 | 28.32 | 0.43 |
| | fibula | UMCZ T448 | T448-B2 | 1980 | 2695 | 2475 | 2750 | 21 | 25 | 5610 | 6820 | 39.82 | 0.21 |
| | | | T448-B1 | 2090 | 2805 | 2640 | 2695 | 16 | 25 | 5610 | 6875 | 40.97 | 0.18 |
| | | | | | | | | | | | | | |
| *Trirachodon* | radius | CGP1/79a | R1 | 825 | 925 | 800 | 825 | 50 | 75 | 2875 | 3625 | 25.96 | 0.47 |
| | ulna | CGP1/79b | U1 | 725 | 875 | 500 | 800 | 58 | 58 | 2675 | 3125 | 25 | 0.5 |
| | femur | NMQR3282a | Tri1-BII 1 | 1265 | 1265 | 1375 | 1815 | 51 | 61 | 5445 | 6435 | 24.07 | 0.52 |
| | | | Tri1-BII 2 | 1430 | 2365 | 1815 | 2035 | 37 | 30 | 5280 | 6050 | 33.74 | 0.33 |
| | femur | SAM-PK-K5881a | Tri-1pro | 1485 | 1540 | 1485 | 2145 | 28 | 50 | 4510 | 6435 | 30.4 | 0.38 |
| | | | Tri-2dis | 1650 | 880 | 1760 | 2090 | 25 | 53 | 4785 | 5555 | 30.85 | 0.41 |
| | tibia | NMQR3282b | Tri3-B 1 | 1320 | 825 | 1375 | 1430 | 60 | 50 | 5995 | 5005 | 22.5 | 0.55 |
| | | | Tri3-B 2 | 1430 | 1540 | 1375 | 1210 | 40 | 43 | 5005 | 5115 | 27.45 | 0.45 |
| | tibia | SAM-PK-K5881c | TRI 1B 1 | 990 | 935 | 1045 | 1045 | 38 | 55 | 4125 | 5005 | 21.99 | 0.56 |
| | | | | | | | | | | | | | |
| *Tritylodon* | humerus | B/P/I/4785a | TY5-BII 1 | 3410 | 4180 | 3080 | 2585 | 28 | 30 | 8030 | 8415 | 40.3 | 0.19 |
| | | | TY5-BI 1 | 3080 | 3025 | 3080 | 3575 | 35 | 33 | 8085 | 8415 | 38.67 | 0.23 |
| | humerus | B/P/I/5160 | TY3-BI 1 | 1980 | 2090 | 1705 | 1925 | 63 | 36 | 7150 | 5995 | 29.29 | 0.41 |
| | | | TY3-BII 1 | 1375 | 3025 | 3630 | 2420 | 50 | 51 | 7755 | 8250 | 32.65 | 0.35 |
| | radius | B/P/I/5167 | TY1-BII 2 | 1485 | 1595 | 1595 | 2475 | 30 | 50 | 4730 | 6820 | 30.95 | 0.38 |
| | | | TY1-BII 3 | 1925 | 2750 | 1595 | 1815 | 31 | 43 | 5225 | 6930 | 33.26 | 0.34 |
| | radius | B/P/I/4785b | TY5-BII 1 | 450 | 2200 | 625 | 1075 | 18 | 49 | 1525 | 4500 | 36.1 | 0.29 |
| | | | TY5-BI 1 | 700 | 2025 | 575 | 1075 | 16 | 46 | 1675 | 4250 | 36.92 | 0.26 |

# APPENDIX 3:

Relative bone wall thickness values from earlier studies for comparison with results in this study

Appendix 3: Relative bone wall thickness values from earlier studies for comparison with results in this study. An * indicates data calculated from r/t values in a study conducted by Magwene (1993).

| Genus | Common name | Reference | Lifestyle habit | Humerus | Radius | Femur | Tibia |
|---|---|---|---|---|---|---|---|
| *Alligator* | alligator | | semi-aquatic | | | 35.6 | |
| *Alligator mississippiensis* | alligator | * | semi-aquatic | | | 29.71 | |
| *Alligator olsoni* | alligator | * | semi-aquatic | | | 34.53 | |
| *Amphibolurus barbatus* | agamid lizard | * | generalised, terrestrial | | | 21.89 | |
| *Anolis cristatellus* | anole lizard | * | generalised, terrestrial | | | 25 | |
| *Chamaeleo vulgaris* | chamaeleon | * | arboreal | | | 22.79 | |
| *Crocodylus niloticus* | Nile crocodile | Chinsamy, 1991 | semi-aquatic | | | 36.3 | |
| *Crotaphytus collaris* | collared lizard | * | generalised, terrestrial | | | 20 | |
| *Cyclura carinata* | Turks Island lizard | * | generalised, terrestrial | | | 20 | |
| *Eumeces fasciatus* | five-lined skink | * | generalised, terrestrial | | | 27.52 | |
| *Gerrhonotus grantis* | anguid lizard | * | burrower and rock climber | | | 33.36 | |
| *Heloderma suspectum* | gila monster | * | burrower and rock climber | | | 38.33 | |
| *Phrynosoma douglassii* | Douglass's horned lizard | * | fossorial | | | 32.89 | |
| *Iguana tuberculata* | iguana | * | generalised, terrestrial | | | 19.08 | |
| *Ptychozoon homalocephalum* | gecko | * | generalised, terrestrial | | | 25 | |
| *Sauromalus* | common chuckwalla lizard | * | generalised, terrestrial | | | 25.49 | |
| *Sceloporus clarkii* | Clarke's spiny lizard | * | rock climber | | | 33.33 | |
| *Sceloporus magister* | iguanid | * | generalised, terrestrial | | | 29.2 | |
| *Sceloporus occiedentalis* | iguanid | * | generalised, terrestrial | | | 27.6 | |
| *Sceloporus spinosus* | iguanid | * | generalised, terrestrial | | | 33.33 | |
| *Sphenodon punctatus* | tuatara | * | generalised, terrestrial | | | 27.49 | |
| *Varanus arenarius* | monitor | * | generalised, terrestrial | | | 16.67 | |
| *Varanus nuchalis* | monitor | * | generalised, terrestrial | | | 15.48 | |
| *Varanus salvator* | water monitor | * | semi-aquatic | | | 19.1 | |
| *Hippopotamus* | hippo | Wall, 1983 | semi-aquatic | 35 | 32.5 | 44 | 38.9 |
| *Choeropsis* | pygmy hippo | Wall, 1983 | semi-aquatic | 31.6 | 34.4 | 32.9 | 31.3 |
| *Odobenus* | walrus | Wall, 1983 | semi-aquatic | 25.32 | 32.8 | 40.1 | 23.1 |
| *Trichechus* | manatee | Wall, 1983 | fully aquatic | 54.2 | 54.2 | | |
| *Zalophus* | sea lion | Wall, 1983 | semi-aquatic | 29 | 31 | 48.1 | 36.3 |
| *Castor* | beaver | Wall, 1983 | semi-aquatic | 52.5 | | 43.3 | |

| Genus | Common name | Reference | Lifestyle habit | Humerus | Radius | Femur | Tibia |
|---|---|---|---|---|---|---|---|
| *Ceratotherium* | white rhino | Wall, 1983 | generalised, terrestrial | 33.8 | 26.2 | 25.2 | 26.6 |
| *Bison* | bison | Wall, 1983 | generalised, terrestrial | 17.9 | 17.1 | 19.4 | 18.7 |
| *Tapirus* | tapir | Wall, 1983 | generalised, terrestrial | 22.3 | 19.4 | 19.5 | 23.8 |
| *Rangifer* | caribou | Wall, 1983 | generalised, terrestrial | 16.2 | 22.6 | 18.3 | 21.1 |
| *Taurotragus* | eland | Wall, 1983 | generalised, terrestrial | 27.7 | 20.5 | 21.9 | 21.8 |
| *Okapia* | okapi | Wall, 1983 | generalised, terrestrial | 26.2 | 20.7 | 23.2 | 23.7 |
| *Tragelaphus* | kudu | Wall, 1983 | generalised, terrestrial | 25.9 |  | 21.7 | 25.1 |
| *Cervus* | eld deer | Wall, 1983 | generalised, terrestrial | 21.2 | 23.2 | 19.7 | 24.1 |
| *Hippotragus* | Roan antelope | Wall, 1983 | generalised, terrestrial | 28.1 | 26.5 | 25.1 | 24.9 |
| *Alces* | moose | Wall, 1983 | generalised, terrestrial | 19.7 | 12.6 | 14.6 | 14.5 |
| *Gazella* | gazelle | Wall, 1983 | generalised, terrestrial | 20.3 |  | 17.8 | 24.2 |
| *Connochaetes* | gnu | Wall, 1983 | generalised, terrestrial | 21.5 | 22.1 | 24.1 | 22.1 |
| *Procyon* | racoon | Wall, 1983 | generalised, terrestrial | 18.7 |  | 20.7 |  |
| *Alces machlis* | moose | * | generalised, terrestrial |  |  | 18.41 |  |
| *Arctomys* | marmot | * | generalised, terrestrial |  |  | 17.23 |  |
| *Auchenia glama* | llama | * | generalised, terrestrial |  |  | 18 |  |
| *Bison Americanus* | bison | * | generalised, terrestrial |  |  | 14.65 |  |
| *Bos* | domestic ox | * | generalised, terrestrial |  |  | 23.47 |  |
| *Bos bubalis* | ox | * | generalised, terrestrial |  |  | 23.61 |  |
| *Bubalis* | buffalo | * | generalised, terrestrial |  |  | 23.58 |  |
| *Camelus* | camel | * | generalised, terrestrial |  |  | 15.34 |  |
| *Capra* | Ibex (goat) | * | generalised, terrestrial |  |  | 21.12 |  |
| *Cariacus macrotis* | deer | * | generalised, terrestrial |  |  | 15.81 |  |
| *Cavia* | cavy (rodent) | * | generalised, terrestrial |  |  | 14.58 |  |
| *Cephalophus* | duiker | * | generalised, terrestrial |  |  | 18.34 |  |
| *Connochaetes* | wildebeest | * | generalised, terrestrial |  |  | 20.5 |  |
| *Dasyprocta* | agouti (rodent) | * | generalised, terrestrial |  |  | 18.12 |  |
| *Didelphis virginiana* | opossum | * | arboreal |  |  | 22.79 |  |
| *Echidna* | spiny anteater | * | fossorial |  |  | 21.28 |  |
| *Elephas africanus* | african elephant | * | generalised, terrestrial |  |  | 20.2 |  |
| *Elephas indicus* | asiatic elephant | * | generalised, terrestrial |  |  | 27.34 |  |
| *Equus burchelli* | Burchell's zebra | * | generalised, terrestrial |  |  | 23.51 |  |

| Genus | Common name | Reference | Lifestyle habit | Humerus | Radius | Femur | Tibia |
|---|---|---|---|---|---|---|---|
| *Equus caballus* | domestic horse | * | generalised, terrestrial | | | 22.53 | |
| *Equus hemionus* | Kiang wild ass | * | generalised, terrestrial | | | 20.55 | |
| *Erinaceus* | hedgehog | * | generalised, terrestrial | | | 22.91 | |
| *Erithizon* | new world porcupine | * | fossorial | | | 33.76 | |
| *Gazella granti* | gazelle | * | generalised, terrestrial | | | 22.08 | |
| *Giraffa* | giraffe | * | generalised, terrestrial | | | 25.14 | |
| *Heteromys* | spiny mouse | * | generalised, terrestrial | | | 10.54 | |
| *Kobus ellipsiprymnus* | antelope | * | generalised, terrestrial | | | 17.93 | |
| *Lepus* | hare | * | generalised, terrestrial | | | 17.42 | |
| *Manis* | pangolin | * | digs open termite nests | | | 22.65 | |
| *Mephitis* | skunk | * | generalised, terrestrial | | | 12.5 | |
| *Mule* | mule | * | generalised, terrestrial | | | 14.29 | |
| *Mus rattus* | black rat | * | generalised, terrestrial | | | 17.13 | |
| *Mus sylvaticus* | wood field-mouse | * | generalised, terrestrial | | | 20.84 | |
| *Ornithorhynchus* | platypus | * | semi-aquatic | | | 16.87 | |
| *Ovibos moschatus* | musk-ox | * | generalised, terrestrial | | | 8.58 | |
| *Ovis* | sheep | * | generalised, terrestrial | | | 22.64 | |
| *Ovis montana* | sheep | * | generalised, terrestrial | | | 19.64 | |
| *Phacochoerus* | warthog | * | fossorial | | | 20.78 | |
| *Procavia* | rock hyrax | * | rock climber | | | 27.5 | |
| *Putorius* | mink | * | generalised, terrestrial | | | 14.57 | |
| *Putorius* | mink | * | generalised, terrestrial | | | 28.18 | |
| *Rangifer* | reindeer | * | generalised, terrestrial | | | 19.4 | |
| *Raphiceros* | steinbok | * | generalised, terrestrial | | | 22.45 | |
| *Rhinoceros bicornis* | rhino | * | generalised, terrestrial | | | 38.2 | |
| *Scalopus* | atopogale (rodent) | * | generalised, terrestrial | | | 16.67 | |
| *Sciurus* | squirrel | * | arboreal | | | 9.71 | |
| *Solenodon paradoxus* | atopogale (rodent) | * | generalised, terrestrial | | | 15.2 | |
| *Sorex* | shrew | * | generalised, terrestrial | | | 28.63 | |
| *Sus* | domestic pig | * | generalised, terrestrial | | | 13.93 | |
| *Sus scrofa* | wild boar | * | generalised, terrestrial | | | 17.45 | |
| *Tamandua* | Tamandua anteater | * | arboreal | | | 30.96 | |

| Genus | Common name | Reference | Lifestyle habit | Humerus | Radius | Femur | Tibia |
|---|---|---|---|---|---|---|---|
| *Tapirus* | tapir | * | generalised, terrestrial | | | 15.74 | |
| *Tragulus javanicus* | mouse deer | * | generalised, terrestrial | | | 6.9 | |
| *Trichosurus* | phalanger (Aus. marsupial) | * | generalised, terrestrial | | | 19.05 | |
| *Tupaia* | tree-shrew | * | arboreal | | | 18.35 | |
| *Viverra* | civet | * | generalised, terrestrial | | | 20.09 | |
| *Heterocephalus glaber* | naked mole r+B10at | | fossorial | | | 31.03 | |

# APPENDIX 4:

Fourier Transform Infra-red Indices:

4(a) Fourier Transform Infra-red BPI

4(b) Fourier Transform Infra-red API

4(c) Fourier Transform Infra-red BAI

4(d) Fourier Transform Infra-red PCI

Appendix 4a: Fourier Transform Infra-red BPI

| Genus | Specimen number | Frequency at 1415cm$^{-1}$ | Frequency at 605cm$^{-1}$ | Absorbance at 1415cm$^{-1}$ | Absorbance at 605cm$^{-1}$ | Total |
|---|---|---|---|---|---|---|
| *Giraffa camelopardalis* | 1a | 1415.9 | 603.77 | 0.37824 | 1.1642 | 0.325 |
| | pretreated 1b | 1413.6 | 604.18 | 0.38333 | 1.2033 | 0.319 |
| | | | | | | |
| *Crocodylus niloticus* | CROC6 | 1416.5 | 604.16 | 0.51635 | 0.90527 | 0.57 |
| | CROC7 | 1416.7 | 604.21 | 0.45616 | 0.79089 | 0.577 |
| | CROC8 | 1417 | 604.26 | 0.52204 | 0.86058 | 0.607 |
| | CROC9 | 1416 | 604.21 | 0.54701 | 0.89898 | 0.608 |
| | CROC10 | 1417.1 | 604.37 | 0.48582 | 0.74162 | 0.655 |
| | CROC11 | 1416.3 | 604.06 | 0.42236 | 0.83836 | 0.504 |
| | CROC12 | 1416.7 | 604.15 | 0.4934 | 0.90362 | 0.546 |
| | CROC13 | 1416.3 | 603.09 | 0.40308 | 0.72653 | 0.555 |
| | CROC14 | 1416 | 604.21 | 0.29721 | 0.60633 | 0.49 |
| | | | | | | |
| *Varanus* | 1 | 1417.7 | 604.1 | 0.34908 | 0.48243 | 0.724 |
| | | | | | | |
| *Sivatherium hendeyi* | SAM-PQL43928 | 1419.9 | 604.24 | 0.26157 | 0.74372 | 0.352 |
| | | | | | | |
| *Cynognathus* | SAM-PK-K3029 | 1426.9 | 603.78 | 0.54215 | 0.81096 | 0.6685 |
| | B/P/I/1675d | 1427.8 | 604.17 | 0.47332 | 0.89311 | 0.53 |
| | | | | | | |
| *Diademodon* | UMCZ T504a | 1428.6 | 604.29 | 0.62663 | 1.1748 | 0.533 |
| | UMCZ T504b | 1428.7 | 603.96 | 0.78734 | 1.282 | 0.614 |
| | | | | | | |
| *Trirachodon* | SAM-PK-K5881(1) | 1424.6 | 603.98 | 0.44398 | 0.72695 | 0.611 |

Appendix 4b: Fourier Transform Infra-red API

| Genus | Specimen number | Frequency at 1540cm$^{-1}$ | Frequency at 605cm$^{-1}$ | Absorbance at 1540cm$^{-1}$ | Absorbance at 605cm$^{-1}$ | Total |
|---|---|---|---|---|---|---|
| *Giraffa camelopardalis* | 1a | 1543.7 | 603.77 | 0.24897 | 1.1642 | 0.214 |
| | pretreated 1b | 1544.5 | 604.18 | 0.23563 | 1.2033 | 0.196 |
| | | | | | | |
| *Crocodylus niloticus* | CROC6 | 1543.3 | 604.16 | 0.33413 | 0.90527 | 0.369 |
| | CROC7 | 1538.4 | 604.21 | 0.25121 | 0.79089 | 0.318 |
| | CROC8 | 1542.3 | 604.26 | 0.3229 | 0.86058 | 0.375 |
| | CROC9 | 1541.2 | 604.21 | 0.35347 | 0.89898 | 0.393 |
| | CROC10 | 1540.2 | 604.37 | 0.30777 | 0.74162 | 0.415 |
| | CROC11 | 1542.4 | 604.06 | 0.25858 | 0.83836 | 0.308 |
| | CROC12 | 1540.6 | 604.15 | 0.30565 | 0.90362 | 0.338 |
| | CROC13 | 1542 | 604.09 | 0.25663 | 0.72653 | 0.353 |
| | CROC14 | 1538.2 | 604.21 | 0.19194 | 0.60633 | 0.317 |
| | | | | | | |
| *Varanus* | 1 | 1544.4 | 604.1 | 0.29044 | 0.48243 | 0.602 |
| | | | | | | |
| *Sivatherium hendeyi* | SAM-PQL43928 | 1543.5 | 604.24 | 0.1679 | 0.74372 | 0.226 |
| | | | | | | |
| *Cynognathus* | SAM-PK-K3029 | 1542.3 | 603.78 | 0.30378 | 0.81096 | 0.3746 |
| | B/P/I/1675d | 1540 | 604.17 | 0.26439 | 0.89311 | 0.296 |
| | | | | | | |
| *Diademodon* | UMCZ T504a | 1542.4 | 604.29 | 0.24333 | 1.1748 | 0.207 |
| | UMCZ T504b | 1554.5 | 1.282 | 0.3904 | 1.282 | 0.305 |
| | | | | | | |
| *Trirachodon* | SAM-PK-K5881(1) | 1543.3 | 603.98 | 0.23931 | 0.72695 | 0.329 |

Appendix 4c: Fourier Transform Infra-red BAI

| Genus | Specimen number | Frequency at 1415cm$^{-1}$ | Frequency at 1540cm$^{-1}$ | Absorbance at 1415cm$^{-1}$ | Absorbance at 1540cm$^{-1}$ | Total |
|---|---|---|---|---|---|---|
| *Giraffa camelopardalis* | 1a | 1415.9 | 1543.7 | 0.37824 | 0.24897 | 1.519 |
| | pretreated 1b | 1413.6 | 1544.5 | 0.38333 | 0.23563 | 1.627 |
| | | | | | | |
| *Crocodylus niloticus* | CROC6 | 1416.5 | 1543.3 | 0.51635 | 0.33413 | 1.545 |
| | CROC7 | 1416.7 | 1538.4 | 0.45616 | 0.25121 | 1.816 |
| | CROC8 | 1417 | 1542.3 | 0.52204 | 0.3229 | 1.617 |
| | CROC9 | 1416 | 1541.2 | 0.54701 | 0.35341 | 1.548 |
| | CROC10 | 1417.1 | 1540.2 | 0.48582 | 0.30777 | 1.579 |
| | CROC11 | 1416.3 | 1542.4 | 0.42236 | 0.25858 | 1.633 |
| | CROC12 | 1416.7 | 1540.6 | 0.4934 | 0.30565 | 1.614 |
| | CROC13 | 1416.3 | 1542 | 0.40308 | 0.25663 | 1.571 |
| | CROC14 | 1416.8 | 1538.2 | 0.29721 | 0.19194 | 1.548 |
| | | | | | | |
| *Varanus* | 1 | 1417.7 | 1544.4 | 0.34908 | 0.29044 | 1.202 |
| | | | | | | |
| *Sivatherium hendeyi* | SAM-PQL43928 | 1419.9 | 1543.5 | 0.26157 | 0.1679 | 1.558 |
| | | | | | | |
| *Cynognathus* | SAM-PK-K3029 | 1426.9 | 1542.3 | 0.54215 | 0.30378 | 1.785 |
| | B/P/I/1675d | 1427.8 | 1540 | 0.47332 | 0.26439 | 1.79 |
| | | | | | | |
| *Diademodon* | UMCZ T504a | 1428.6 | 1542.4 | 0.62663 | 0.24333 | 2.575 |
| | UMCZ T504b | 1428.7 | 1554.5 | 0.78734 | 0.3904 | 2.017 |
| | | | | | | |
| *Trirachodon* | SAM-PK-K5881(1) | 1424.6 | 1543.3 | 0.44398 | 0.23931 | 1.855 |

Appendix 4d: Fourier Transform Infra-red PCI

| Genus | Specimen number | Frequency at 565cm$^{-1}$ | Frequency at 605cm$^{-1}$ | Frequency at 590cm$^{-1}$ | Absorbance at 565cm$^{-1}$ | Absorbance at 605cm$^{-1}$ | Absorbance at 590cm$^{-1}$ | Total |
|---|---|---|---|---|---|---|---|---|
| *Giraffa camelopardalis* | 1a | 567.17 | 603.77 | 589.91 | 1.3509 | 1.1642 | 0.79809 | 3.151 |
| | pretreated 1b | 566.06 | 604.18 | 590.11 | 1.4343 | 1.2033 | 0.69437 | 3.799 |
| | | | | | | | | |
| *Crocodylus niloticus* | CROC6 | 566.48 | 604.16 | 590.29 | 1.0442 | 0.90527 | 0.72242 | 2.7 |
| | CROC7 | 568.66 | 604.21 | 590.83 | 0.92242 | 0.79089 | 0.61957 | 2.765 |
| | CROC8 | 566.32 | 604.26 | 590.66 | 0.99777 | 0.86058 | 0.70001 | 2.655 |
| | CROC9 | 566.3 | 604.21 | 590.38 | 1.0423 | 0.89898 | 0.73594 | 2.638 |
| | CROC10 | 566.27 | 604.37 | 590.48 | 0.84591 | 0.74162 | 0.60615 | 2.619 |
| | CROC11 | 567.98 | 604.06 | 590.17 | 0.98008 | 0.83836 | 0.6523 | 2.788 |
| | CROC12 | 567.83 | 604.15 | 590.39 | 1.0513 | 0.90362 | 0.70612 | 2.769 |
| | CROC13 | 567.81 | 603.09 | 590.24 | 0.83611 | 0.72653 | 0.57819 | 2.703 |
| | CROC14 | 566.61 | 604.21 | 590.09 | 0.71918 | 0.60633 | 0.46826 | 2.831 |
| | | | | | | | | |
| *Varanus* | 1 | 564.39 | 604.1 | 590.34 | 0.54439 | 0.48243 | 0.41017 | 2.503 |
| | | | | | | | | |
| *Sivatherium hendeyi* | SAM-PQL43928 | 568.14 | 604.24 | 590.03 | 0.78147 | 0.74372 | 0.46457 | 3.283 |
| | | | | | | | | |
| *Cynognathus* | SAM-PK-K3029 | 567.44 | 603.78 | 589.78 | 0.75839 | 0.81096 | 0.51079 | 3.072 |
| | B/P/I/1675d | 568.52 | 604.17 | 590.1 | 0.85793 | 0.89311 | 0.53087 | 3.298 |
| | | | | | | | | |
| *Diademodon* | UMCZ T504a | 569.81 | 604.29 | 589.69 | 1.043 | 1.1748 | 0.5699 | 3.892 |
| | UMCZ T504b | 568.24 | 603.96 | 589.92 | 1.1472 | 1.282 | 0.6966 | 3.488 |
| | | | | | | | | |
| *Trirachodon* | SAM-PK-K5881(1) | 568.53 | 603.98 | 590.18 | 0.76528 | 0.72695 | 0.45564 | 3.275 |

# APPENDIX 5:

Fourier Transform Infra-red indices taken from Sponheimer and Lee-Thorp (1999a)

Appendix 5: Fourier Transform Infra-red indices taken from Sponheimer and Lee-Thorp (1999a)

| Genus | Common name | BPI | API | BAI | PCI | $CO_3\%_{wt}$ |
|---|---|---|---|---|---|---|
| *Raphicerus melanotis* | greysbok | 0.22 | 0.071 | 3.1 | 3.6 | 2.9 |
| *Syncerus caffer* | buffalo | 0.27 | 0.092 | 2.9 | 3.5 | 3.4 |
| *Damaliscus dorcas* 1 | bontebok | 0.35 | 0.12 | 2.9 | 3.5 | 4.2 |
| *Damaliscus dorcas* 2 | bontebok | 0.23 | 0.061 | 3.8 | 3.6 | 3 |
| *Papio cynocephalus* | baboon | 0.16 | 0.05 | 3.1 | 3.8 | 2.3 |

# APPENDIX 6:

## $\delta^{13}C$ and $\delta^{18}O$ isotope signatures

Appendix 6: $\delta^{13}C$ and $\delta^{18}O$ isotope signatures

| Genus | Specimen number | $\delta^{13}C$ | Converted value | Mean | $\delta^{18}O$ | Converted value | Mean |
|---|---|---|---|---|---|---|---|
| *Crocodylus* | CROC1 (1) | -3.533 | -3.982 | -6.49 | -2.842 | -3.166 | -3.73 |
| *niloticus* | CROC1 (2) | -5.403 | -5.906 | | -1.723 | -2.027 | |
| | CROC1 (3) | -6.693 | -7.233 | | -3.995 | -4.34 | |
| | CROC1 (4) | -8.253 | -8.838 | | -5.016 | -5.379 | |
| | | | | | | | |
| | CROC2 (1) | -5.009 | -5.5 | -5.91 | -2.104 | -2.415 | -3.87 |
| | CROC2 (2) | -5.662 | -6.172 | | -4.018 | -4.363 | |
| | CROC2 (3) | -4.773 | -5.257 | | -3.61 | -3.948 | |
| | CROC2 (4) | -5.881 | -6.397 | | -3.289 | -3.621 | |
| | | | | | | | |
| | CROC3 (1) | -3.941 | -4.401 | -5.19 | -3.197 | -3.528 | -4.26 |
| | CROC3 (2) | -4.934 | -5.423 | | -3.793 | -4.134 | |
| | CROC3 (3) | -5.134 | -5.629 | | -4.454 | -4.807 | |
| | CROC3 (4) | -4.801 | -5.286 | | -4.233 | -4.582 | |
| | | | | | | | |
| *Thrinaxodon* | B/P/I/5020(1) | -11.433 | -12.111 | -12.8 | -10.373 | -10.833 | -11.6 |
| | BP/I/5020(2) | -11.89 | -12.581 | | -10.762 | -11.229 | |
| | BP/I/5020(3) | -12.411 | -13.117 | | -11.216 | -11.691 | |
| | BP/I/5020(4) | -12.622 | -13.334 | | -12.025 | -12.515 | |
| | | | | | | | |
| *Cynognathus* | SAM-PK-K3029 (1) | -11.199 | -11.88 | -11.6 | -12.389 | -12.9 | -13.3 |
| | SAM-PK-K3029 (2) | -10.536 | -11.2 | | -12.394 | -12.91 | |
| | SAM-PK-K3029 (3) | -11.319 | -12.01 | | -13.116 | -13.64 | |
| | SAM-PK-K3029 (4) | -10.766 | -11.43 | | -13.183 | -13.71 | |
| | | | | | | | |
| | B/P/I/1675d (4) | -10.968 | -11.072 | -10.8 | -12.605 | -10.794 | -11.1 |
| | B/P/I/1675d (5) | -10.491 | -10.584 | | -13.179 | -11.393 | |
| | | | | | | | |
| *Diademodon* | UMCZ T472 (1) | -13.417 | -14.152 | -14.3 | -13.645 | -14.164 | -13.8 |
| | UMCZ T472 (2) | -13.117 | -13.843 | | -13.779 | -14.3 | |
| | UMCZ T472 (3) | -12.982 | -13.704 | | -13.632 | -14.15 | |
| | UMCZ T472 (4) | -13.788 | -14.534 | | -13.389 | -13.903 | |
| | UMCZ T472 (5) | -14.301 | -15.062 | | -12.069 | -12.559 | |
| | | | | | | | |
| | UMCZ T471 (1) | -12.078 | -12.774 | -12.4 | -15.087 | -15.632 | -13 |
| | UMCZ T471 (2) | -11.534 | -12.214 | | -13.816 | -14.338 | |
| | UMCZ T471 (3) | -11.761 | -12.448 | | -10.021 | -10.474 | |
| | UMCZ T471 (4) | -11.556 | -12.237 | | -11.137 | -11.61 | |
| | | | | | | | |
| | UMCZ T473 (1) | -11.786 | -12.474 | -13.8 | -15.2 | -15.747 | -13.5 |
| | UMCZ T473 (2) | -13.31 | -14.042 | | -12.421 | -12.918 | |
| | UMCZ T473 (3) | -13.23 | -13.96 | | -14.022 | -14.548 | |
| | UMCZ T473 (4) | -13.359 | -14.092 | | -13.527 | -14.043 | |
| | UMCZ T473 (5) | -13.284 | -14.015 | | -12.115 | -12.606 | |
| | UMCZ T473 (6) | -13.387 | -14.121 | | -10.648 | -11.113 | |
| | | | | | | | |
| | UMCZ T474 (1) | -12.961 | -13.683 | -13 | -11.481 | -11.961 | -13.7 |
| | UMCZ T474 (2) | -11.829 | -12.518 | | -14.136 | -14.663 | |
| | UMCZ T474 (3) | -11.948 | -12.64 | | -14.196 | -14.724 | |
| | | | | | | | |
| | UMCZ T487 (1) | -12.701 | -13.415 | -13.2 | -14.22 | -14.749 | -15 |

| Genus | Specimen number | $\delta^{13}C$ | Converted value | Mean | $\delta^{18}O$ | Converted value | Mean |
|---|---|---|---|---|---|---|---|
| *Diademodon* | UMCZ T487 (2) | -12.336 | -13.04 | | -14.884 | -15.425 | |
| | UMCZ T487 (3) | -12.711 | -13.426 | | -15.691 | -16.246 | |
| | UMCZ T487 (4) | -12.53 | -13.239 | | -16.017 | -16.578 | |
| | UMCZ T487 (5) | -12.608 | -13.32 | | -15.828 | -16.386 | |
| | UMCZ T487 (6) | -12.098 | -12.794 | | -9.901 | -10.352 | |
| | | | | | | | |
| | UMCZ T504a (1) | -13.82 | -14.567 | -14.3 | -15.564 | -16.117 | -15.1 |
| | UMCZ T504a (2) | -12.971 | -13.693 | | -13.92 | -14.444 | |
| | UMCZ T504a (3) | -13.584 | -14.324 | | -11.74 | -12.224 | |
| | UMCZ T504a (4) | -13.739 | -14.483 | | -15.479 | -16.031 | |
| | UMCZ T504a (5) | -12.95 | -13.671 | | -15.007 | -15.55 | |
| | UMCZ T504a (6) | -14.258 | -15.017 | | -15.834 | -16.392 | |
| | | | | | | | |
| | UMCZ T470 (1) | -12.259 | -12.961 | -13.3 | -15.489 | -16.041 | -15.2 |
| | UMCZ T470 (2) | -13.121 | -13.848 | | -14.241 | -14.77 | |
| | UMCZ T470 (3) | -12.249 | -12.95 | | -14.635 | -15.171 | |
| | UMCZ T470 (4) | -12.492 | -13.2 | | -14.338 | -14.869 | |
| | UMCZ T470 (5) | -12.256 | -12.957 | | -13.896 | -14.419 | |
| | UMCZ T470 (6) | -12.089 | -12.786 | | -15.257 | -15.805 | |
| | UMCZ T470 (7) | -13.602 | -14.342 | | -14.556 | -15.091 | |
| | | | | | | | |
| | UMCZ T443 (1) | -12.692 | -13.406 | -14.1 | -13.126 | -13.635 | -12.9 |
| | UMCZ T443 (2) | -13.331 | -14.064 | | -13.662 | -14.181 | |
| | UMCZ T443 (3) | -13.56 | -14.3 | | -12.684 | -13.185 | |
| | UMCZ T443 (4) | -14.221 | -14.979 | | -11.698 | -12.182 | |
| | UMCZ T443 (5) | -13.664 | -14.406 | | -13.076 | -13.584 | |
| | UMCZ T443 (6) | -12.693 | -13.407 | | -9.915 | -10.366 | |
| | | | | | | | |
| *Trirachodon* | SAM-PK-K5881 2(1) | -10.865 | -10.887 | -10.9 | -13.819 | -11.814 | -12 |
| | SAM-PK-K5881 2(2) | -10.831 | -10.853 | | -13.137 | -11.133 | |
| | SAM-PK-K5881 2(3) | -10.97 | -11.686 | | -15.048 | -13.042 | |
| | | | | | | | |
| | SAM-PK-K5881 3(1) | -13.355 | -13.413 | -11.6 | -13.682 | -11.678 | -9.7 |
| | SAM-PK-K5881 3(2) | -9.752 | -9.758 | | -9.714 | -7.714 | |